ALLEVIATION OF EFFECTIVE PERMEABILITY REDUCTION OF GAS-CONDENSATE DUE TO CONDENSATE BUILDUP NEAR WELLBORE

A Thesis

by

JOSE GILBERTO CARBALLO SALAS

Submitted to the Office of Graduate Studies of
Texas A&M University
in partial fulfillment of the requirements for the degree of

MASTER OF SCIENCE

December 2004

Major Subject: Petroleum Engineering

ALLEVIATION OF EFFECTIVE PERMEABILITY REDUCTION OF GAS-CONDENSATE DUE TO CONDENSATE BUILDUP NEAR WELLBORE

A Thesis

by

JOSE GILBERTO CARBALLO SALAS

Submitted to the Office of Graduate Studies of
Texas A&M University
in partial fulfillment of the requirements for the degree of

MASTER OF SCIENCE

Approved as to style and content by:

_____	_____
William D. McCain Jr. (Chair of Committee)	W. John Lee (Member)
_____	_____
Robert R. Berg (Member)	Stephen A. Holditch (Head of Department)

December 2004

Major Subject: Petroleum Engineering

ABSTRACT

Alleviation of Effective Permeability Reduction of Gas-Condensate due to Condensate Buildup Near Wellbore. (December 2004)

José Gilberto Carballo Salas, B.S.,

Universidad Simon Bolivar, Venezuela

Chair of Advisory Committee: Dr. William D. McCain Jr.

When the reservoir pressure is decreased below dew point pressure of the gas near the wellbore, gas-condensate wells start to decrease production because condensate is separated from the gas around the wellbore causing a decrease in gas relative permeability. This effect is more dramatic if the permeability of the reservoir is low. The idea proposed for reducing this problem is to eliminate the irreducible water saturation near the wellbore to leave more space for the gas to flow and therefore increase the productivity of the well. In this research a simulation study was performed to determine the range of permeabilities where the cylinder of condensate will seriously affect the well's productivity, and the distance the removal of water around the wellbore has to be extended in order to have acceleration of production and an increase in the final reserves.

A compositional-radial reservoir was simulated with one well in the center of 109 grids. Three gas-condensate fluids with different heptanes plus compositions (4, 8 and 11 mole %), and two irreducible water saturations were used. The fitting of the Equation of State (EOS) was performed using the method proposed by Aguilar and McCain. Several simulations were performed with several permeabilities to determine the permeabilities for which the productivity is not affected by the presence of the cylinder of condensate.

At constant permeability, various radii of a region of zero initial water saturation around the wellbore were simulated and comparisons of the effects of removal of irreducible water on productivity were made.

Reservoirs with permeabilities lower than 100 mD showed a reduction in the ultimate reserves due to the cylinder of condensate. The optimal radius of water removal

depends on the fluid composition and the irreducible water saturation of the reservoir. The expected increase in reserves due to water removal varies from 10 to 80 % for gas production and from 4 to 30% for condensate production.

DEDICATION

I kindly dedicate this thesis:

To my beautiful and wonderful wife Maria, for all her support, patience and love,

To my parents, and

To God.

ACKNOWLEDGEMENTS

In this section I would like to thank all the people that contributed to realization of this thesis to:

- Dr W. McCain Jr.: for all the knowledge and guidance and also for being an example of academic excellence.
- My wife Maria: for giving me important advice and ways to improve the thesis.
- Dr T. Blasingame: for being the right help at the right time during my studies**.**
- Dr J. Lee and Dr R. Berg**:** for being part of my committee.
- All the professors, staff and friends of the petroleum department: for their knowledge and help during the last two years.

TABLE OF CONTENTS

CHAPTER Page

LIST OF TABLES

Page

LIST OF FIGURES

Page

Page

Page

CHAPTER I

INTRODUCTION

Gas-condensate reservoirs have fluid behavior that differs from oil reservoirs. Gas condensates are present as a single-phase gas when the reservoir pressure exceeds the dew point pressure of the gas. When the reservoir is produced and the pressure decreases the heaviest components of the fluid will form a liquid phase, condensate, which does not flow to the wellbore

Even when the average reservoir pressure is above the dew point pressure, near the wellbore there is a zone where the pressure is below the dew point pressure of the gas; in this zone the gas will drop part of its liquids before entering the wellbore. This region is called "near wellbore condensate deposition" or "condensate cylinder". This cylinder of condensate decreases severely the gas relative permeability around the wellbore. Thus the productivity of the gas is severely reduced.

Deddy, *et al.* (1994)[1] define in their work that the near wellbore condensate accumulation is an "extremely important factor" explaining the reasons for some wells productivities being reduced by 50%.

Barnum, *et al.* (1995)[2] found that the condensation of hydrocarbon liquids can severely restrict the gas productivity, and that the gas recoveries are expected to be below 50% of the original gas in place.

One of the ideas to improve the productivity of the gas-condensate wells is to eliminate the water saturation around the wellbore in order to leave more space for the gas and the condensate to flow. This study is a reservoir simulation to determine the permeability at which the cumulative gas production will be affected by this cylinder of condensate and also to evaluate the effect of the removal of the water saturation near the wellbore. When the water is removed the reservoir will have 2 regions;

This thesis follows the style and format of the *Journal of Petroleum Technology.*

a treated region near the wellbore up to a certain diameter and the normal reservoir outside this region.

This study provides the theoretical support for use in the design of this process in field practice.

1.1 Research Objectives

The main objectives of this research are:

1. Determine the permeability limit for which the gas condensate cylinder will not affect the cumulative production of the reservoir.

2. Determine the optimum radius of treatment for three different fluids and two different irreducible water saturations, and quantify the associated increase in cumulative production.

CHAPTER II

LITERATURE REVIEW

Several methods have been proposed for improving well productivity for gas-condensate wells.

Dehane, *et al.* (2000)[3] discussed that horizontal wells reduced the pressure drawdown (compared to a vertical well); this reduction in the drawdown reduces the amount of condensation of liquids around the wellbore. The problem with this approach is that the drawdown of the well has to be controlled from the wellhead. It also has the problem that in reservoirs with poor or no pressure maintenance, when the average reservoir pressure is below the dew point the problem of liquid condensation will still exist.

Wang, *et al.* (2000)[4] studied the behavior of hydraulic fracturing in gas condensate wells and concluded that the liquid deposition around the wellbore in low permeability reservoirs is a factor that can greatly reduce the well productivity index. They stated that liquid deposition will increase the length of the fracture necessary to have the same value of production. Once again in hydraulic fracturing the idea is to reduce the pressure drawdown of the near wellbore formation in order to avoid liquid deposition.

Tarek, *et al.* (2000)[5] studied the effectiveness of injecting lean gas, nitrogen and carbon dioxide (CO_2) using a huff'n puff injection technique to remove the liquid deposition near the wellbore. The results of this study show that the gases injected can actually increase the liquid deposition around the wellbore. Large quantities of gases must be injected in order to assure liquid evaporation. Those amounts depend on the pressure of the reservoir, the liquid content of the gas, and the composition of the injection fluid. The study concluded that the huff 'n puff method is a viable option because it might reduce the liquid saturation near the wellbore but no dynamic study was presented to explain how often the treatment must be performed.

Jamaludin, *et al.* (2001)[6] concluded that a mixture of CO_2 and propane has the ability to vaporize the condensate liquids near the wellbore.

Du, *et al.* (2000)[7] studied the use of solvents to improve the productivity of gas-condensate reservoirs, in studies performed with cores they showed that methanol injection can substantially improve the gas relative permeability because of the miscible displacement of the water and condensate. Further, the beneficial effects of the methanol injection are more pronounced with high initial water saturations. In addition, this method is less expensive than alternatives such as hydraulic fracturing.

Al-Anazi, *et al.* (2000)[8] showed a field test of a methanol treatment in the Hatter's Pond field where the injection of 1000 barrels of methanol caused an increased in production by 100% the first four months and 50% thereafter, the improvement is explained to be due to the water and condensate removal near the wellbore.

El-Banbi and McCain (2000)[9] described the process of the formation of the cylinder of condensate and showed how the relative permeabilities of gas and liquid change with time in the reservoir. This paper shows that near the wellbore the condensate concentration has a maximum at the beginning and then after the reservoir pressure decreases below the dew point pressure of the gas, the amount of condensate near the wellbore decreases.

CHAPTER III

DESCRIPTION OF THE RESERVOIR-SIMULATION PARAMETERS

3.1 Fitting of the EOS for Use in the Simulation

One of the most important steps in a compositional reservoir simulation is the tuning of the EOS. In this research the method used for this propose is the one proposed by Aguilar and McCain (2003)[10]. This method was chosen because it is a systematic and consistent way of performing the tuning. During matching of the volumetric data special attention was taken in matching the liquid saturation data from the constant volume depletion (CVD) test. This parameter has a very important effect in the results of the reservoir simulation. The fluid compositions of the three fluids studied are given in **Table 3.1**.

Table 3.1 Molar Composition of the Studied Fluids

	Fluid A Mole Fraction	Fluid B Mole Fraction	Fluid C Mole Fraction
H2S	0.0394	0.0017	0.0000
N2	0.1086	0.0752	0.0030
CO2	0.0238	0.0131	0.0435
C1	0.6643	0.6565	0.6255
C2	0.0650	0.0819	0.0999
C3	0.0281	0.0414	0.0500
IC4	0.0052	0.0075	0.0131
NC4	0.0103	0.0180	0.0220
IC5	0.0032	0.0065	0.0103
NC5	0.0034	0.0078	0.0093
C6	0.0057	0.0100	0.0147
C7+	0.0430	0.0804	0.1087

3.1.1 Match of Fluid A Data (4 mole % C7+)

Fig. 3.1 to Fig. 3.5 present the match of the data obtained for fluid A, The points represent the laboratory data and the line represents the behavior calculated with the tuned EOS.

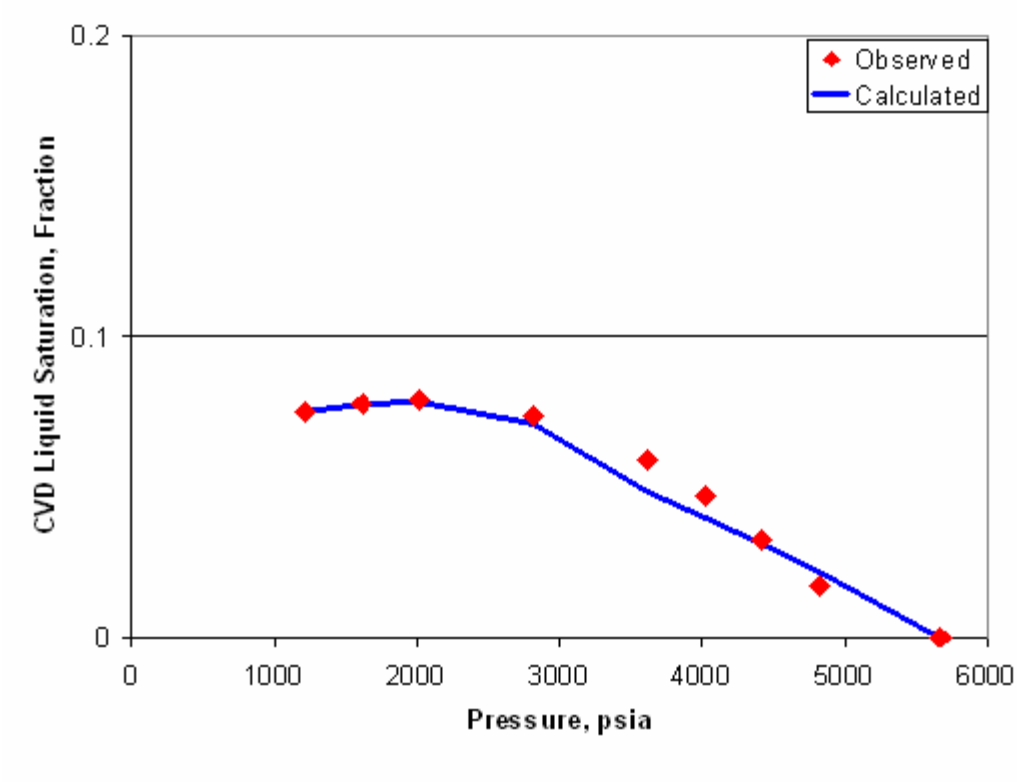

Fig. 3.1 CVD Liquid Saturation for Fluid A (4 mole % C7+)

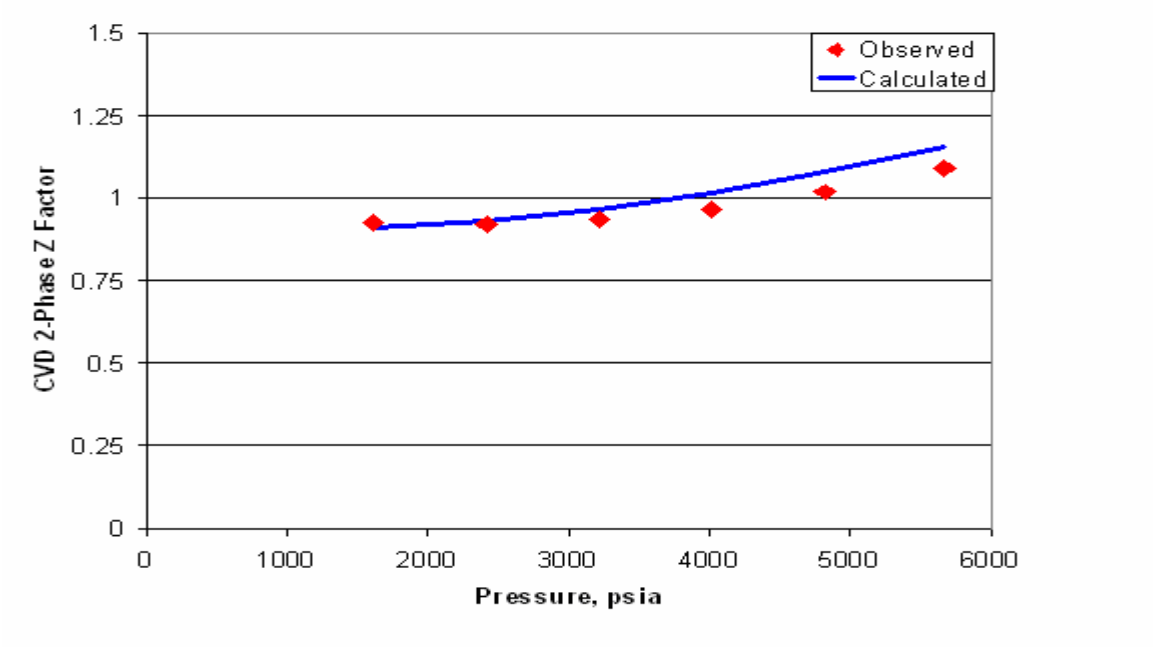

Fig. 3.2 CVD 2 Phase Z Factor for Fluid A (4 mole % C7+)

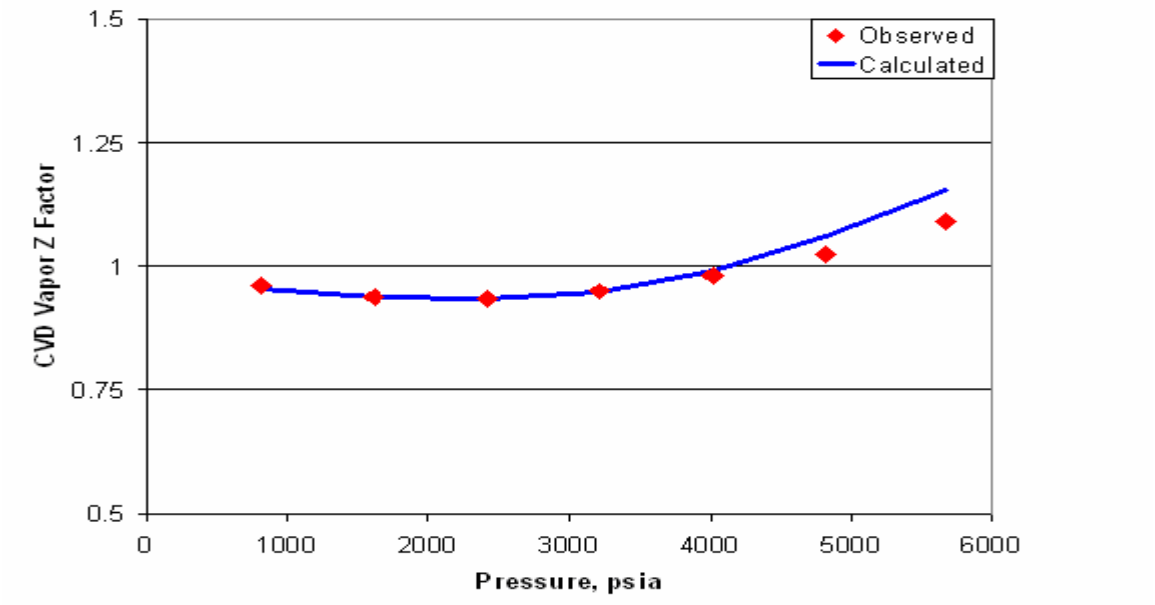

Fig. 3.3 CVD Vapor Z Factor for Fluid A (4 mole % C7+)

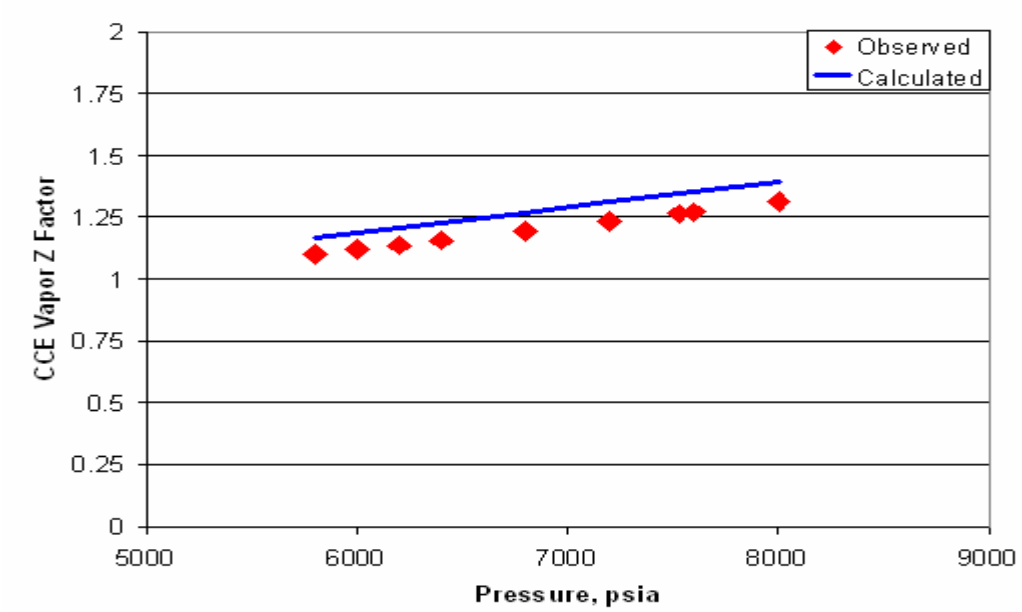

Fig. 3.4 CCE Vapor Z Factor for Fluid A (4 mole % C7+)

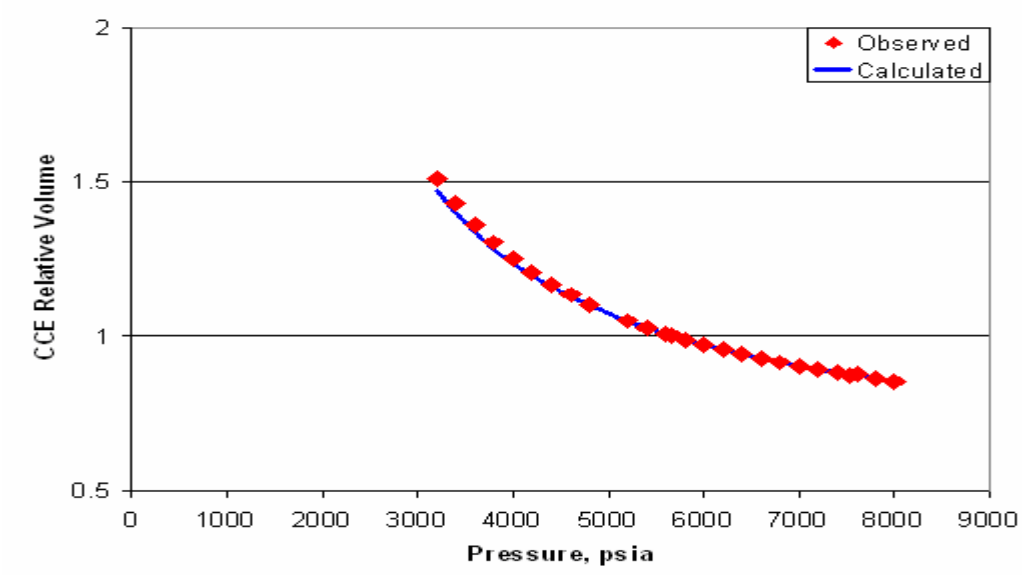

Fig. 3.5 CCE Relative Volume for Fluid A (4 mole % C7+)

3.1.2 Match of Fluid B Data (8 mole % C7+)

Fig. 3.6 to **Fig. 3.10** present the match of the data obtained for fluid B, The points represent the laboratory data and the line represents the behavior calculated with the tuned EOS.

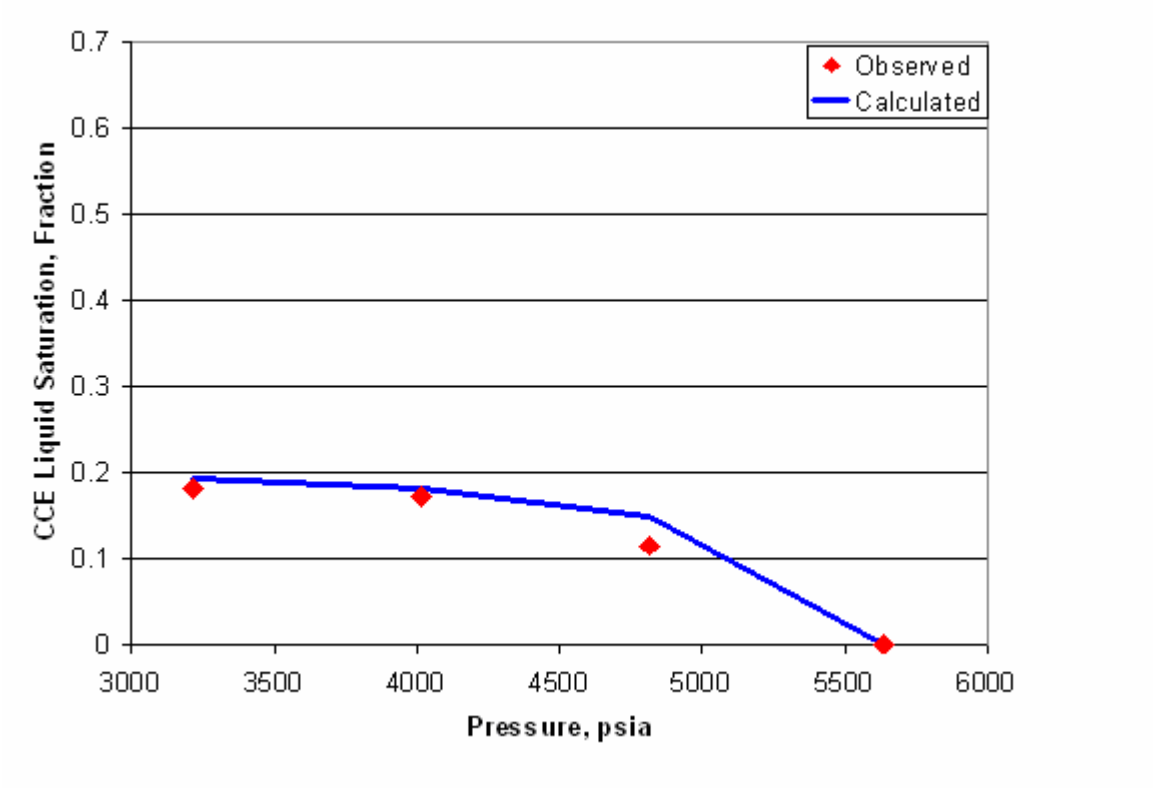

Fig. 3.6 CCE Liquid Saturation for Fluid B (8 mole % C7+)

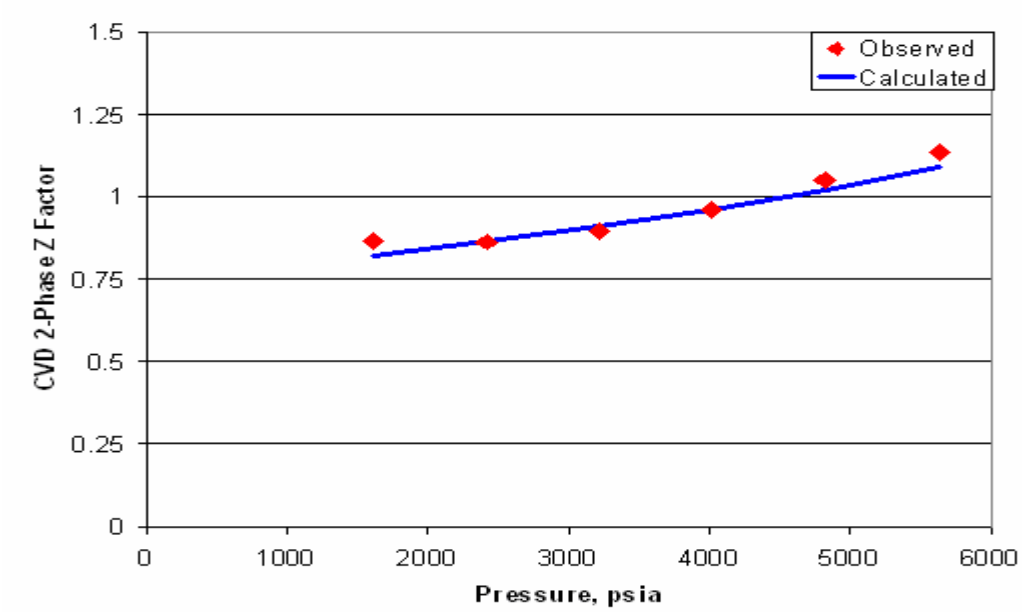

Fig. 3.7 CVD 2 Phase Z Factor for Fluid B (8 mole % C7+)

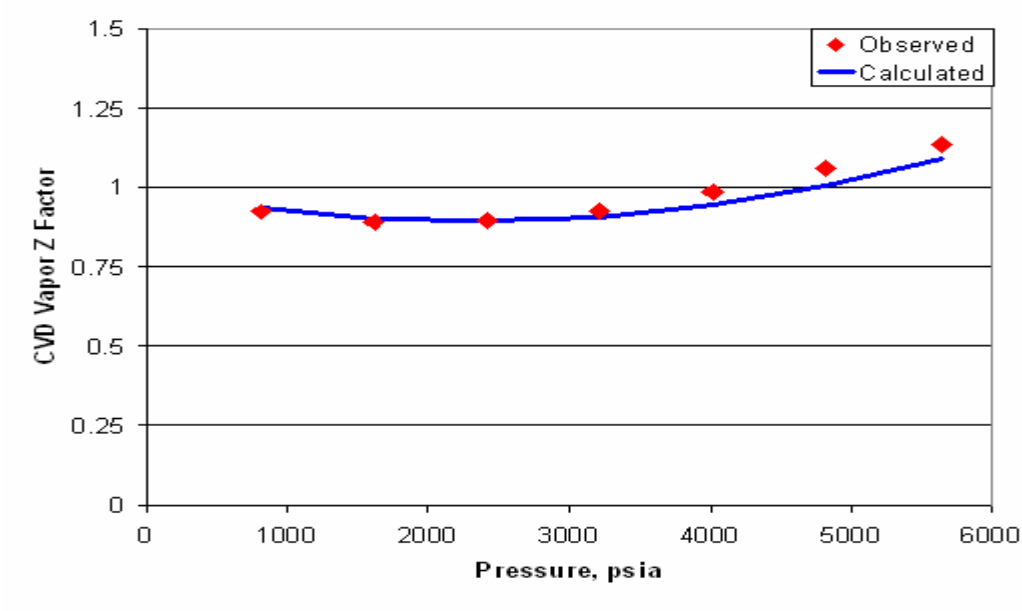

Fig. 3.8 CVD Vapor Z Factor for Fluid B (8 mole % C7+)

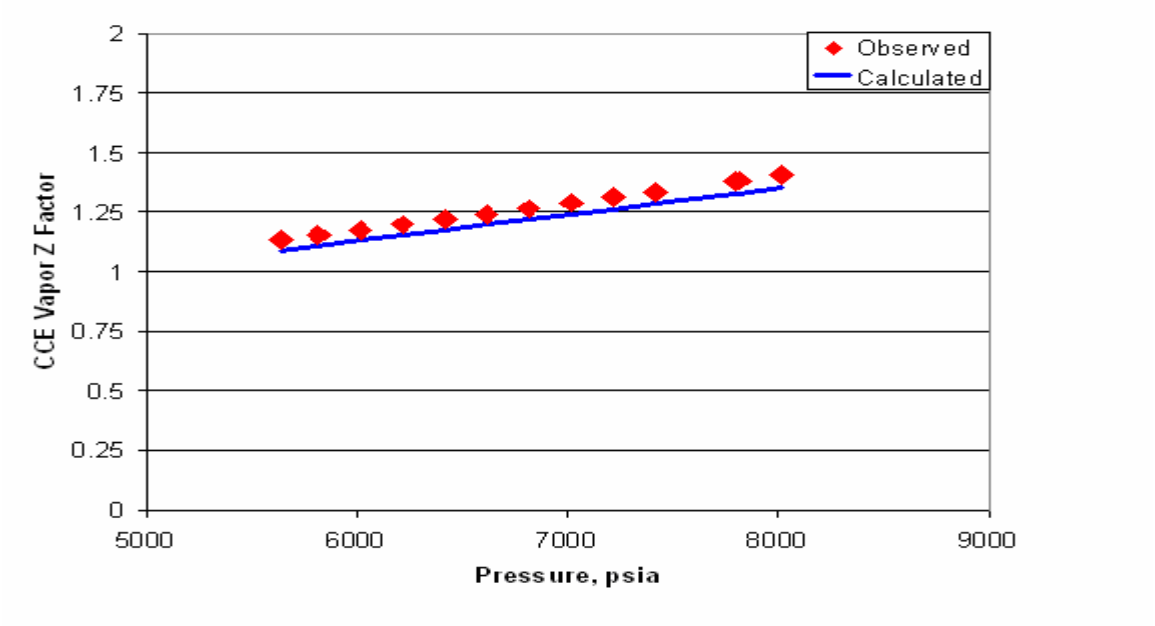

Fig. 3.9 CCE Vapor Z Factor for Fluid B (8 mole % C7+)

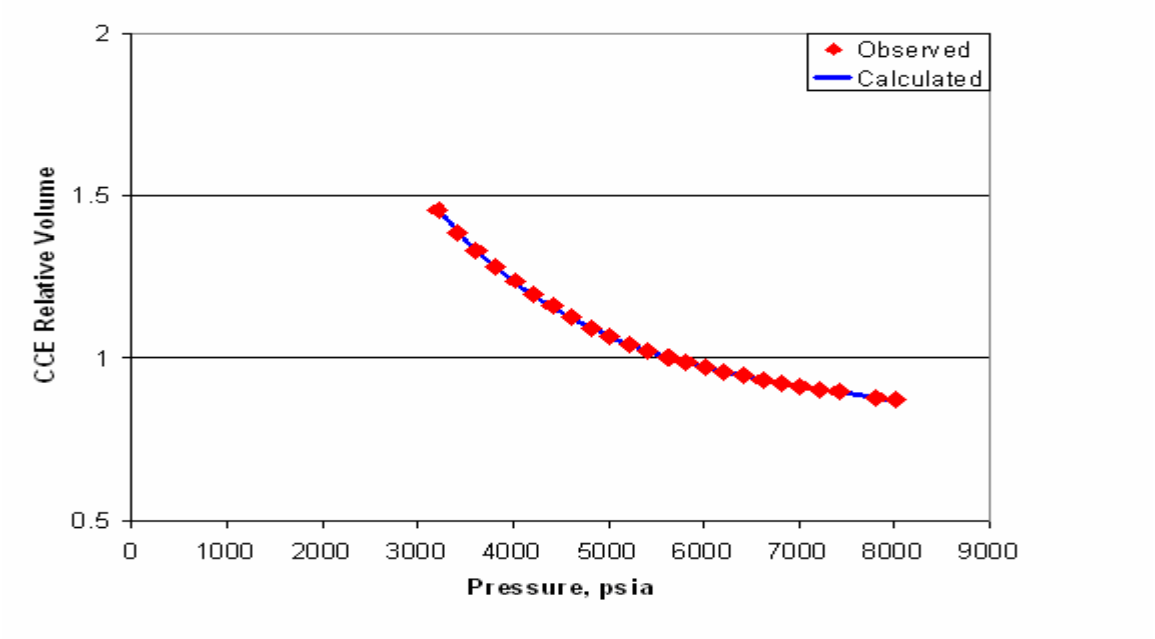

Fig. 3.10 CCE Relative Volume for Fluid B (8 mole % C7+)

3.1.3 Match of Fluid C Data (11 mole % C7+)

Fig. 3.11 to **Fig 3.15** present the match of the data obtained for fluid C, The points represent the laboratory data and the line represents the behavior calculated with the tuned EOS.

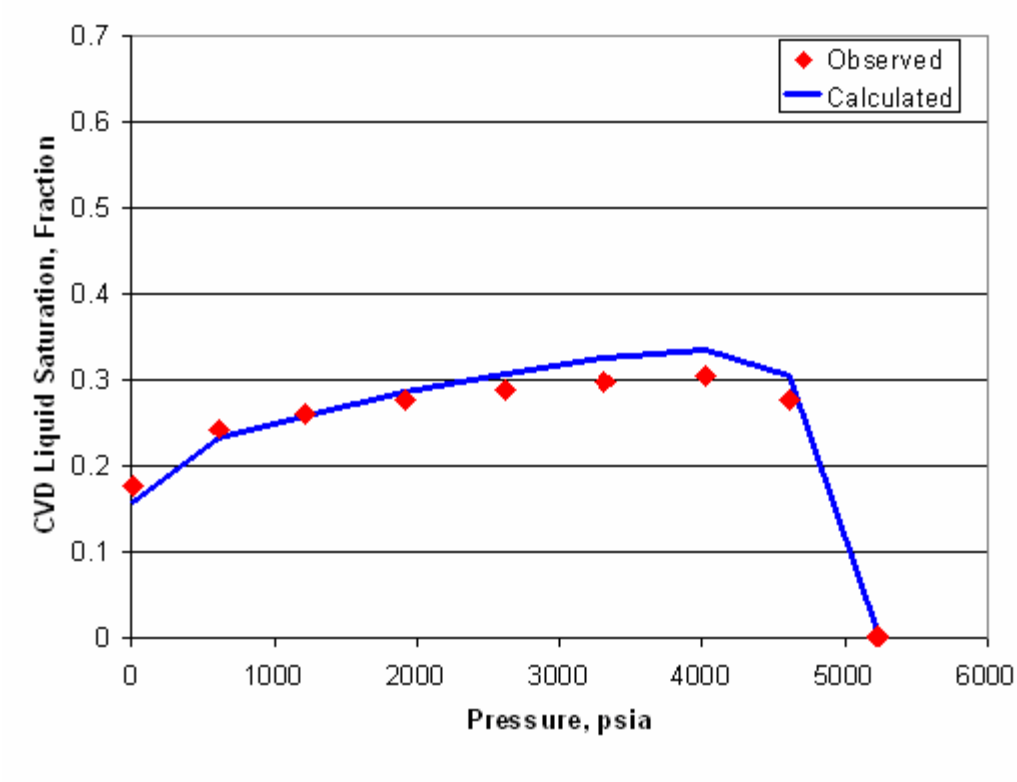

Fig. 3.11 CVD Liquid Saturation for Fluid C (11 mole % C7+)

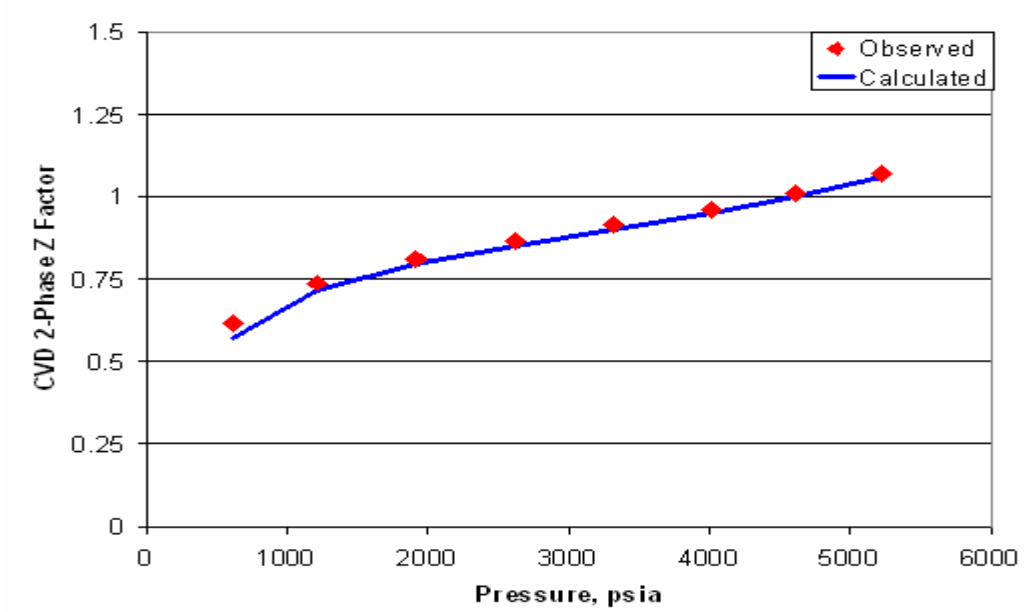

Fig. 3.12 CVD 2 Phase Z Factor for Fluid C (11 mole % C7+)

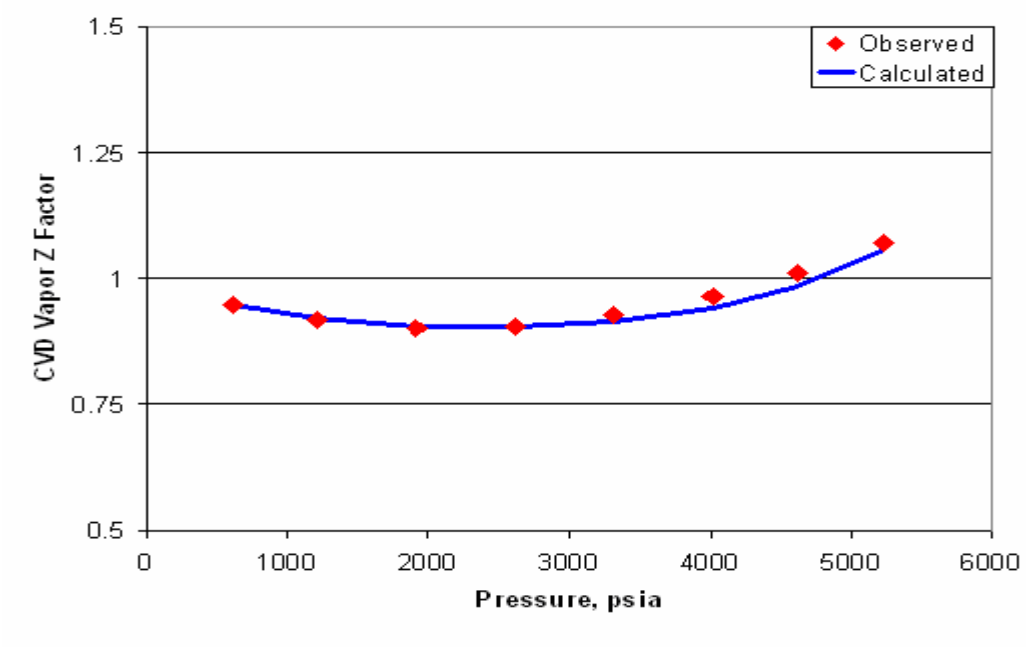

Fig. 3.13 CVD Vapor Z Factor for Fluid C (11 mole % C7+)

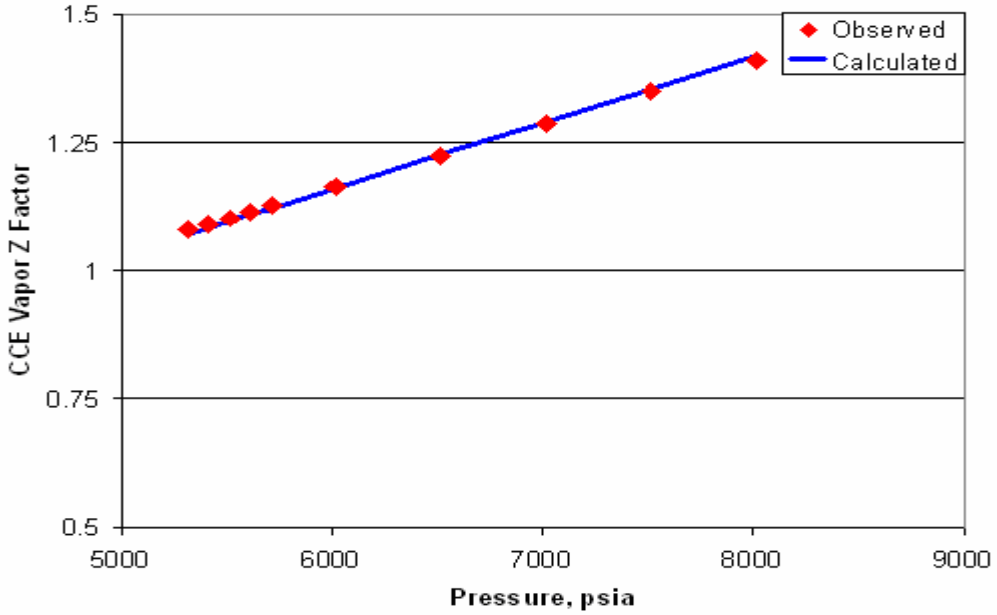

Fig. 3.14 CCE Vapor Z Factor for Fluid C (11 mole % C7+)

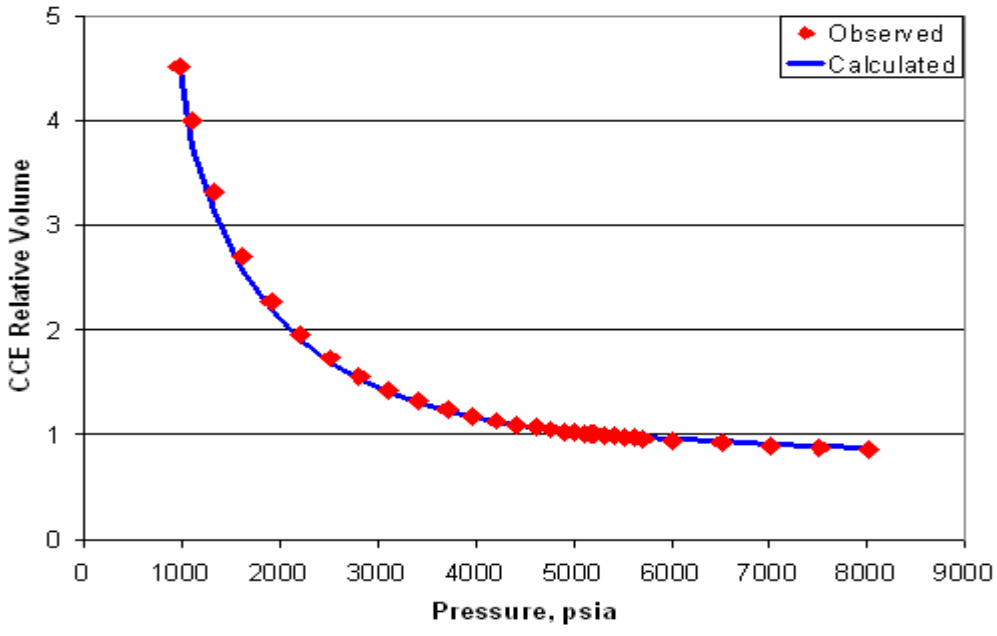

Fig. 3.15 CCE Relative Volume for Fluid C (11 mole % C7+)

3.2 Rock Property Data Used in the Simulation

Two sets of rock-property data were used: one for an irreducible water saturation of 20% and another for 41%. In order to generate the rock property data for the treated zone, the permeability curves of the reservoir were extrapolated until reaching zero irreducible water saturation. The process will be explained in the following section.

3.2.1 Irreducible Water Saturation of 41 %

The following figures present the rock curves used in the reservoir simulation for the case in which the irreducible water saturation is 41%.

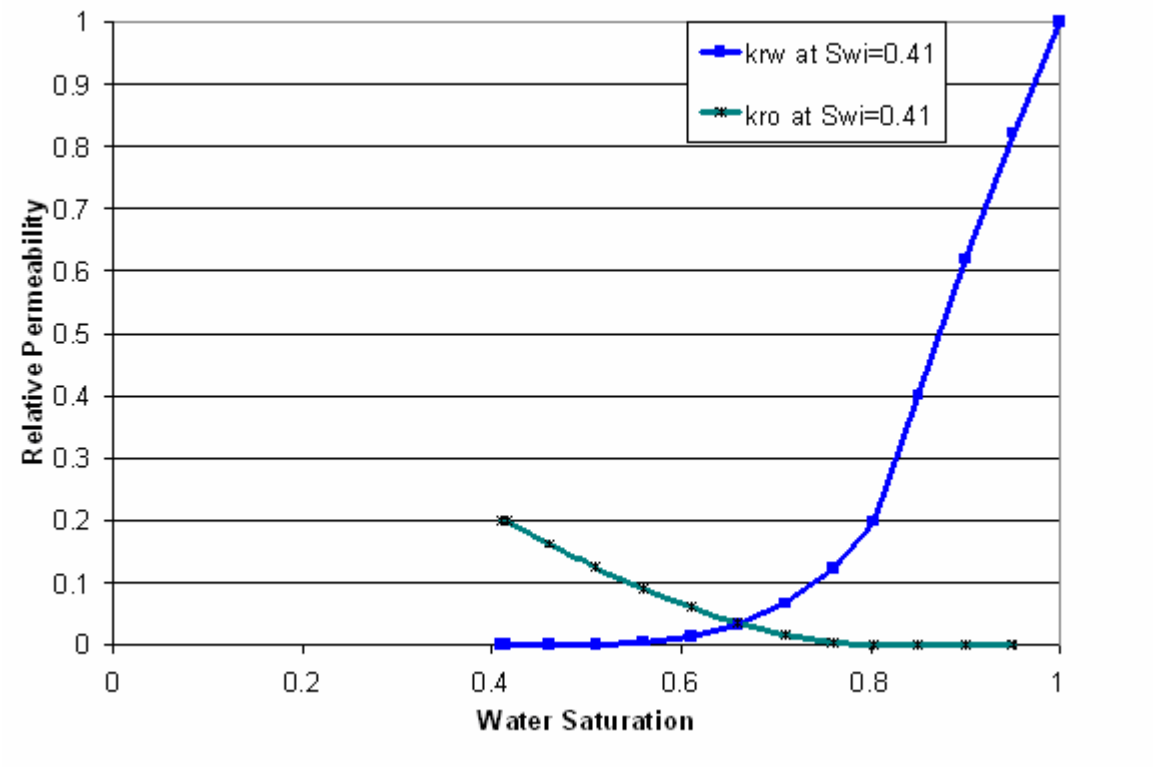

Fig. 3.16 Oil and Water Relative Permeability curves Swi=0.41

Fig. 3.16 presents the oil and water relative permeability curves for the case of irreducible water saturation equal to 0.41. Notice that krow= 0.2 at the maximum oil saturation.

The data of Fig 3.16 can be used to make a curve of relative permeability to oil versus oil saturation, this curve is presented in the **Fig. 3.17** where we can find in green the data presented in Fig. 3.16. The red points are the extrapolation made from the oil relative permeability which are going to be used in the treated region (Swi=0).

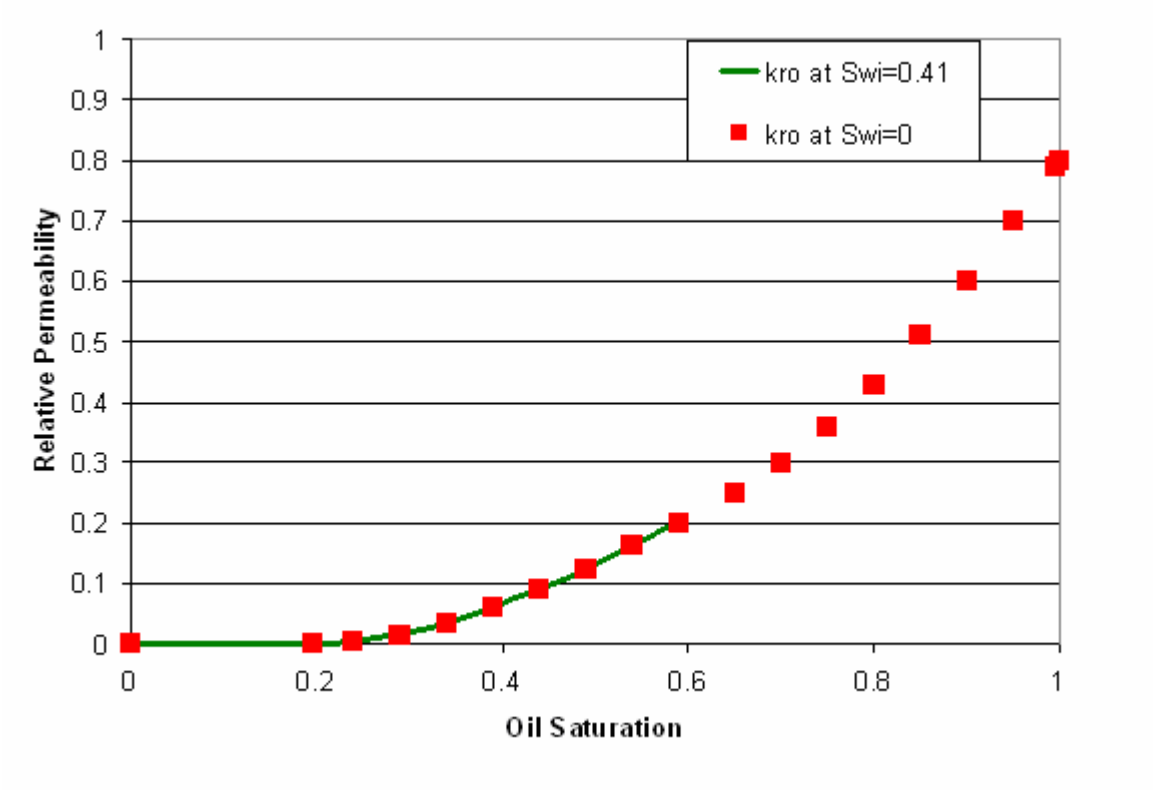

Fig. 3.17 Oil Relative Permeability Curves vs Oil Saturation for Swi=0.41 and Swi=0

Fig. 3.17 shows, as in Fig. 3.16, that the minimum oil saturation to flow is 0.2 and that the curve passes through 0.2 at the maximum oil saturation (Somax=0.59), it also shows in red the extrapolation to kro=0.8 for the new maximum oil saturation (new

Somax=1). These data will be used to create the relative permeability curve for the water free zone.

Fig. 3.18 presents the relative permeabilities of oil and water for the treated region (Swi=0).

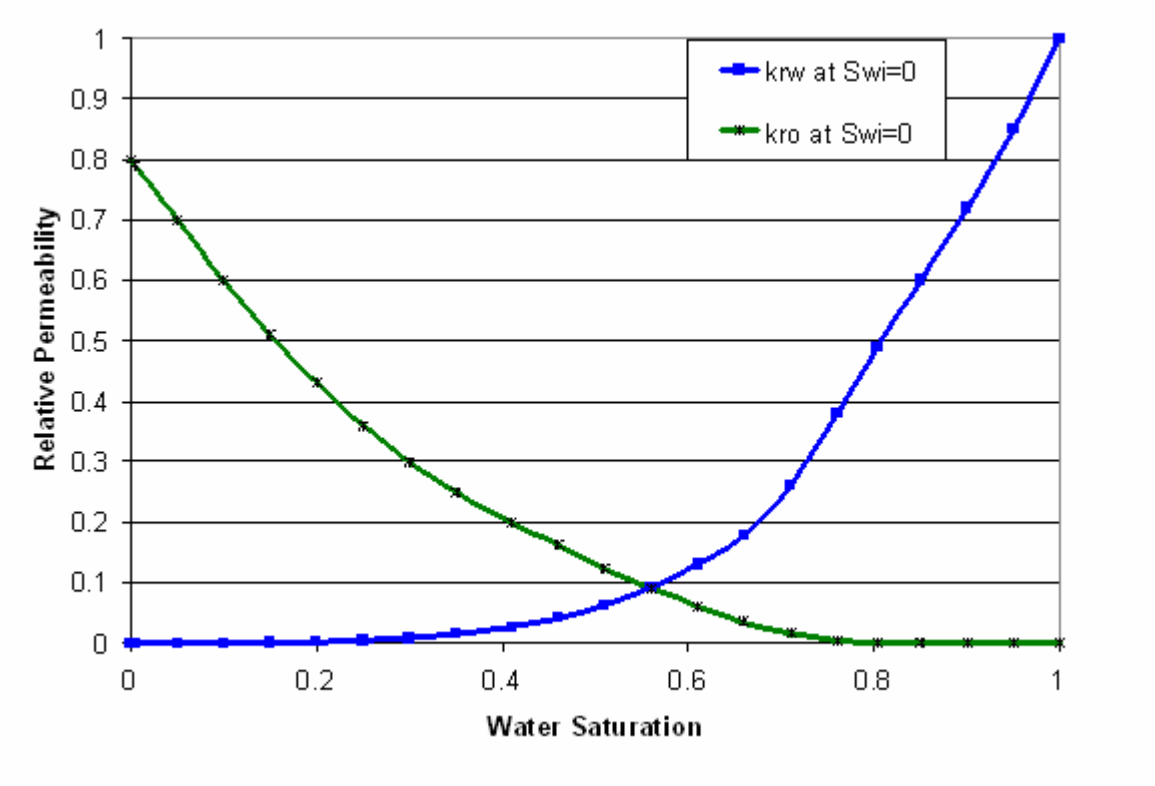

Fig. 3.18 Oil and Water Relative Permeability curves for the treated zone (Swi=0) of the reservoir at Swi=0.41

Fig. 3.19 presents the oil and gas relative permeability curves vs gas saturation at Swi=0.41.

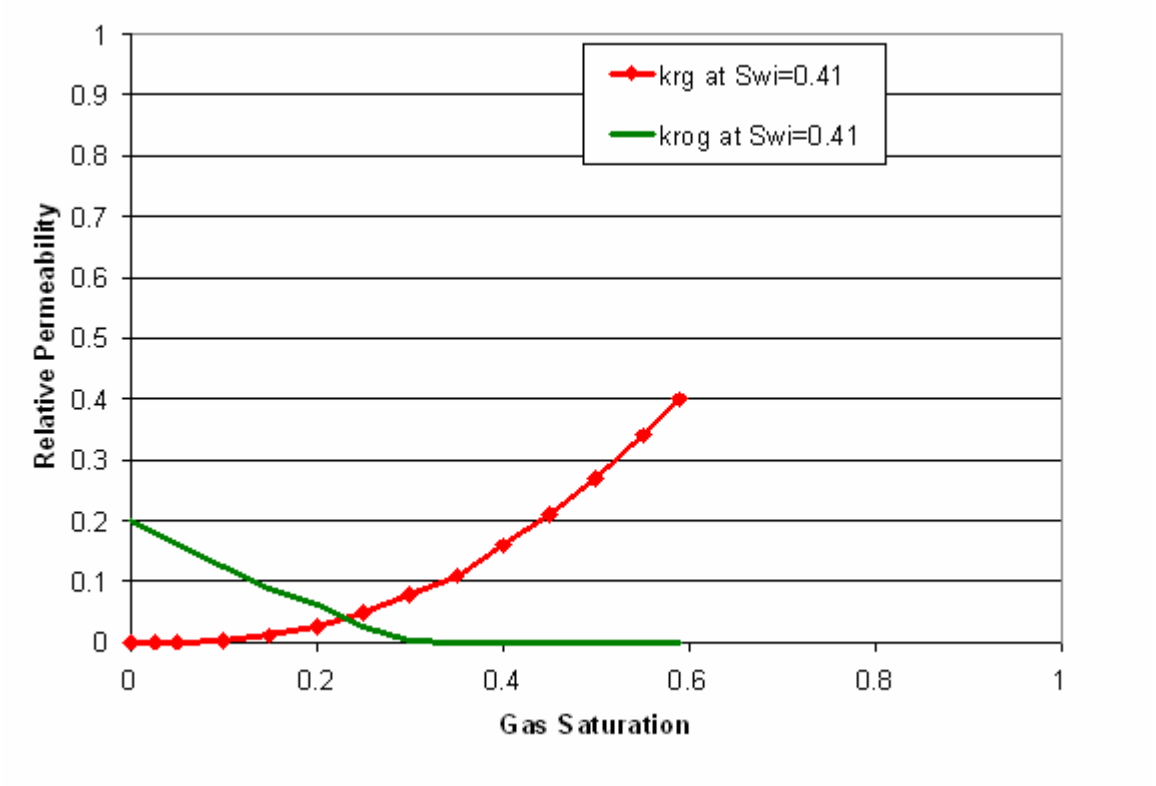

Fig. 3.19 Oil and Gas Relative Permeability Curves at Swi=0.41

Fig. 3.19 shows that at the maximum oil saturation, krog=0.2 as expected from Fig. 3.16 and at maximum gas saturation, krg= 0.4, The curves start from 0.59 which corresponds to 1-Swi. From these curves a graph of the krog versus oil saturation was prepared.

Fig 3.20 presents the oil relative permeability in gas (krog) vs oil saturation for the case of Swi=0.41 in green and also presents the extrapolation for the case of Swi=0 in red.

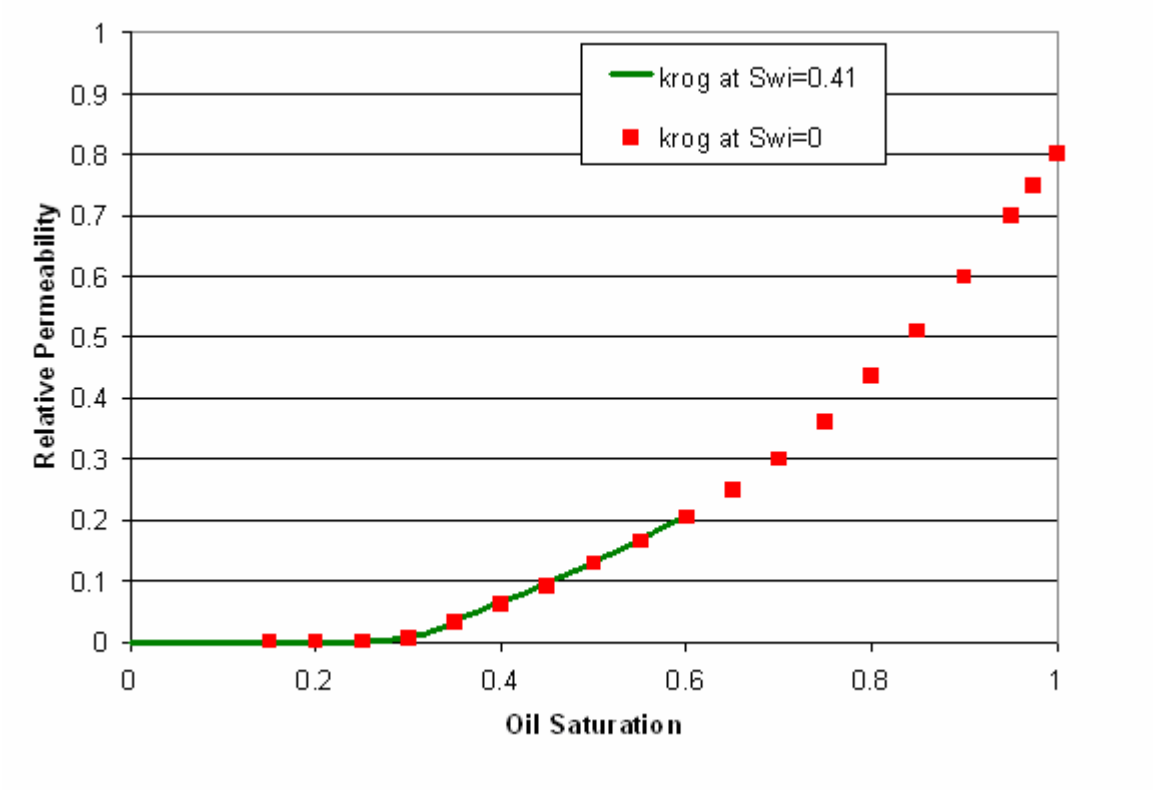

Fig. 3.20 Oil in Gas Relative Permeability Curves vs Oil Saturation

Fig. 3.20 shows that at the maximum oil saturation krog=0.8 as expected from Fig. 3.17.

Fig. 3.21 presents the relative permeabilities of oil and gas for the treated region (Swi=0).

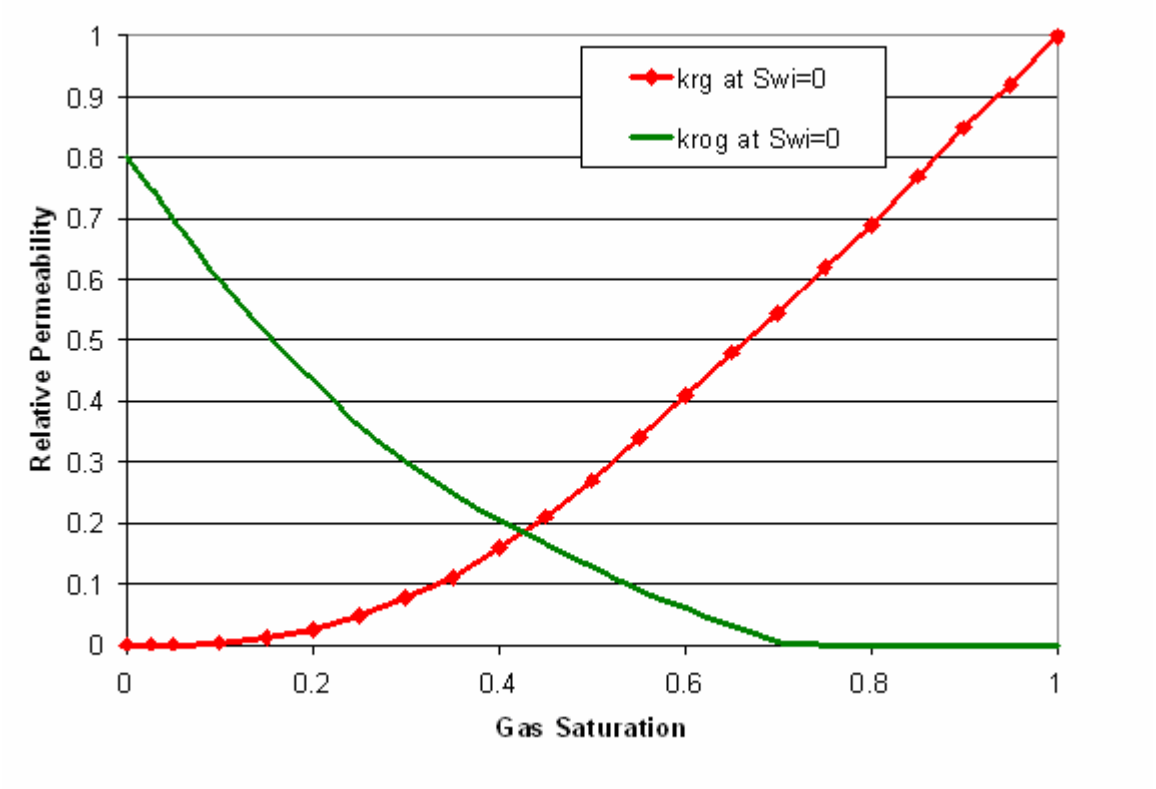

Fig. 3.21 Oil and Gas Relative Permeability Curves for the Treated Zone (Swi=0) of the Reservoir at Swi=0.41

Fig. 3.21 shows that the graph starts from 0 and ends at 1. The krg curve was extrapolated to one and the krog curve was extrapolated. It can also be seen that the oil relative permeability curve has an end point of 0.8 at the maximum oil saturation which is consistent with Fig 3.18.

Fig 3.22 shows in green the capillary pressure curves used in the region of Swi=0.41 and in blue the capillary pressure curves used in the treated zone (Swi=0).

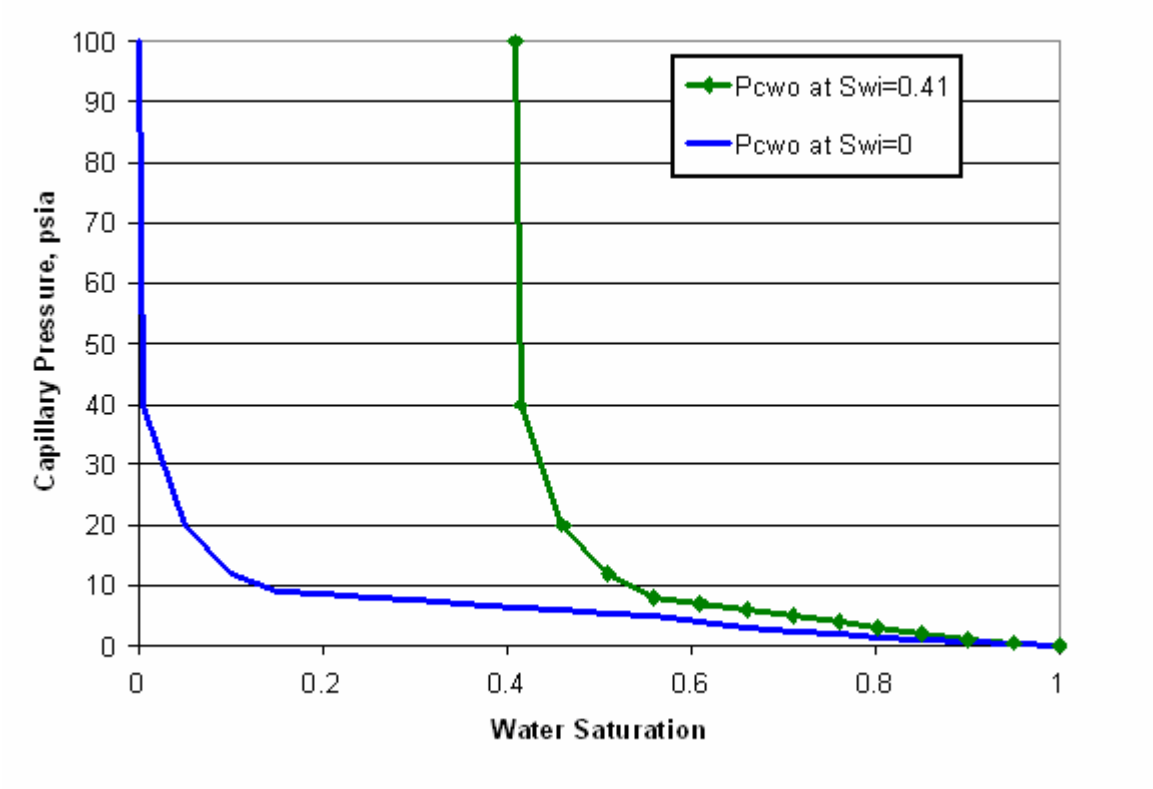

Fig. 3.22 Capillary Pressure Curves at Swi=0.41 and its Treated Zone (Swi=0)

3.2.2 Irreducible Water Saturation of 20 %

The following figures present the relative permeability and capillary pressure data used in the reservoir simulation for the case in which the irreducible water saturation is 20 %, with its corresponding water-free zone.

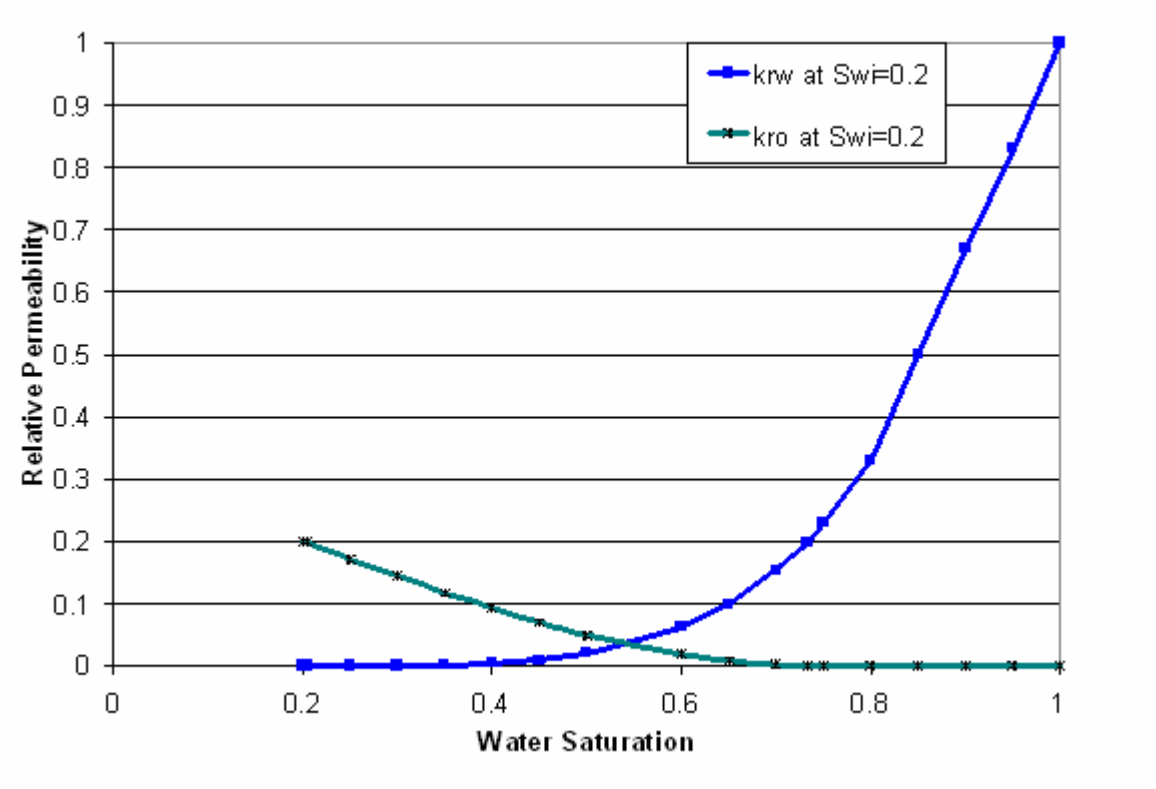

Fig. 3.23 Oil and Water Relative Permeability Curves at Swi=0.2

Fig. 3.23 presents the oil and water relative permeability curves for the case of irreducible water saturation equal to 0.2. Notice that krow= 0.2 at the maximum oil saturation.

The data of Fig 3.23 can be used to create a curve of relative permeability to oil versus oil saturation; this curve is presented in the **Fig. 3.24** where on the green line are the data presented in Fig. 3.23. The red points are the extrapolation made from the oil relative permeability, these will be used in the treated region (Swi=0).

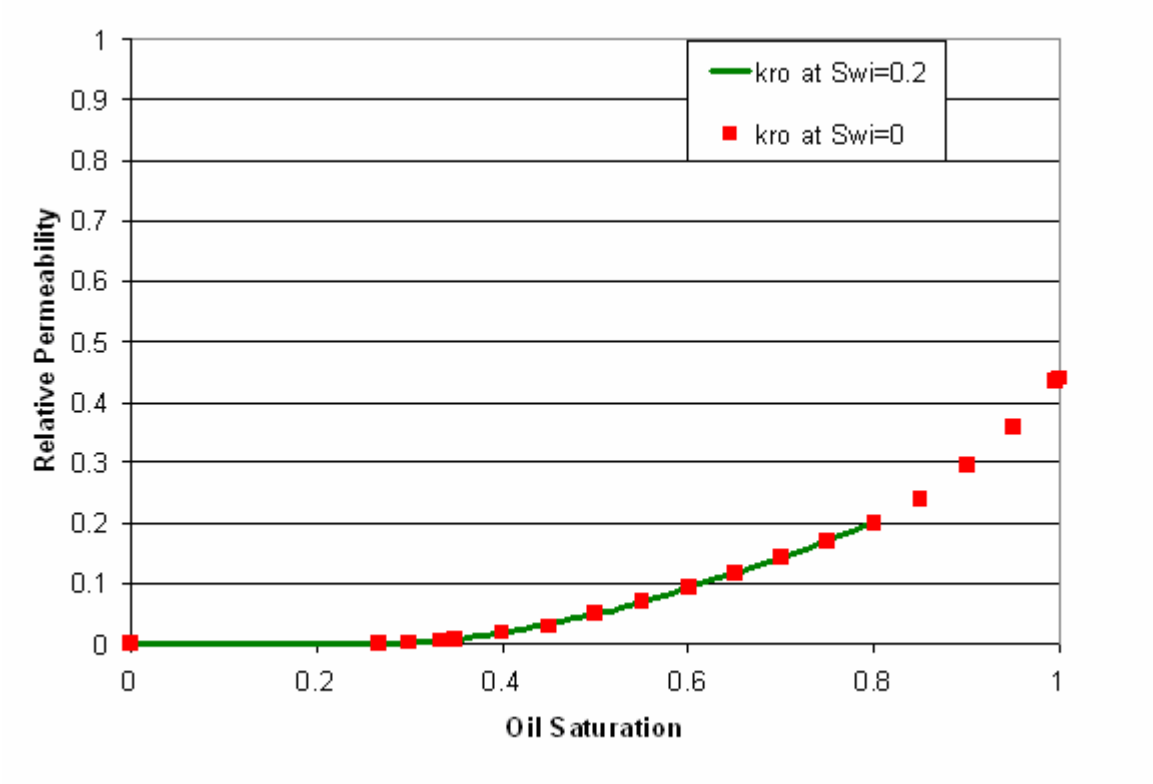

Fig. 3.24 Oil Relative Permeability Curves vs Oil Saturation for Swi=0.2 and Swi=0

Fig. 3.24 shows as in Fig. 3.23 that the minimum oil saturation to flow is 0.24 and that the oil curve passes through 0.2 at the maximum oil saturation (Somax=0.8), also shown in red is the extrapolation made to kro=0.44 for the new maximum oil saturation (Somax=1). These data will be used to create the relative permeability curve for the water free zone.

Fig. 3.25 presents the relative permeability of oil and water for the treated region (Swi=0).

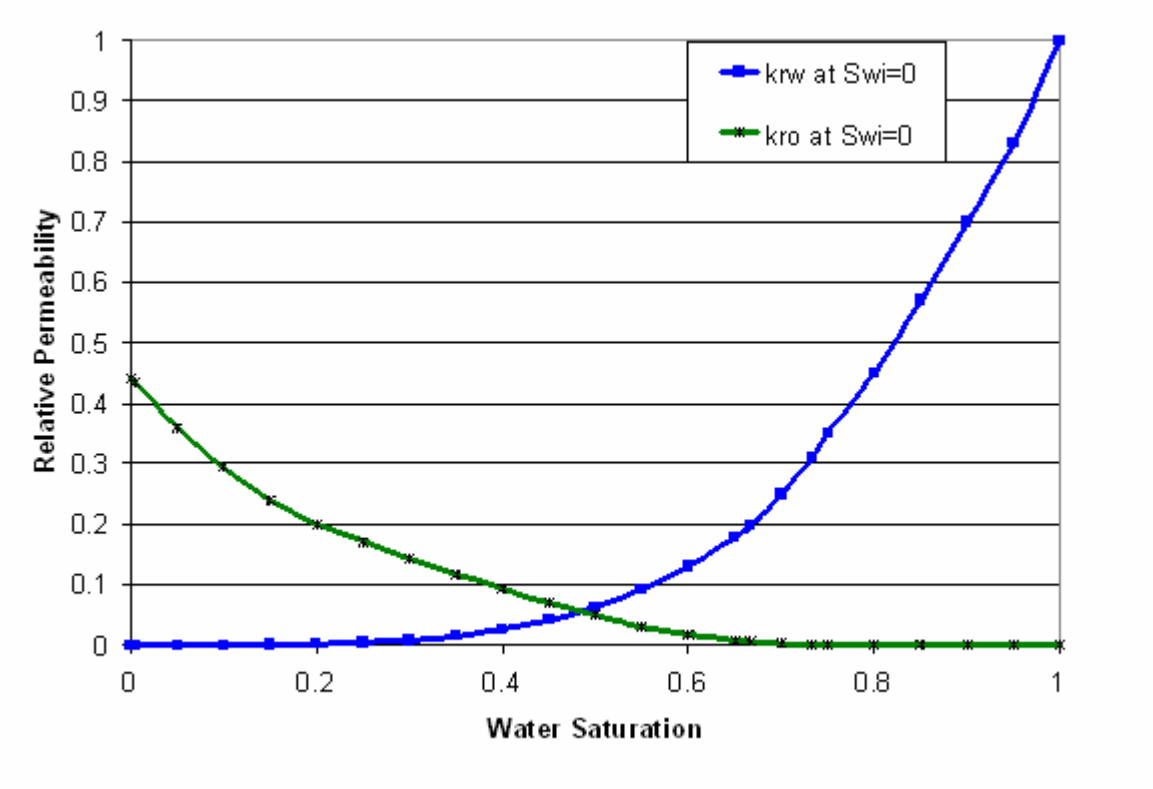

Fig. 3.25 Oil and Water Relative Permeability Curves for the Treated Zone (Swi=0)

Fig. 3.26 presents the oil and gas relative permeability curves vs gas saturation at Swi=0.2.

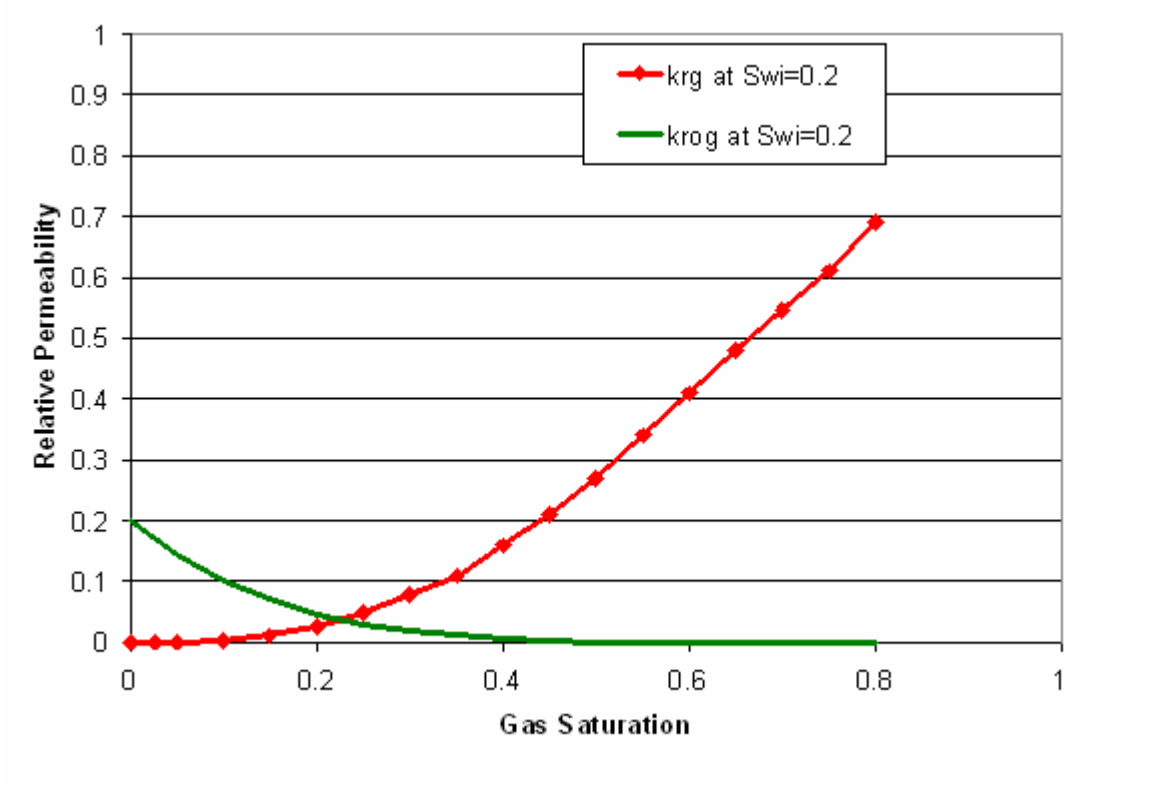

Fig. 3.26 Oil and Gas Relative Permeability Curves at Swi=0.2

It can be seen in Fig. 3.26 that at the maximum oil saturation krog=0.2 as expected from Fig. 3.23 and at the maximum gas saturation krg= 0.69. Also the curves start from 0.8 which corresponds to 1-Swi.

Fig 3.27 presents the oil relative permeability in gas (krog) vs oil saturation for the case of Swi=0.2 in green and also presents its extrapolation for the case of Swi=0 in red.

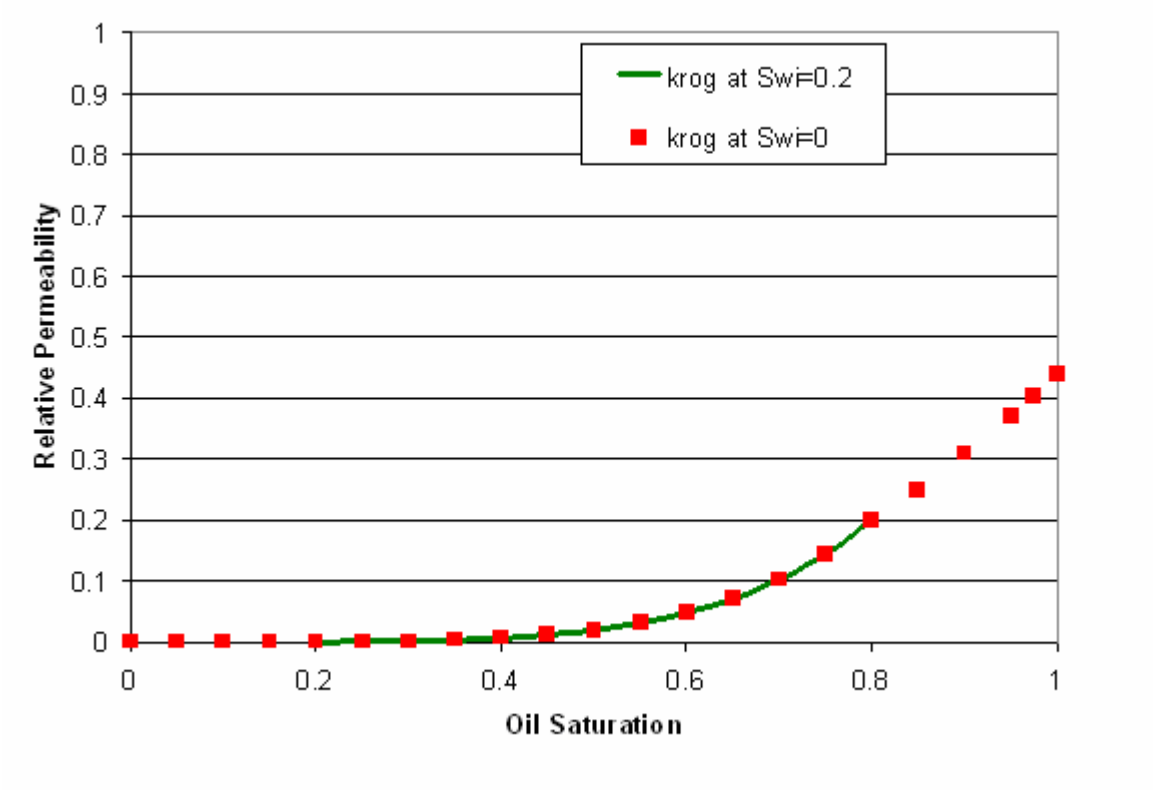

Fig. 3.27 Oil in Gas Relative Permeability Curves vs Oil Saturation

Fig 3.27 can be compared with Fig 3.26. The point of krog at the maximum oil saturation is equal to 0.44 as expected (for the water free zone).

Fig. 3.28 presents the relative permeability of oil and gas for the treated region (Swi=0).

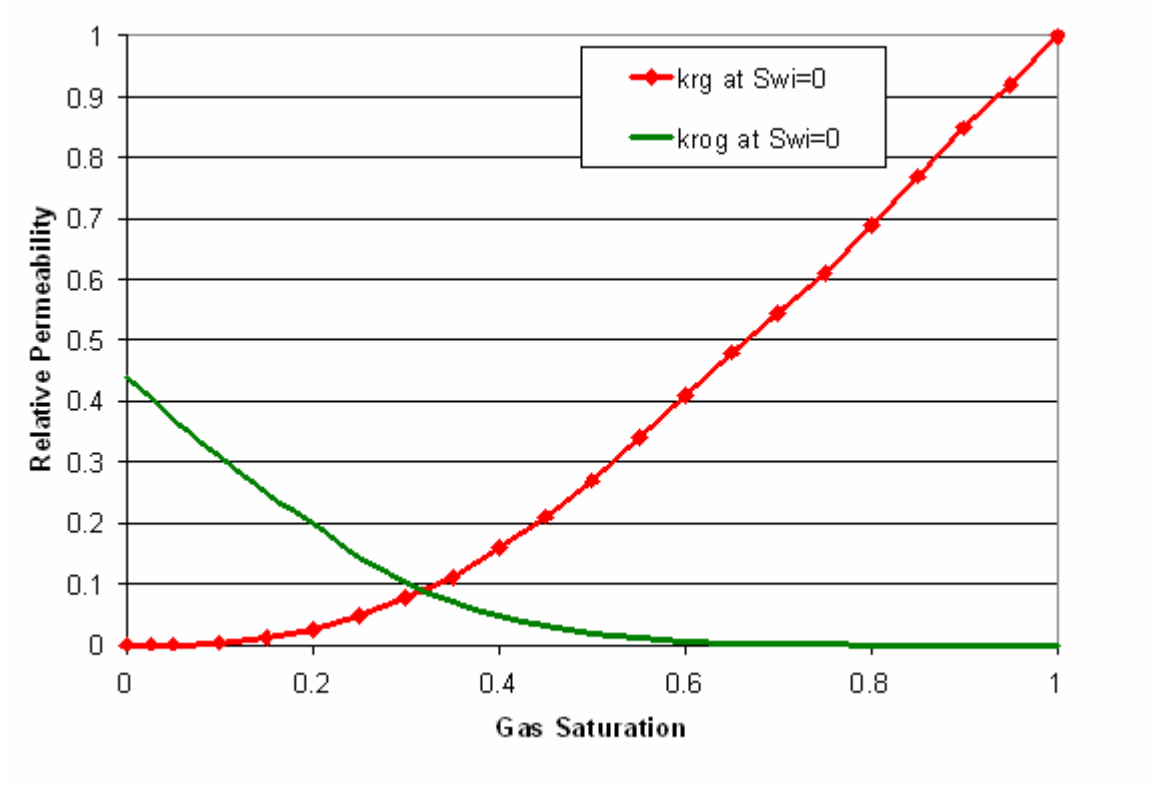

Fig. 3.28 Oil and Gas Relative Permeability Curves for the Treated Zone (Swi=0) of the Reservoir at Swi=0.2

Fig. 3.28 shows that the graph goes from 0 to 1. The krg curve was extrapolated to one and the krog curve was extrapolated and displaced to start at one. The krog curve has an end point of 0.44 at the maximum oil saturation which is consistent with Fig 3.25.

Fig 3.29 shows in green the capillary pressure curves used in the region of Swi=0.41 and in blue the capillary pressure curves used in the treated zone.

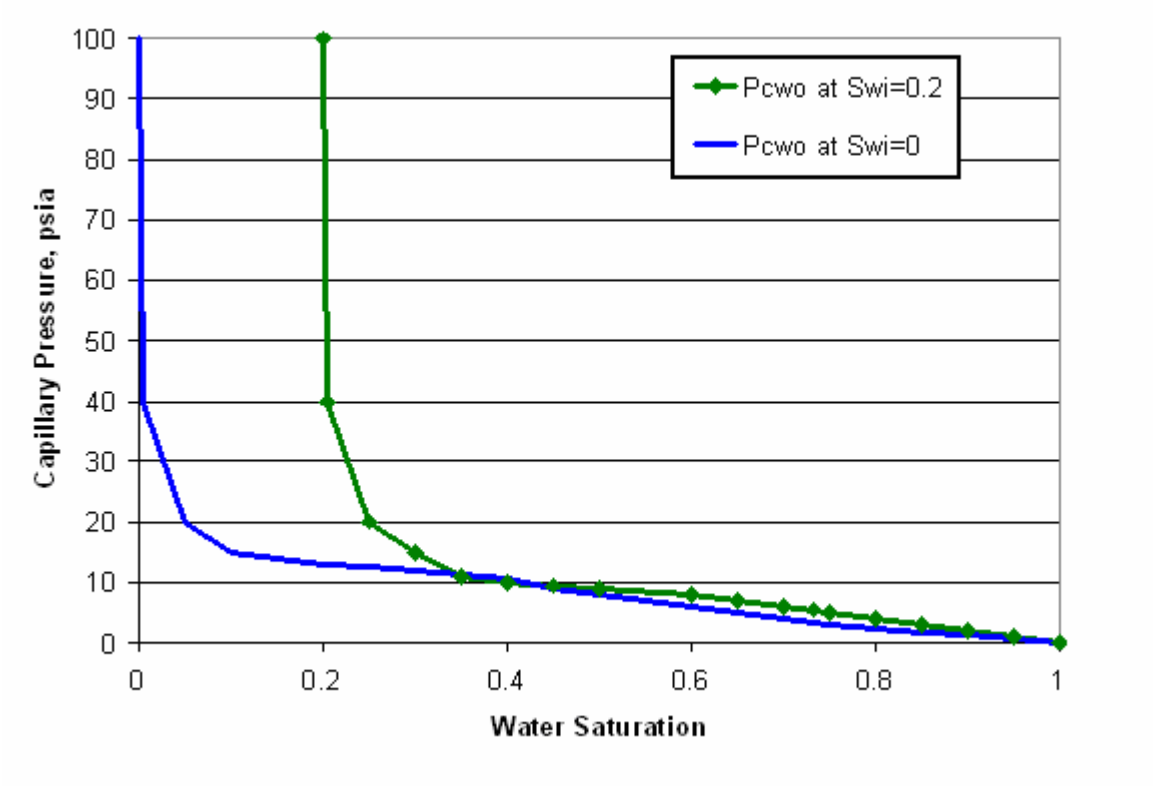

Fig. 3.29 Capillary Pressure Curves at Swi=0.2 and its Treated Zone (Swi=0)

3.3 Simulation Parameters

3.3.1 Grid

The grid selected to perform the simulation is a one layer radial 109 cell model, a picture of the grid is presented in **Fig. 3.30**

The grid follow a spacing approximately logarithmical, which means the grids are smaller near the wellbore and bigger far from the wellbore, the griding was not exactly logarithmical in order to facilitate the definition of the radius of treatment.

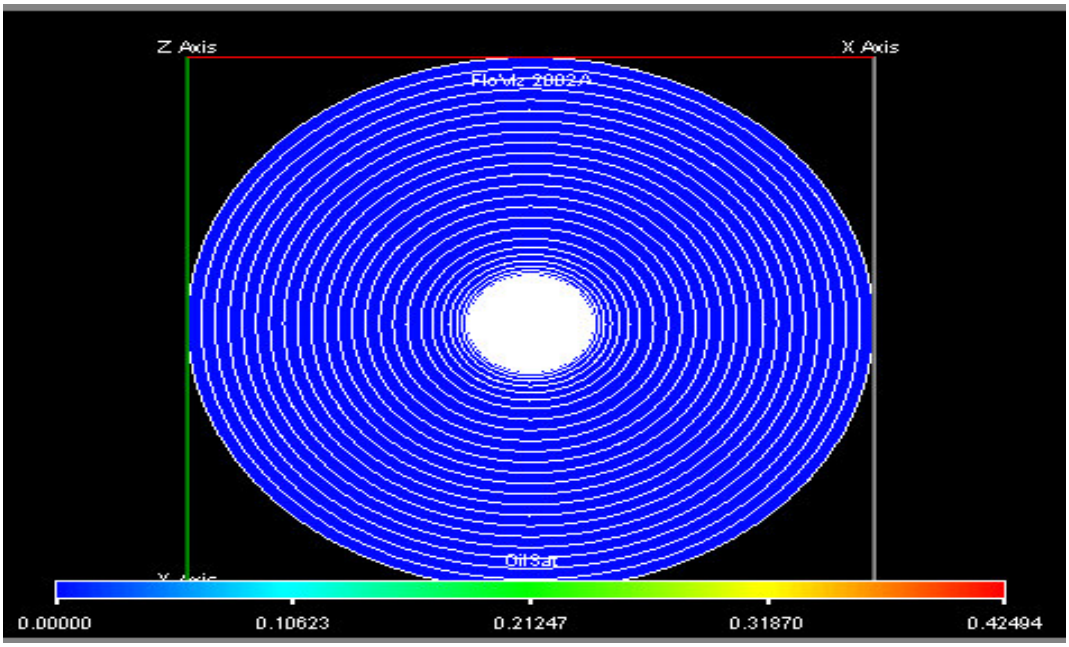

Fig. 3.30 Grid Selected

Fig. 3.30 shows the fine refinement in the grid around the wellbore. A transversal projection of the grid can be seen in **Fig. 3.31**

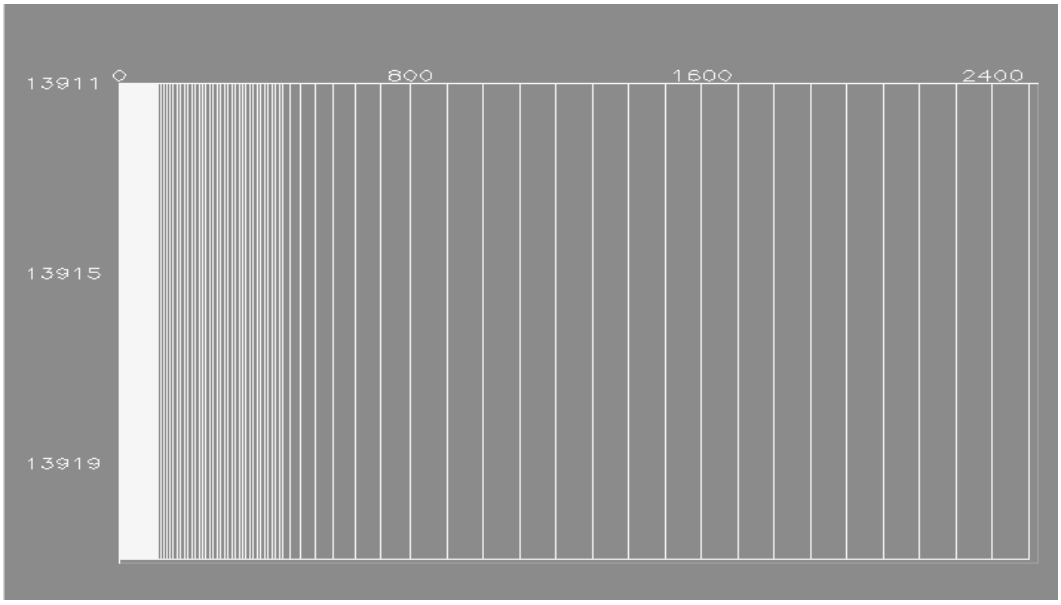

Fig. 3.31 Transversal View of the Grid

3.3.2 Simulation Constraints

The simulation was preformed using several assumptions, first the reservoir initial pressure is set at 2000 psia above the dew point pressure of the gas for every case; this means that the initial reservoir pressure varies with the fluid. The production rate of the simulation was controlled by the well head pressure: its value was constant at 1000 psi. The Gray correlation was used to link bottom-hole and well-head pressure. The reservoir radius was 2500 feet (area of approximately 450 acres) The reservoir had no skin and was homogeneous; the ratio of net to gross was 1. The reservoir was produced by natural depletion.

In the case of a treated reservoir the simulation had two regions: a treated region near the wellbore within a radius of treatment where the irreducible water saturation is zero and the rest of the reservoir in which water saturation was not changed (20 or 41 %, depending on the case). The simulations were performed considering that the reservoir had two regions beginning at the start of the simulation. This analysis compared the treated-reservoir results with the results obtained with a reservoir of similar characteristics, but without treatment.

CHAPTER IV

RESULTS AND ANALYSIS

As it was previously mentioned, the objectives of this study are to determine when the problem of the condensate deposition will affect the gas reserves, and how far should the water be eliminated to have a significant increase in production. These questions will be considered in 3 parts. First the reservoir permeability will be changed until a limit is found where the deposition of condensate does not affect the recoveries of the gas. Second the reservoir parameters of the treated and non treated reservoir will be compared and studied. And third the determination of the optimum radius of treatment was based on production results.

4.1 Limits of the Problem

Several simulations were performed to investigate the limit of the permeability where the problem of the condensate deposition is going to affect the reservoir production. These simulations were done considering that reservoir had no treatment. One parameter, permeability, was varied in order to see the effect of that variable on the final cumulative production.

4.1.1 Base Case

This analysis started with a reservoir with a thickness of 10 feet of thickness, fluid C (C7+ = 11 mole %), and an irreducible water saturation of 41%. The simulations were performed varying the reservoir permeability from 5 mD to 300 mD. **Fig. 4.1** shows the gas production rate over time and **Fig. 4.2** shows the cumulative gas production over time.

In every case it can be observed that the gas production rate has an inflection point near the beginning of the production. This point corresponds in every case to the point where the average reservoir pressure declines below the dew point pressure of the gas.

Fig. 4.2 shows that the same cumulative production is attained when the reservoir permeability is above 100 mD. Lowering the value of permeability below 100 mD will decrease the final amount of reserves from the reservoir

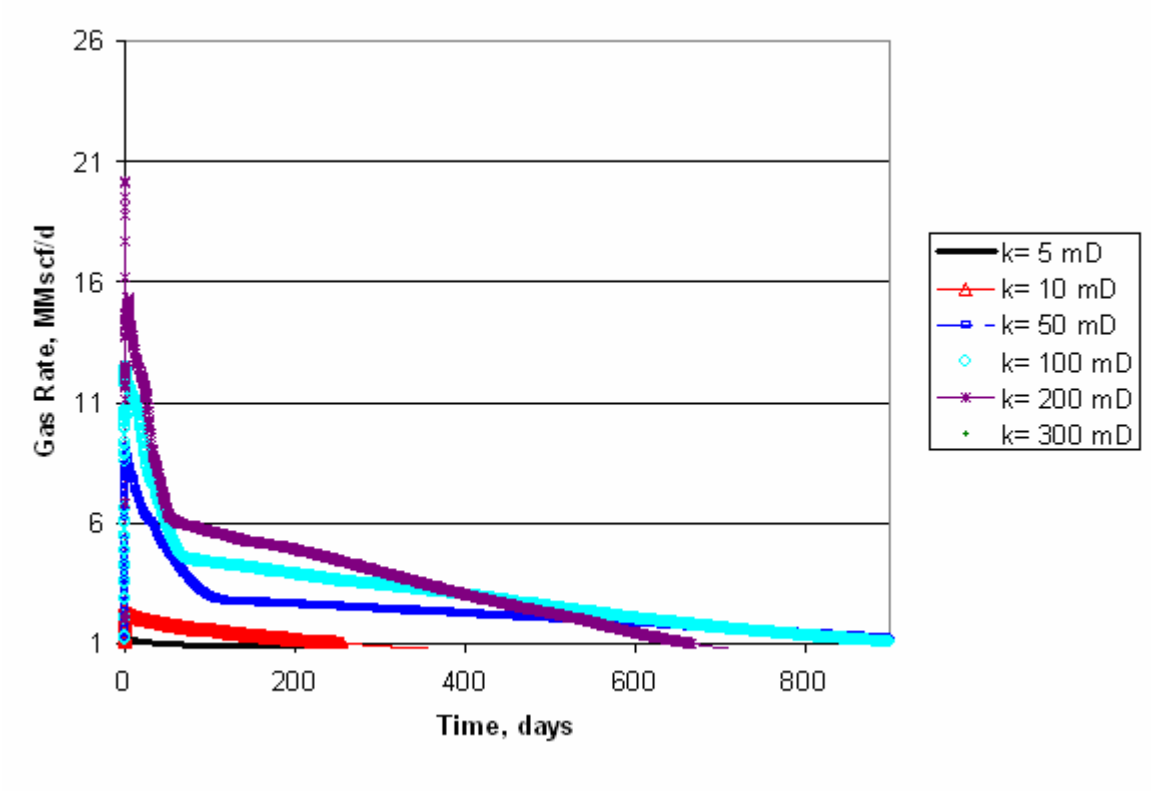

Fig. 4.1 Gas Rate vs Time, Fluid C (11 mole % C7+), Swi=0.41, h=10 feet

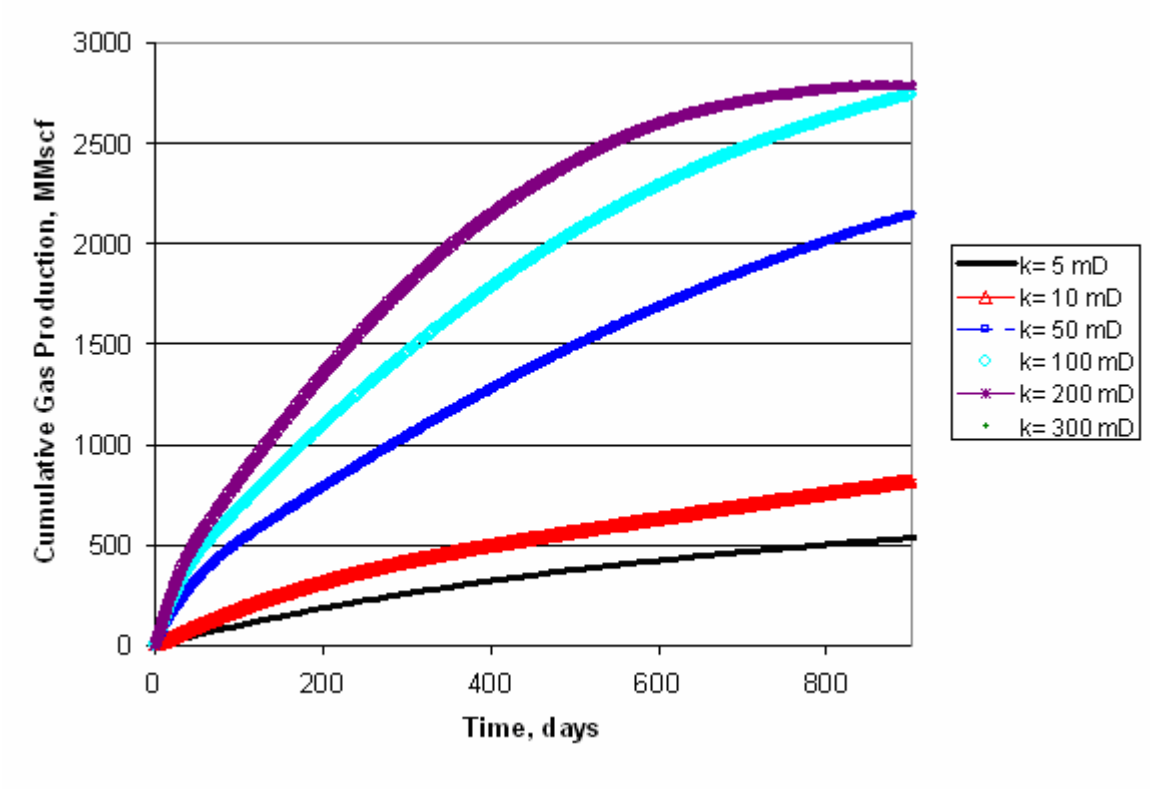

Fig. 4.2 Cumulative Gas Production vs Time, Fluid C (11 mole % C7+), Swi=0.41, h=10 feet

Fig. 4.3 shows the cumulative condensate production from the reservoir. The cumulative condensate production will be the same when the permeability of the reservoir is 100 mD or larger.

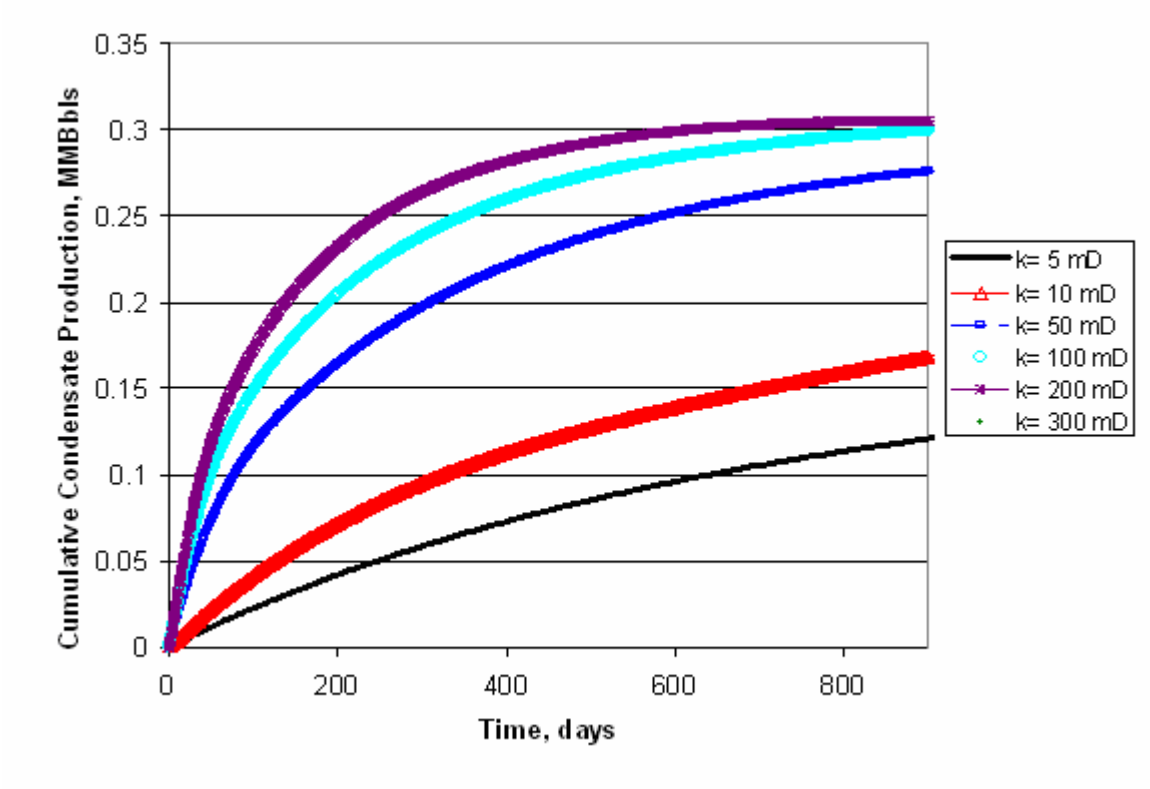

Fig. 4.3 Cumulative Condensate Production vs Time for Fluid C (11 mole % C7+), Swi=0.41, h=10 feet

4.1.2 Effect on the Fluid Composition

Fig. 4.4 and **Fig. 4.5** show the cumulative gas production vs time for h = 10 feet for fluid A and B respectively. A permeability of 100 mD continues to be the limit below which the cumulative gas produced starts to decrease

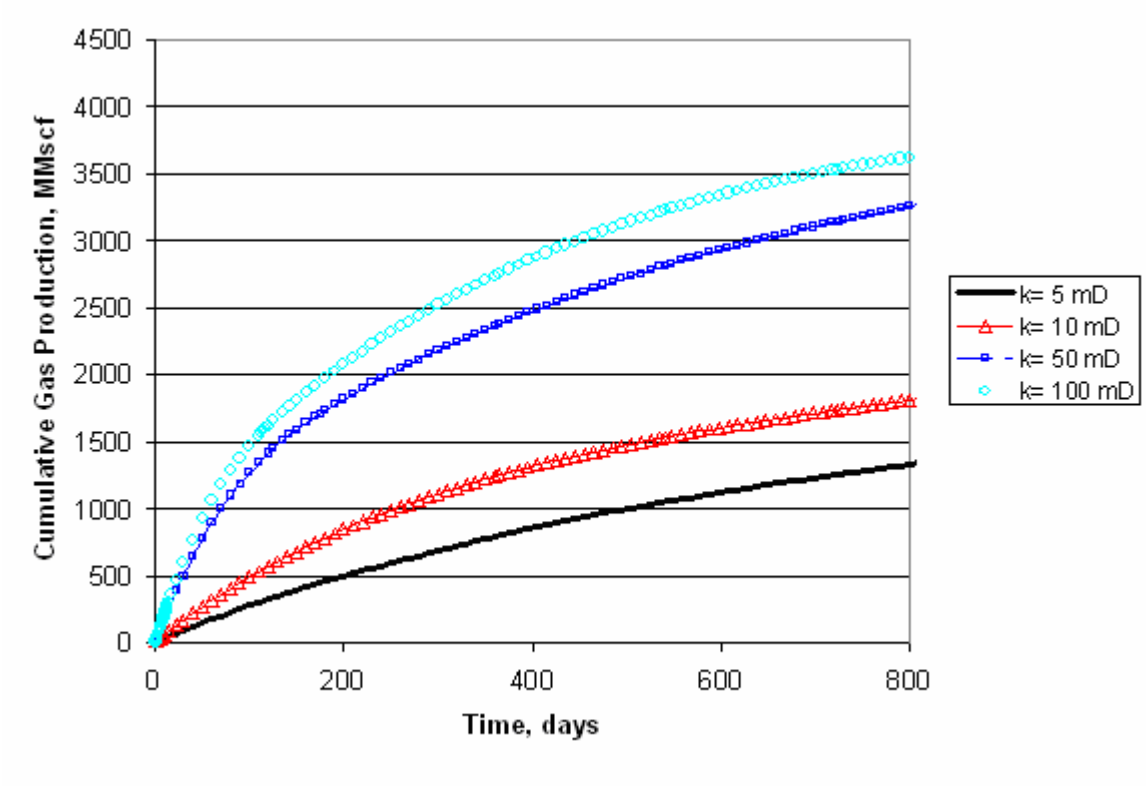

Fig. 4.4 Cumulative Gas Production vs Time for Fluid A (4 mole % C7+), Swi=0.41, h=10 feet

Fig. 4.4 shows that the reservoir at 50 mD does not reach the same level of cumulative gas production as the reservoir at 100 mD; therefore in order to avoid losing gas production the reservoir have to has a permeability larger than 100 mD (limit= 100 mD).

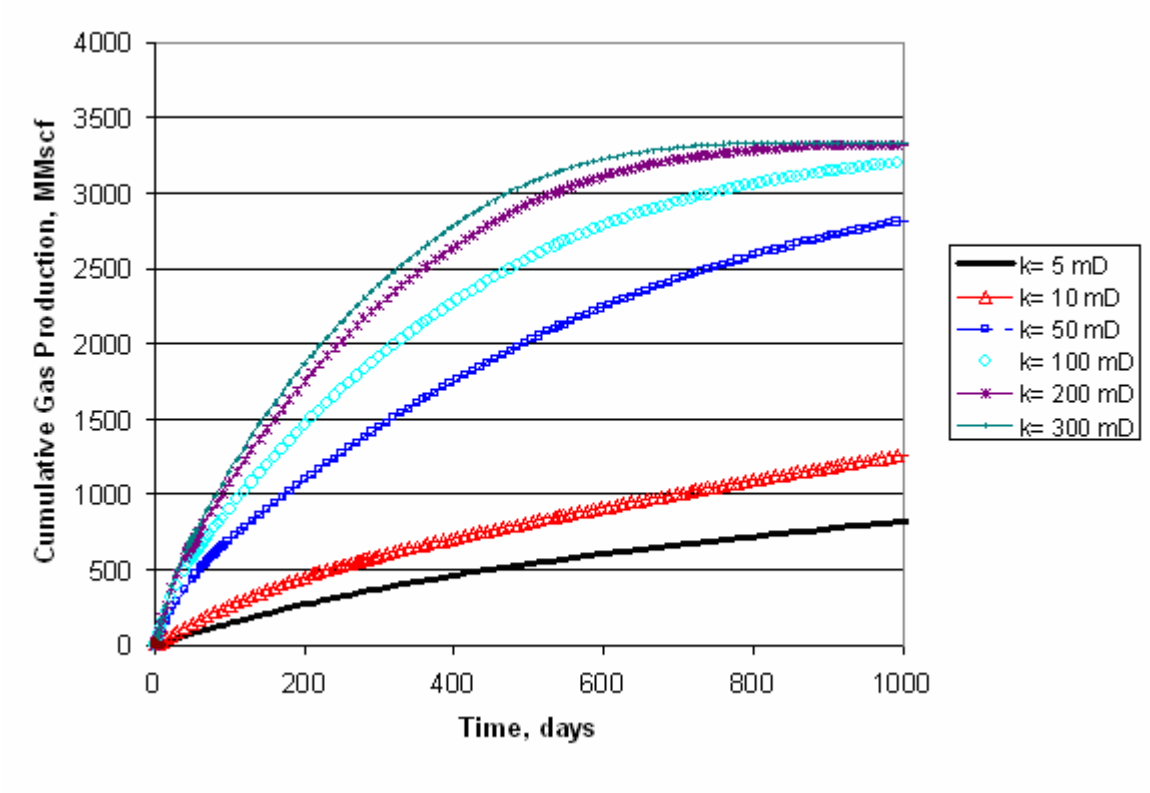

Fig. 4.5 Cumulative Gas Production vs Time for Fluid B (8 mole % C7+), Swi=0.41, h=10 feet

4.1.3 Effect on the Thickness

It was observed in general that an increase in the thickness will reduced the minimum permeability for which the problem of condensate deposition will not affect the cumulative final production. **Fig. 4.6, Fig. 4.7** and **Fig. 4.8** show the cumulative gas production for fluids A, B and C for the case of h=50 mD. This time for fluids A and B the same cumulative production will be obtained at permeabilities of 50 mD or above; but in the case of fluid C the same cumulative gas production will be obtained for permeabilities of 100 mD or above.

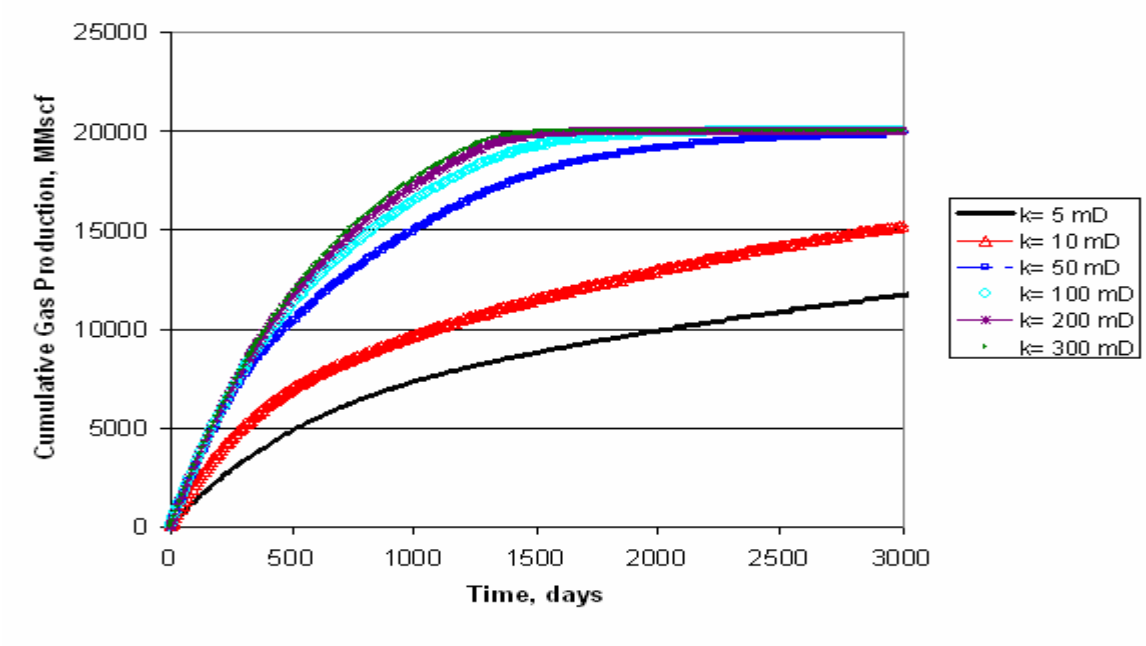

Fig. 4.6 Cumulative Gas Production vs Time for Fluid A (4 mole % C7+), Swi=0.41, h=50 feet

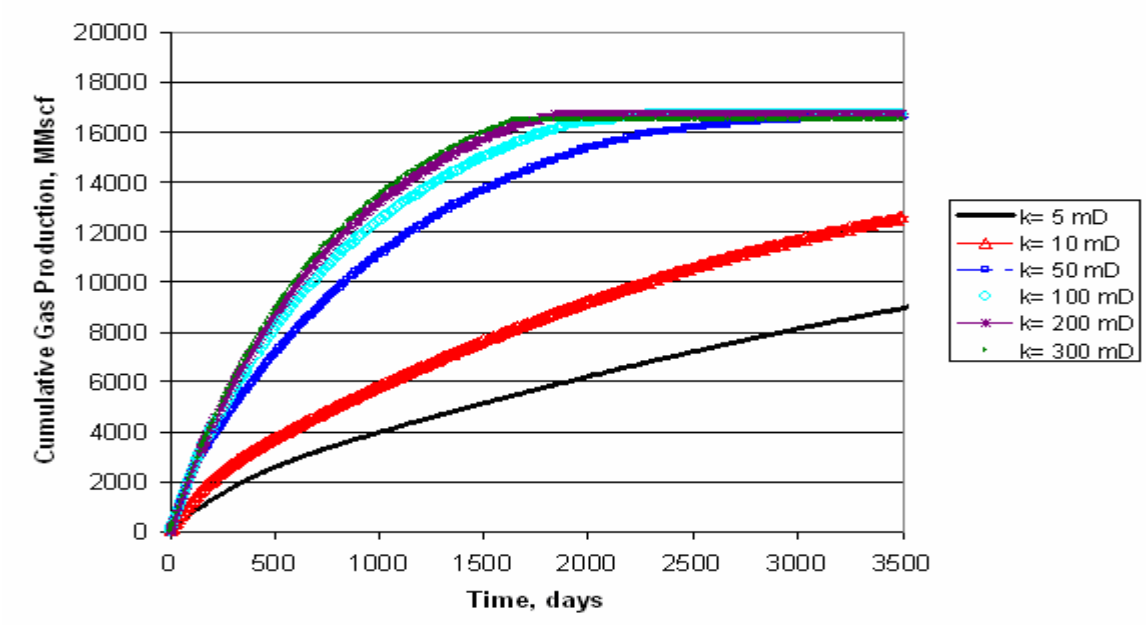

Fig. 4.7 Cumulative Gas Production vs Time for Fluid B (8 mole % C7+), Swi=0.41, h=50 feet

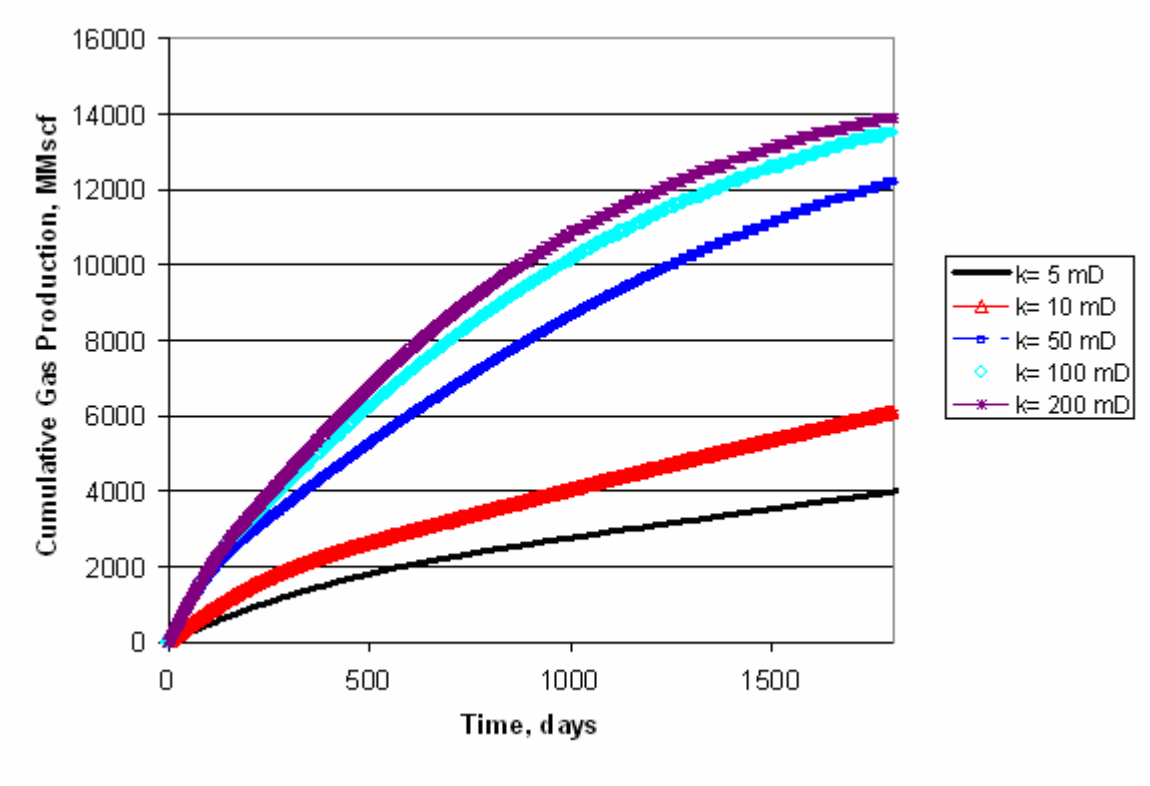

Fig. 4.8 Cumulative Gas Production vs Time for Fluid C (11 mole % C7+), Swi=0.41, h=50 feet

Consequently it is possible to assert that the limit depends on the kh of the reservoir and also on the C7+ content of the fluid.

4.1.4 Effect on Water Saturation

The effect of the water saturation is observed in the following figures. Cumulative gas production is given for fluid A, B and C at a thickness of 50 feet and an irreducible water saturation of 20% in **Fig. 4.9**, **Fig. 4.10** and **Fig. 4.11** respectively. The figures show that the limit of the permeability does not vary with the water content. As in the previous case it continues to be 50 mD for fluids A and B and 100 mD for fluid C when the thickness is 50 feet.

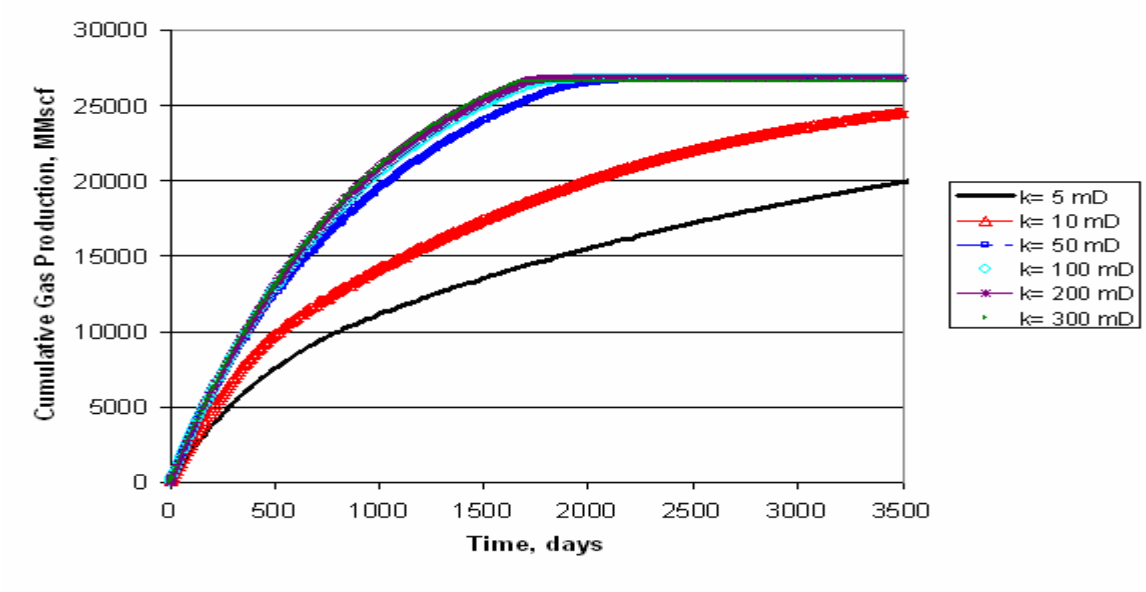

Fig. 4.9 Cumulative Gas Production vs Time for Fluid A (4 mole % C7+), Swi=0.2, h=50 feet

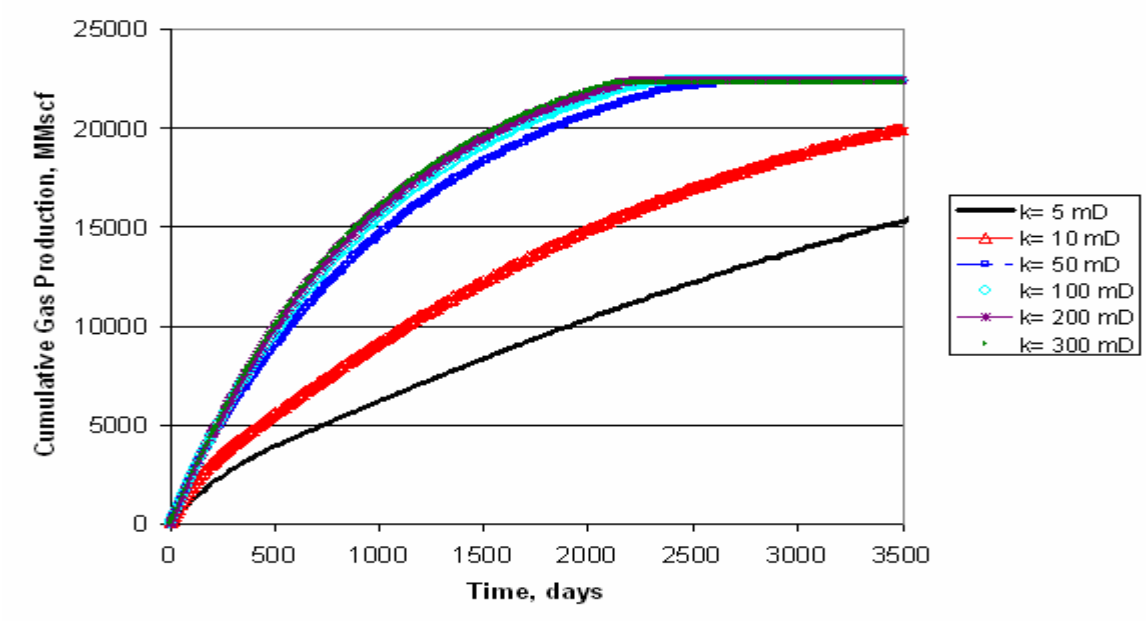

Fig. 4.10 Cumulative Gas Production vs Time for Fluid B (8 mole % C7+), Swi=0.2, h=50 feet

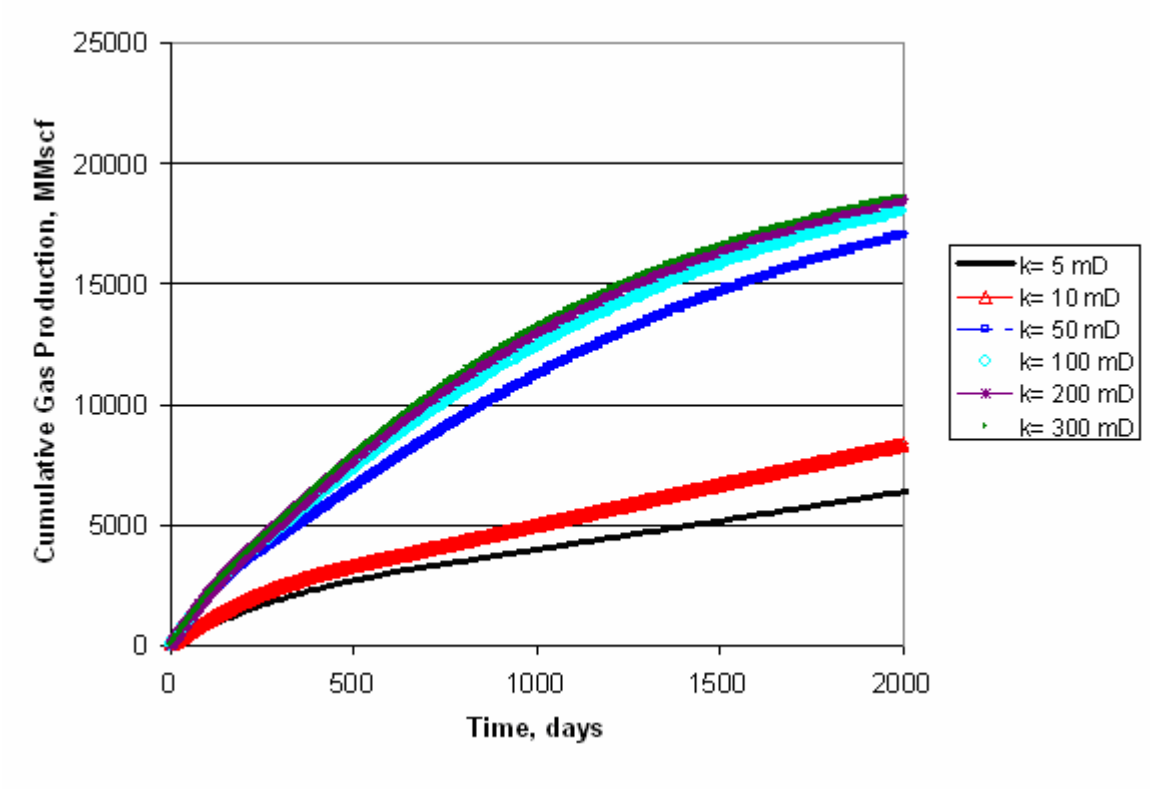

Fig. 4.11 Cumulative Gas Production vs Time for Fluid C (11 mole % C7+), Swi=0.2, h=50 feet

Appendix A shows other results for fluids A, B and C for different water saturations, and permeabilities.

It can be concluded that for reservoirs with permeability higher to 100 mD the problem of the condensate deposition will not affect the ultimate gas recoveries from the reservoir, and that this result is independent of the C7+ fraction of the gas in place, the reservoir thickness, and the irreducible water saturation of the reservoir.

As the reservoir thickness increases the limit of permeability will decrease depending on the C7+ content of the reservoir.

4.2 Description of the Proposed Solution

This section shows the reservoir behavior of the ring of condensate and how this behavior is affected by the treatment of the reservoir. As an example, this section will consider the case with fluid C in place, Swi is 0.2 and h is 10 feet. The treated region will be 100 feet just to illustrate the physical changes of the reservoir.

4.2.1 Differences Production Profiles

Fig. 4.12 shows the gas production rate for a reservoir of 10 mD, 10 feet of thickness, fluid C and Swi equal to 0.2 for two cases; one with treatment and another without treatment. The treatment consists of the removal of all the water near the wellbore to a radius of 100 feet. Figure 4.12 shows that there is a significant acceleration of production. **Fig. 4.13** shows the cumulative gas produced over time. The cumulative production at the end of 800 days has increased by 35 % due to eliminating the irreducible water saturation near wellbore. **Fig. 4.14** shows the cumulative condensate produced over time, in this case an increase of condensate production of approximately 14 % is observed. Finally **Fig. 4.15** shows the condensate rate over time.

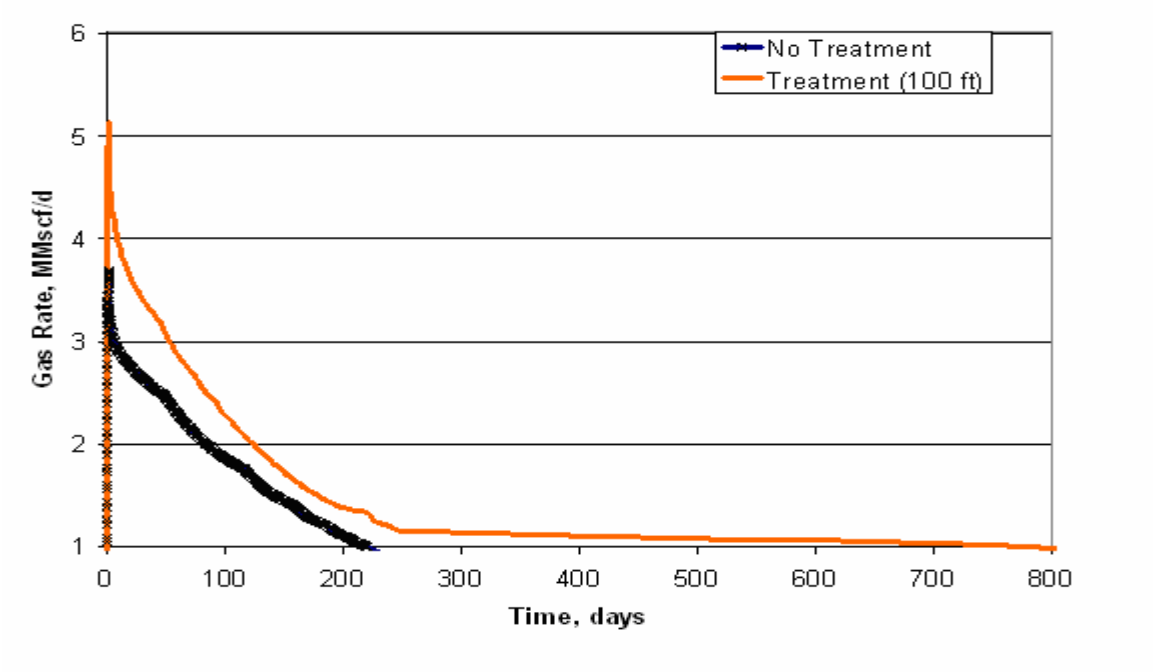

Fig. 4.12 Gas Production Rate vs Time for Fluid C (11 mole % C7+), Swi=0.2, h=10 feet, k=10 mD

Fig. 3.20 shows that the initial gas relative permeability for the non treated reservoir is 0.7, The treated reservoir the reservoir has 2 regions: the first region, from the wellbore to a radius of 100 feet, where the water was removed and thus the gas relative permeability is 1 and a second region from 100 to 2500 feet where Swi is equal to 0.2 and the gas relative permeability is 0.7. As it is explained in the Appendix B the treated reservoir has an equivalent gas relative permeability of 0.864 which represents an increase of 23% with respect to the reservoir with no treatment. Fig 4.12 shows that the differences in gas rates for the beginning of the simulation are approximately 33 % (3 vs 4 MMSCFD for the non-treated and treated case respectively) which is consistent with the expected increase in gas permeability.

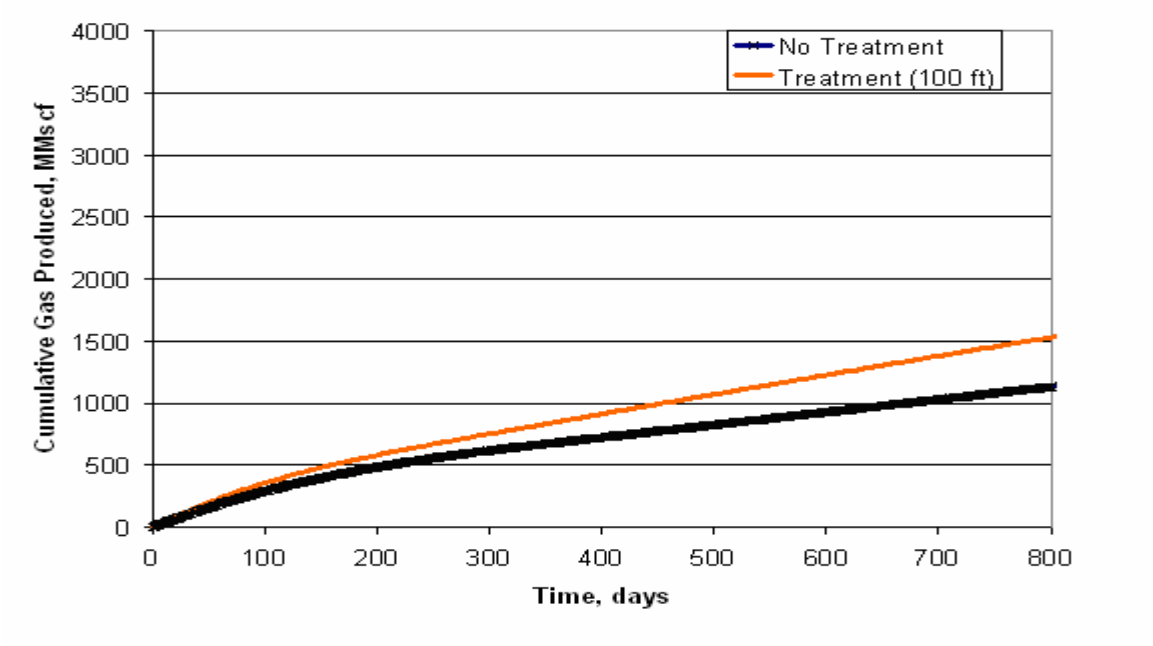

Fig. 4.13 Cumulative Gas Production vs Time for Fluid C (11 mole % C7+), Swi=0.2, h=10 feet, k=10 mD

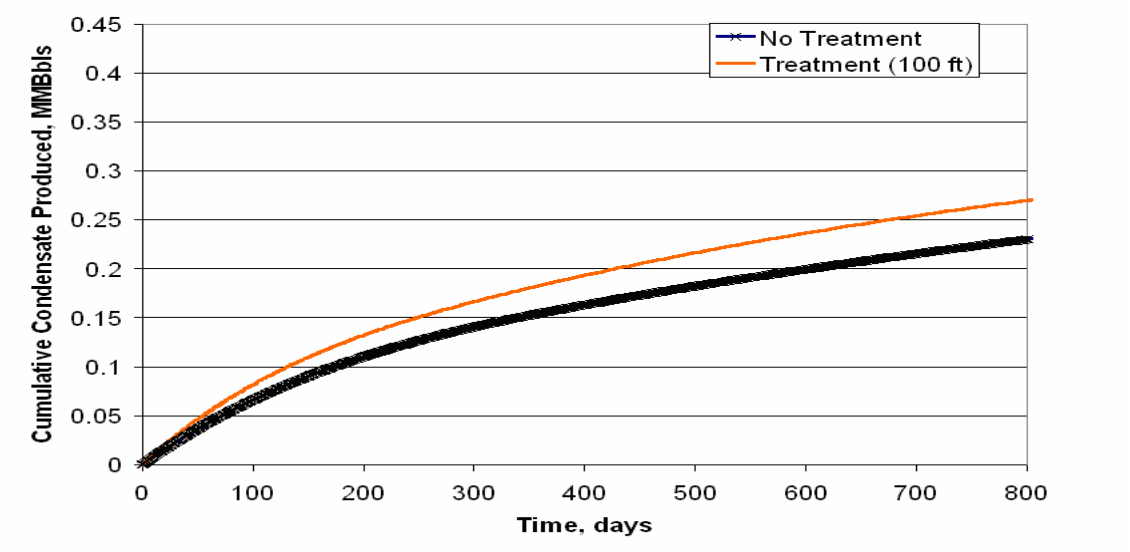

Fig. 4.14 Cumulative Condensate Production vs Time for Fluid C (11 mole % C7+), Swi=0.2, h=10 feet, k=10 mD

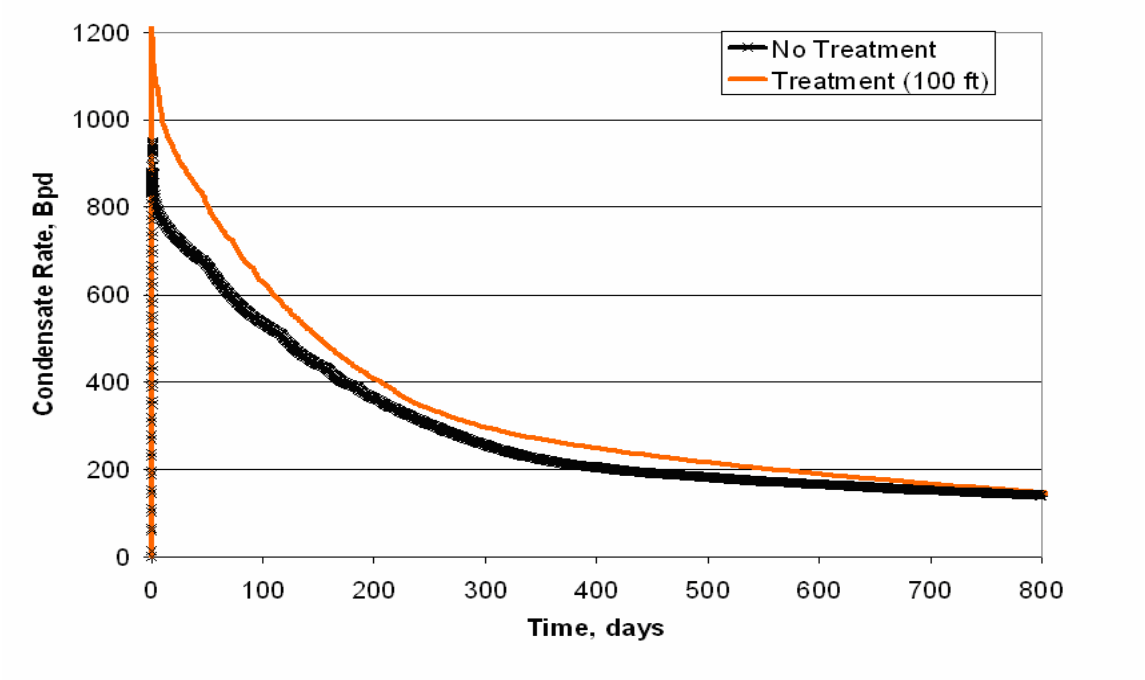

Fig. 4.15 Condensate Production Rate vs Time for Fluid C (11 mole % C7+), Swi=0.2, h=10 feet, k=10 mD

Fig. 4.15 shows an increase of approximately 33% in condensate production at the beginning of the simulation.

4.2.2 Differences in Condensate Saturation in the Reservoir

Fig 4.16 shows the increase in condensate saturation with time for the reservoir with fluid C (10 mD and h=10 feet) without treatment, **Fig 4.17** shows the same graph for the same reservoir with 100 feet of treatment.

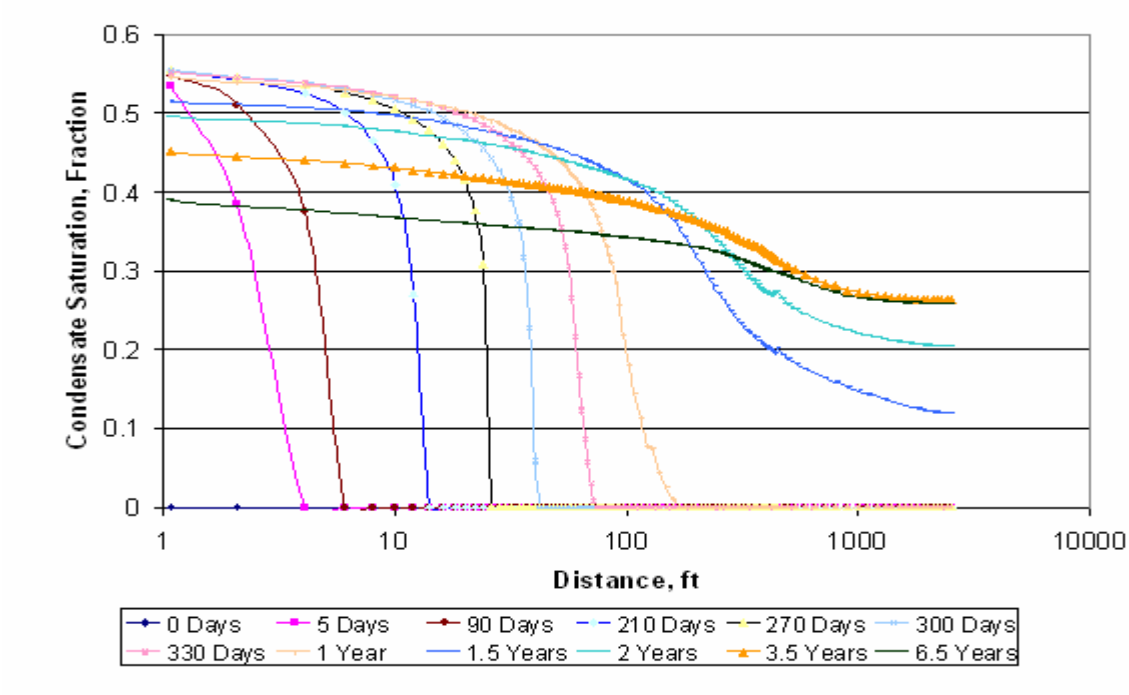

Fig. 4.16 Condensate Saturation vs Distance for Fluid C (11 mole % C7+), Swi=0.2, h=10 feet, k=10 mD, no Treatment

Fig 4.16 shows that at the beginning of the simulation the reservoir has no condensate, after 5 days of producing the reservoir the condensate saturation around the wellbore is approximately 55%. In this case the water saturation in the reservoir is 20 %, therefore at this time the gas saturation is approximately 25%. Another interesting aspect is that the reservoir pressure falls completely below the dew point pressure for the gas between 1 and 1.5 years; this effect can be seen on the graph by the fact that the blue line corresponding to 1.5 years shows the entire reservoir with a condensate saturation greater than zero.

Fig 4.16 also shows that in the limits of the reservoir distances greater than 1000 feet the condensate saturation is approximately 0.26 for 6.5 years. If 20% of irreducible water is taken into account, the condensate occupies 32.5 % of the space of the hydrocarbon phase. This result is consistent with the CVD test, Fig 3.11, in which the

liquid saturation is approximately 33 % at the same conditions of pressure and temperature.

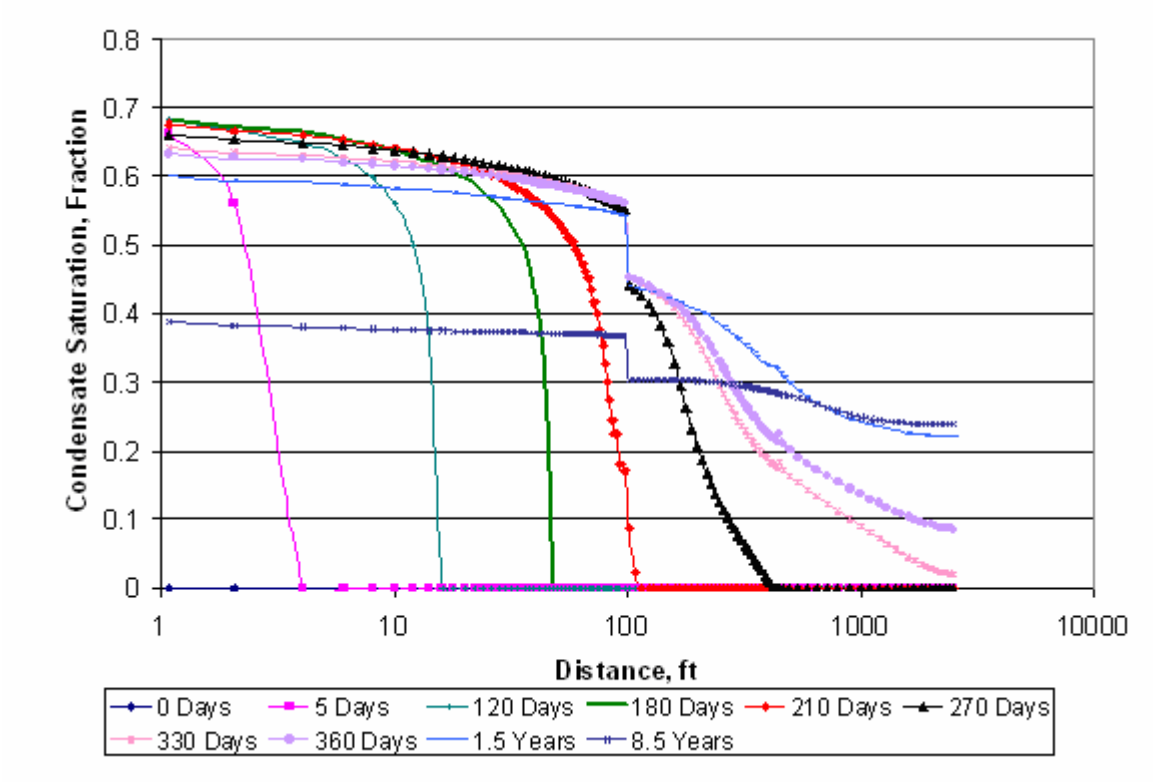

Fig. 4.17 Condensate Saturation vs Distance for Fluid C (11 mole % C7+), Swi=0.2, h=10 feet, k=10 mD, 100 feet of Treatment

Fig 4.17 is the reservoir presented in Fig. 4.16 with a treatment of 100 feet of reservoir performed. This means that the reservoir from the well to 100 radial feet away has a water saturation of zero. After 100 feet the reservoir has an irreducible water saturation of 0.2. This is the reason a discontinuity can be observed in the condensate saturation profile.

For example the line of 270 Days has a condensate saturation of 0.58 before the discontinuity and just after the discontinuity the condensate saturation is approximately 0.45. These numbers follow a logical trend because after the results observed in the Fig

4.16 one can expect that this line would be continuous if the water saturation were continuous, and if the effect of the water saturation is corrected (the correction would be 1-Swi) the number of 0.58 will be altered to be 0.464.

The values of the condensate saturation for the cells far from the well are again approximately 0.26 for 8.5 years as the previous case. This is the value expected as in Fig. 4.16.

The near-wellbore region in this case has a condensate saturation of 0.67, this value is more important than the value of 0.55 obtained for the case with no treatment, the difference between the two cases is that the reservoir in Fig 4.17 has no water, and once again it is possible to find the factor (1-Swi) between the case with no treatment and the case with treatment. Even if the condensate saturation is larger in the treatment case, the gas saturation is increased because for the treatment case the near-wellbore region has only condensate and gas without water and therefore the gas saturation in the treatment case is 0.33 in contrast to 0.25 for the case with no treatment. This increase in the condensate and the gas saturation will increase the gas and the condensate production of the reservoir since the relative permeabilities will be larger.

Fig 4.15 also shows that in this case the reservoir pressure passes below the dew point pressure of the gas between 330 and 360 days.

4.2.3 Differences in Gas Saturation in the Reservoir

Fig 4.18 shows the gas saturation for the reservoir with fluid C (10 mD and h=10 feet) without treatment, **Fig 4.19** shows the same graph for the same reservoir with 100 feet of treatment.

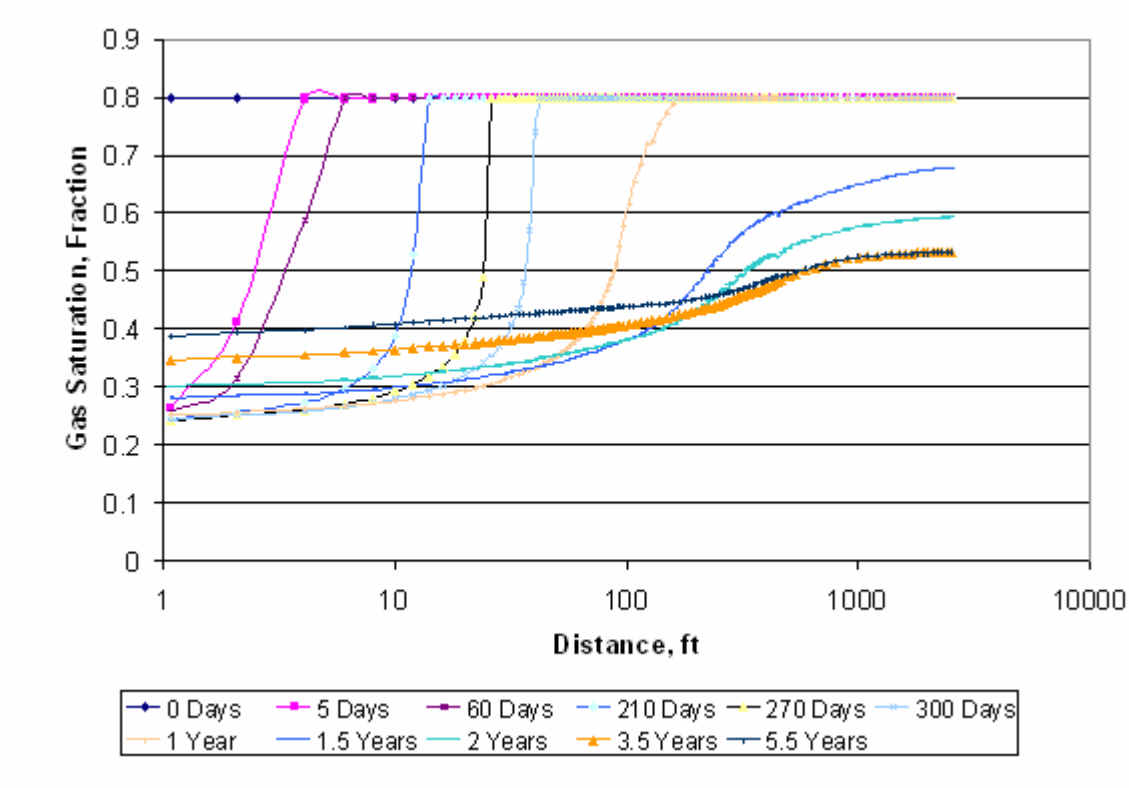

Fig. 4.18 Gas Saturation vs Distance for Fluid C (11 mole % C7+), Swi=0.2, h=10 feet, k=10 mD, no Treatment

Fig 4.18 shows that at the beginning of the simulation the reservoir has a gas saturation of 0.8. After 5 days of production, the gas saturation around the wellbore is approximately 0.25 which is consistent with the result encountered in Fig 4.16.

It can also be seen that the reservoir pressure falls completely below the dew point pressure of the gas between 1 and 1.5 years; this effect can be seen in the graph by the blue line corresponding to 1.5 years presents a gas saturation under 80 % throughout the reservoir.

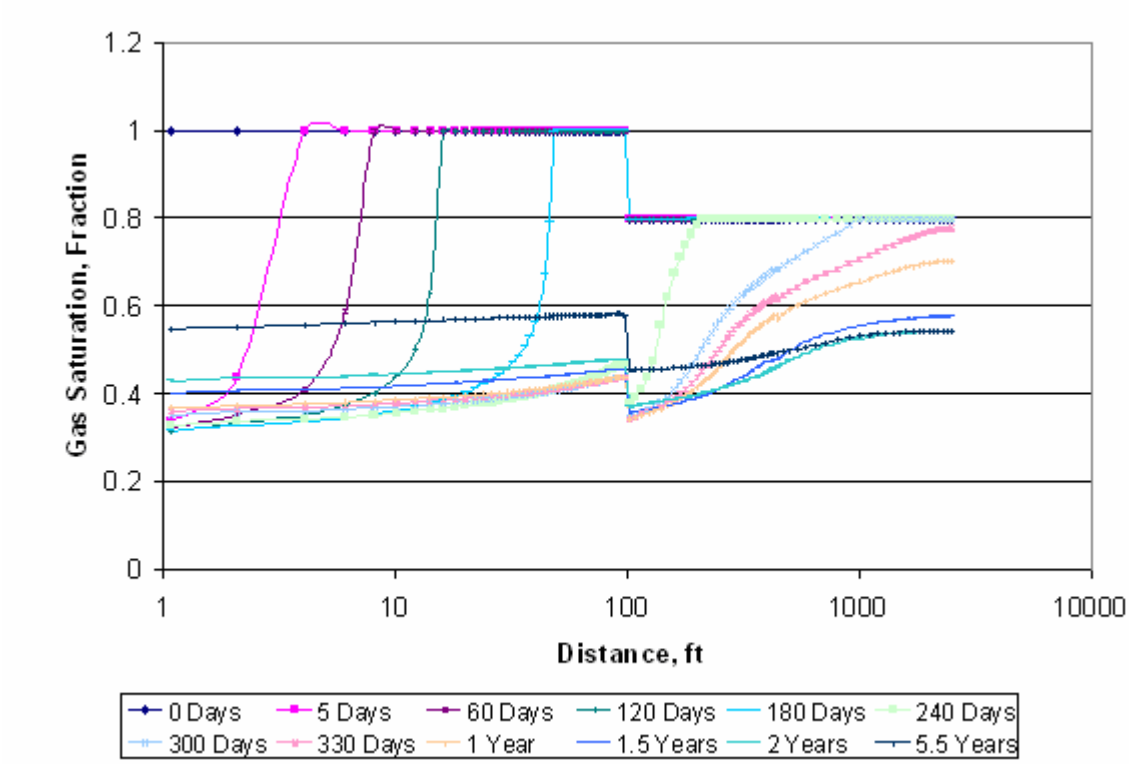

Fig. 4.19 Gas Saturation vs Distance for Fluid C (11 mole % C7+), Swi=0.2, h=10 feet, k=10 mD, 100 feet of Treatment

Fig 4.19 is the reservoir presented in Fig. 4.18 with a radial treatment of 100 feet of reservoir. This means that the reservoir from the well to a radial distance of 100 feet has a water saturation of zero. With a radial distance greater than 100 feet the reservoir has an irreducible water saturation of 0.2. This is the reason why a discontinuity can be observed in the gas saturation profile.

A factor of 1-Swi can be observed between the values of the lines at the same time before and after the discontinuity.

Comparison of Fig 4.18 and Fig 4.19 shows that the gas saturation near the wellbore changed from 0.25 to 0.33 due to the treatment of the reservoir.

Fig 4.19 also shows that in this case the reservoir pressure passes below the dew point pressure of the gas between 330 and 365 days.

4.2.4 Differences in Condensate Permeability

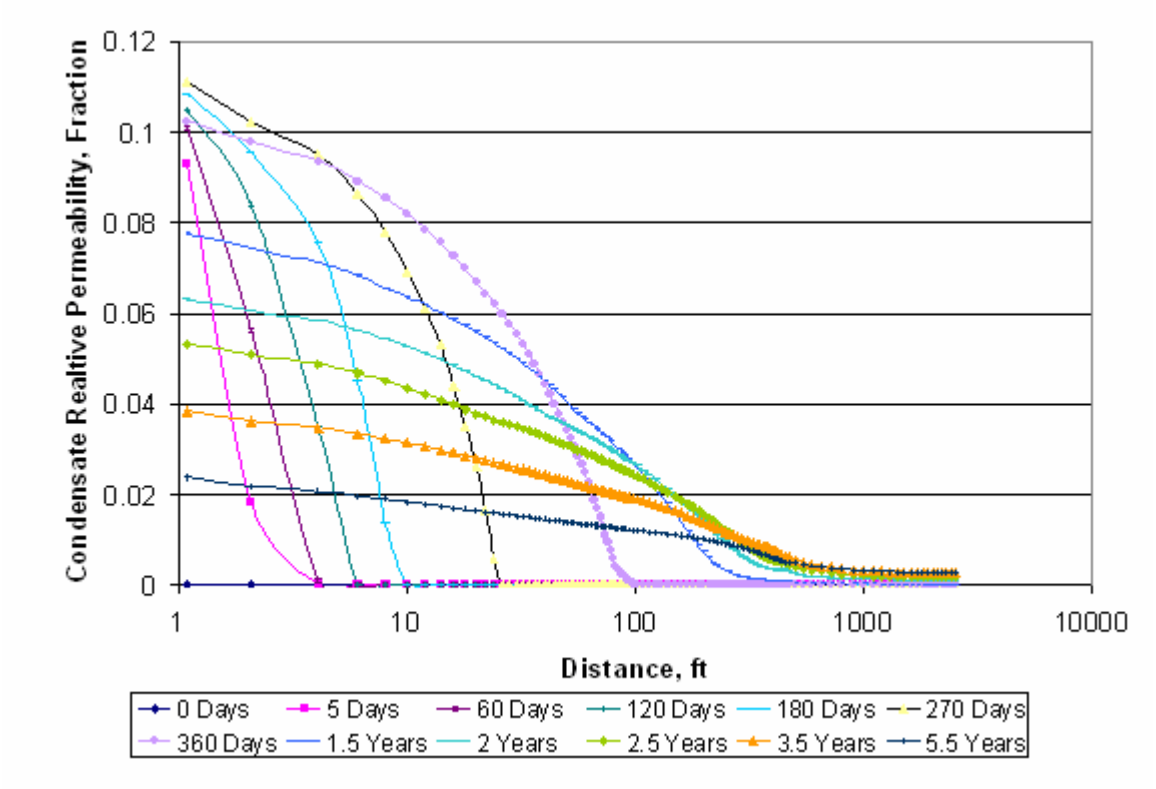

Fig. 4.20 Condensate Relative Permeability vs Distance for Fluid C (11 mole % C7+), Swi=0.2, h=10 feet, k=10 mD, no Treatment

Fig. 4.20 shows that the condensate relative permeability for the base case is at most 0.11. This is the relative permeability that will allow all the liquid deposited around the wellbore to be produced.

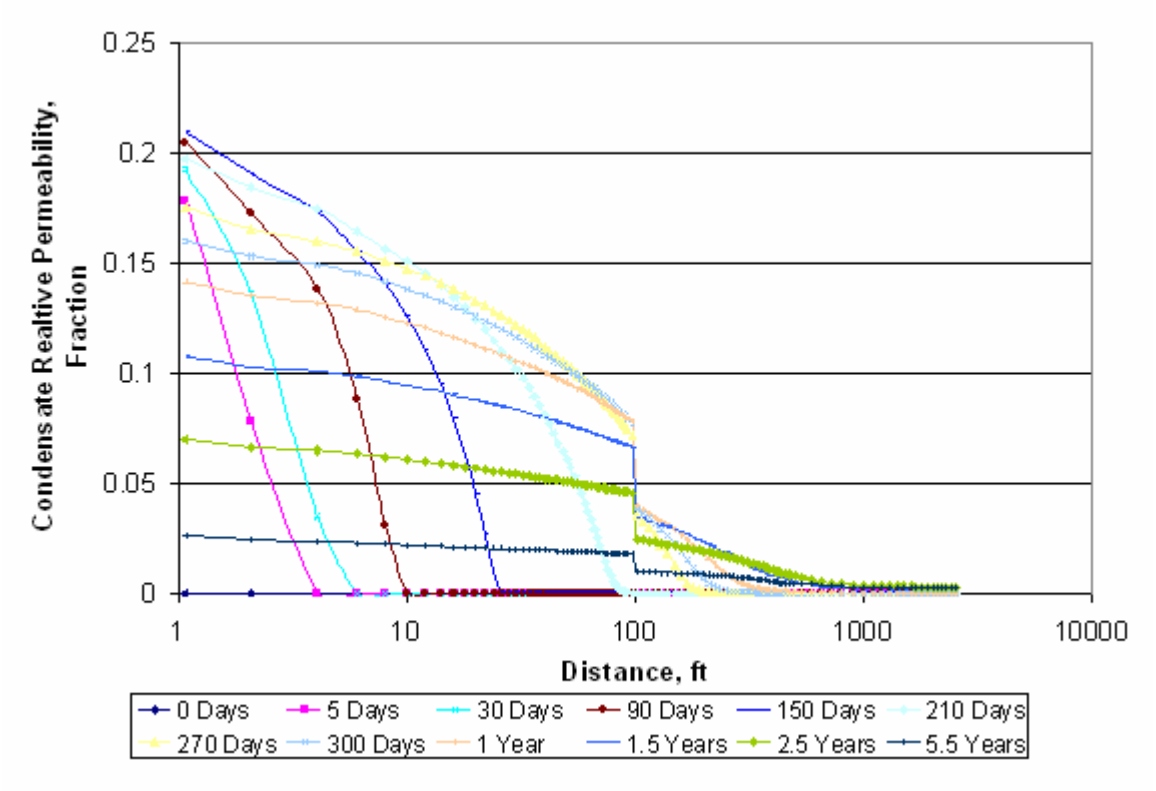

Fig. 4.21 Condensate Relative Permeability vs Distance for Fluid C (11 mole % C7+), Swi=0.2, h=10 feet, k=10 mD, 100 feet of Treatment

Fig. 4.21 shows that the condensate relative permeability for the treated case is double the relative permeability of the base case, this is the direct effect of the increased condensate saturation near the wellbore. The discontinuities presented in this graph again are caused by the change from the treated to the non treated region of the reservoir.

4.2.5 Differences in Gas Permeability

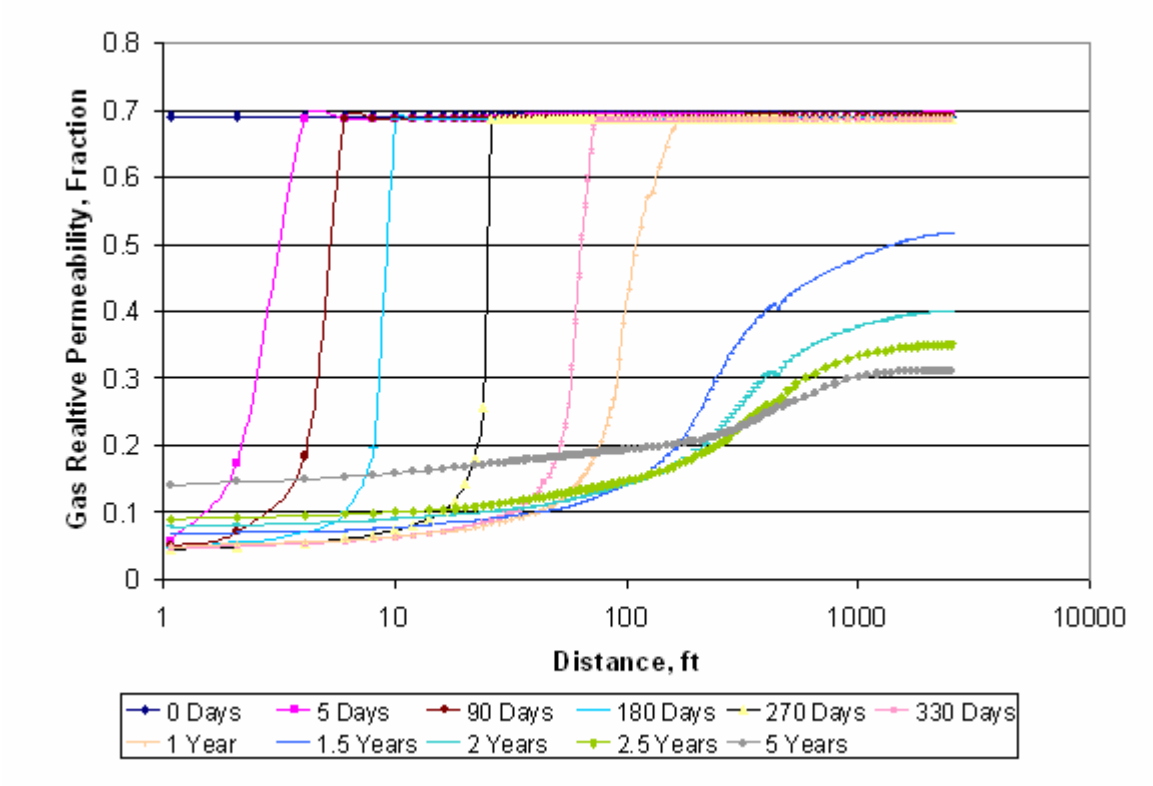

Fig. 4.22 Gas Relative Permeability vs Distance for Fluid C (11 mole % C7+), Swi=0.2, h=10 feet, k=10 mD, no Treatment

Fig. 4.22 shows the gas relative permeability for the no treatment case; the reservoir starts with a gas relative permeability of 0.69 which is the value expected from Fig. 3.26. After 5 days the relative permeability around the reservoir decreases to almost 0.05; this effect is due to the condensate deposition around the wellbore and the resulting decrease in the gas saturation.

The external part of the reservoir, 1000 feet and more, has a gas relative permeability of approximately 0.3. This value also corresponds with the value expected from Fig. 3.29 for a value of gas saturation of 0.54.

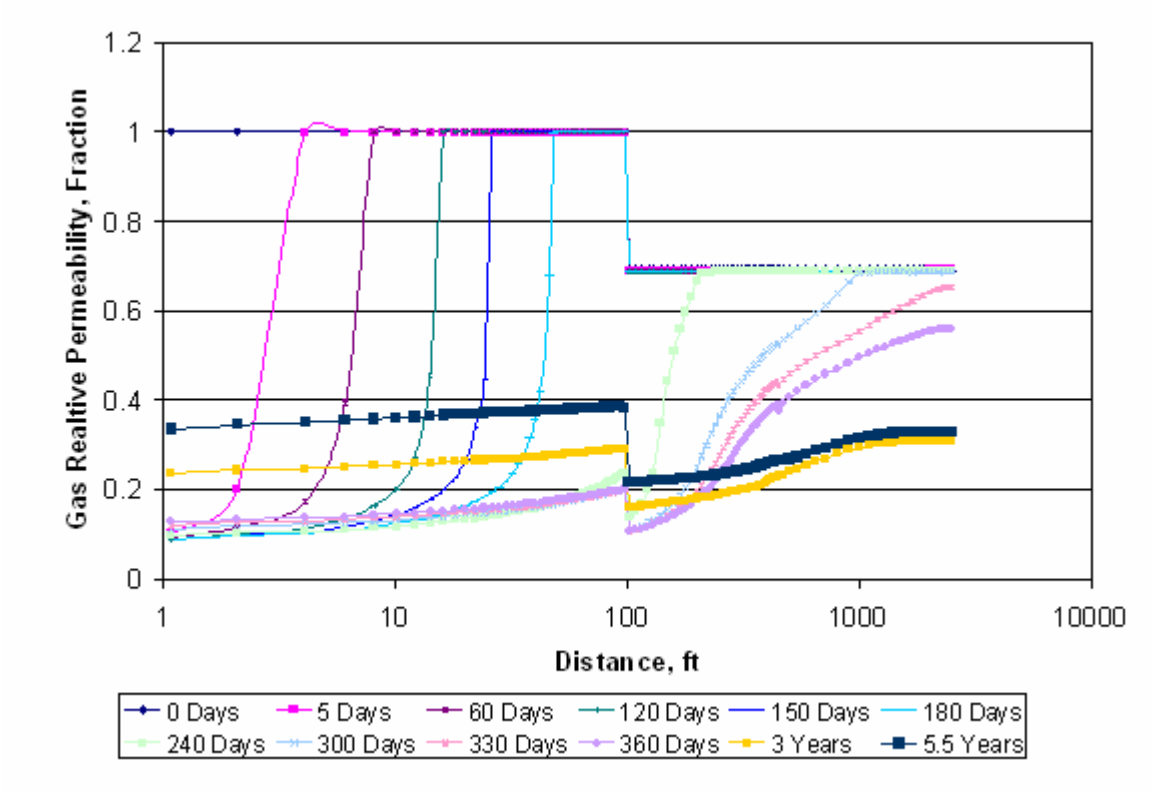

Fig. 4.23 Gas Relative Permeability vs Distance for Fluid C (11 mole % C7+), Swi=0.2, h=10 feet, k=10 mD, 100 feet of Treatment

Fig. 4.23 shows the gas relative permeability for the treated reservoir. The reservoir starts with a gas relative permeability of 1 for the region of less than 100 feet and has a value of 0.69 for the region external to 100 feet. These are the values expected from the Fig. 3.28 (at 100% and 80% gas saturation respectively). The difference between those values is due to differences in gas saturation caused by the removal of water for the region closer to the wellbore.

After 5 days the gas relative permeability around the wellbore decreases to about 0.1. This is due to the condensate deposition and the resulting decrease in the gas saturation. This value is approximately double the value of gas relative permeability associated with the non-treated case.

Again in the outer reservoir the gas relative permeability is approximately 0.3. This value corresponds with the value expected from Fig. 3.28 for a value of gas saturation of 0.54.

4.2.6 Differences in Pressure profile

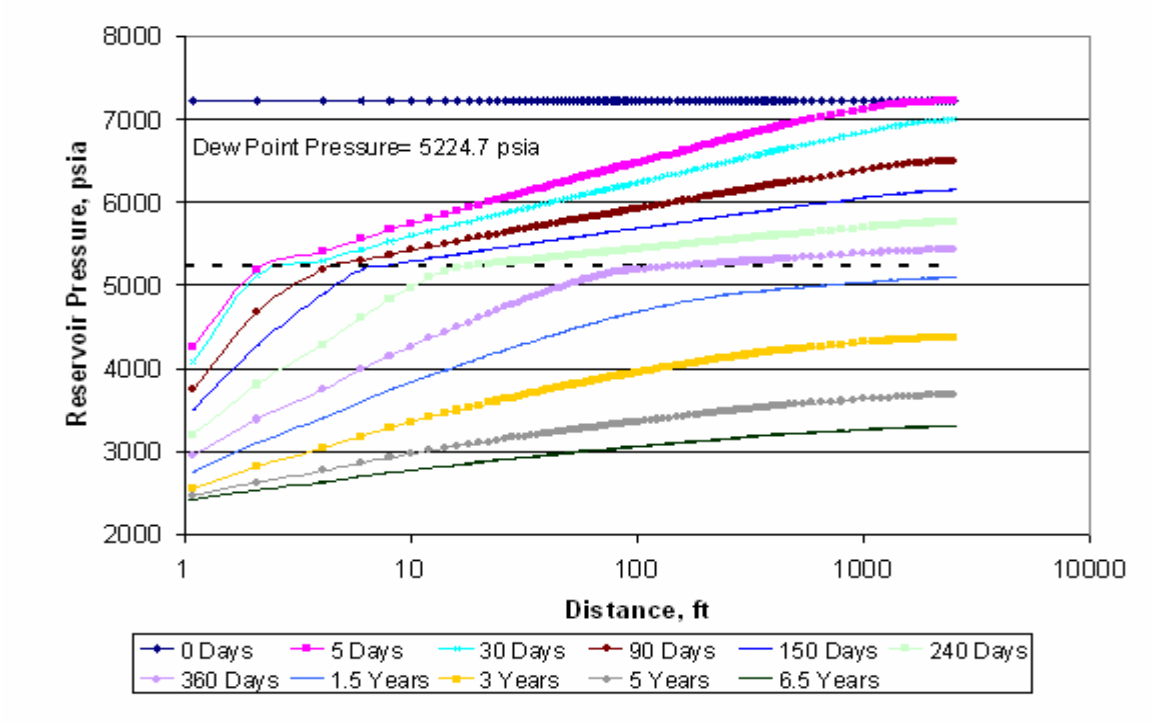

Fig. 4.24 Pressure vs Distance for Fluid C (11 mole % C7+), Swi=0.2, h=10 feet, k=10 mD, no Treatment

Fig. 4.24 shows the pressure through the reservoir for the no treatment case. The initial reservoir pressure is 7224 psia and the dew point pressure of the gas is 5224 psia. After 5 days of production the reservoir pressure near the wellbore has decreased below the dew point pressure. Condensate starts to deposit near the wellbore almost immediately.

As production continues the reservoir is depleted; at approximately 1.5 years pressure throughout the reservoir is below the dew point pressure of the gas.

The pressure near the wellbore starts at 4200 psia and ends at approximately 2500 psia. These pressures are controlled by the well head pressure and the pressure drop in the tubing..

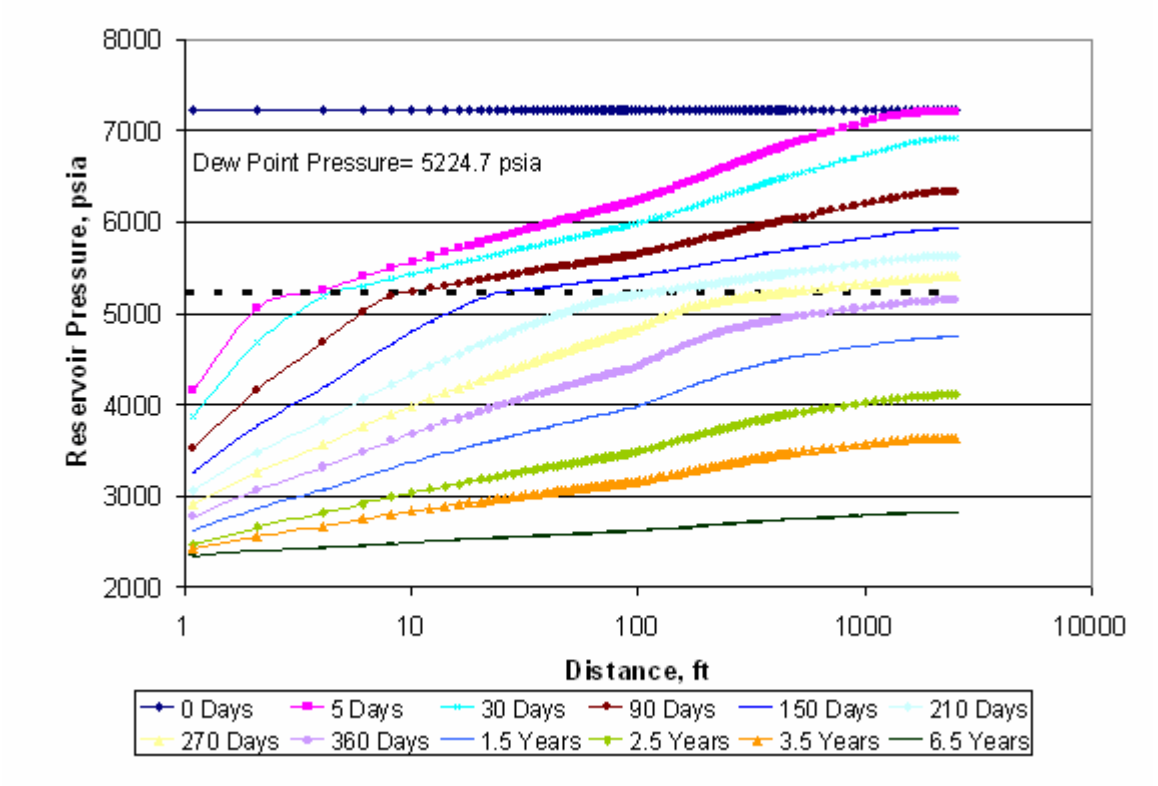

Fig. 4.25 Pressure vs Distance for Fluid C (11 mole % C7+), Swi=0.2, h=10 feet, k=10 mD, 100 feet of Treatment

Fig. 4.25 shows the pressure through the reservoir for the treated case. Again the initial reservoir pressure is 7224 psia and the dew point pressure of the gas is 5224 psia. Again after 5 days of production the reservoir pressure near the wellbore decreases below the dew point pressure.

As production continues the reservoir is depleted; at approximately 360 days the pressure throughout reservoir is below the dew point pressure of the gas.

The pressure near the wellbore starts at 4200 psia and ends at approximately 3500 psia; controlled by the well head pressure and the pressure drop in the tubing..

Appendix C shows another example of the same graphs for fluid C at Swi= 0.41 and a radius of treatment of 100 feet.

4.3 Determination of the Optimum Radius of Treatment

As the radius of treatment increases, the reservoir will produce more gas at a higher production rate. The optimum radius of treatment will be considered as the smallest radius of treatment for which any further increase does not represent an important gain on the cumulative gas production with respect to the case of no treatment.

In the following section the variation of the optimum radius of treatment with respect to reservoir thickness, irreducible water saturation, fluid composition and permeability will be discussed. The presentation of results will start with the case of fluid C, k=10 mD Swi=0.41, h=10 feet, and then all the parameters will be changed one at a time to observe the effect of these changes on the optimum radius of treatment and the associated increase in cumulative gas production.

4.3.1 Base Case

Fig. 4.26 presents the gas production rate vs time for Fluid C at k=10 mD for several radii of treatment. **Fig. 4.27** presents the cumulative gas production over time associated with this case.

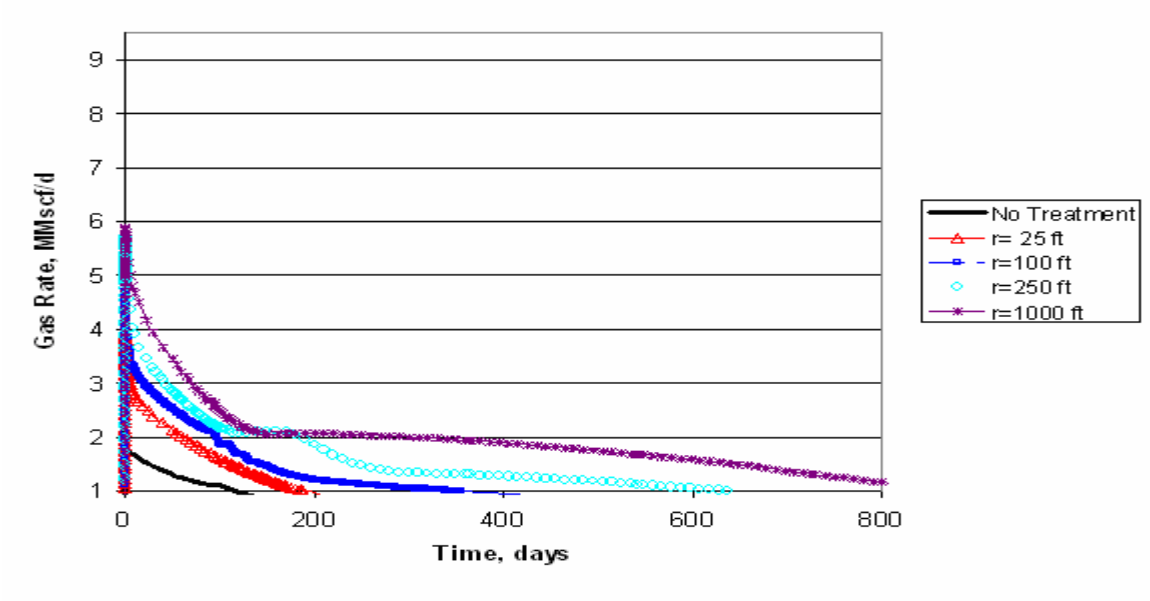

Fig. 4.26 Gas Production Rate vs Time for Several Radius of Treatment, Fluid C (11 mole % C7+), Swi=0.41, h=10 feet, k=10 mD

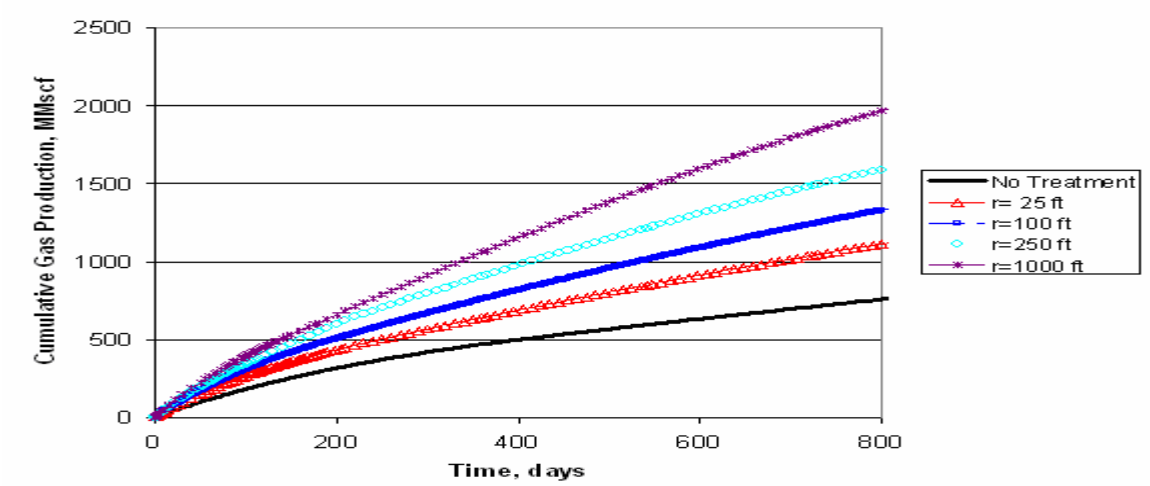

Fig. 4.27 Cumulative Gas Production vs Time for Several Radius of Treatment, Fluid C (11 mole % C7+), Swi=0.41, h=10 feet, k=10 mD

Fig. 4.27 shows that the increase in the ultimate recoveries from the reservoir is approximately 100% over the no treatment case for a treatment of 250 feet.

The costs of the treatment are assumed to be directly proportional to the volume of the treatment required. As the reservoir has a constant height the cost of the treatment will be proportional to the area of treatment. As the surface is circular the area of treatment is proportional to the radius squared, therefore the following analysis will be performed based on the squared radius of the treatment.

The incremental differences among the cumulative gas production for the treated cases and the non-treated case for several radii of treatment. at various points in time will be used to determine the optimum radius of treatment.

Fig. 4.28 shows the incremental changes in cumulative production with respect to the non-treated case plotted against volume of treatment represented by the treatment radius squared. The increase in incremental cumulative gas production are minimal at treatment volumes greater than 62500 radius squared. Thus for this case the optimum radius of treatment is 250 feet.

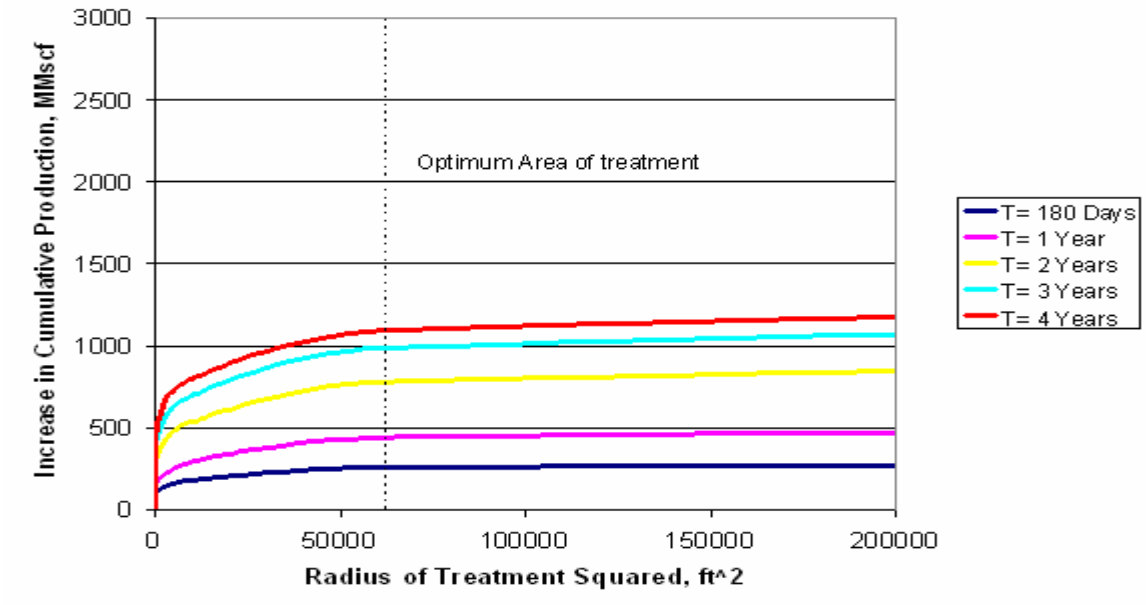

Fig. 4.28 Increment in Cumulative Gas Production vs Radius of Treatment Squared , Fluid C (11 mole % C7+), Swi=0.41, h=10 feet, k=10 mD

The following section shows how the optimum radii of treatment vary with changes in some reservoir parameters.

4.3.2 Effect on Thickness

Fig. 4.29 shows the incremental increase in cumulative gas production with respect to the non-treated case against the treatment radius squared for fluid C at Swi=0.41, k= 10 mD, altering the reservoir thickness to 50 feet. The optimum radius of treatment is again 250 feet (R^2= 62500 ft^2) he optimum radius of treatment appears to be independent of reservoir thickness.

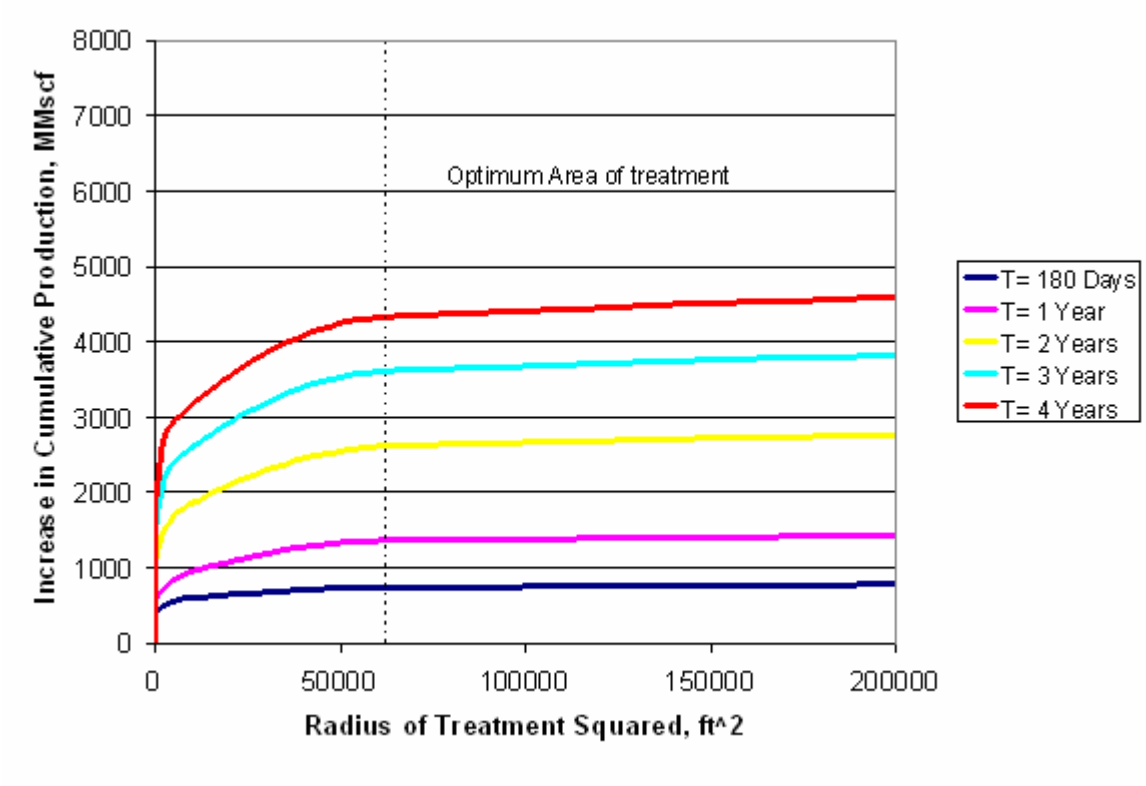

Fig. 4.29 Increment in Cumulative Gas Production vs Radius of Treatment Squared , Fluid C (11 mole % C7+), Swi=0.41, h=50 feet, k=10 mD

4.3.3 Effect of Permeability

Fig. 4.30 shows the incremental increase in cumulative gas production with respect to the base case against the treatment radius squared for fluid C at Swi=0.41, h= 10 feet with reservoir permeability changed to 50 mD. The optimum radius remains 250 feet (R^2= 62500 ft^2) , the optimum radius of treatment appears to be independent of the permeability.

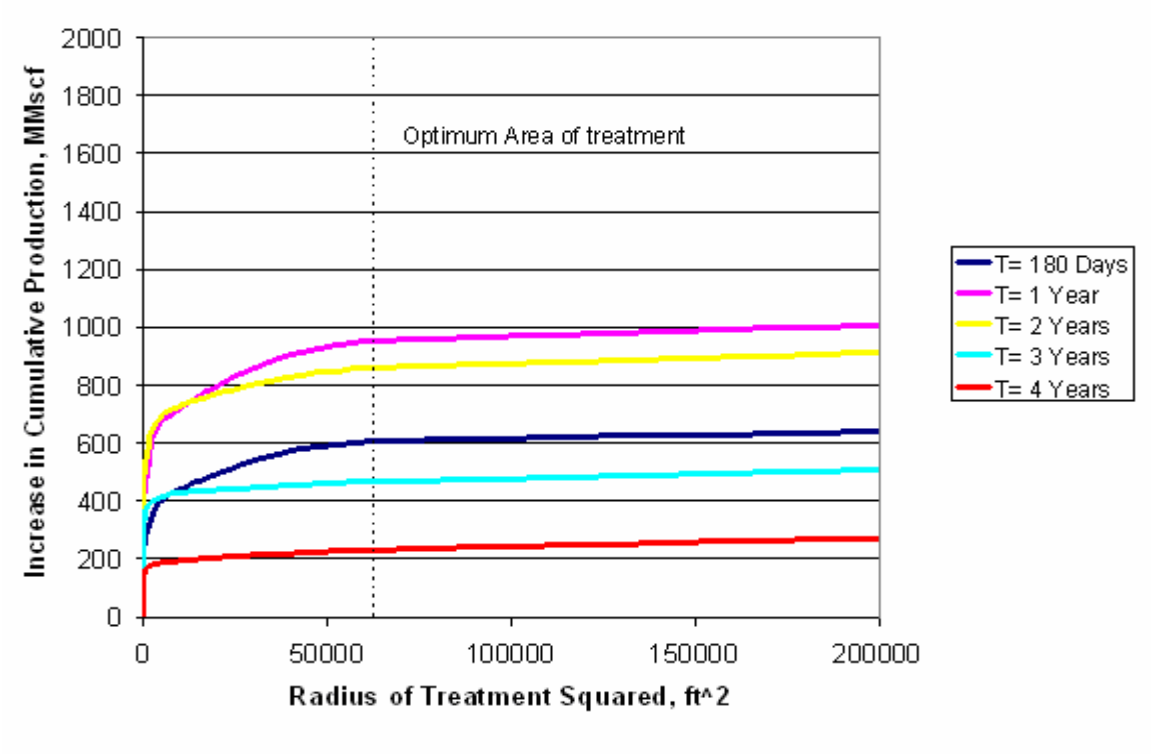

Fig. 4.30 Increment in Cumulative Gas Production vs Radius of Treatment Squared , Fluid C (11 mole % C7+), Swi=0.41, h=10 feet, k=50 mD

4.3.4 Effect of Water Saturation

Fig. 4.31 shows the incremental changes in cumulative gas production with respect to the base case against the treatment radius squared for fluid C at h= 10 feet and

k= 10 mD with irreducible water saturation changed to Swi=0.2. The optimum radius of treatment is 100 feet (R^2= 10000 ft^2). Irreducible water saturation appears to have a serious effect on the optimum radius of treatment.

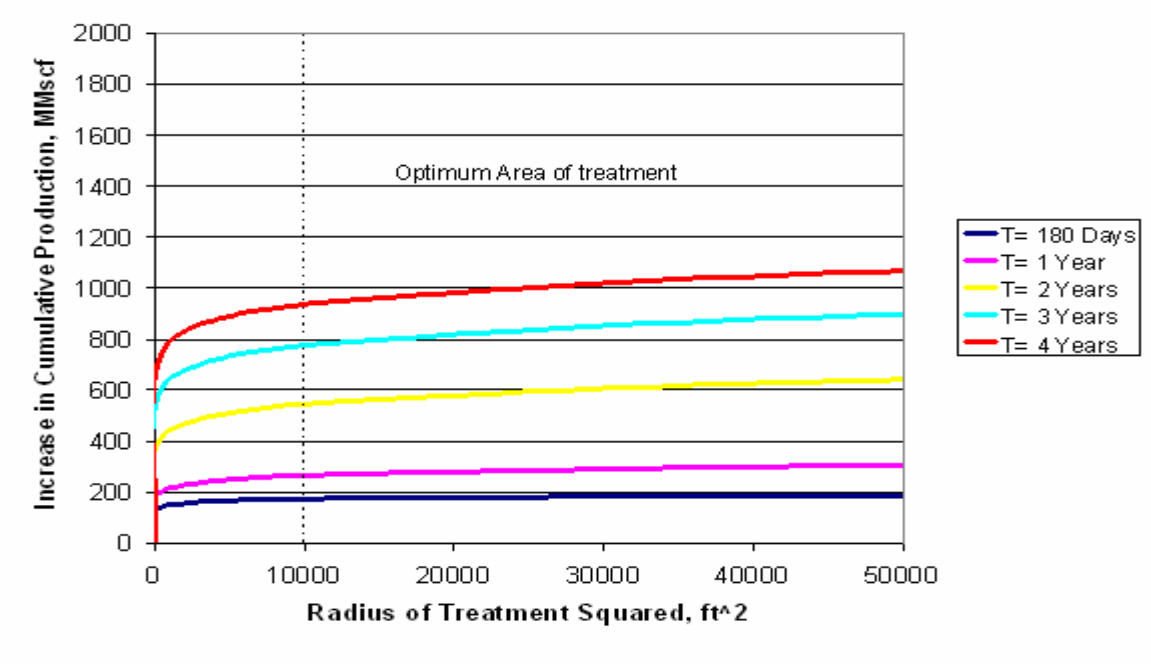

Fig. 4.31 Increment in Cumulative Gas Production vs Radius of Treatment Squared , Fluid C (11 mole % C7+), Swi=0.2, h=10 feet, k=10 mD

4.3.5 Effect on Fluid Composition

Fig. 4.32 shows the increases in incremental cumulative gas production with respect to the base case against the treatment radius squared for fluid B at Swi=0.2, h= 10 feet and k= 10 mD. The optimum radius is 200 feet (R^2= 40000 ft^2): at radii above this value the increases in incremental cumulative gas production are minimal.

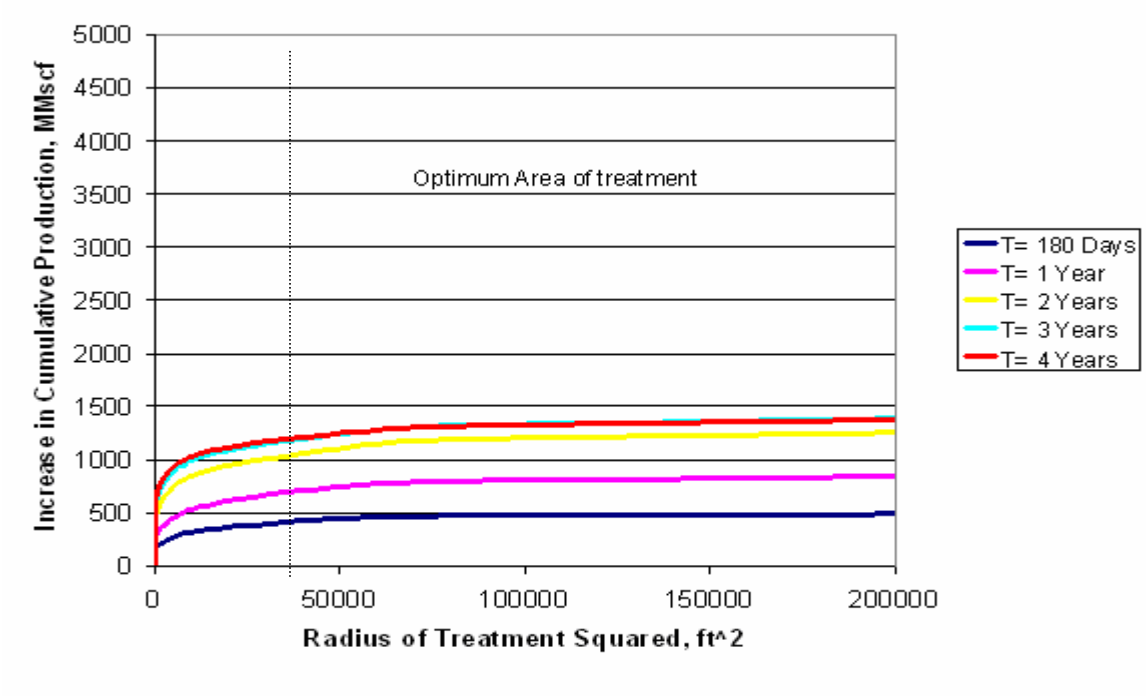

Fig. 4.32 Increment in Cumulative Gas Production vs Radius of Treatment Squared , Fluid B (8 mole % C7+), Swi=0.41, h=10 feet, k=10 mD

Fig. 4.33 shows the increases in incremental cumulative gas production with respect to the base case against the treatment radius squared for fluid A at Swi=0.2, h= 10 feet and k= 10 mD. The optimum radius is 100 feet (R^2= 10000 ft^2). Thus the composition of the reservoir gas, represented by the mole percent of heptanes plus, has an important effect on the optimum radius of treatment.

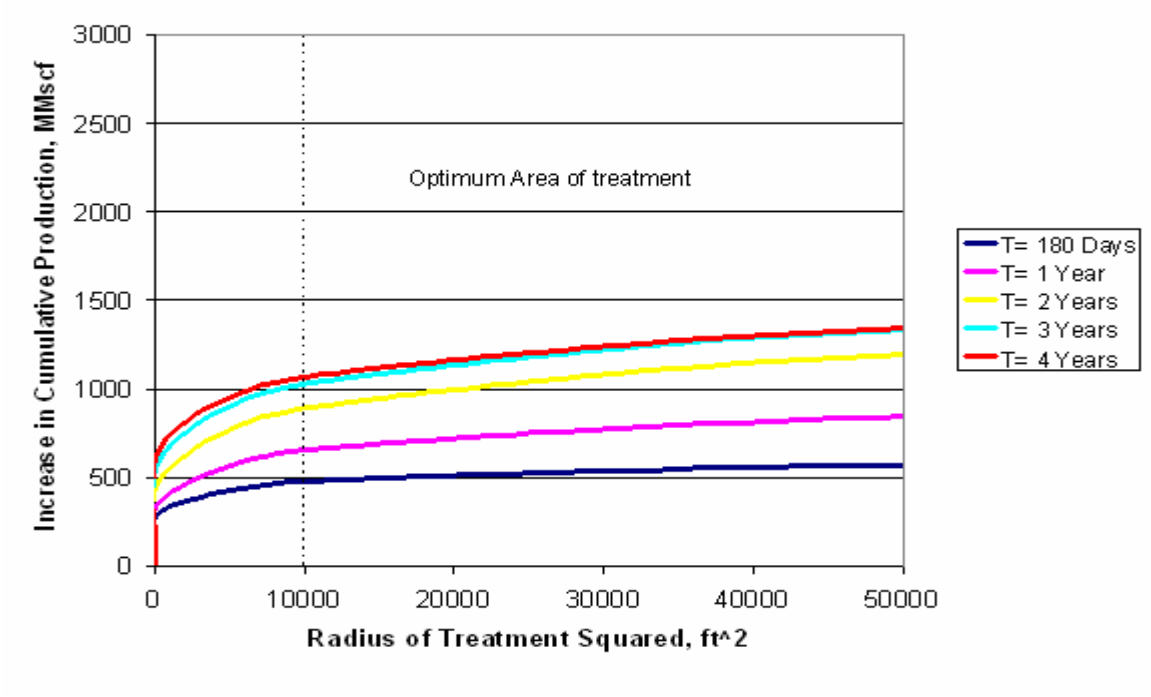

Fig. 4.33 Increment in Cumulative Gas Production vs Radius of Treatment Squared , Fluid A (4 mole % C7+), Swi=0.41, h=10 feet, k=10 mD

Appendix D shows the gas production rates, the cumulative gas productions over time, and the increases in the incremental cumulative gas production over the radii of treatment squared for the all the cases studied.

4.3.6 Effect of the Tubing Diameter

The base value of tubing diameter in this study was 4.5 inches. This section will examine the effect of the size of the tubing on the optimum radii of treatment. For this section only fluid B will be considered with tubing diameters of 3.5 , 2.875 and 2.375 inches. Irreducible water saturations of 41 and 20 % will be investigated. The results show that the tubing diameter does not affect the optimum radii of treatment.

Fig 4.34 shows the increase in cumulative gas production for the case of a tubing diameter of 2.375 inches.

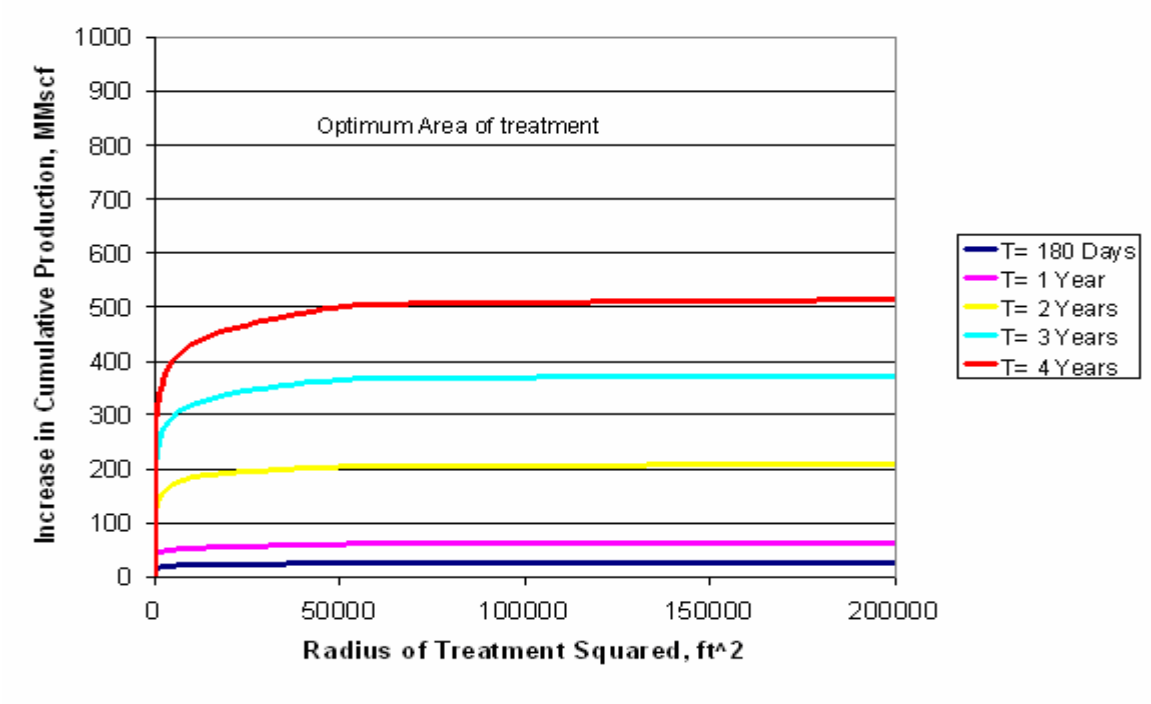

Fig. 4.34 Increase in Cumulative Gas Production vs Time for Fluid B (4 mole % C7+), Swi=0.41, h=10 feet, 10 mD, Tub Diam= 2.375 inches

Fig. 4.34 shows that the optimum radius of treatment does not change due to a change in tubing diameter, and it continues to be 200 feet as shown in Fig 4.32.

Appendix E shows the results obtained for the other tubing sizes and irreducible water saturations.

4.3.7 Summary of the Expected Increase in Gas and Condensate Production

As discussed in the previous sections the determination of the radius of investigation depends mainly on the composition of the reservoir fluid and the irreducible water saturation in the reservoir and it is not sensitive to the permeability or the reservoir thickness. **Table 4.1** summarizes the optimum treatment radii for the different conditions. **Table 4.2** and **Table 4.3** summarize the improvements in cumulative gas and condensate at the optimum radii of treatment for 10 and 50 mD respectively considering that the wells produce to an abandonment production rate of 1 MMscf/d. **Table 4.4** and **Table 4.5** summarize the improvements in cumulative gas and condensate production at the optimum radii of treatment for 10 and 50 mD respectively considering that the wells produce to an abandonment rate of 0.5 MMscf/d.

Table 4.1 Optimum Treatment Radius

Fluid	% C7	Optimum Treatment Radius (ft)	
		Swi=20%	Swi=41%
A	4	25	100
B	8	80	200
C	11	100	250

Table 4.2 Expected Gas and Condensate Recoveries for the Base Case and Optimum Radius of Treatment for 10 mD and Production Limit of 1 MMSCFD

Fluid	C7+ mole%	K mD	h ft	Swi % of pore volume	Optimum ft	Base Case % of GIP	Optimum Case % of GIP	Base Case % of OIP	Optimum Case % of OIP
C	11	10	10	41	250	14.8	31.0	13.7	19.2
C	11	10	50	41	250	31.6	50.8	20.4	24.1
B	8	10	10	41	200	21.9	42.3	19.1	27.4
B	8	10	50	41	200	38.2	54.5	28.2	33.9
A	4	10	10	41	100	29.9	45.2	29.4	37.1
A	4	10	50	41	100	46.0	58.3	40.1	43.0
C	11	10	10	20	100	13.5	22.1	12.7	17.0
C	11	10	50	20	100	36.9	49.0	22.4	24.7
B	8	10	10	20	80	37.2	45.2	27.4	30.3
B	8	10	50	20	80	51.0	54.6	33.5	34.4
A	4	10	10	20	25	41.7	47.0	37.5	39.6
A	4	10	50	20	25	52.3	55.7	42.9	43.5

Table 4.3 Expected Gas and Condensate Recoveries for the Base Case and Optimum Radius of Treatment for 50 mD and Production Limit of 1 MMSCFD

Fluid	C7+ mole%	K mD	h ft	Swi % of pore volume	Optimum ft	Base Case % of GIP	Optimum Case % of GIP	Base Case % of OIP	Optimum Case % of OIP
C	11	50	10	41	250	39.2	54.5	22.9	25.0
C	11	50	50	41	250	50.0	55.4	25.5	26.6
B	8	50	10	41	200	44.9	57.6	31.1	34.4
B	8	50	50	41	200	56.3	58.7	36.1	36.7
A	4	50	10	41	100	49.2	59.5	41.6	43.6
A	4	50	50	41	100	55.9	60.5	44.8	45.9
C	11	50	10	20	100	49.1	52.8	24.7	25.1
C	11	50	50	20	100	53.3	54.1	26.1	26.1
B	8	50	10	20	80	52.1	55.2	33.7	34.7
B	8	50	50	20	80	57.4	57.4	36.1	36.1
A	4	50	10	20	25	53.2	56.4	43.1	43.5
A	4	50	50	20	25	59.0	59.0	45.8	45.8

Table 4.4 Expected Gas and Condensate Recoveries for the Base Case and Optimum Radius of Treatment for 10 mD and Production Limit of 0.5 MMSCFD

Fluid	C7+ mole %	K mD	h ft	Swi % of pore volume	Optimum ft	Base Case % of GIP	Optimum Case % of GIP	Base Case % of OIP	Optimum Case % of OIP
C	11	10	10	41	250	19.4	39.4	16.9	21.6
C	11	10	50	41	250	37.2	53.9	22.7	24.8
B	8	10	10	41	200	24.7	45.6	20.9	28.9
B	8	10	50	41	200	43.8	57.0	30.6	34.5
A	4	10	10	41	100	34.3	50.5	33.0	39.5
A	4	10	50	41	100	48.4	59.3	41.3	43.3
C	11	10	10	20	100	21.2	35.9	17.1	21.4
C	11	10	50	20	100	42.6	49.8	23.4	24.7
B	8	10	10	20	80	43.8	50.2	30.3	32.7
B	8	10	50	20	80	54.6	55.6	34.8	34.8
A	4	10	10	20	25	46.9	51.8	37.5	39.6
A	4	10	50	20	25	55.0	57.5	44.5	44.6

Table 4.5 Expected Gas and Condensate Recoveries for the Base Case and Optimum Radius of Treatment for 50 mD and Production Limit of 0.5 MMSCFD

Fluid	C7+ mole %	K mD	h ft	Swi % of pore volume	Optimum ft	Base Case % of GIP	Optimum Case % of GIP	Base Case % of OIP	Optimum Case % of OIP
C	11	50	10	41	250	44.0	54.8	24.1	25.1
C	11	50	50	41	250	53.1	55.6	26.0	26.6
B	8	50	10	41	200	48.8	58.2	32.6	34.5
B	8	50	50	41	200	57.0	58.7	36.4	36.7
A	4	50	10	41	100	52.5	60.9	43.1	43.9
A	4	50	50	41	100	58.7	60.5	45.7	45.9
C	11	50	10	20	100	51.7	53.6	25.2	25.3
C	11	50	50	20	100	54.4	54.4	26.2	26.2
B	8	50	10	20	80	55.9	57.1	35.1	35.2
B	8	50	50	20	80	57.6	57.6	36.3	36.3
A	4	50	10	20	25	57.7	58.9	44.7	44.7
A	4	50	50	20	25	59.9	59.9	46.1	46.1

Table 4.2 to 4.5, shows that the difference between the optimum and the non treated case appears to be larger when the reservoir permeability and thickness are low. The improvement expected from the treatment also appears to increase when the heptanes plus composition of the reservoir fluid, the irreducible water saturation and the abandonment production rate are larger.

Table 4.2 shows that for fluid C (11 mole % C7+), h=10 feet, Swi=0.41, k=10mD and production limit of 1 MMscf/d, the increase in cumulative gas production with respect to the base case is 109 %, and the increase in cumulative condensate production is 40 %; these values are the maximum increases found using the treatment.

Table 4.5 shows that for fluid A (4 mole % C7+), h=50ft, Swi=0.2, 50mD and production limit of 0.5 MMscf/d, the increase in cumulative gas and condensate production is zero.

4.3.8 Methodology Proposed

Since the optimum radius of treatment does not depend on the permeability nor the height of the reservoir, the following method is proposed for determining the radius of treatment of a reservoir.

- With the initial gas-oil ratio of the reservoir and the Eq. 1 the C7+ content of the reservoir fluid can be determined.

$$Y = 13224.2 * X^{-0.856313} \quad \text{.....Eq.1.}$$

Where Y is the C7+ in mole percent of the reservoir fluid and X is the initial gas-oil ratio in $\frac{scf}{STB}$.

- With the heptanes plus mole composition and the irreducible water saturation from the log analysis, the optimum radius of treatment can be obtained from **Fig. 4.35.**

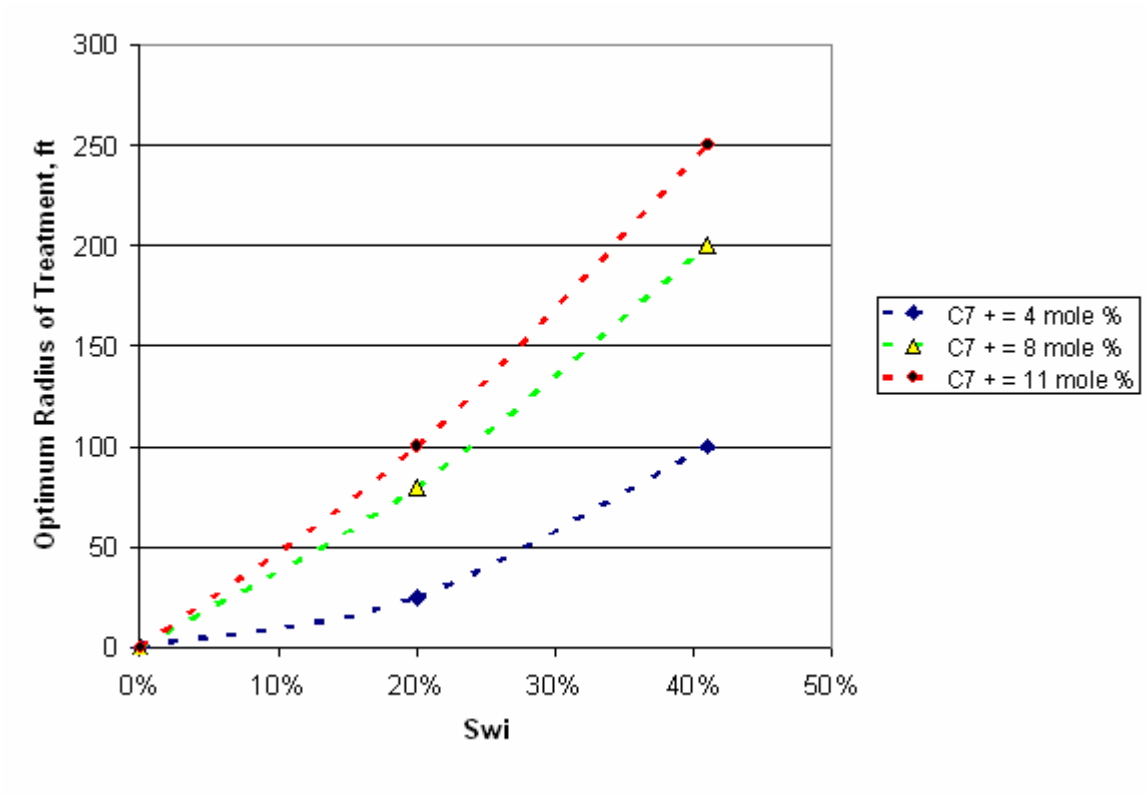

Fig. 4.35 Optimum Radius of Treatment vs Irreducible Water Saturation

CHAPTER V

SUMMARY AND CONCLUSIONS

5.1 Summary

A one-well radial compositional reservoir simulation study was performed to observe the effect of the condensate liquid deposition near wellbore in gas condensate reservoirs. Three fluids were considered at 4, 8 and 11 mole % of heptanes plus composition and 2 irreducible water saturations (20 and 41%) were used to verify the limit of permeability where production is affected by the condensate deposition.

Then, a reservoir with two regions was considered: a treated region near wellbore where the water saturation was reduced to zero and the outer reservoir region where water saturation was unchanged. Several radii of treatment were considered and the optimum radii of the near wellbore zone were selected based on the increase of cumulative gas production compared to the cumulative production of the non-treated case.

5.2 Conclusions

The main conclusions of this study are:

1. When permeabilities are larger than 100 mD, the formation of the condensate in a cylinder around the wellbore will not affect the final cumulative gas recovery of the reservoir.
2. As the values of reservoir thickness increase the lower limit of permeability for which the reservoir reserves might decrease could be less than 100 mD depending on the fluid composition.

3. The optimum radius of treatment will depend on the heptanes plus content of the reservoir fluid and the irreducible water saturation. The permeability and the reservoir thickness appear to have no effect in the optimal radius of treatment.
4. The improvement of cumulative gas and condensate production at the optimum radius of treatment depends on the heptanes plus content of the fluid, the irreducible water saturation, the permeability and the thickness of the reservoir. Higher values of kh are expected to have a lower incremental improvement in gas and condensate recoveries.
5. The cumulative recoveries will also be affected by the limit at which the well is expected to stop producing.
6. Higher values of heptanes plus content of the reservoir fluid and higher values of irreducible water saturation of the reservoir the treatment of the reservoir will give a larger increase in cumulative production with respect to the non-treated case.
7. The effect of removal the water near the wellbore causes acceleration of reserves in every case.
8. The effect of removal the water near the wellbore causes an increase in the cumulative gas and condensate production for values of kh less than 2500 mD-ft.
9. The maximum increase at the optimum radius of treatment with respect to the non-treated case in cumulative gas production found was 109 % and the maximum cumulative condensate production found was 40 %.
10. The optimum radius of treatment can be obtained given the irreducible water saturation and the initial producing gas to oil ratio..
11. The Tubing size appears not to affect the optimum radius of treatment.

NOMENCLATURE

Swi= irreducible water saturation

So = oil saturation

Somax= maximum oil saturation (at Swi)

h = reservoir thickness, feet

k=absolute permeability, mili Darcy

krow=relative permeability to oil in water, dimensionless

krw=relative permeability to water , dimensionless

krog=relative permeability to oil in gas at Swi, dimensionless

krg=relative permeability to gas at Swi, dimensionless

p=pressure, psia

r=radius of the treated zone, feet

Subscripts

av = average

g = gas

i = irreducible

o = oil

w = water

REFERENCES

1. Deddy, A., Kaczorowski, N.J. and Srinivas, B.: "Production Performance of a Retrograde Gas Reservoir: A Case Study of the Arun Field", paper SPE 28749 presented at the SPE Asia Pacific Oil & Gas Conference, Melbourne, Australia, 7-10 November, 1994.

2. Barnum, R.S., Brinkman, F.P., Richardson, T.W. and Spillette, A.G.: "Gas Condensate Reservoir Behaviour: Productivity and Recovery Reduction Due to Condensation", paper SPE 30767 presented at the SPE Annual Technical Conference & Exhibition, Dallas, Texas, 22-25 October, 1995.

3. Dehane, A., Tiab, D., Osisanya, S.O.: "Performance of Horizontal Wells in Gas-Condensate Reservoirs, Djebel Bissa Field, Algeria", paper SPE 65504 presented at the SPE/Petroleum Society of CIM International Conference on Horizontal Well Technology, Calgary, Canada, 6-8 November, 2000.

4. Wang, X., Valko, P.P. and Economides, M.J.: "Production Impairment and Purpose-Built Design of Hydraulic Fractures in Gas Condensate Reservoirs"; paper SPE 64749 presented at the SPE International Oil and Gas Conference and Exhibition, Beijing, China, 7-10 November, 2000.

5. Ahmed, T., Evans, J., Kwan, R.and Vivian, T.: "Wellbore Liquid Blockage in Gas-Condensate Reservoirs", paper SPE 51050 presented at the SPE Eastern Regional Meeting, Pittsburgh, USA, 9-11 November, 1998.

6. Jamaluddin, A.K.M., Ye, S., Thomas, J., D'Cruz, D. and Nighswander, J.: "Experimental and Theoretical Assestment of Using Propane to Remediate Liquid Buildup in Condensate Reservoirs", paper SPE 71526 presented at the SPE Annual Technical Conference and Exhibition, New Orleans, USA, 30 September- 3 October, 2001.

7. Du, L., Walker, J.G., Pope, G.A., Sharma, M.M. and Wang, P.: "Use of Solvent to Improve the Productivity of Gas Condensate Wells", paper SPE 62935 presented at the SPE Annual Technical Conference and Exhibition, Dallas, Texas, 1-4 October, 2000.

8. Al-Anazi, H.A., Walker, J.G., Pope, G.A., Sharma, M.M., Hackney, D.F.: "A Successful Methanol Treatment in a Gas-Condensate Reservoir: Field Application", paper SPE 80901 presented at the SPE Production and Operations Symposium, Oklahoma City, USA, 22-25 March, 2003.

9. El-Banbi, A.H. and McCain, W.D.,Jr.: "Investigation of Well Productivity in Gas-Condensate Reservoirs", paper SPE 59773 presented at the SPE/CERI Gas Technology Symposium, Calgary, Canada, 3-5 April, 2000.

10. Aguilar, R.A. and McCain, W.D.,Jr.: "An Efficient Tuning Strategy to Calibrate Cubic EOS for Compositional Reservoir Simulation", paper SPE 77382 presented at the SPE Annual Conference and Exhibition, San Antonio, Texas, 29 September- 2 October 2002.

APPENDIX A

DETERMINING THE LIMIT OF THE PERMEABILITY

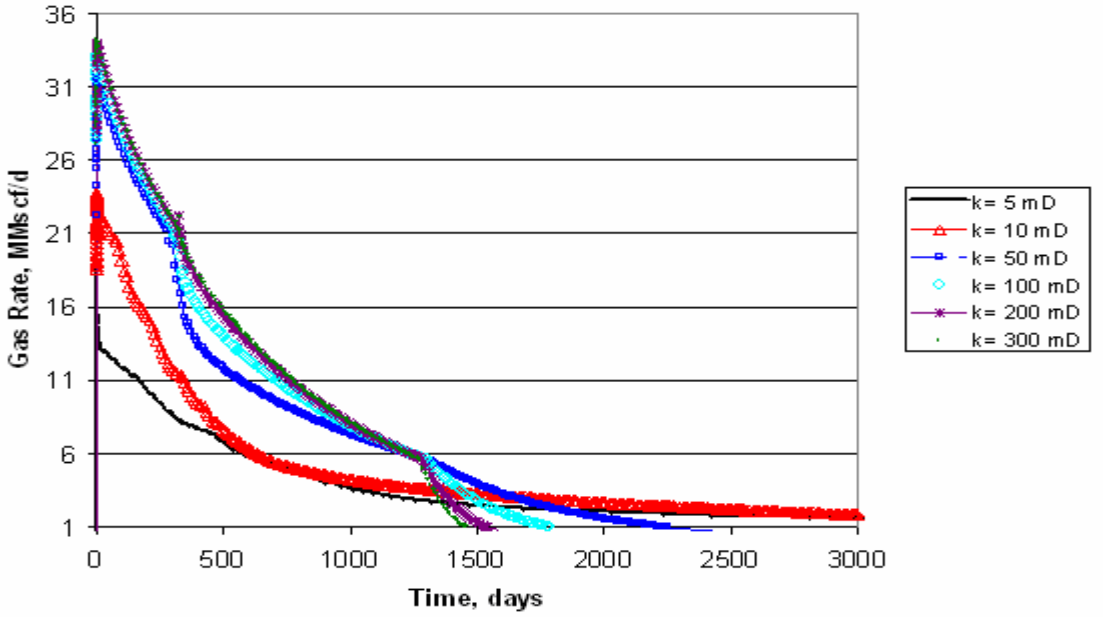

Fig. A.1 Gas Rate vs Time, Fluid A (4 mole % C7+), Swi=0.41, h=50 feet

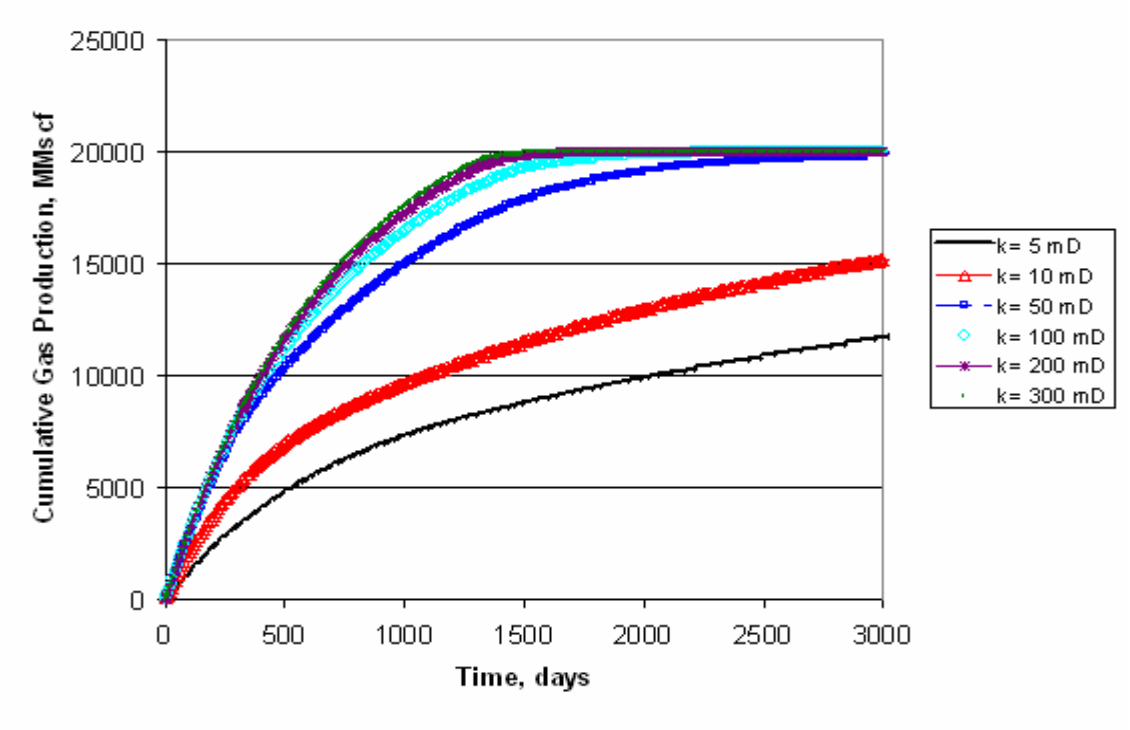

Fig. A.2 Cumulative Gas Production vs Time, Fluid A (4 mole % C7+), Swi=0.41, h=50 feet

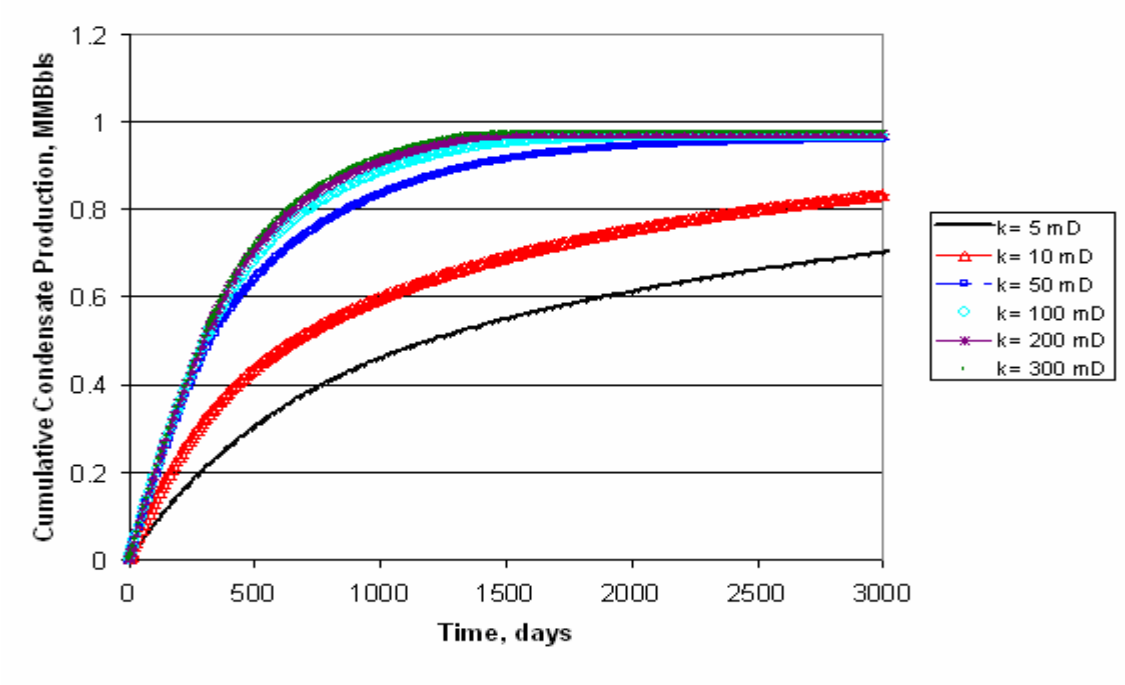

Fig. A.3 Cumulative Condensate Production vs Time, Fluid A (4 mole % C7+), Swi=0.41, h=50 feet

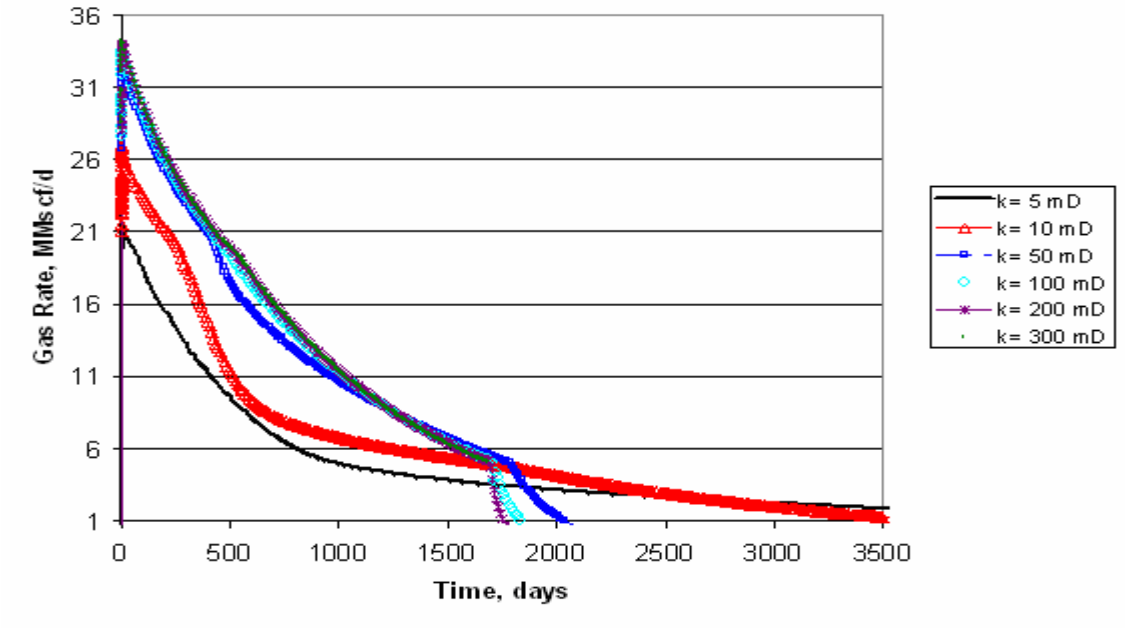

Fig. A.4 Gas Rate vs Time, Fluid A (4 mole % C7+), Swi=0.2, h=50 feet

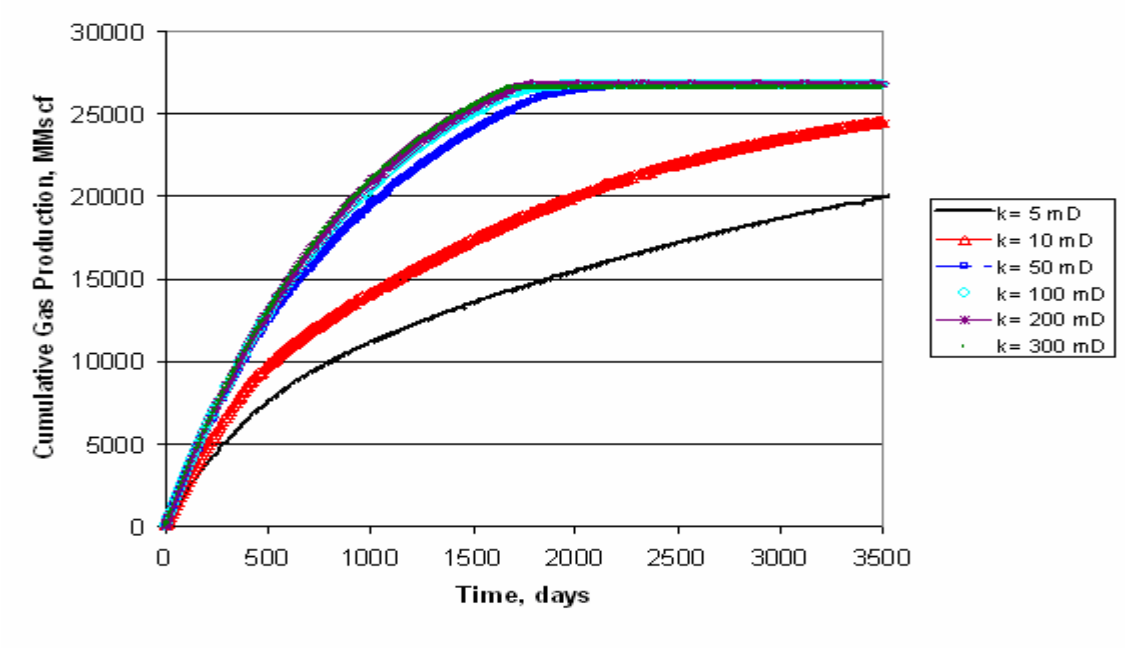

Fig. A.5 Cumulative Gas Production vs Time, Fluid A (4 mole % C7+), Swi=0.2, h=50 feet

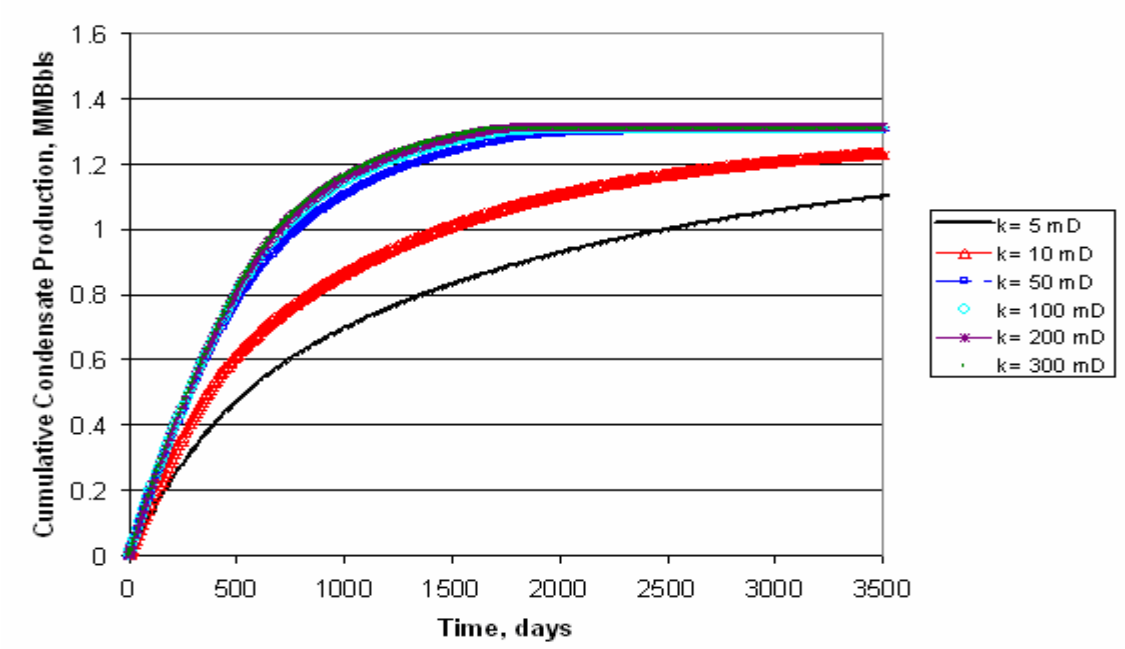

Fig. A.6 Cumulative Condensate Production vs Time, Fluid A (4 mole % C7+), Swi=0.2, h=50 feet

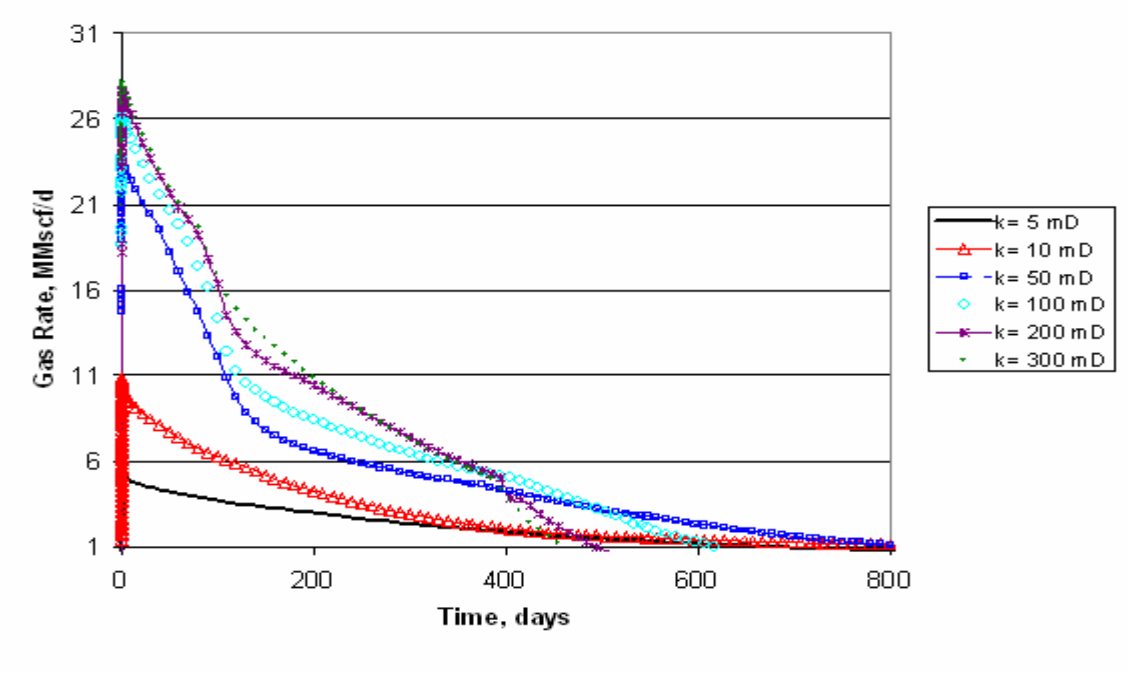

Fig. A.7 Gas Rate vs Time, Fluid A (4 mole % C7+), Swi=0.2, h=10 feet

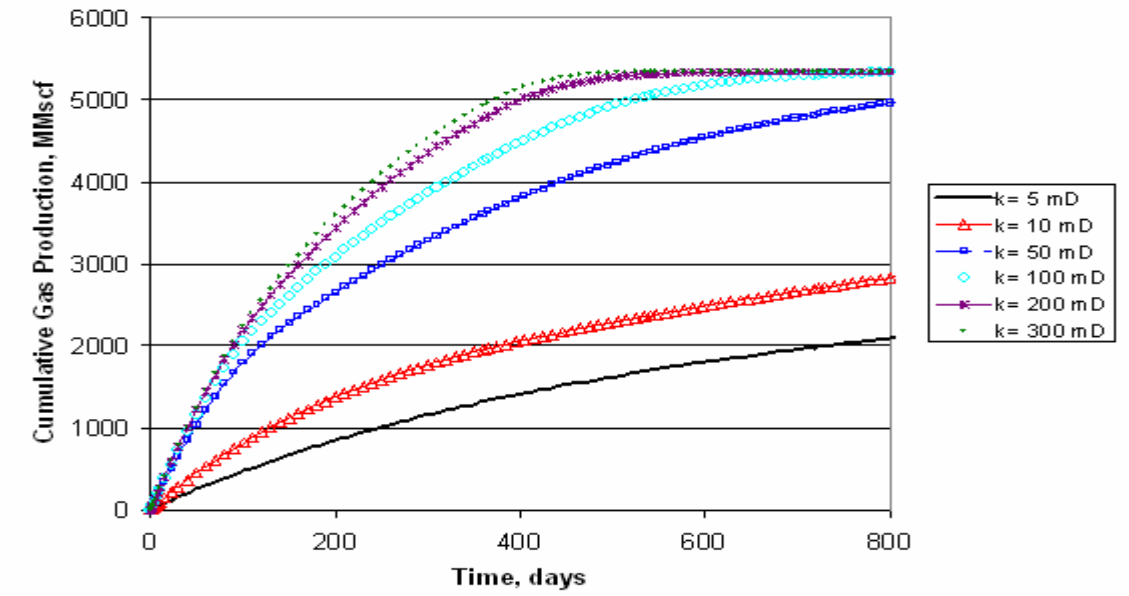

Fig. A.8 Cumulative Gas Production vs Time, Fluid A (4 mole % C7+), Swi=0.2, h=10 feet

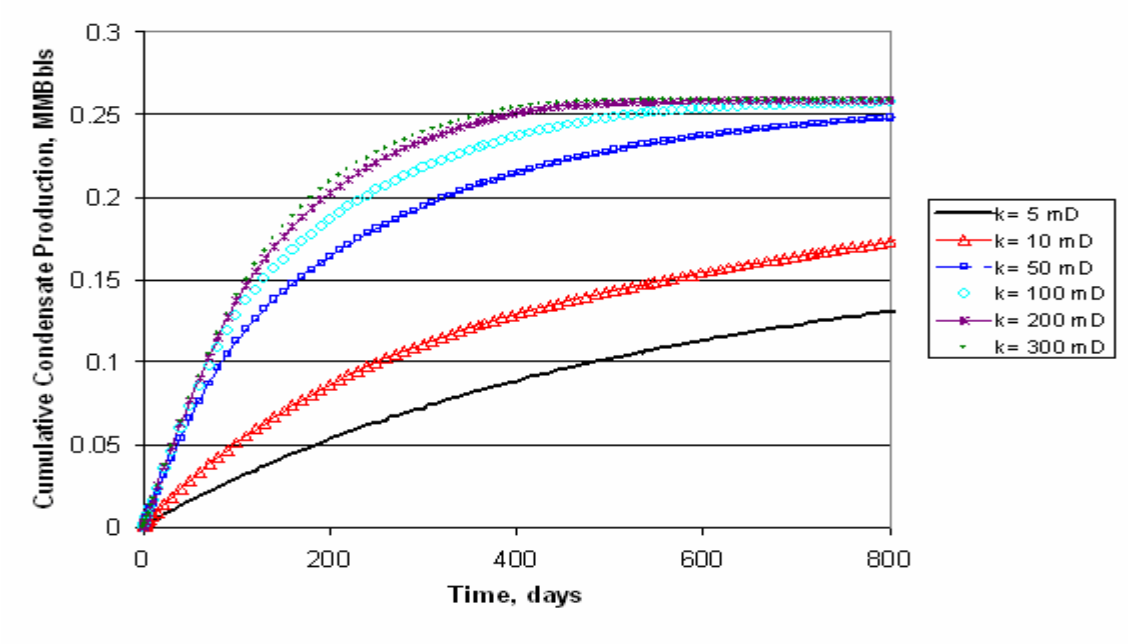

Fig. A.9 Cumulative Condensate Production vs Time, Fluid A (4 mole % C7+), Swi=0.2, h=10 feet

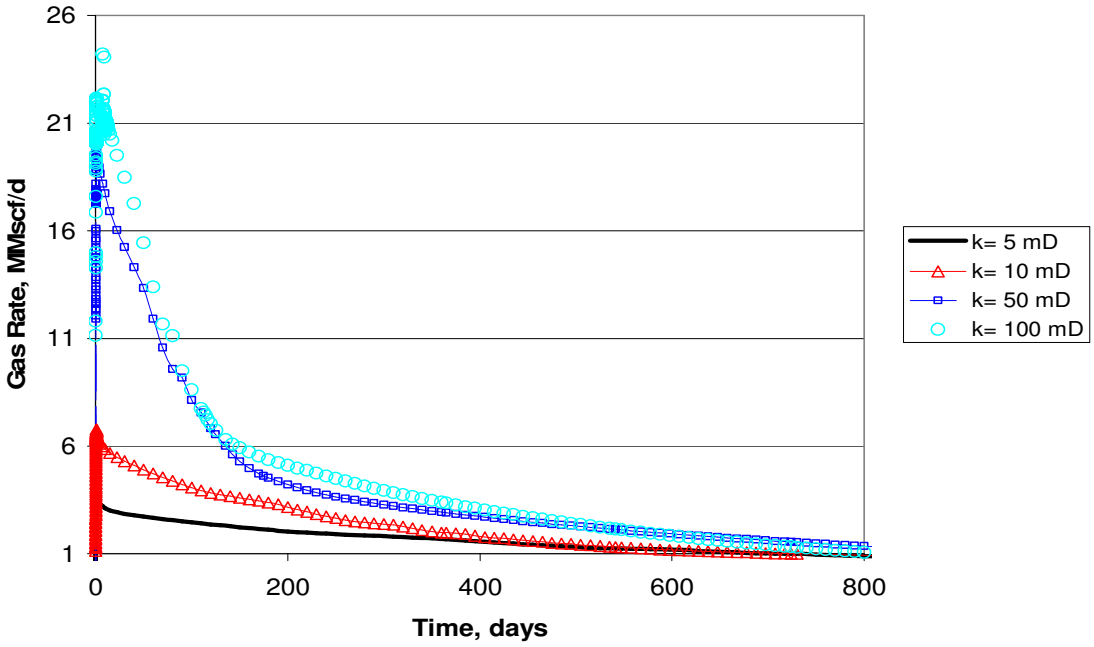

Fig. A.10 Gas Rate vs Time, Fluid A (4 mole % C7+), Swi=0.41, h=10 feet

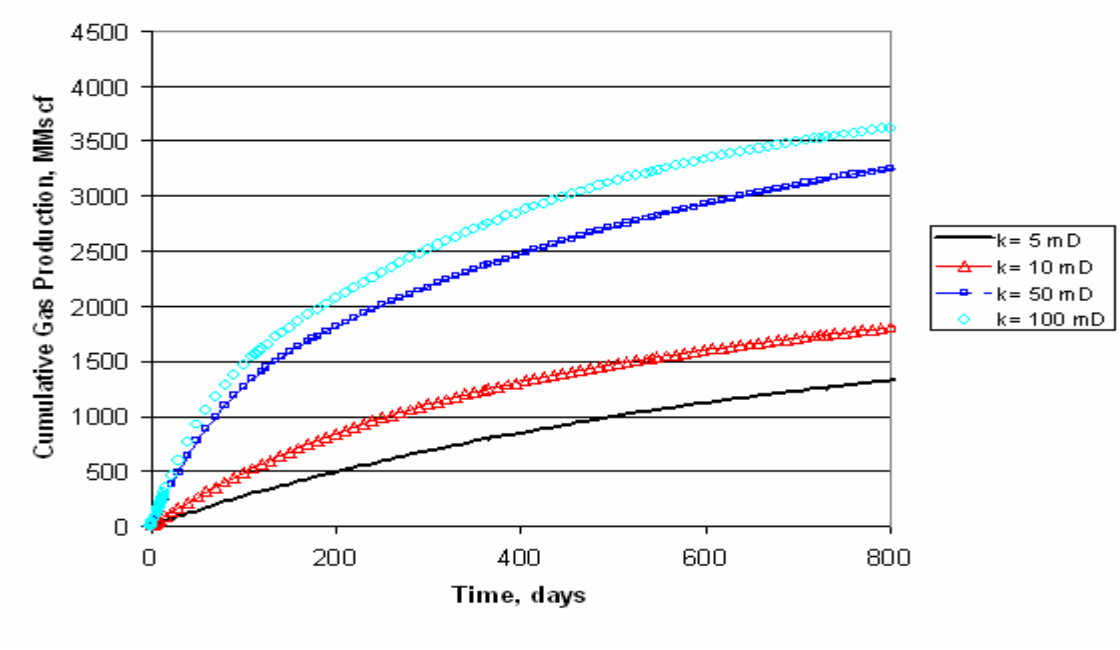

Fig. A.11 Cumulative Gas Production vs Time, Fluid A (4 mole % C7+), Swi=0.41, h=10 feet

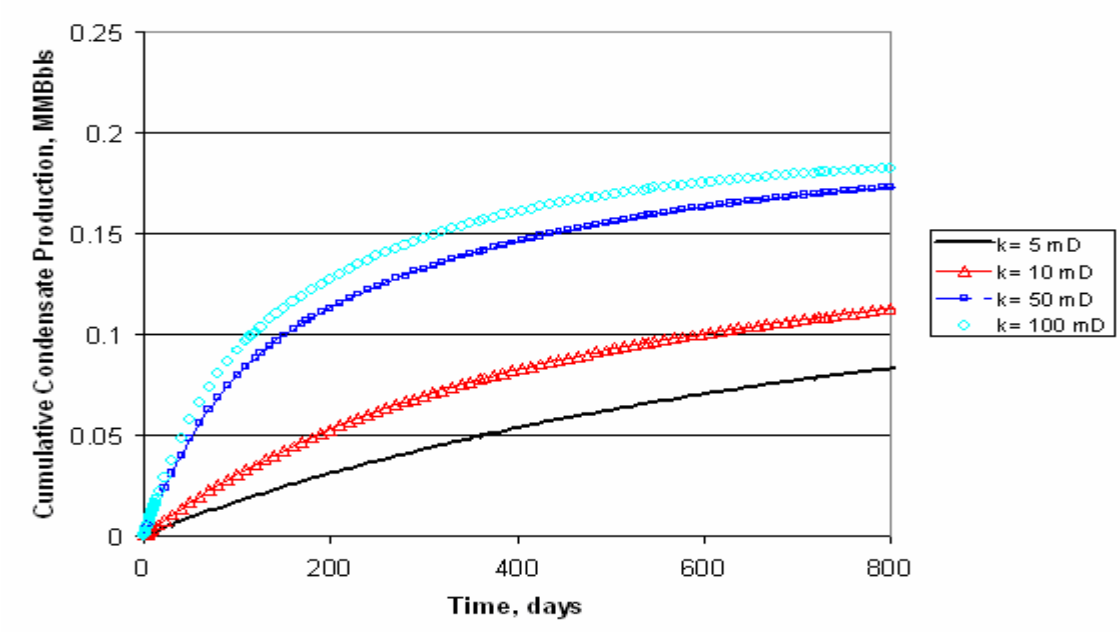

Fig. A.12 Cumulative Condensate Production vs Time, Fluid A (4 mole % C7+), Swi=0.41, h=10 feet

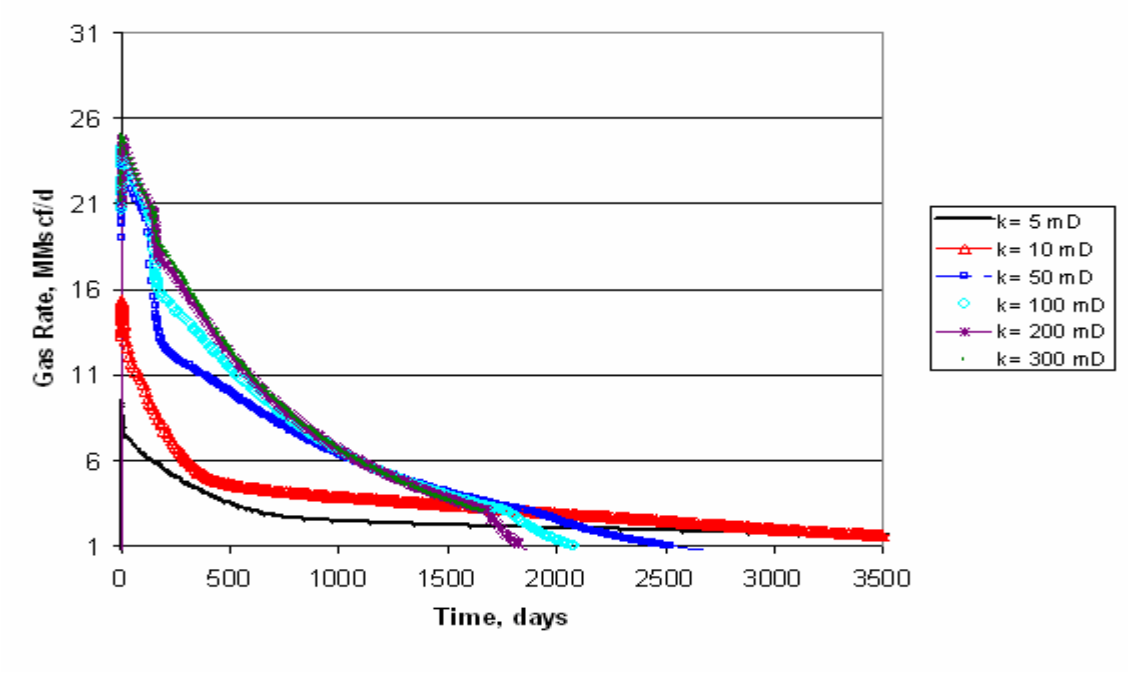

Fig. A.13 Gas Rate vs Time, Fluid B (8 mole % C7+), Swi=0.41, h=50 feet

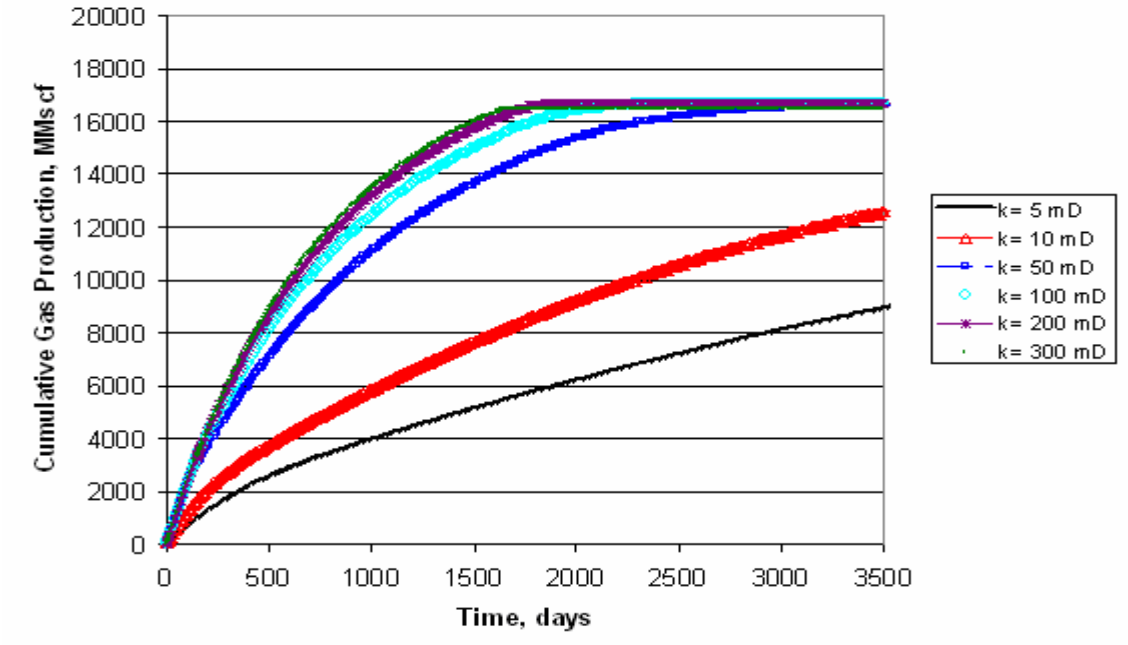

Fig. A.14 Cumulative Gas Production vs Time, Fluid B (8 mole % C7+), Swi=0.41, h=50 feet

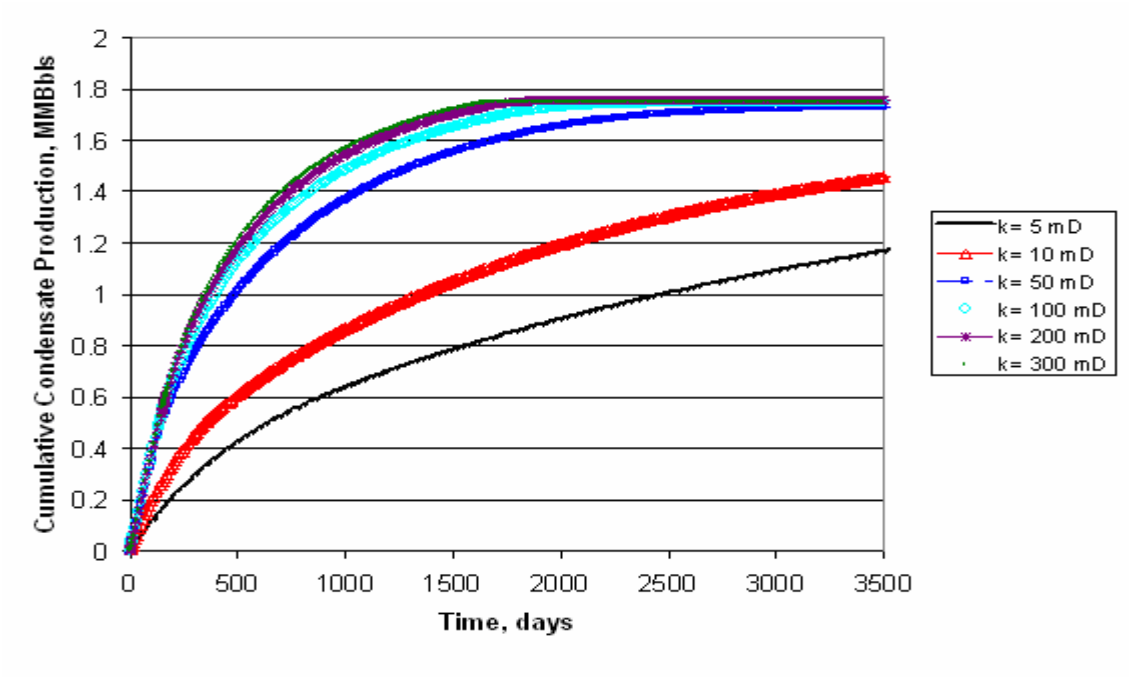

Fig. A.15 Cumulative Condensate Production vs Time, Fluid B (8 mole % C7+), Swi=0.41, h=50 feet

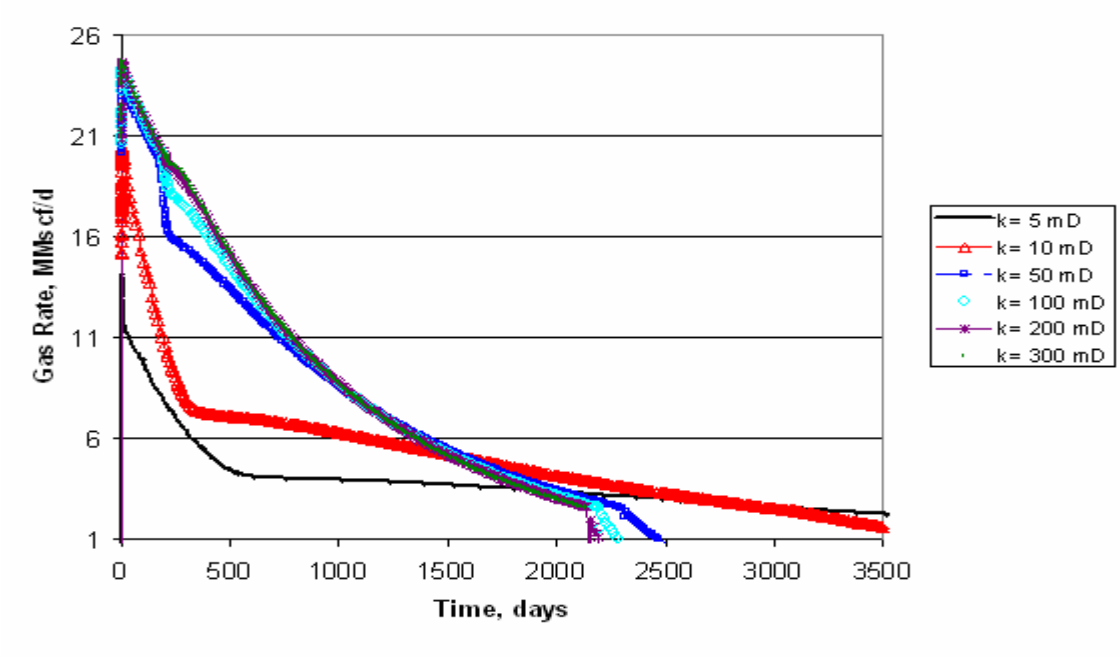

Fig. A.16 Gas Rate vs Time, Fluid B (8 mole % C7+), Swi=0.2, h=50 feet

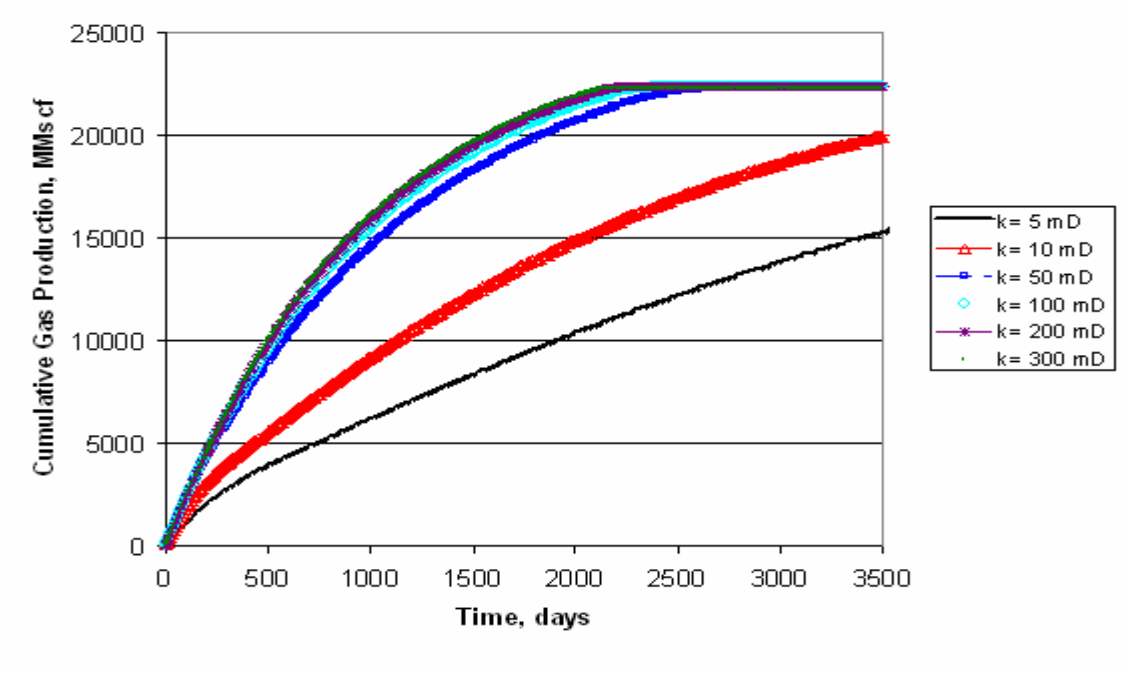

Fig. A.17 Cumulative Gas Production vs Time, Fluid B (8 mole % C7+), Swi=0.2, h=50 feet

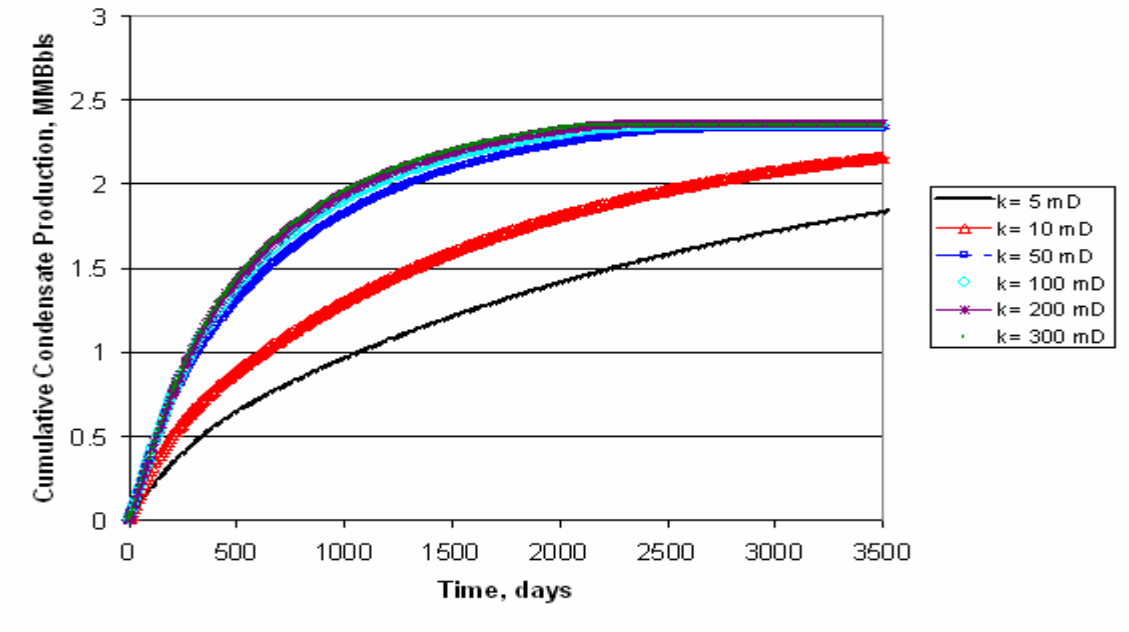

Fig. A.18 Cumulative Condensate Production vs Time, Fluid B (8 mole % C7+), Swi=0.2, h=50 feet

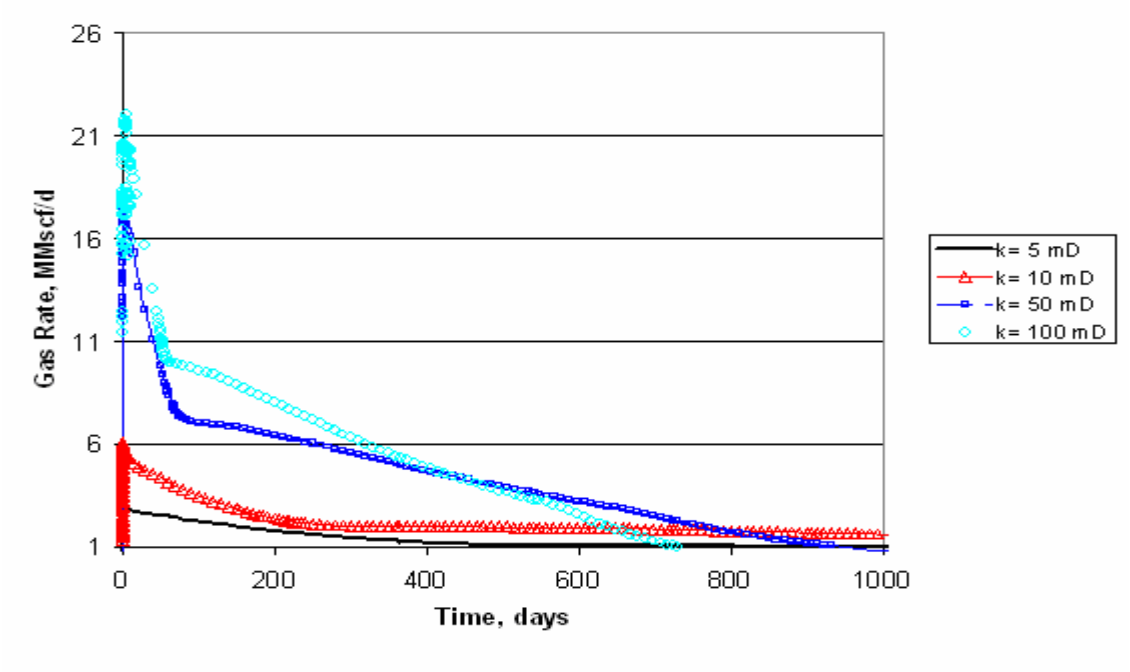

Fig. A.19 Gas Rate vs Time, Fluid B (8 mole % C7+), Swi=0.2, h=10 feet

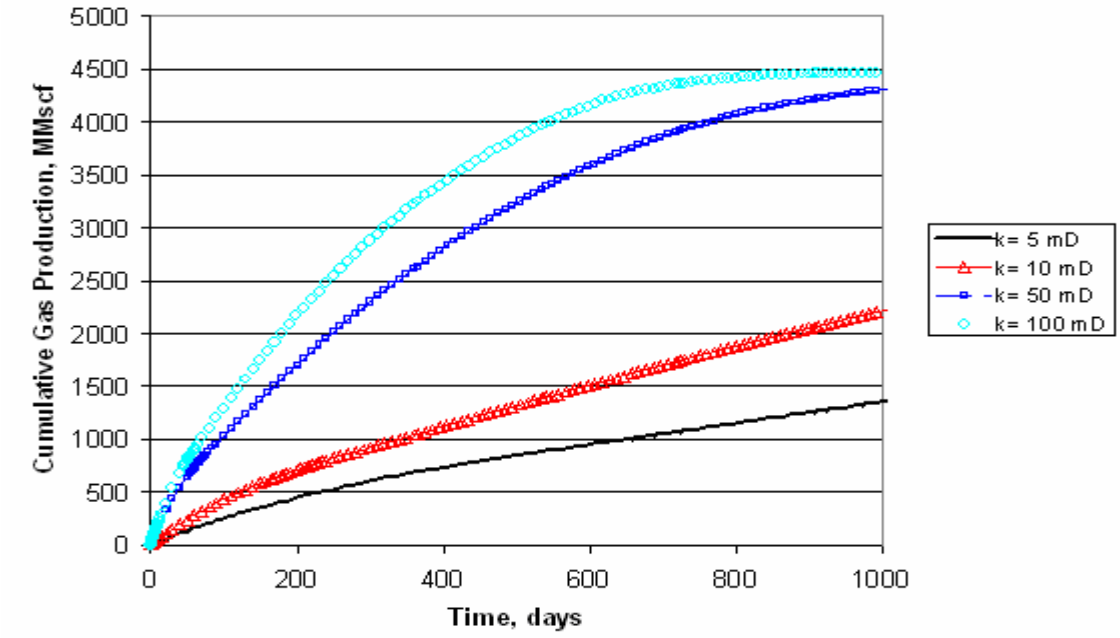

Fig. A.20 Cumulative Gas Production vs Time, Fluid B (8 mole % C7+), Swi=0.2, h=10 feet

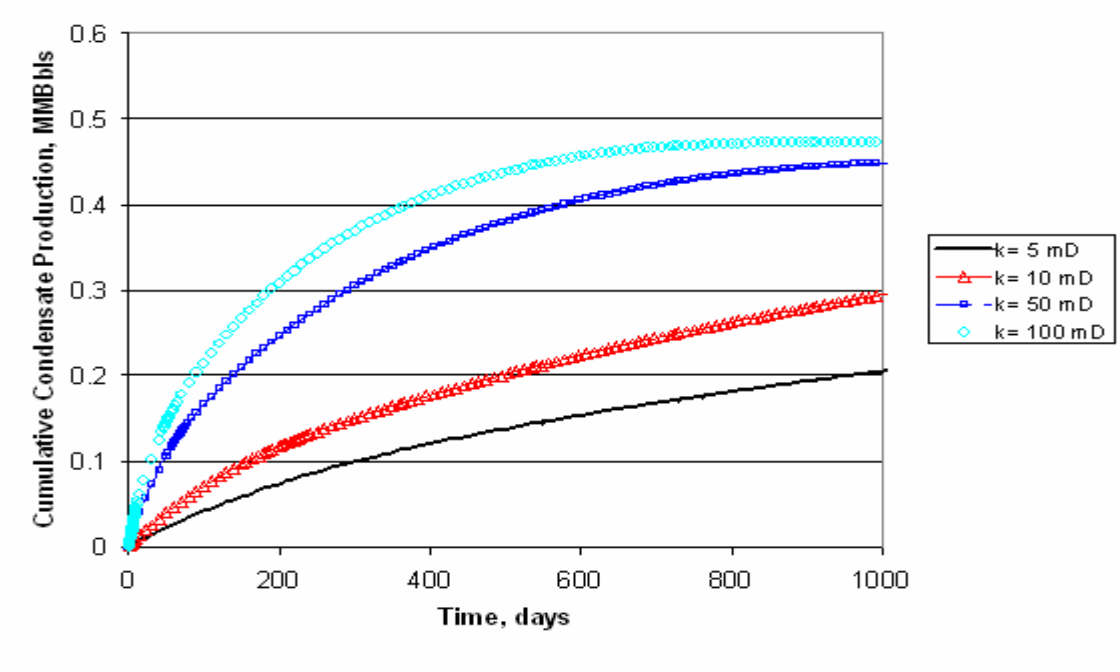

Fig. A.21 Cumulative Condensate Production vs Time, Fluid B (8 mole % C7+), Swi=0.2, h=10 feet

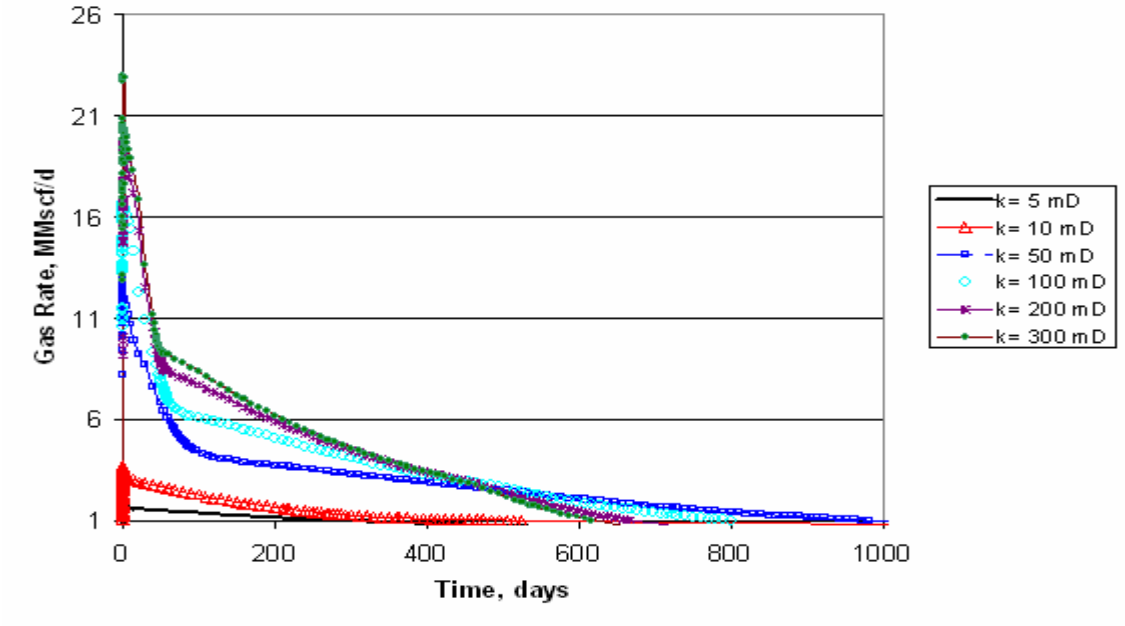

Fig. A.22 Gas Rate vs Time, Fluid B (8 mole % C7+), Swi=0.41, h=10 feet

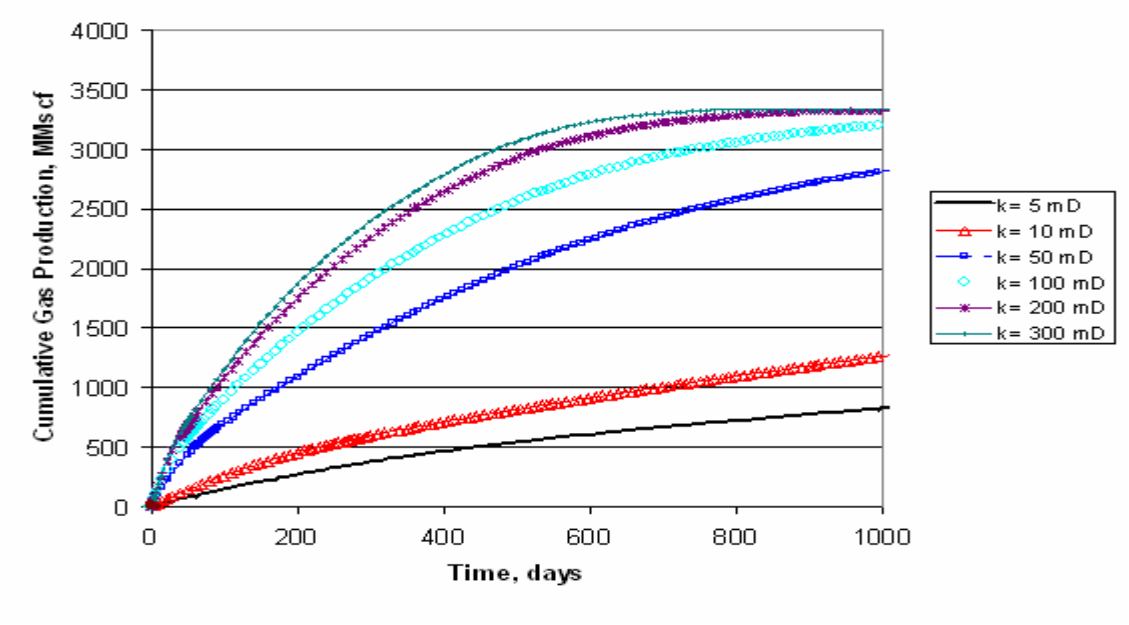

Fig. A.23 Cumulative Gas Production vs Time, Fluid B (8 mole % C7+), Swi=0.41, h=10 feet

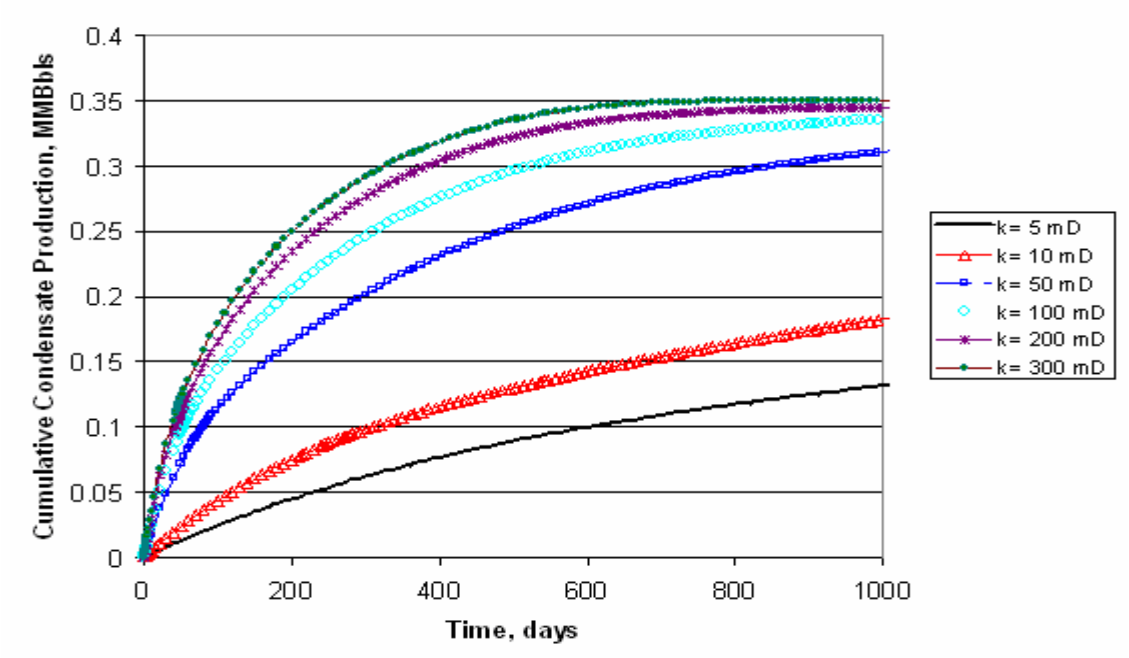

Fig. A.24 Cumulative Condensate Production vs Time, Fluid B (8 mole % C7+), Swi=0.41, h=10 feet

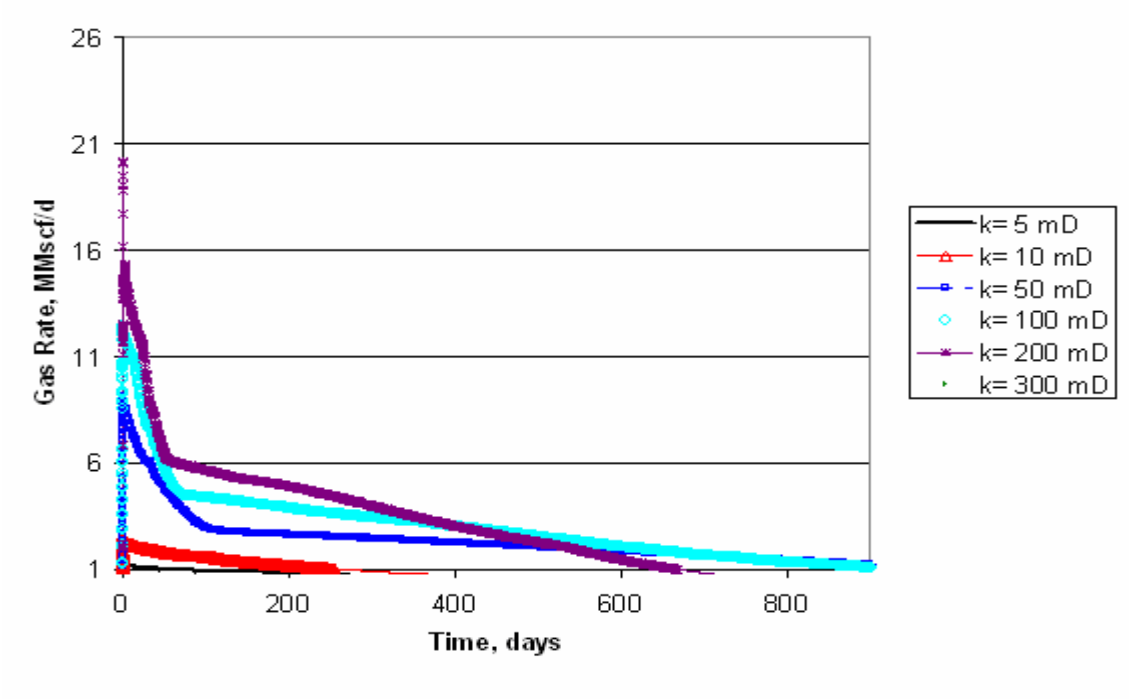

Fig. A.25 Gas Rate vs Time, Fluid C (11 mole % C7+), Swi=0.41, h=10 feet

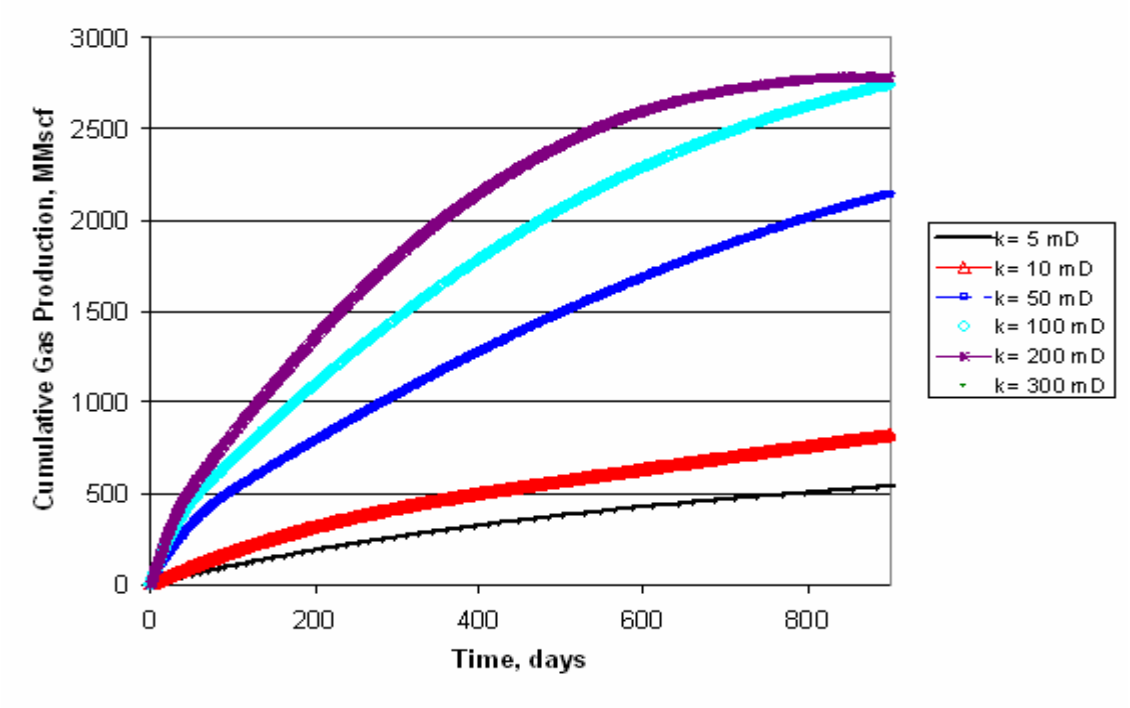

Fig. A.26 Cumulative Gas Production vs Time, Fluid C (11 mole % C7+), Swi=0.41,h=10ft

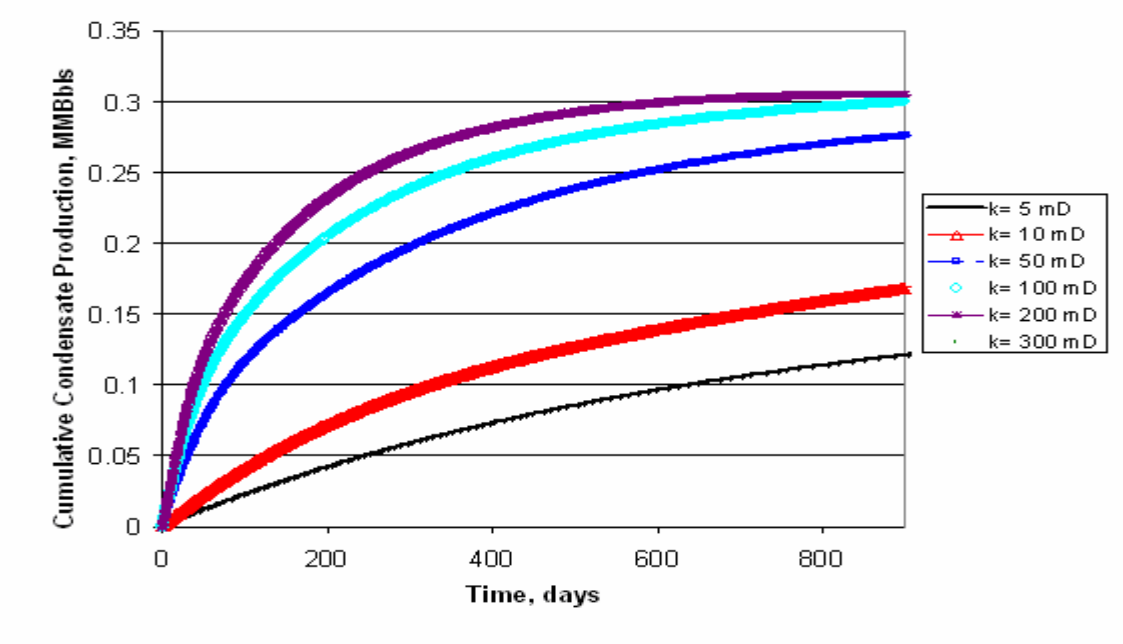

Fig. A.27 Cumulative Condensate Production vs Time, Fluid C (11 mole % C7+), Swi=0.41, h=10 feet

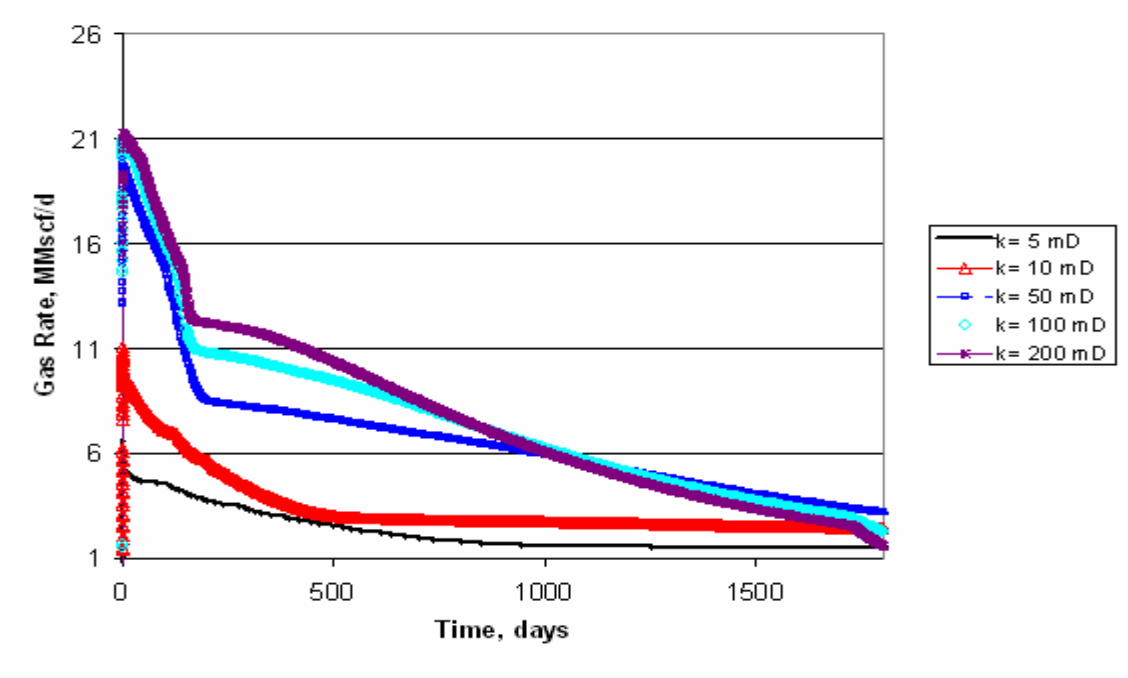

Fig. A.28 Gas Rate vs Time, Fluid C (11 mole % C7+), Swi=0.41, h=50 feet

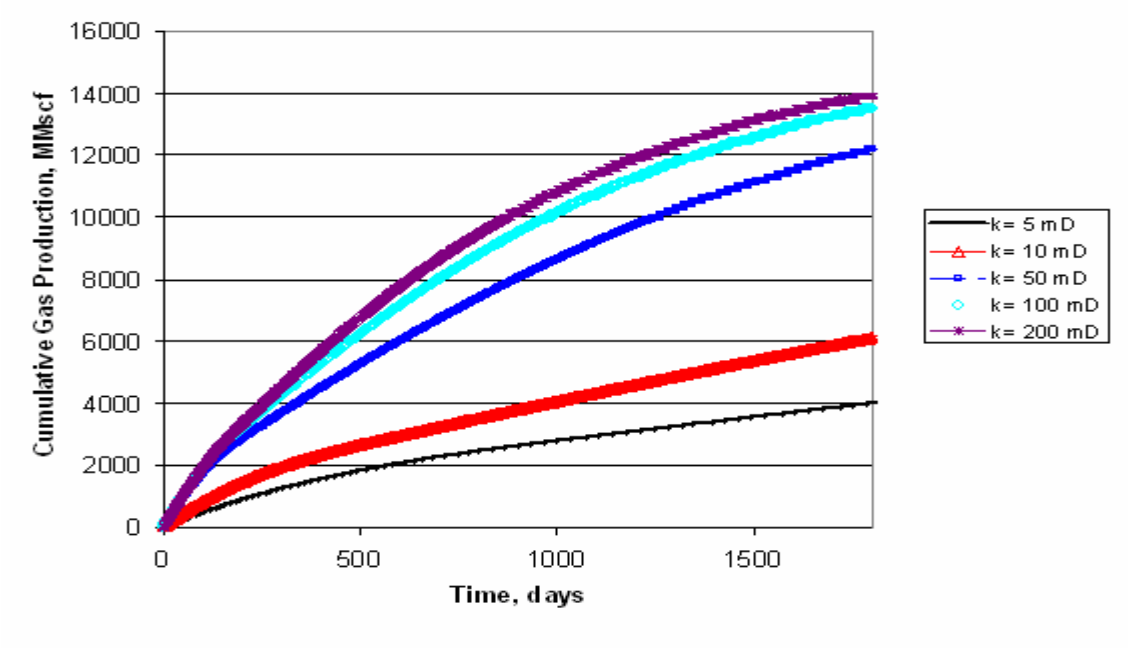

Fig. A.29 Cumulative Gas Production vs Time, Fluid C(11 mole % C7+), Swi=0.41, h=50 feet

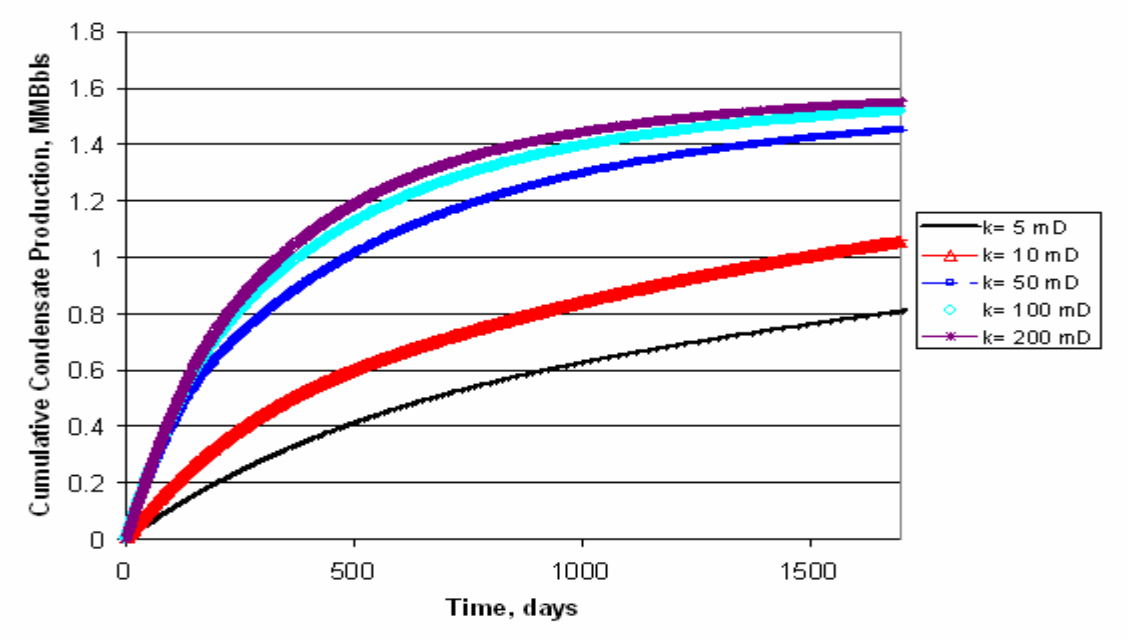

Fig. A.30 Cumulative Condensate Production vs Time, Fluid C (11 mole % C7+), Swi=0.41, h=50 feet

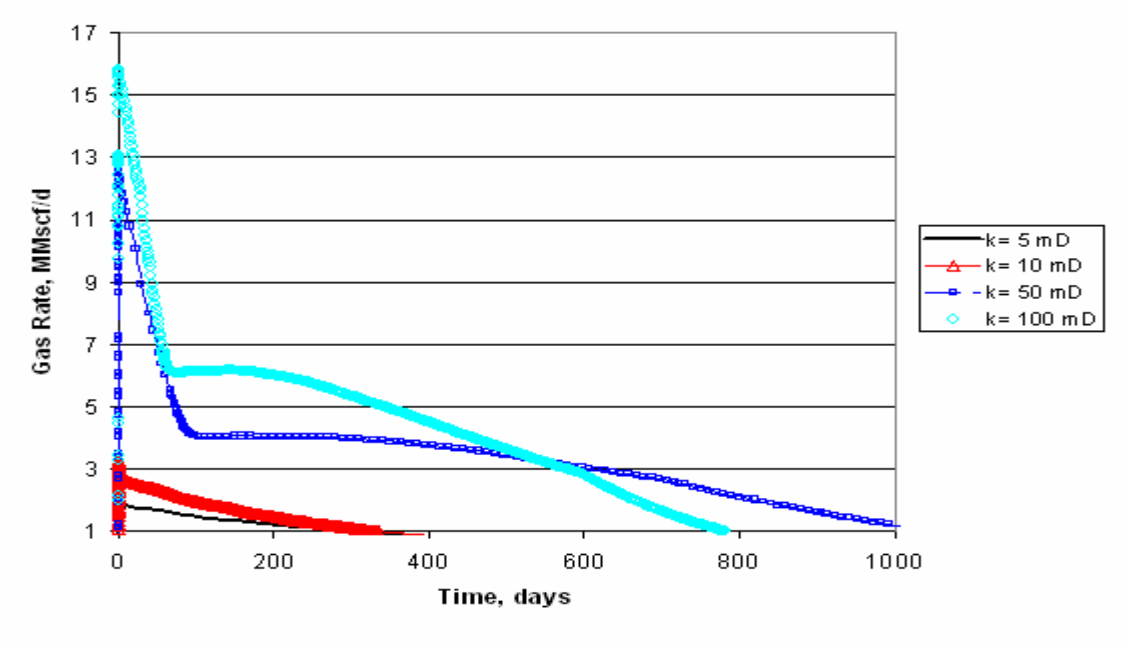

Fig. A.31 Gas Rate vs Time, Fluid C (11 mole % C7+), Swi=0.2, h=10 feet

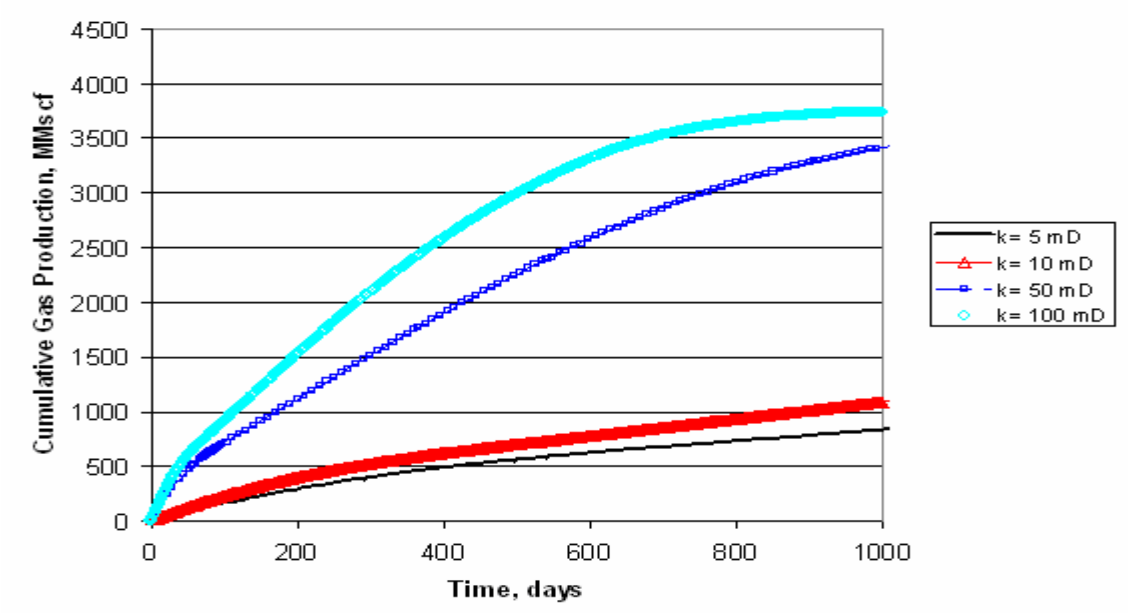

Fig. A.32 Cumulative Gas Production vs Time, Fluid C (11 mole % C7+), Swi=0.2, h=10 feet

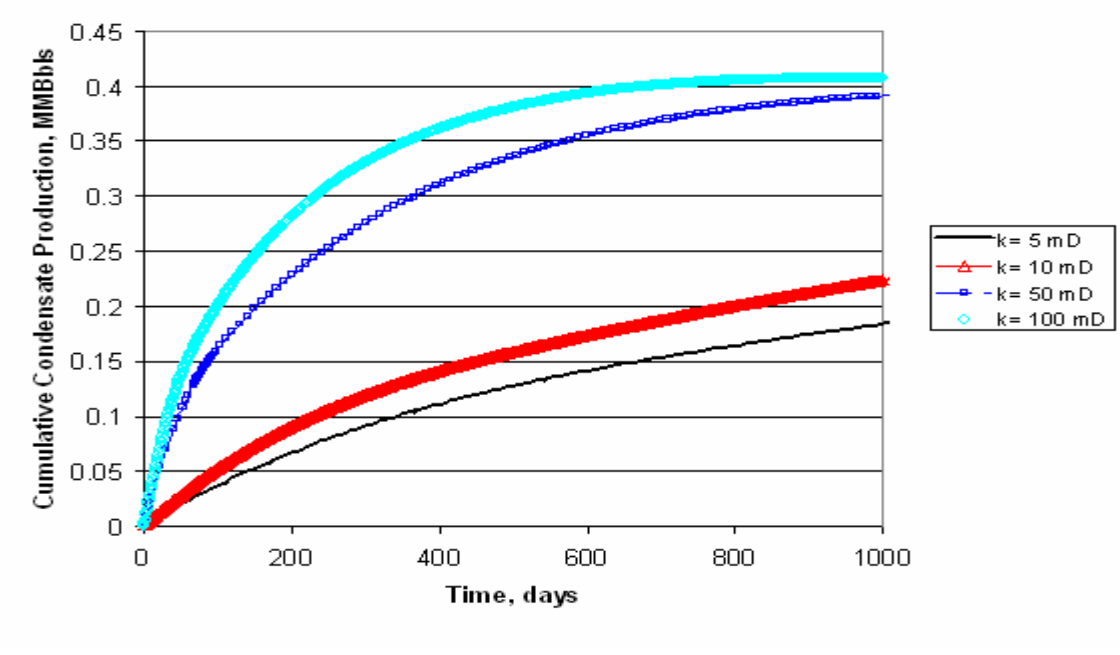

Fig. A.33 Cumulative Condensate Production vs Time, Fluid C (11 mole % C7+), Swi=0.2, h=10 feet

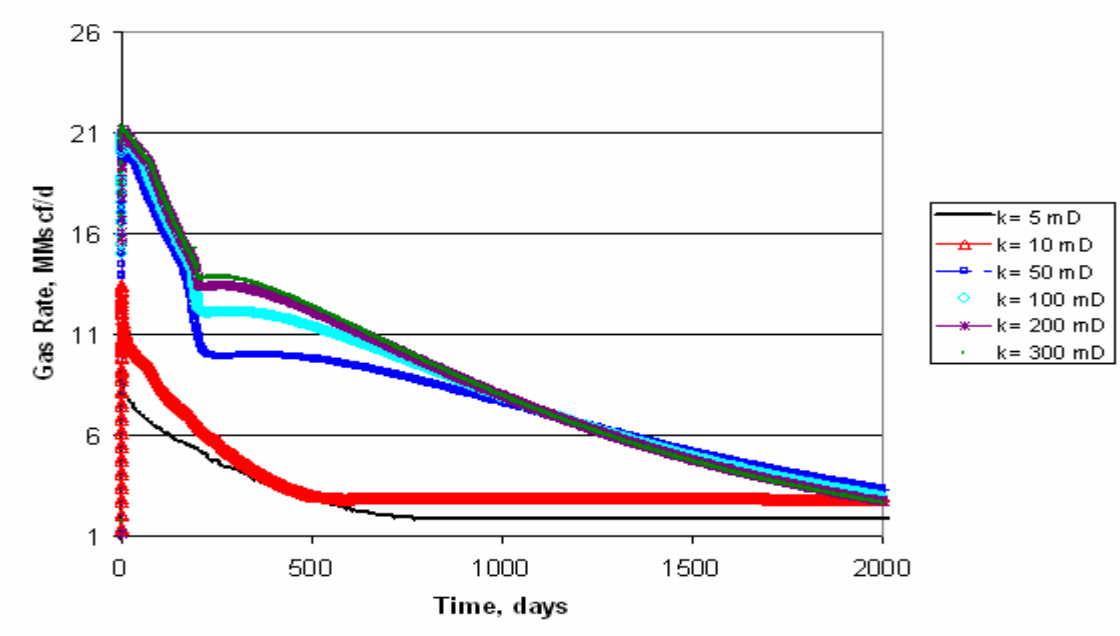

Fig. A.34 Gas Rate vs Time, Fluid C (11 mole % C7+), Swi=0.2, h=50 feet

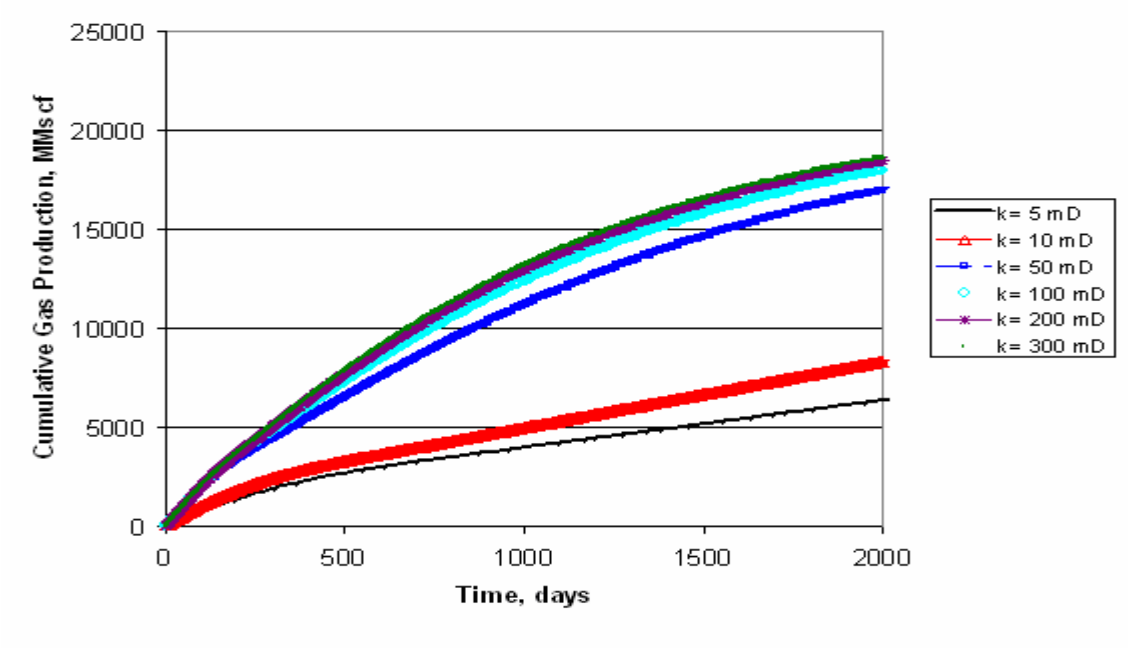

Fig. A.35 Cumulative Gas Production vs Time, Fluid C (11 mole % C7+), Swi=0.2, h=50 feet

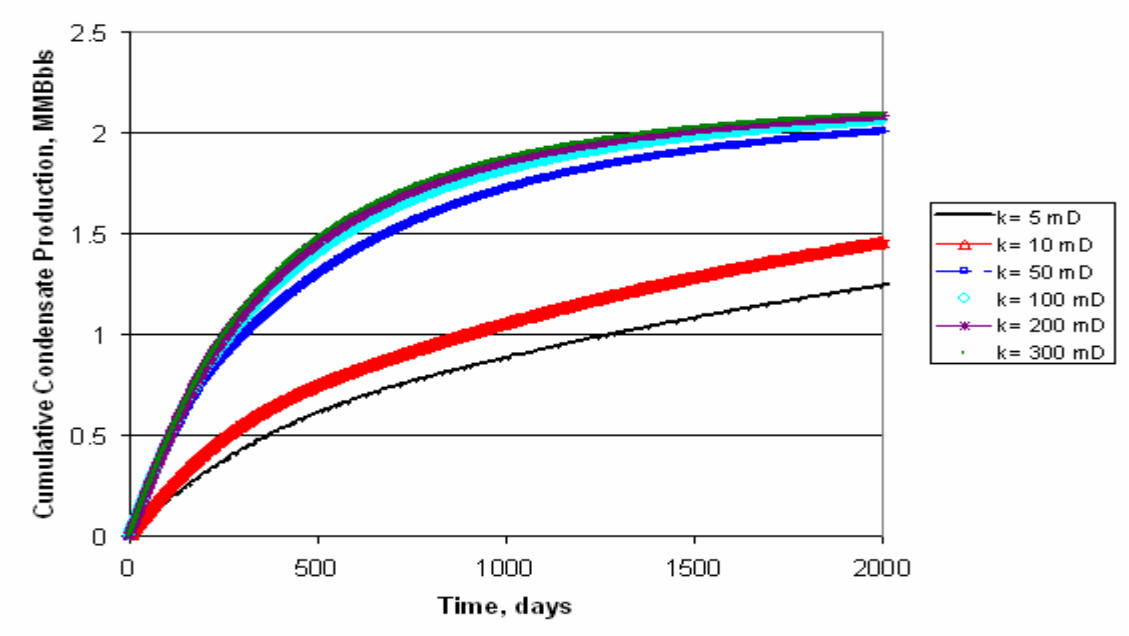

Fig. A.36 Cumulative Condensate Production vs Time, Fluid C (11 mole % C7+), Swi=0.2, h=50 feet

APPENDIX B

INCREASE IN THE INITIAL GAS PERMEABILITY

One of the possible explanations why the reservoir is performing in this behavior is encountered when looking at Darcy's Law. For example in this case Rw=0.375 feet Re1=100 feet , Re= 2500, K1= 1 (permeability of the region near the wellbore), K2=0.7 (permeability of the reservoir without treatment)

Applying the Darcy equation for radial flow for the case without treatment

$$Krgas(eq) = \frac{\ln\left(\frac{\mathrm{Re}}{Rw}\right)}{\frac{\ln\left(\frac{\mathrm{Re}1}{Rw}\right)}{K1} + \frac{\ln\left(\frac{\mathrm{Re}}{\mathrm{Re}1}\right)}{K2}} = \frac{\ln\left(\frac{2500}{0.375}\right)}{\frac{\ln\left(\frac{100}{0.375}\right)}{1} + \frac{\ln\left(\frac{2500}{100}\right)}{0.7}} = 0.864 \text{ .....(Eq. B.1)}$$

For the case with more than 2 regions the equation would be:

$$Krgas(eq) = \frac{\ln\left(\frac{\mathrm{Re}}{Rw}\right)}{\frac{\ln\left(\frac{\mathrm{Re}1}{Rw}\right)}{K1} + \frac{\ln\left(\frac{\mathrm{Re}2}{\mathrm{Re}1}\right)}{K2} + \frac{\ln\left(\frac{\mathrm{Re}3}{\mathrm{Re}1}\right)}{K2}} \text{ .....(Eq. B.2)}$$

APPENDIX C

DESCRIPTION OF THE PROPOSED SOLUTION

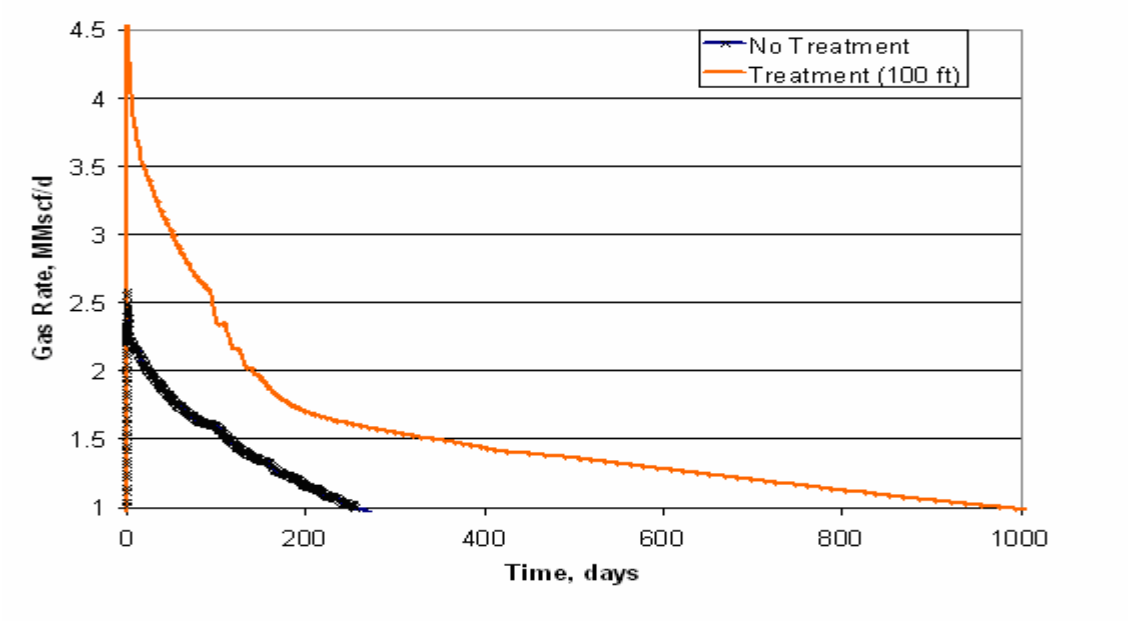

Fig. C.1 Gas Production Rate vs Time for Fluid C (11 mole % C7+), Swi=0.41, h=10 feet, k=10 mD

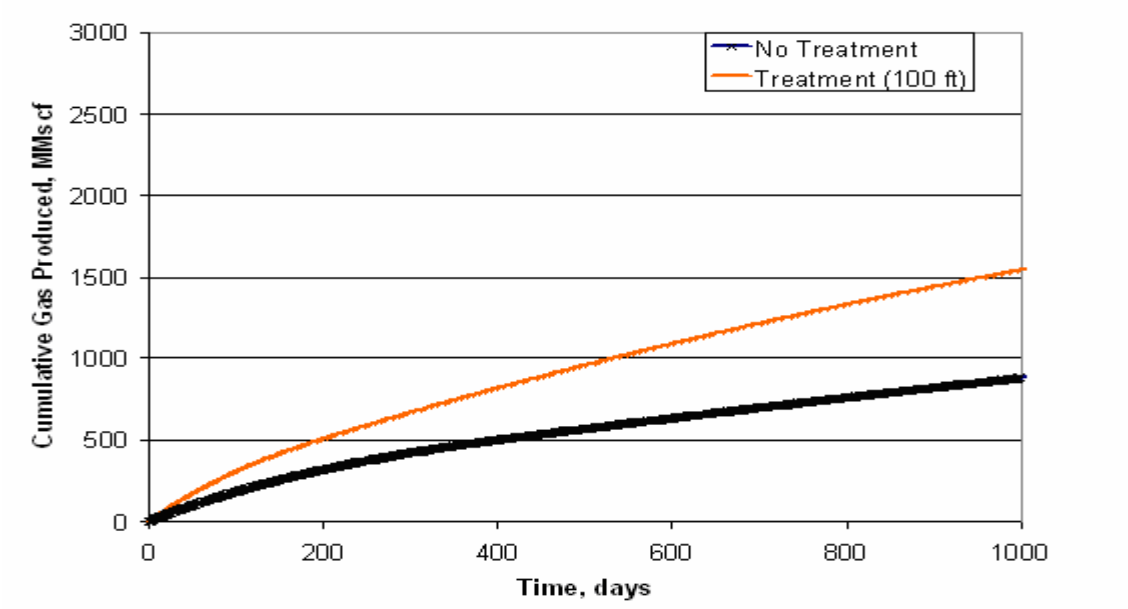

Fig. C.2 Cumulative Gas Production vs Time for Fluid C (11 mole % C7+), Swi=0.41, h=10 feet, k=10 mD

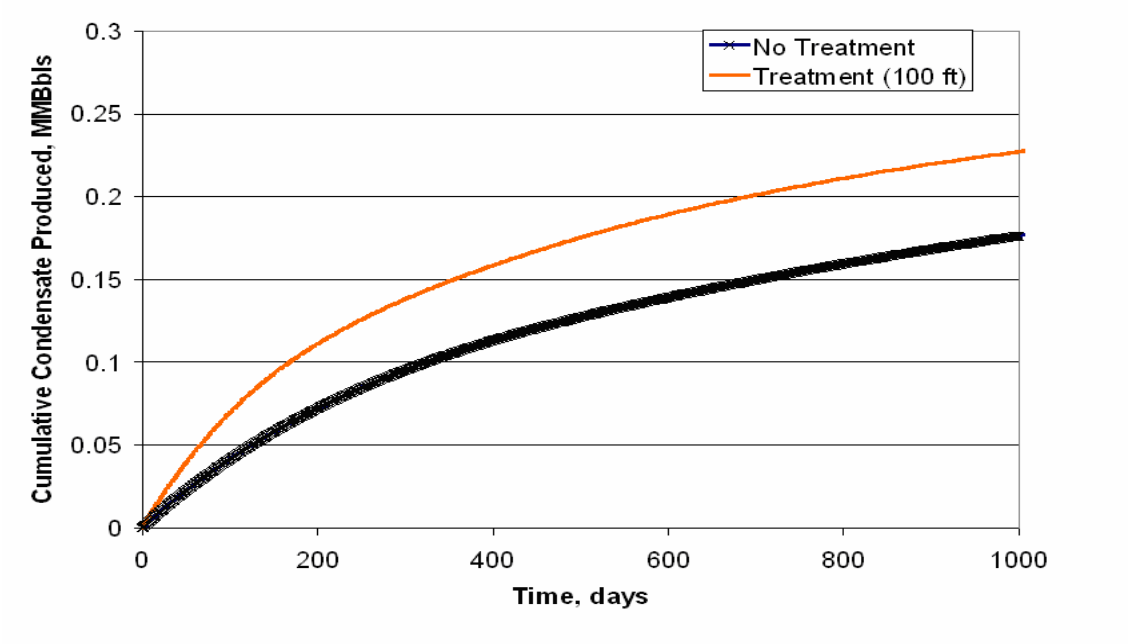

Fig. C.3 Cumulative Condensate Production vs Time for Fluid C (11 mole % C7+), Swi=0.41, h=10 feet, k=10 mD

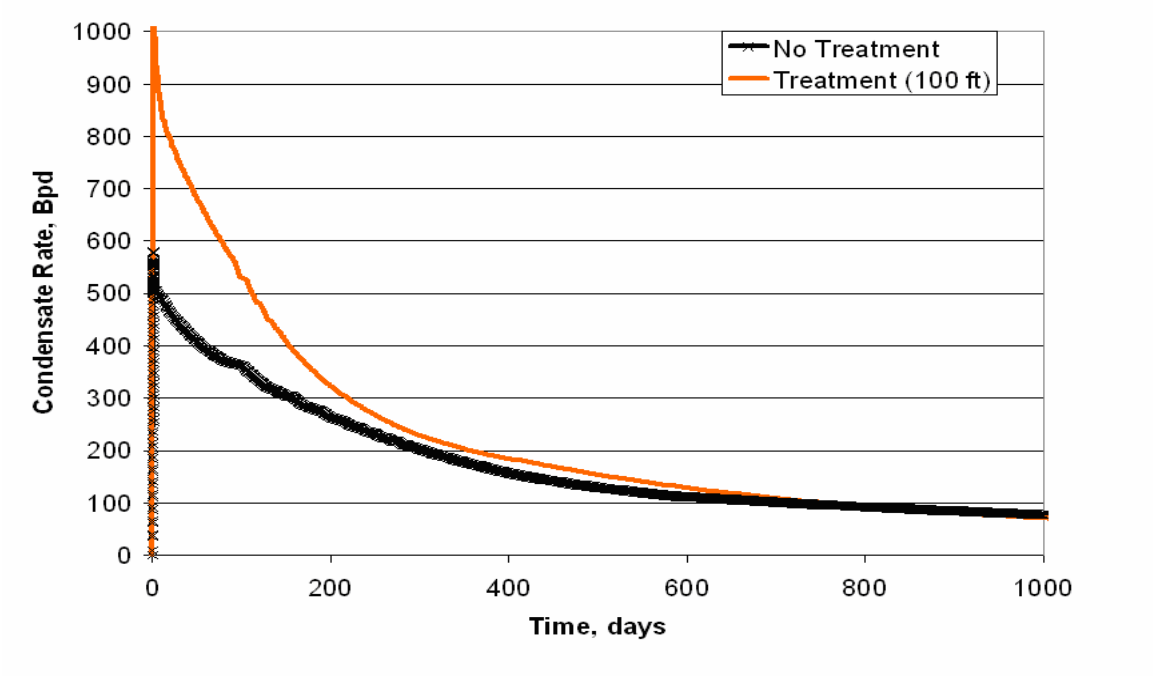

Fig. C.4 Condensate Production Rate vs Time for Fluid C (11 mole % C7+), Swi=0.41, h=10 feet, k=10 mD

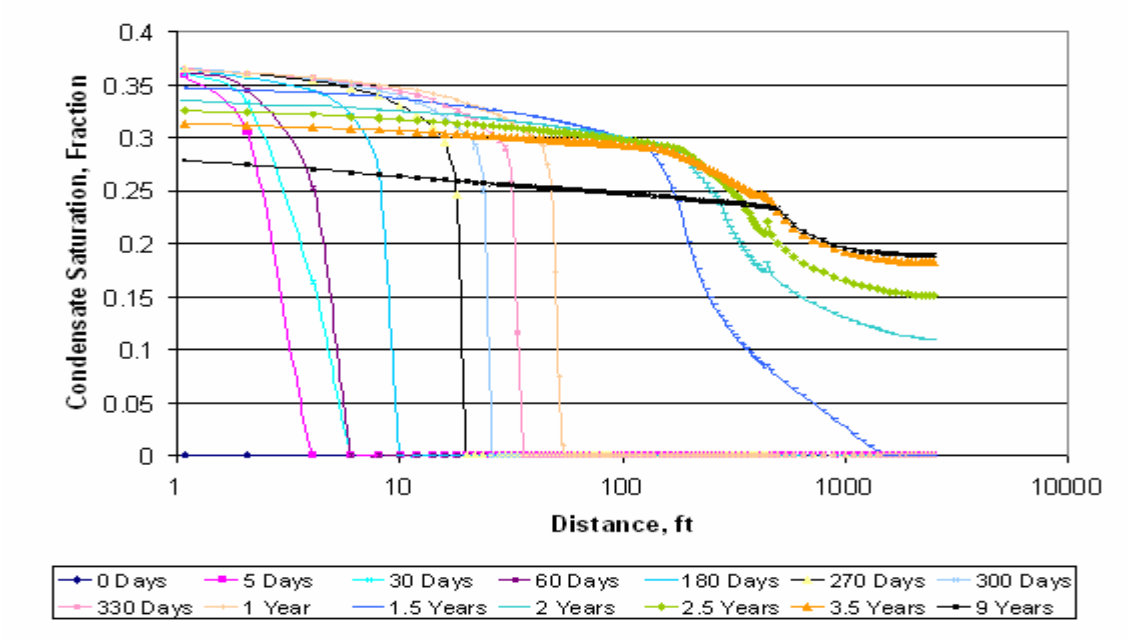

Fig. C.5 Condensate Saturation vs Distance for Fluid C (11 mole % C7+), Swi=0.41, h=10 feet, k=10 mD, no treatment

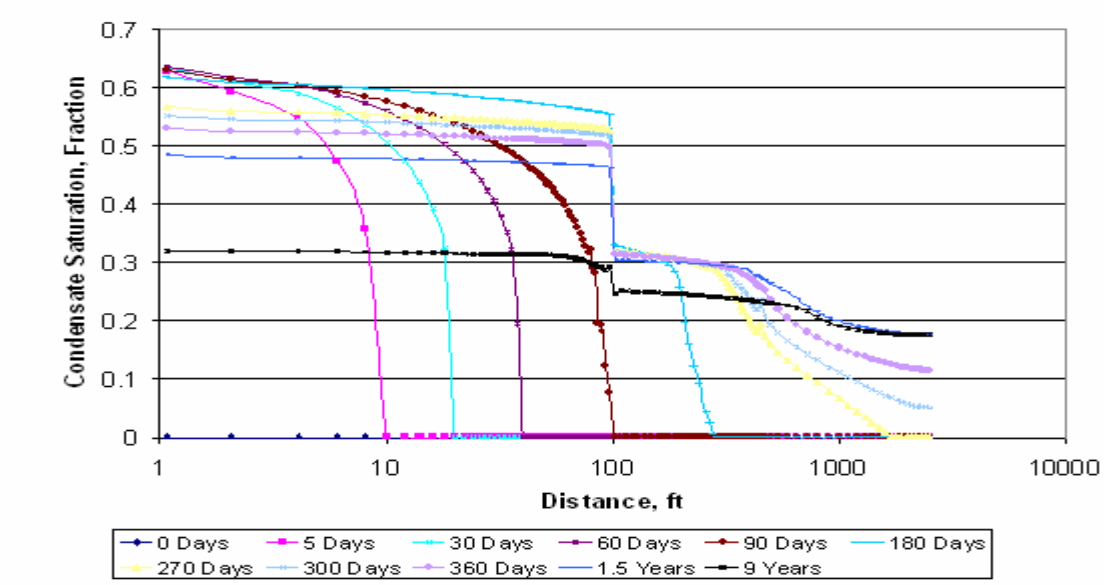

Fig. C.6 Condensate Saturation vs Distance for Fluid C (11 mole % C7+), Swi=0.41, h=10 feet, k=10 mD, 100 feet of treatment

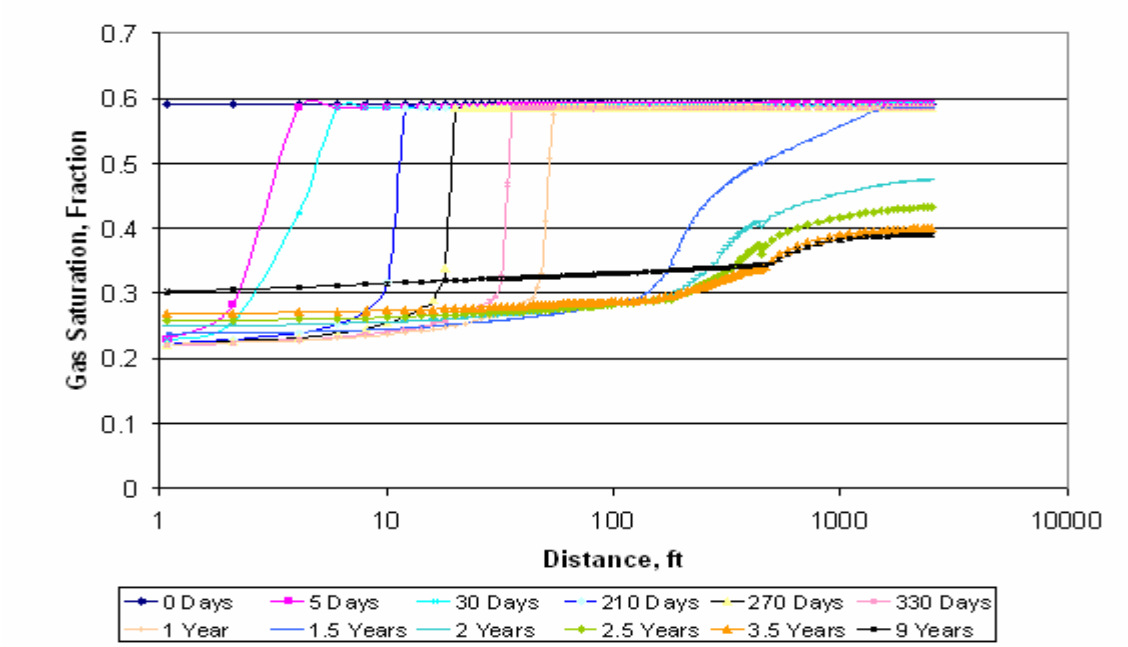

Fig. C.7 Gas Saturation vs Distance for Fluid C (11 mole % C7+), Swi=0.41, h=10 feet, k=10 mD, no treatment

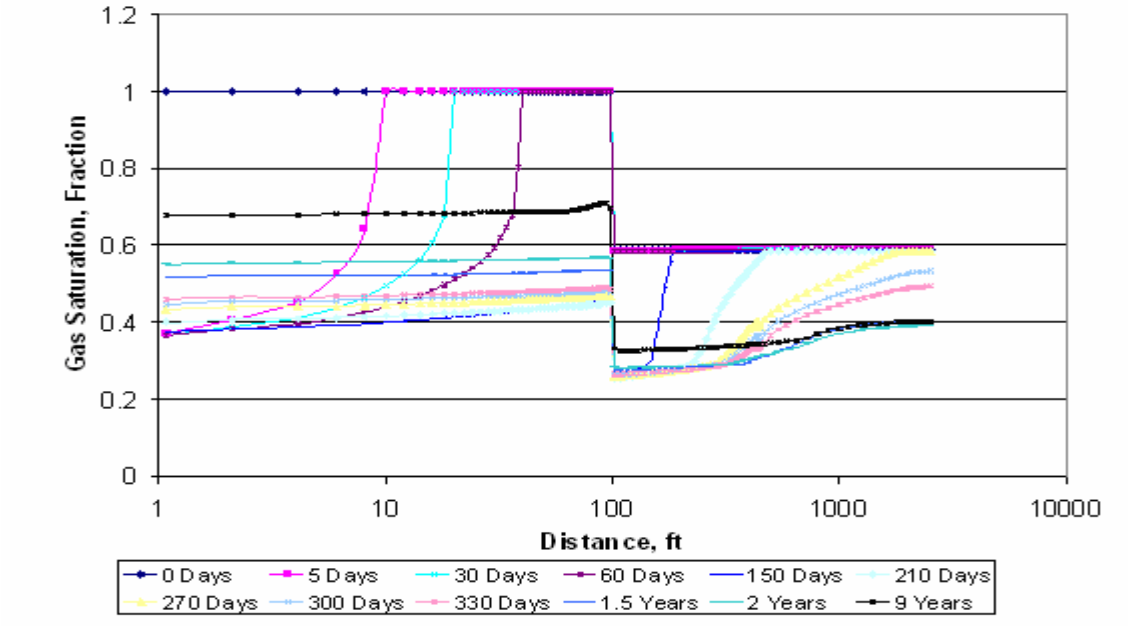

Fig. C.8 Gas Saturation vs Distance for Fluid C (11 mole % C7+), Swi=0.41, h=10 feet, k=10 mD, 100 feet of treatment

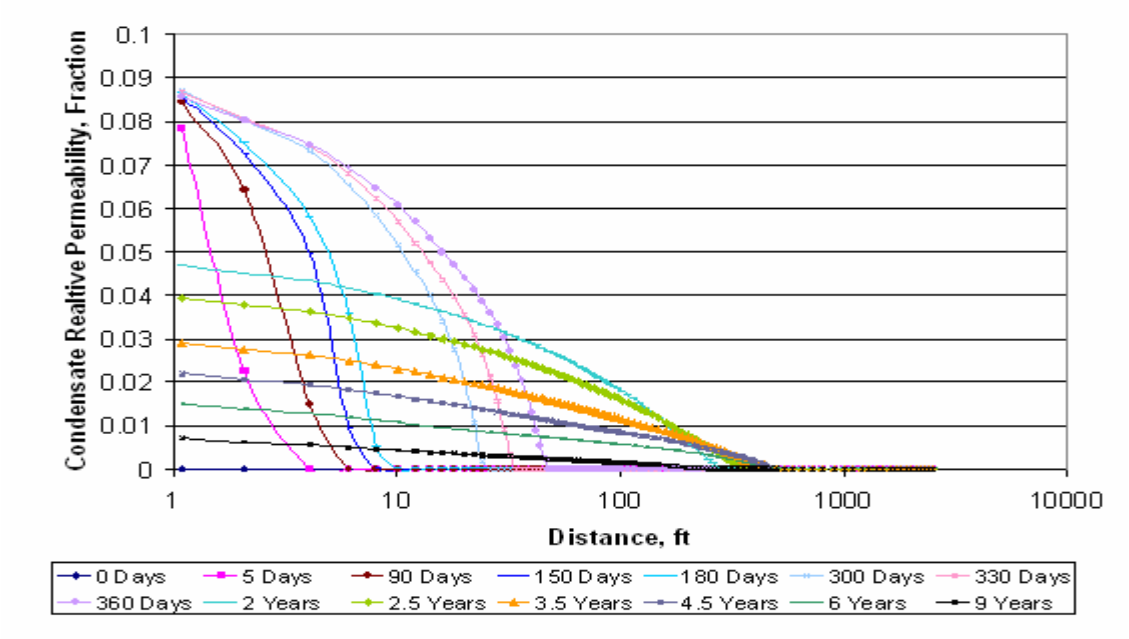

Fig. C.9 Condensate Relative Permeability vs Distance for Fluid C (11 mole % C7+), Swi=0.41, h=10 feet, k=10 mD, no treatment

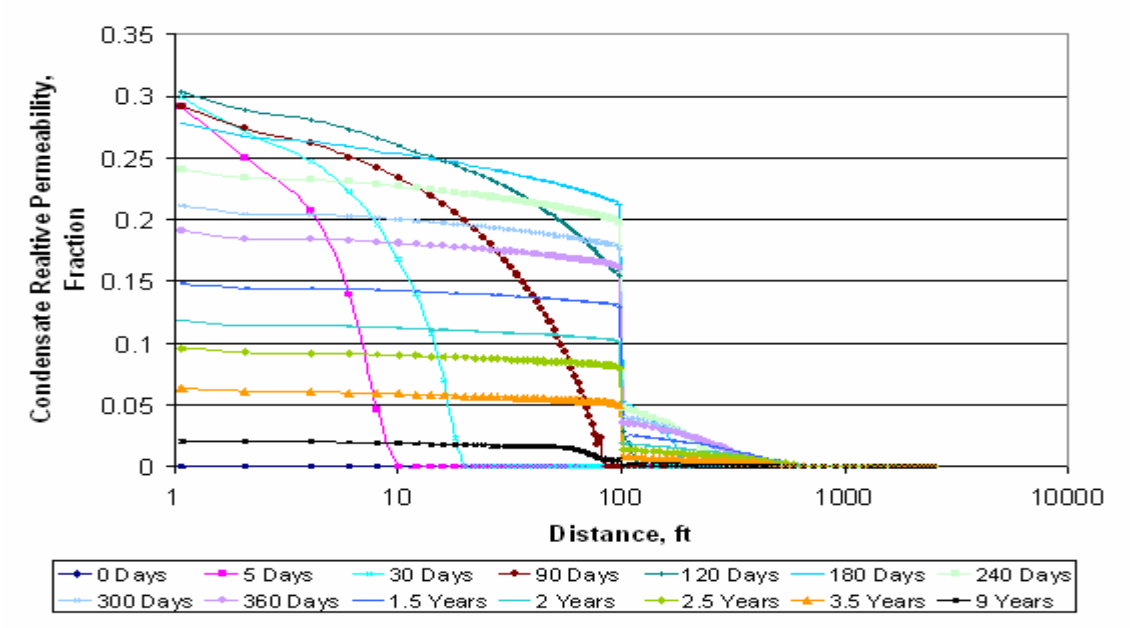

Fig. C.10 Condensate Relative Permeability vs Distance for Fluid C (11 mole % C7+), Swi=0.41, h=10 feet, k=10 mD, 100 feet of treatment

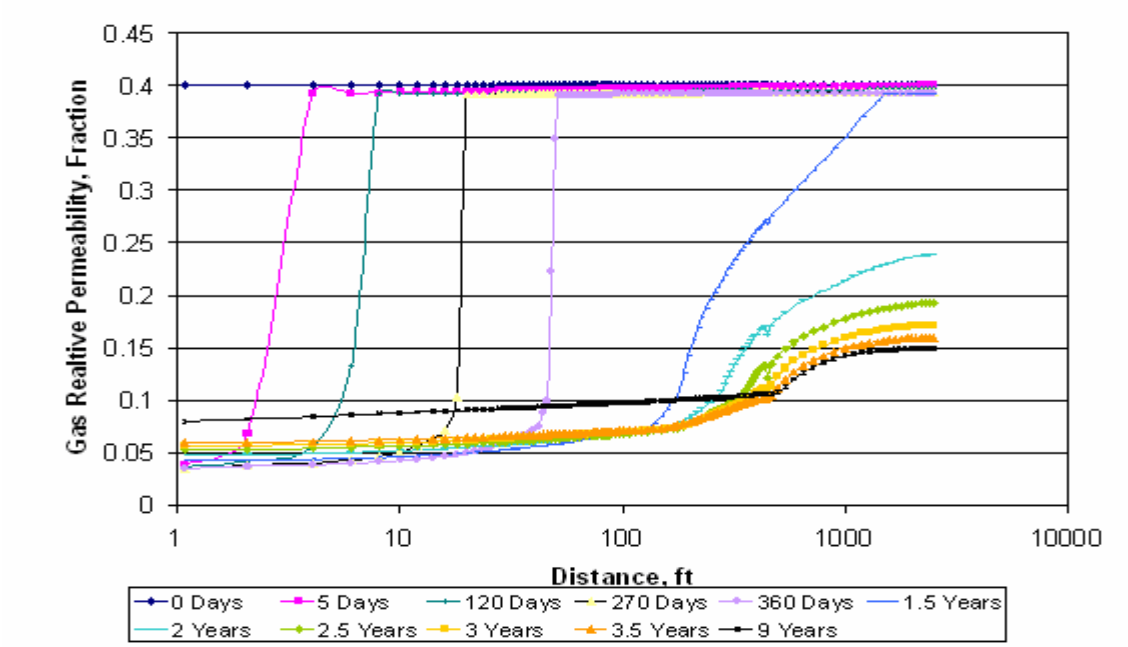

Fig. C.11 Gas Relative Permeability vs Distance for Fluid C (11 mole % C7+), Swi=0.41, h=10 feet, k=10 mD, no treatment

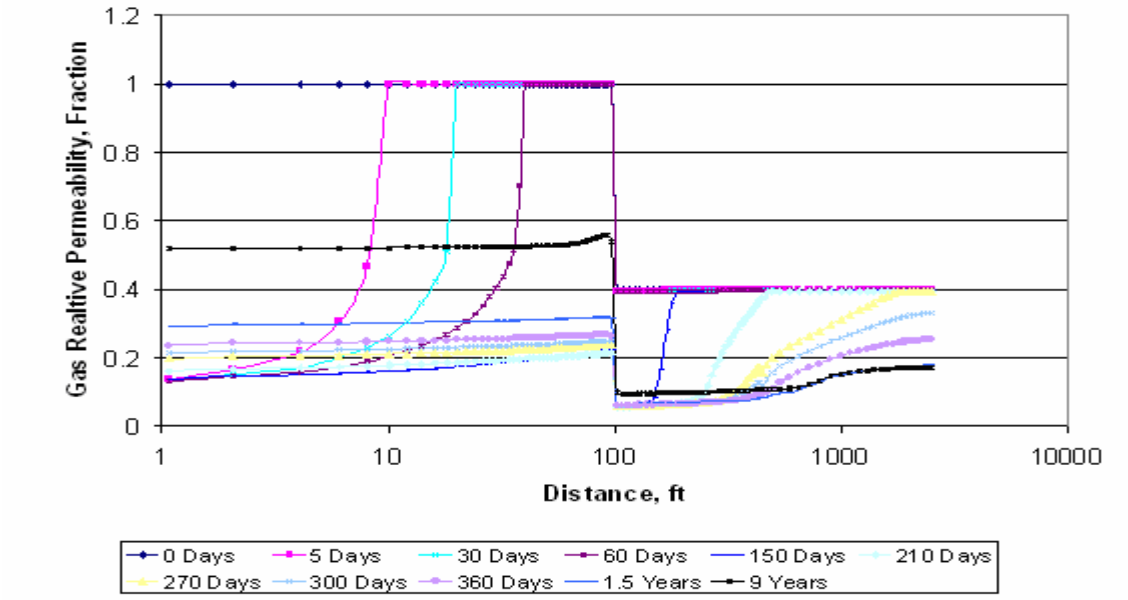

Fig. C.12 Gas Relative Permeability vs Distance for Fluid C (11 mole % C7+), Swi=0.41, h=10 feet, k=10 mD, 100 feet of treatment

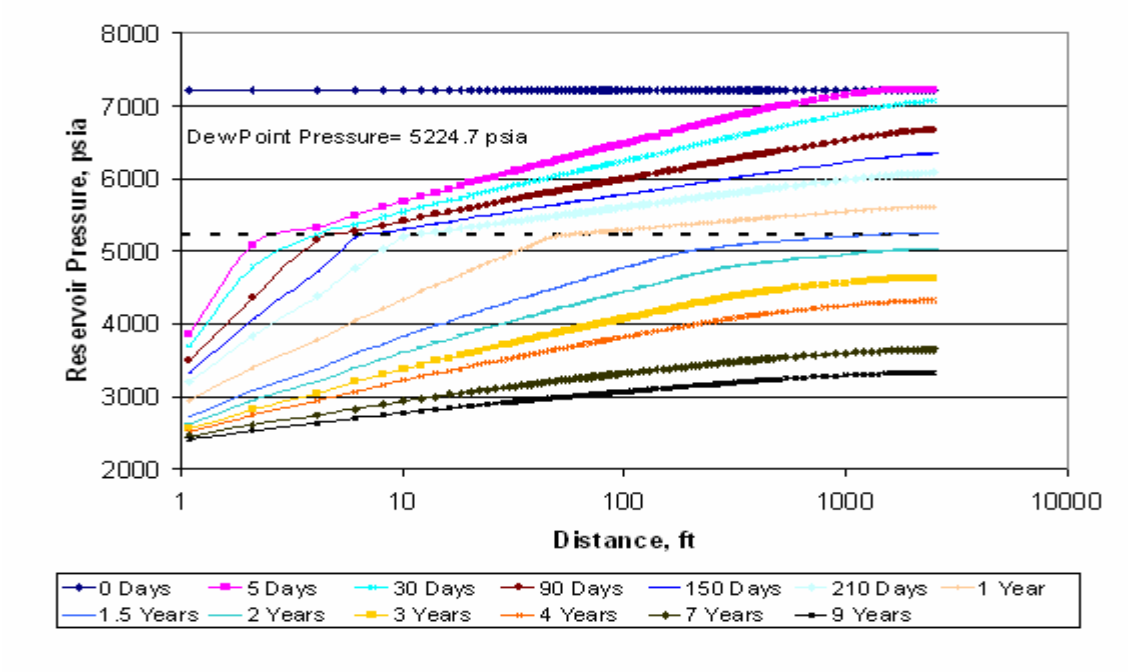

Fig. C.13 Pressure vs Distance for Fluid C (11 mole % C7+), Swi=0.41, h=10 feet, k=10 mD, no treatment

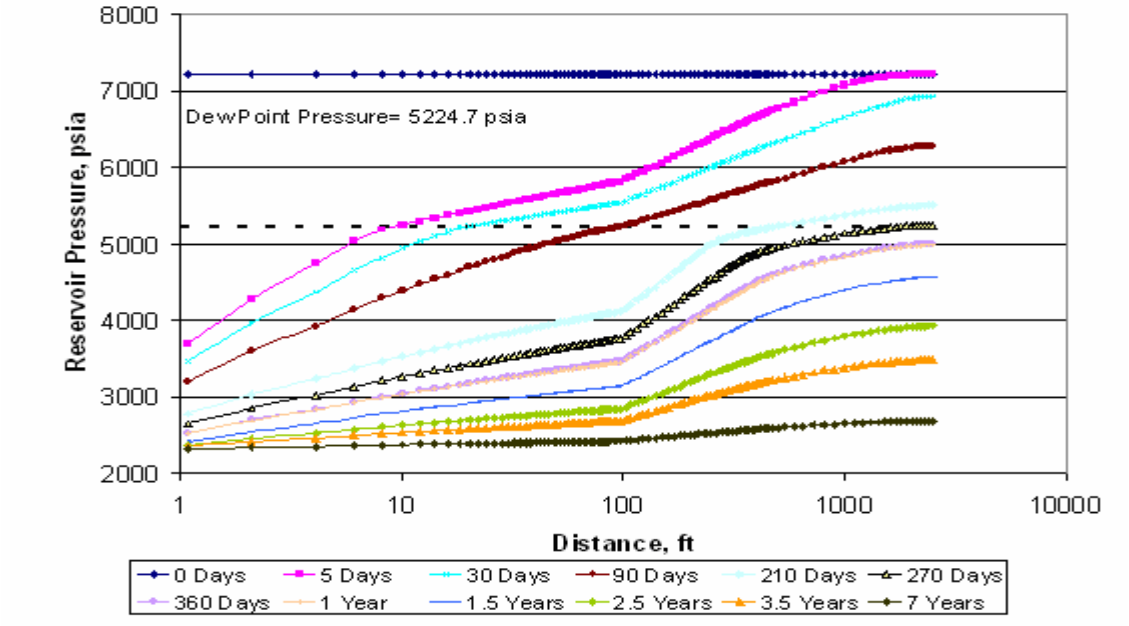

Fig. C.14 Pressure vs Distance for Fluid C (11 mole % C7+), Swi=0.41, h=10 feet, k=10 mD, 100 feet of treatment

APPENDIX D
OPTIMUM RADIUS OF TREATMENT

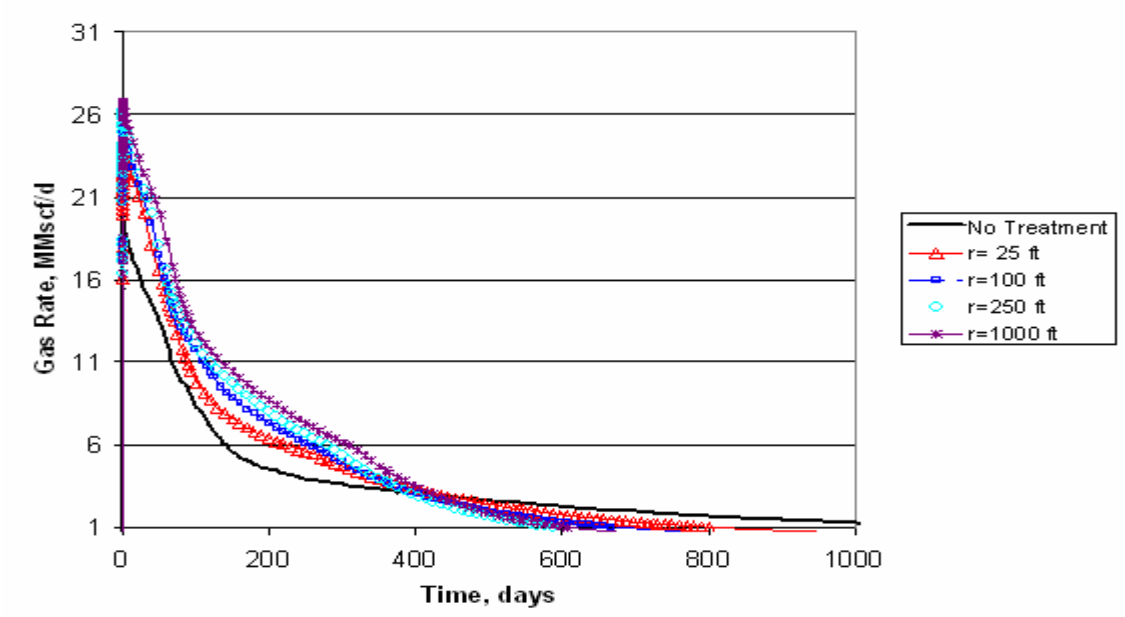

Fig. D.1 Gas Production Rate vs Time for Several Radius of Treatment, Fluid A (4 mole % C7+), Swi=0.41, h=10 feet, k=50 mD

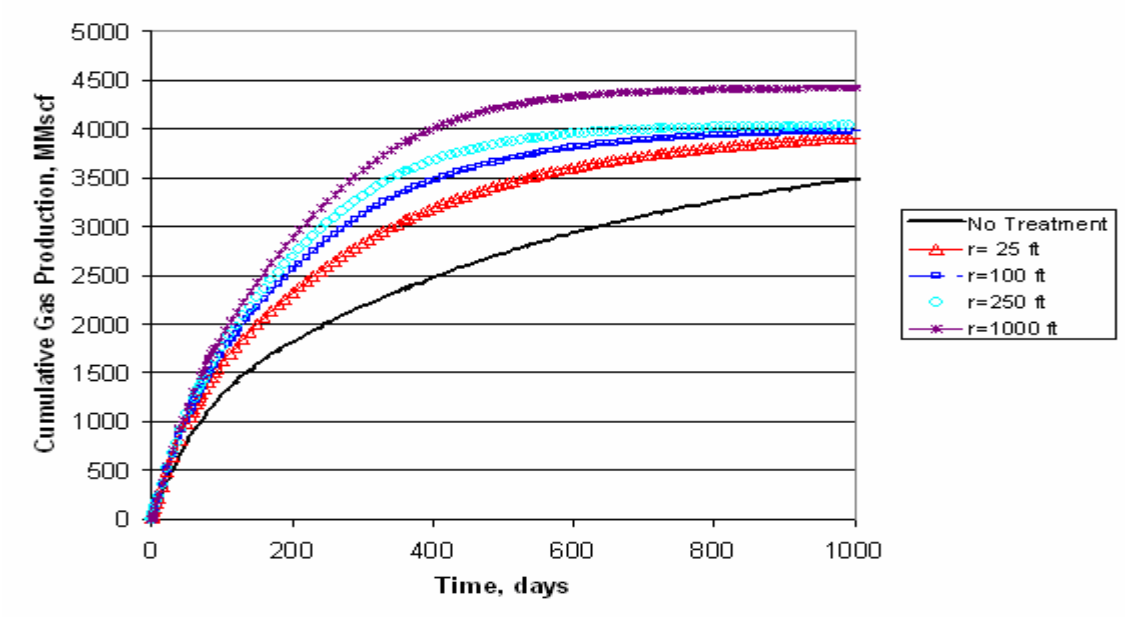

Fig. D.2 Cumulative Gas Production vs Time for Several Radius of Treatment, Fluid A (4 mole % C7+), Swi=0.41, h=10 feet, k=50 mD

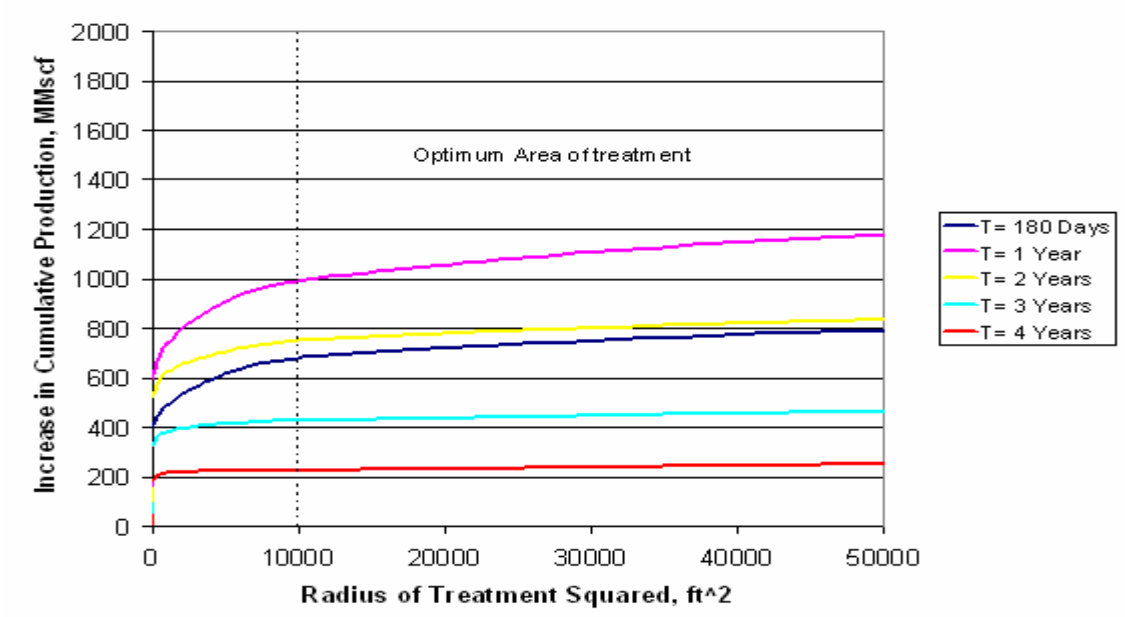

Fig. D.3 Increment in Cumulative Gas Production vs Radius of Treatment Squared , Fluid A (4 mole % C7+), Swi=0.41, h=10 feet, k=50 mD

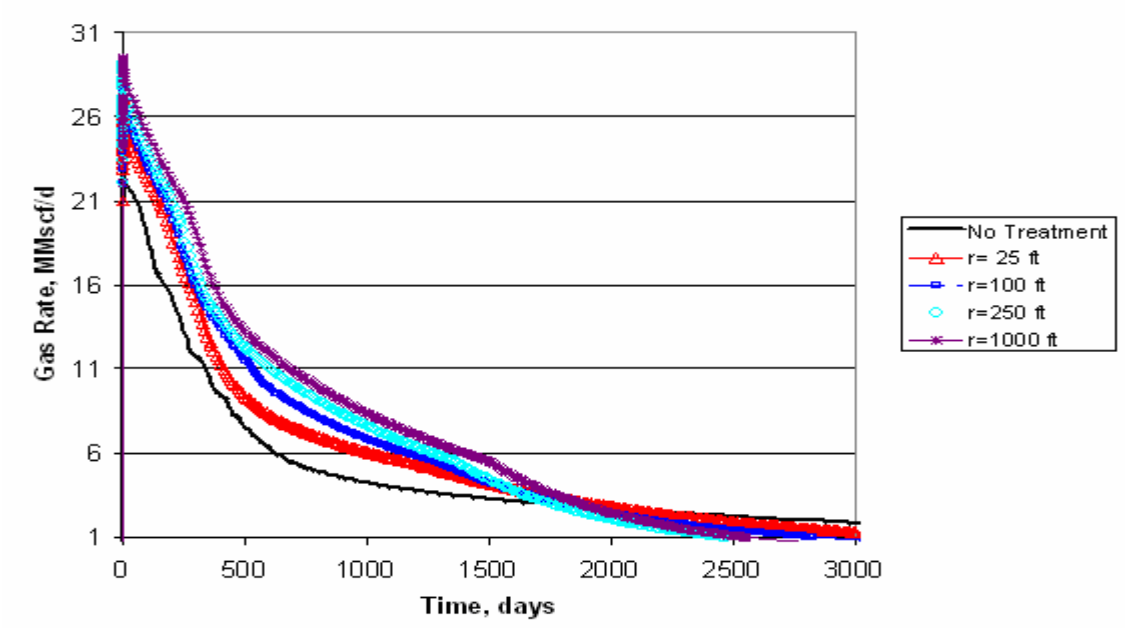

Fig. D.4 Gas Production Rate vs Time for Several Radius of Treatment, Fluid A (4 mole % C7+), Swi=0.41, h=50 feet, k=10 mD

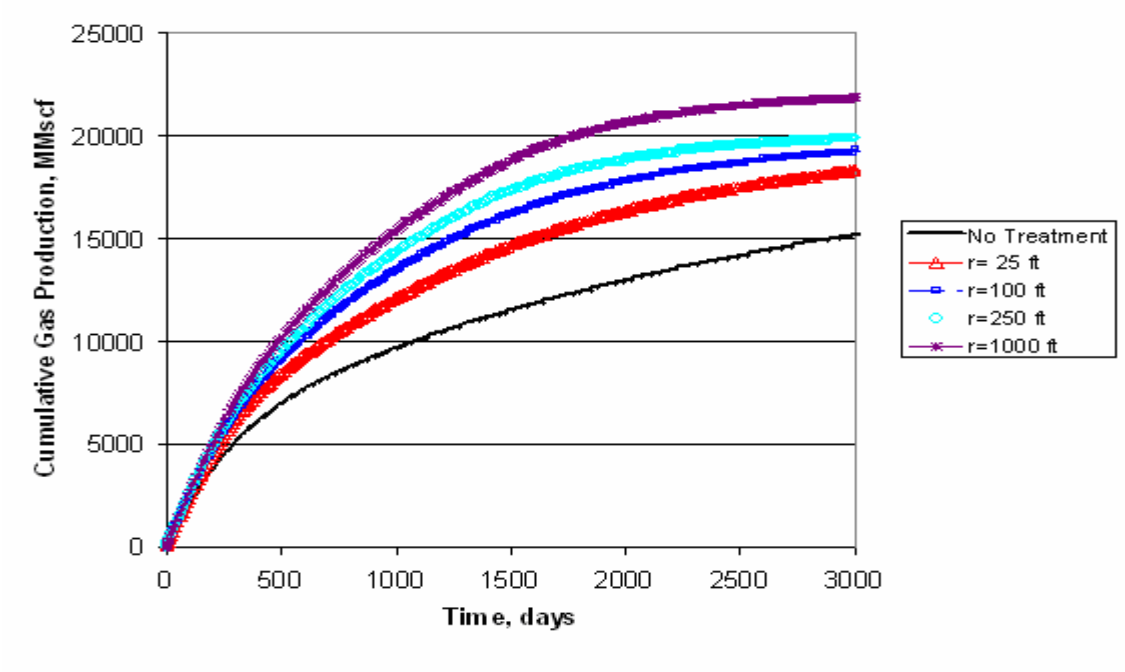

Fig. D.5 Cumulative Gas Production vs Time for Several Radius of Treatment, Fluid A (4 mole % C7+), Swi=0.41, h=50 feet, k=10 mD

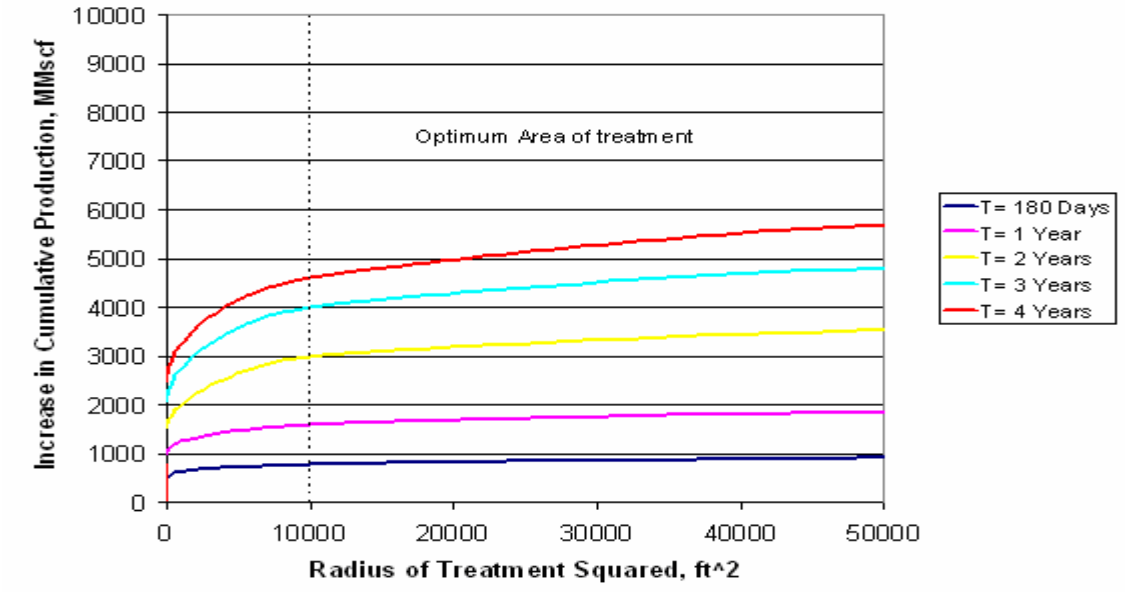

Fig. D.6 Increment in Cumulative Gas Production vs Radius of Treatment Squared , Fluid A (4 mole % C7+), Swi=0.41, h=50 feet, k=10 mD

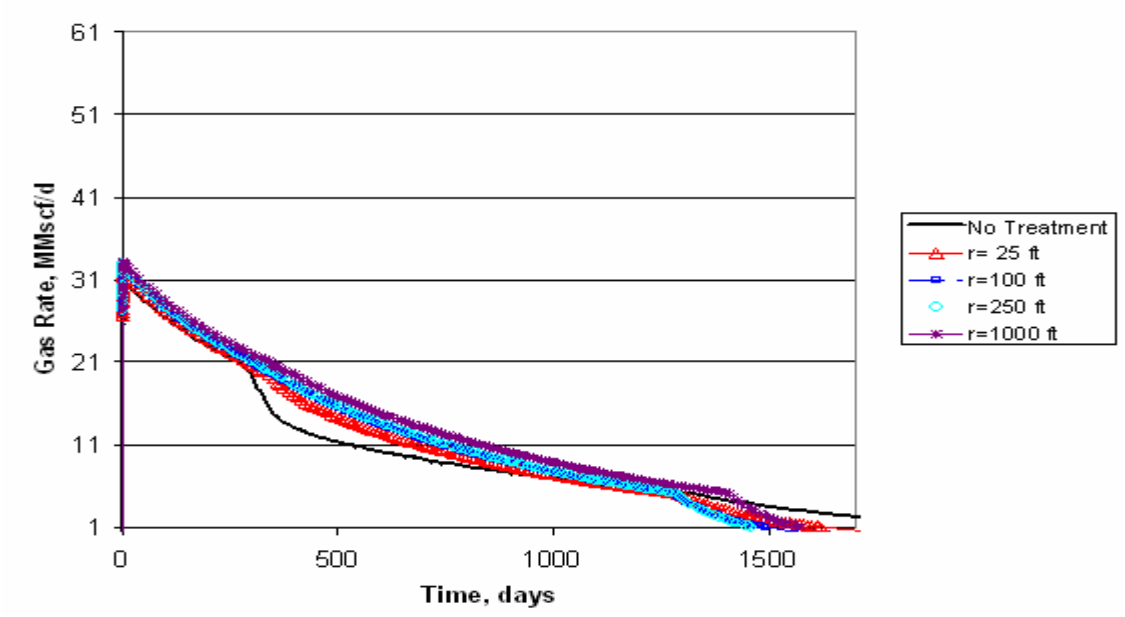

Fig. D.7 Gas Production Rate vs Time for Several Radius of Treatment, Fluid A (4 mole % C7+), Swi=0.41, h=50 feet, k=50 mD

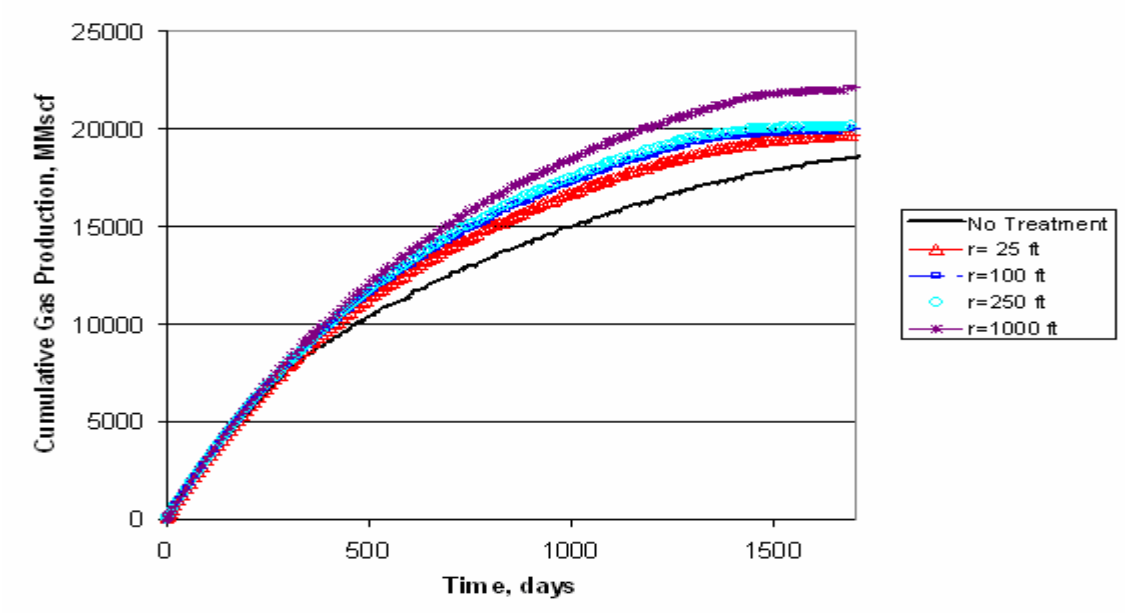

Fig. D.8 Cumulative Gas Production vs Time for Several Radius of Treatment, Fluid A (4 mole % C7+), Swi=0.41, h=50 feet, k=50 mD

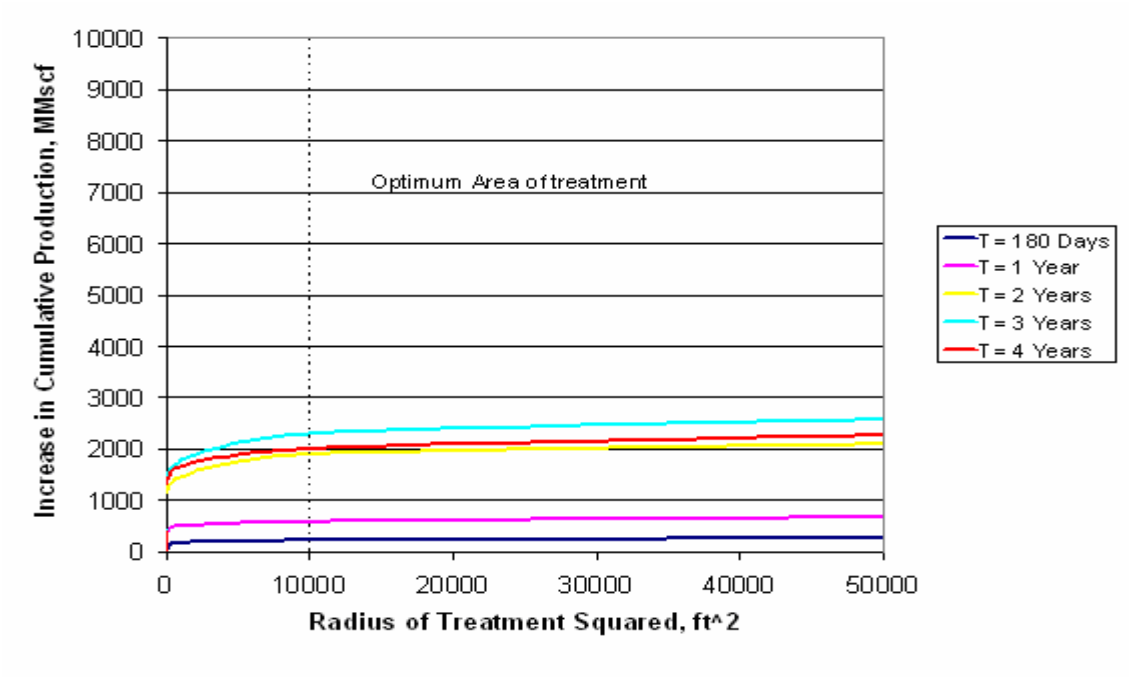

Fig. D.9 Increment in Cumulative Gas Production vs Radius of Treatment Squared , Fluid A (4 mole % C7+), Swi=0.41, h=50 feet, k=50 mD

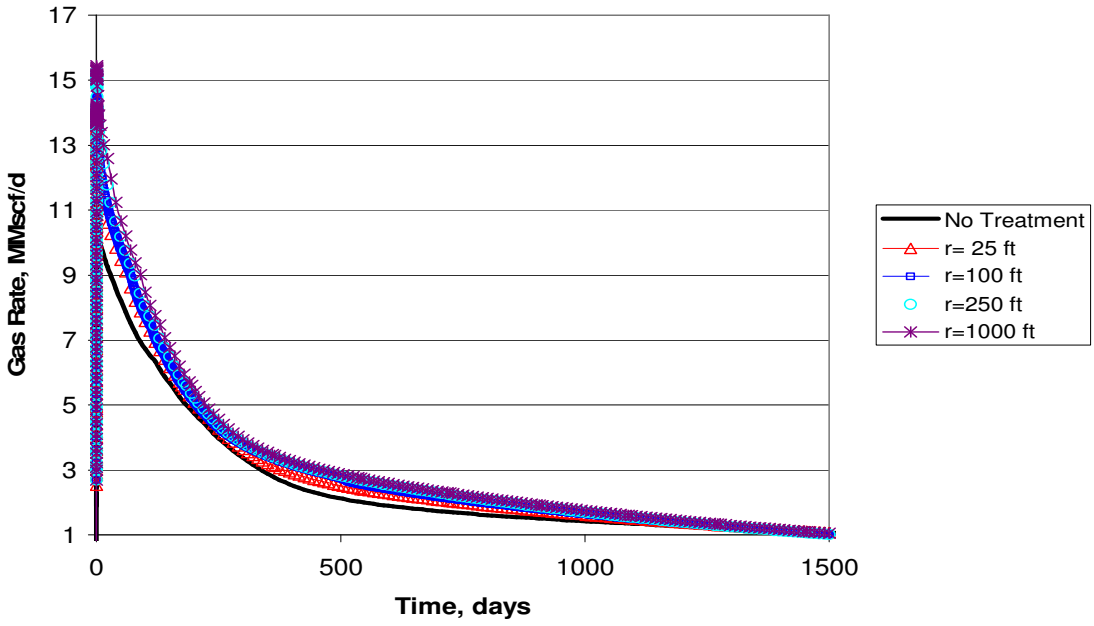

Fig. D.10 Gas Production Rate vs Time for Several Radius of Treatment, Fluid A (4 mole % C7+), Swi=0.2, h=10 feet, k=10 mD

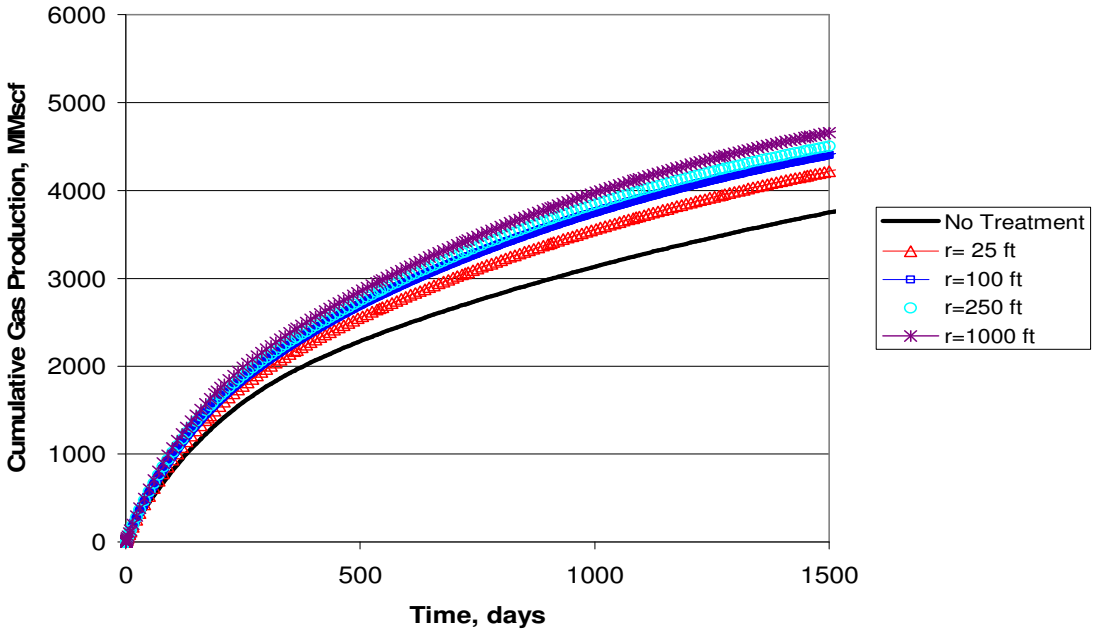

Fig. D.11 Cumulative Gas Production vs Time for Several Radius of Treatment, Fluid A (4 mole % C7+), Swi=0.2, h=10 feet, k=10 mD

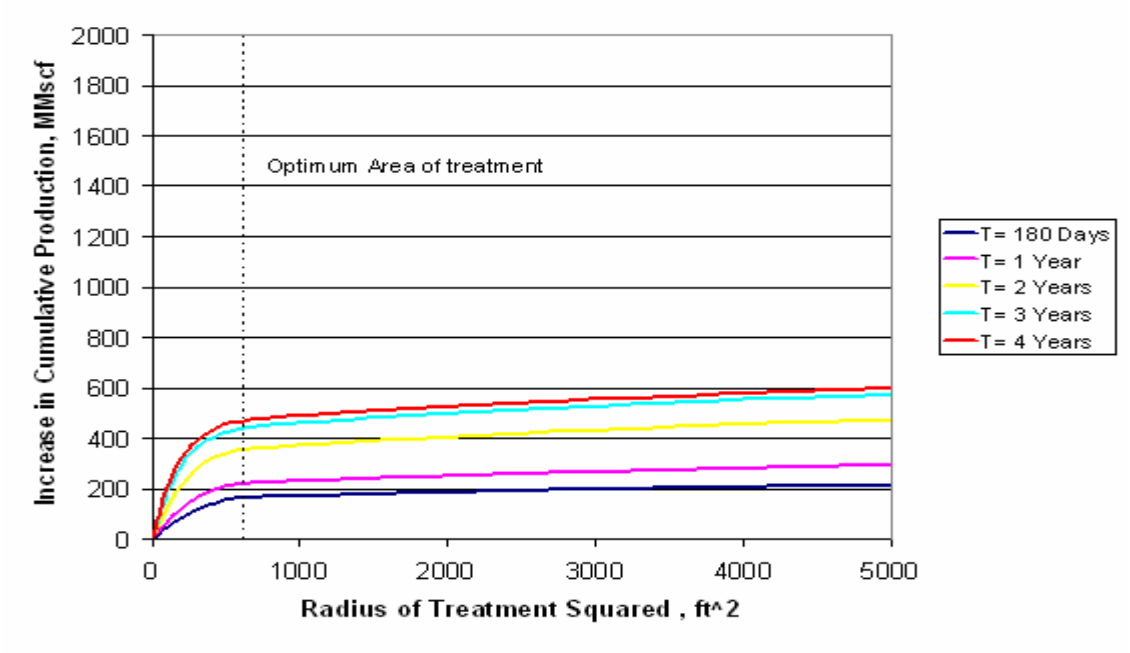

Fig. D.12 Increment in Cumulative Gas Production vs Radius of Treatment Squared , Fluid A (4 mole % C7+), Swi=0.2, h=10 feet, k=10 mD

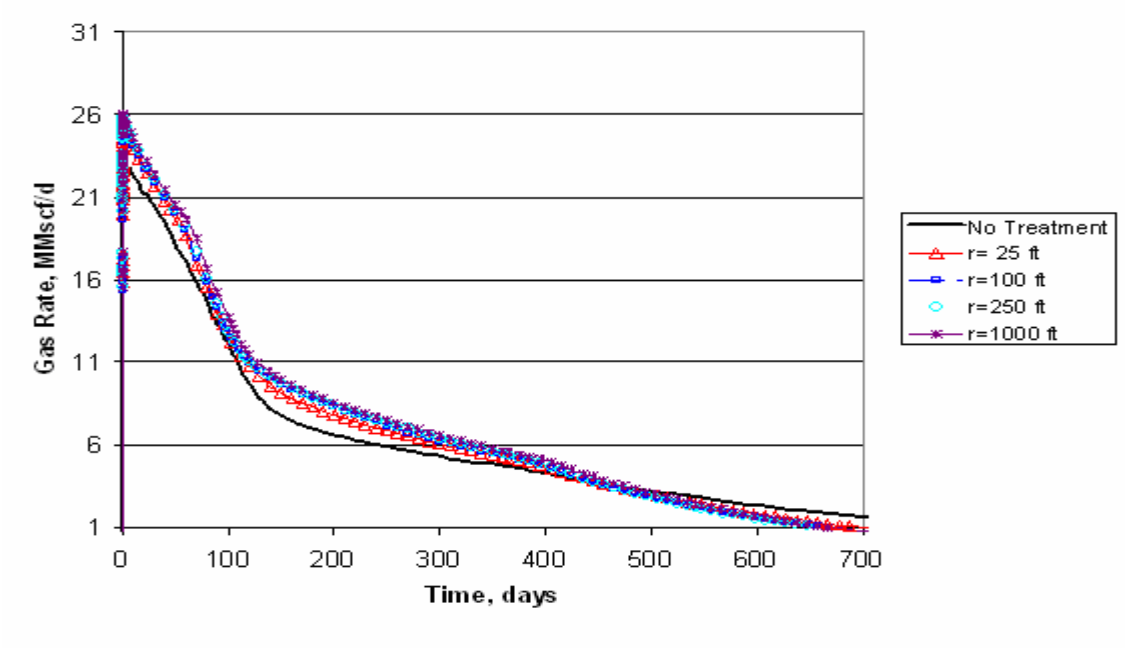

Fig. D.13 Gas Production Rate vs Time for Several Radius of Treatment, Fluid A (4 mole % C7+), Swi=0.2, h=10 feet, k=50 mD

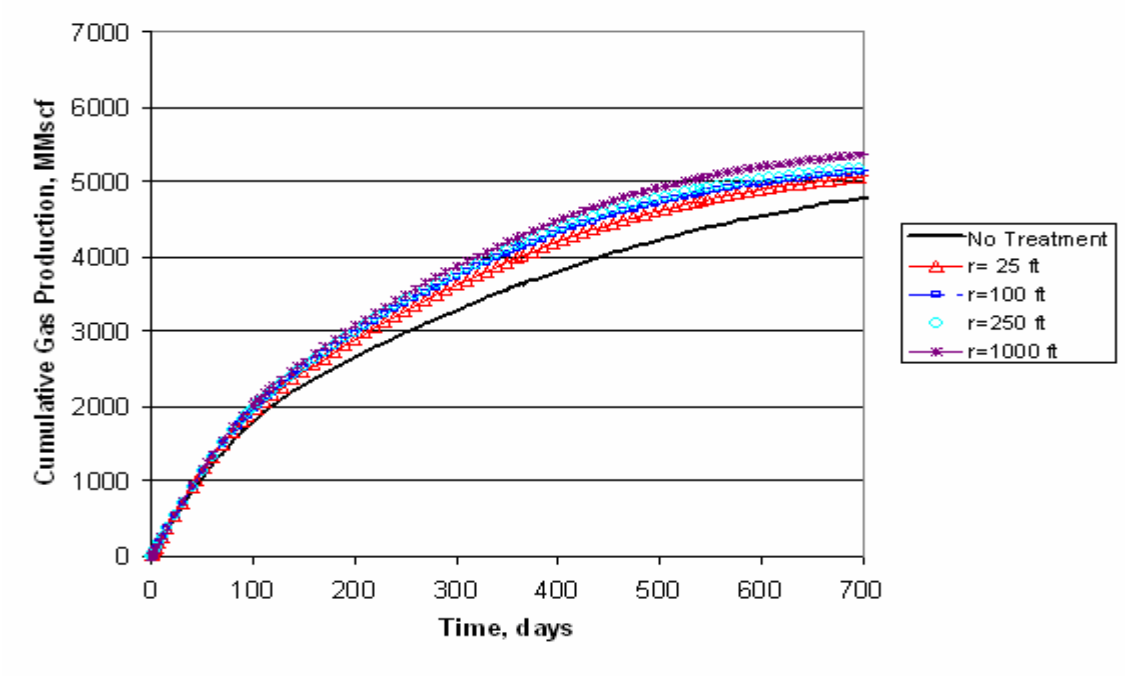

Fig. D.14 Cumulative Gas Production vs Time for Several Radius of Treatment, Fluid A (4 mole % C7+), Swi=0.2, h=10 feet, k=50 mD

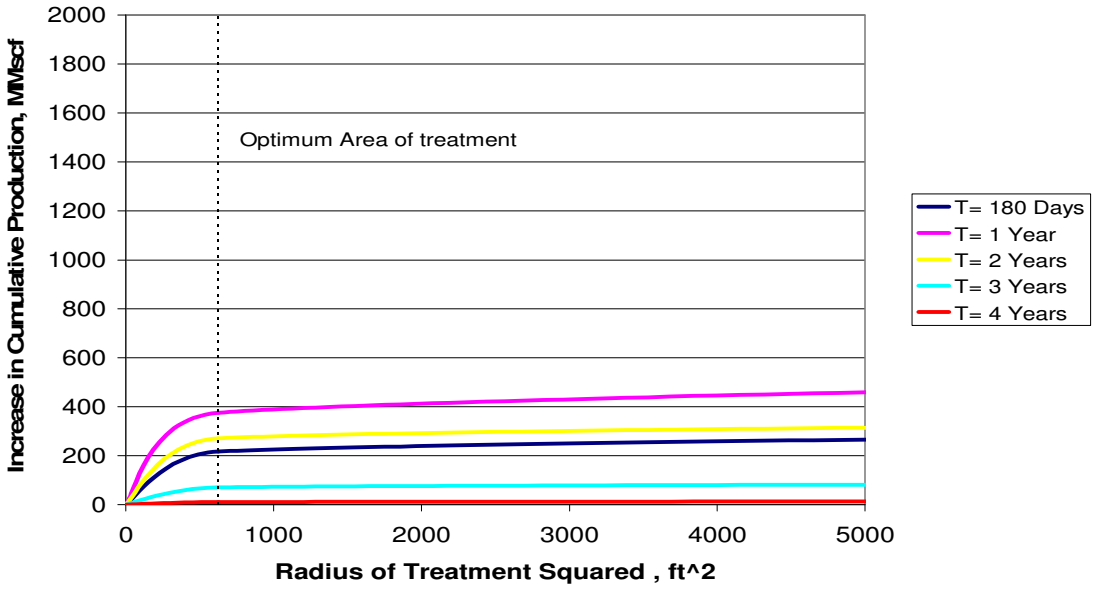

Fig. D.15 Increment in Cumulative Gas Production vs Radius of Treatment Squared , Fluid A (4 mole % C7+), Swi=0.2, h=10 feet, k=50 mD

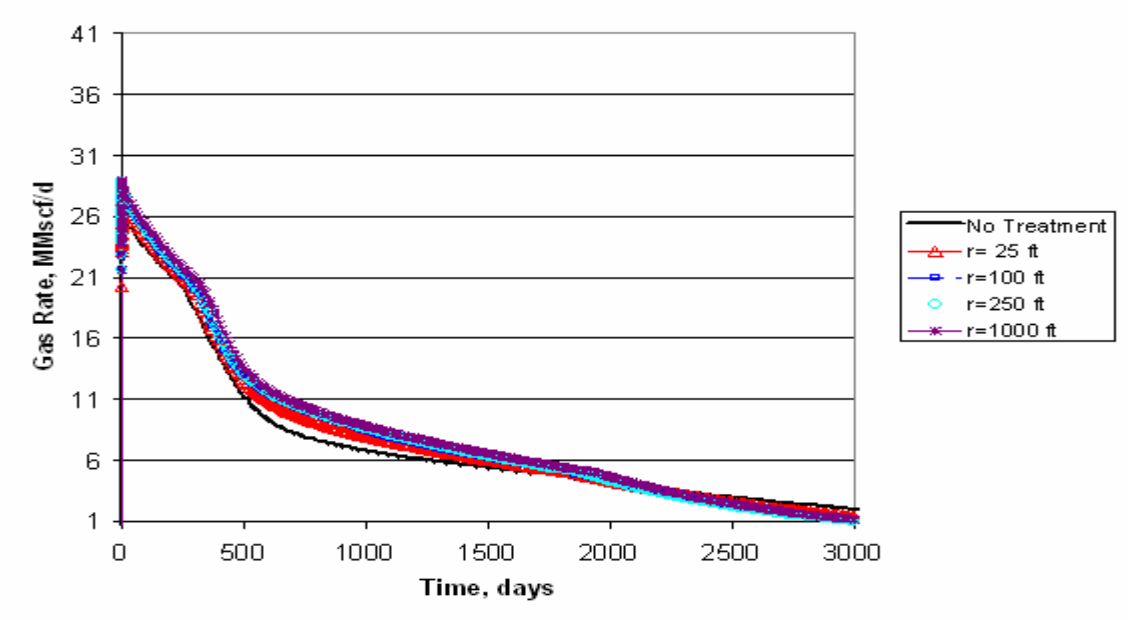

Fig. D.16 Gas Production Rate vs Time for Several Radius of Treatment, Fluid A (4 mole % C7+), Swi=0.2, h=50 feet, k=10 mD

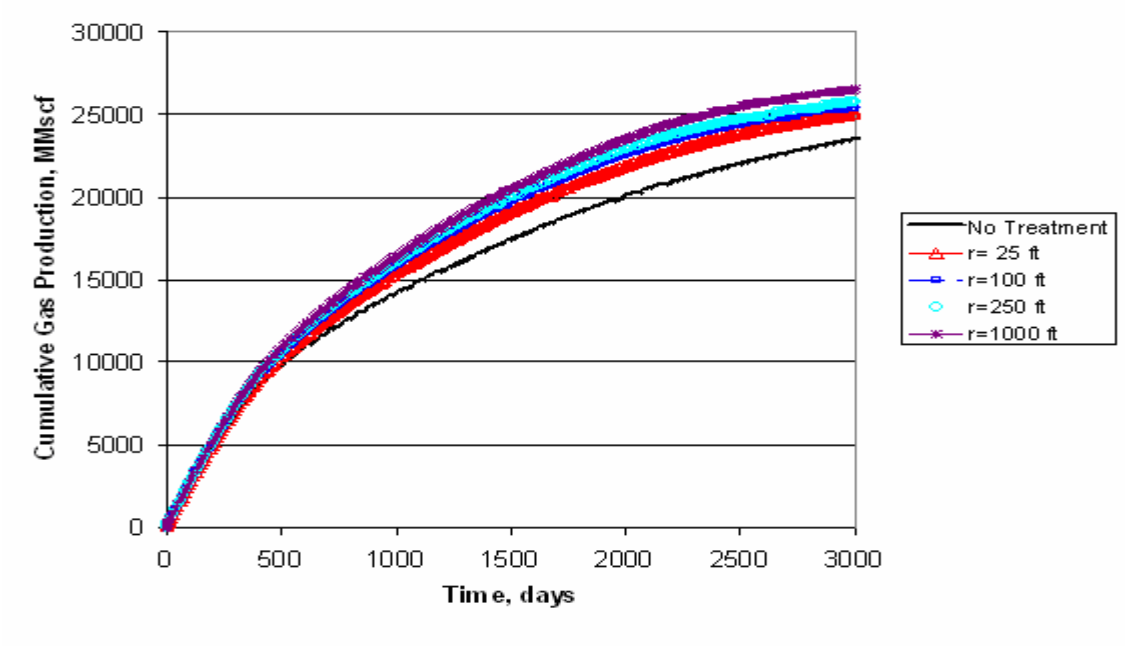

Fig. D.17 Cumulative Gas Production vs Time for Several Radius of Treatment, Fluid A (4 mole % C7+), Swi=0.2, h=50 feet, k=10 mD

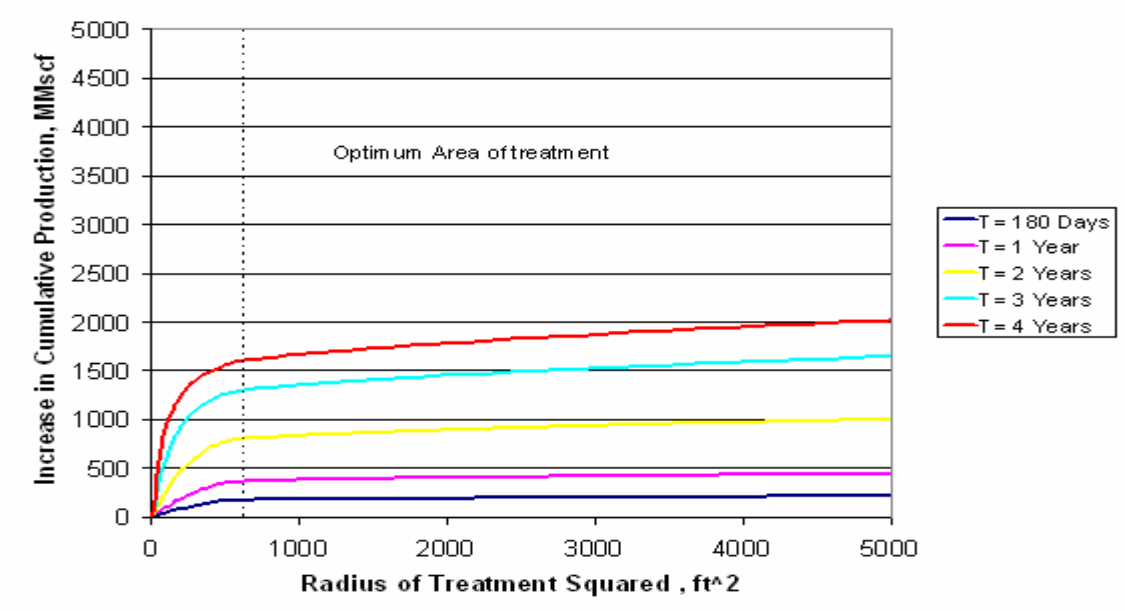

Fig. D.18 Increment in Cumulative Gas Production vs Radius of Treatment Squared , Fluid A (4 mole % C7+), Swi=0.2, h=50 feet, k=10 mD

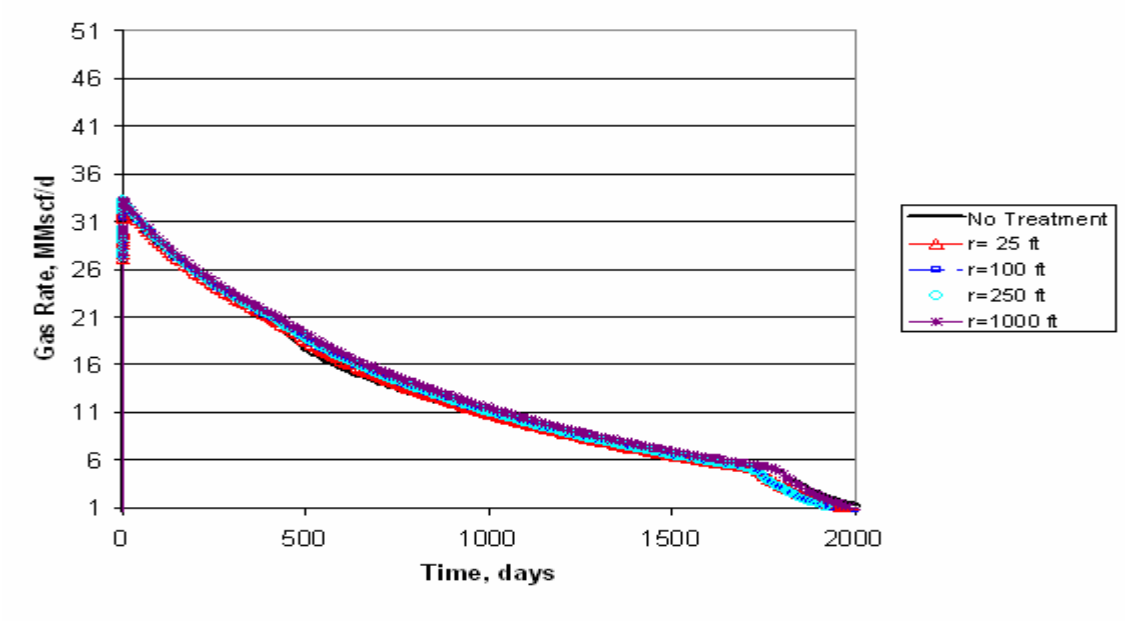

Fig. D.19 Gas Production Rate vs Time for Several Radius of Treatment, Fluid A (4 mole % C7+), Swi=0.2, h=50 feet, k=50 mD

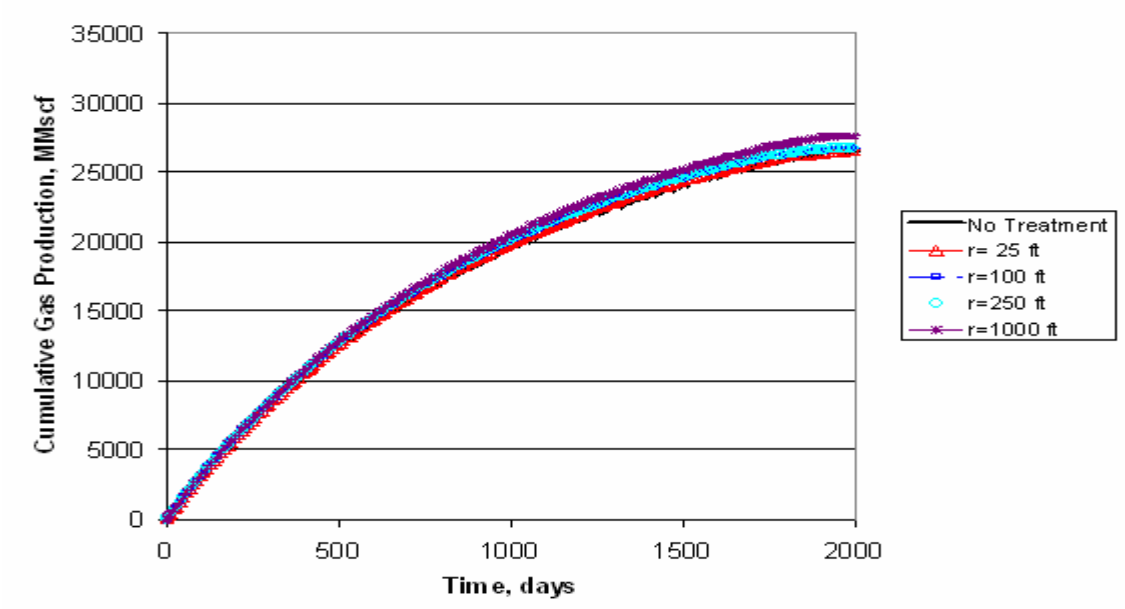

Fig. D.20 Cumulative Gas Production vs Time for Several Radius of Treatment, Fluid A (4 mole % C7+), Swi=0.2, h=50 feet, k=50 mD

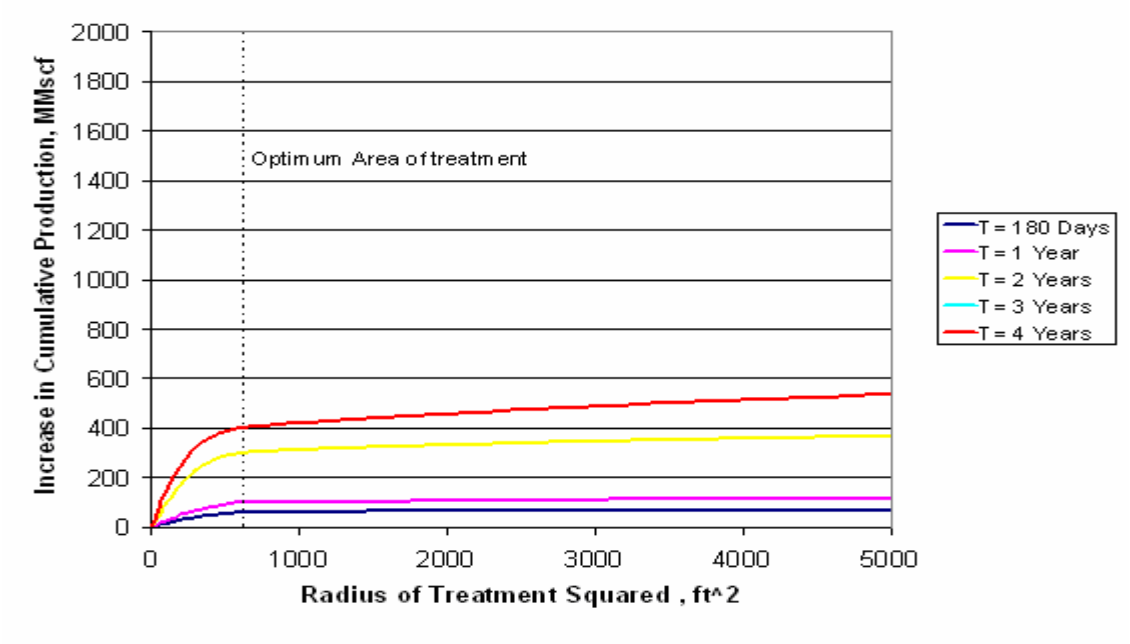

Fig. D.21 Increment in Cumulative Gas Production vs Radius of Treatment Squared , Fluid A (4 mole % C7+), Swi=0.2, h=50 feet, k=50 mD

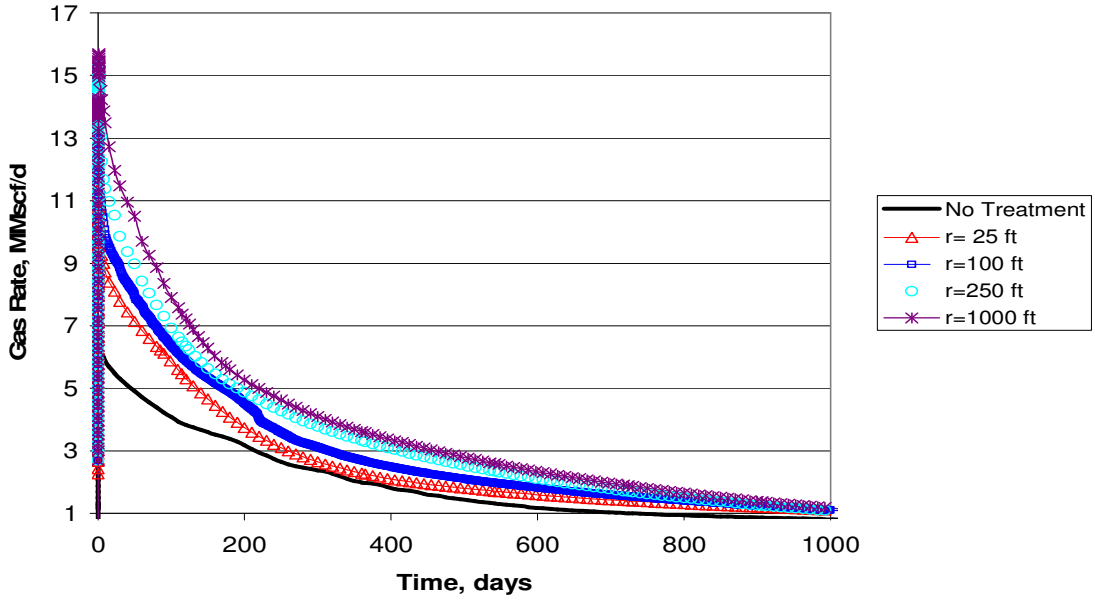

Fig. D.22 Gas Production Rate vs Time for Several Radius of Treatment, Fluid A (4 mole % C7+), Swi=0.41, h=10 feet, k=10 mD

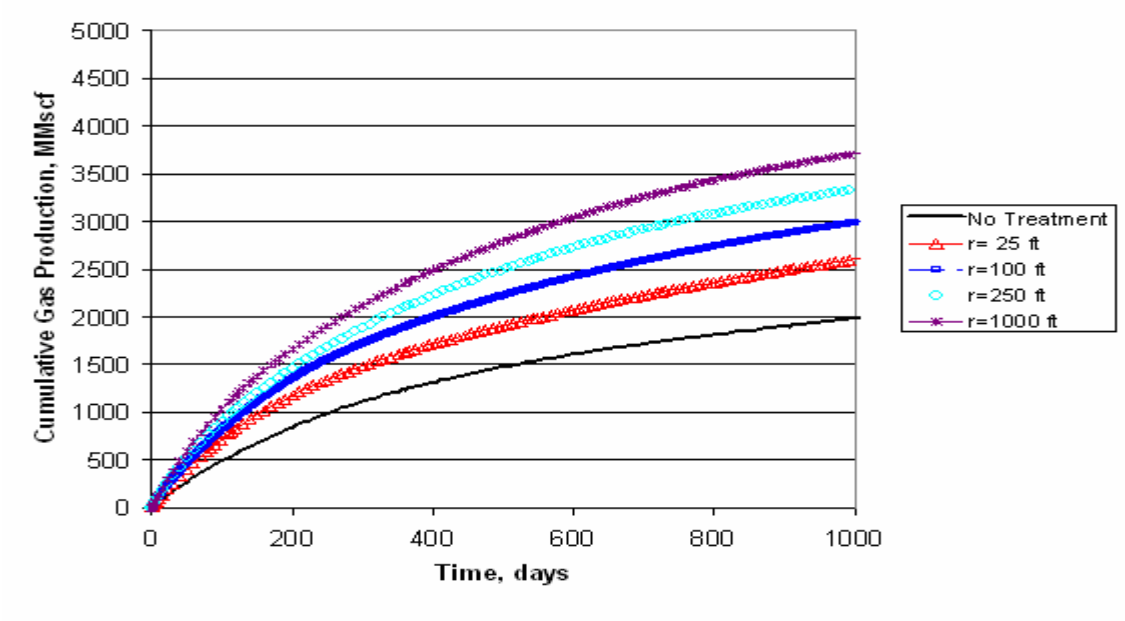

Fig. D.23 Cumulative Gas Production vs Time for Several Radius of Treatment, Fluid A (4 mole % C7+), Swi=0.41, h=10 feet, k=10 mD

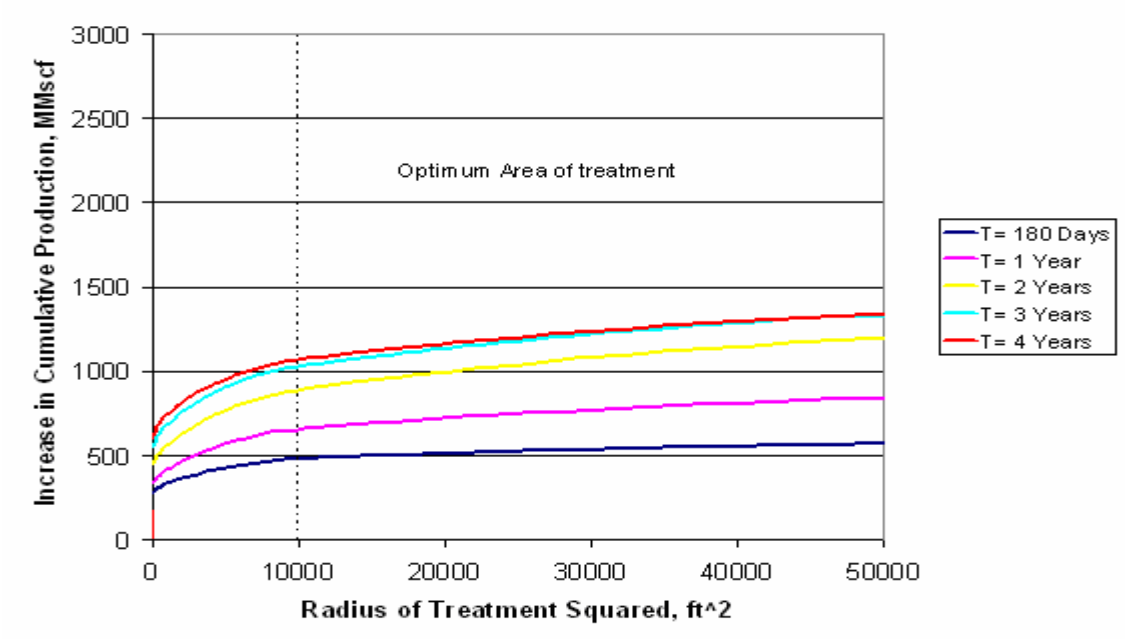

Fig. D.24 Increment in Cumulative Gas Production vs Radius of Treatment Squared , Fluid A (4 mole % C7+), Swi=0.41, h=10 feet, k=10 mD

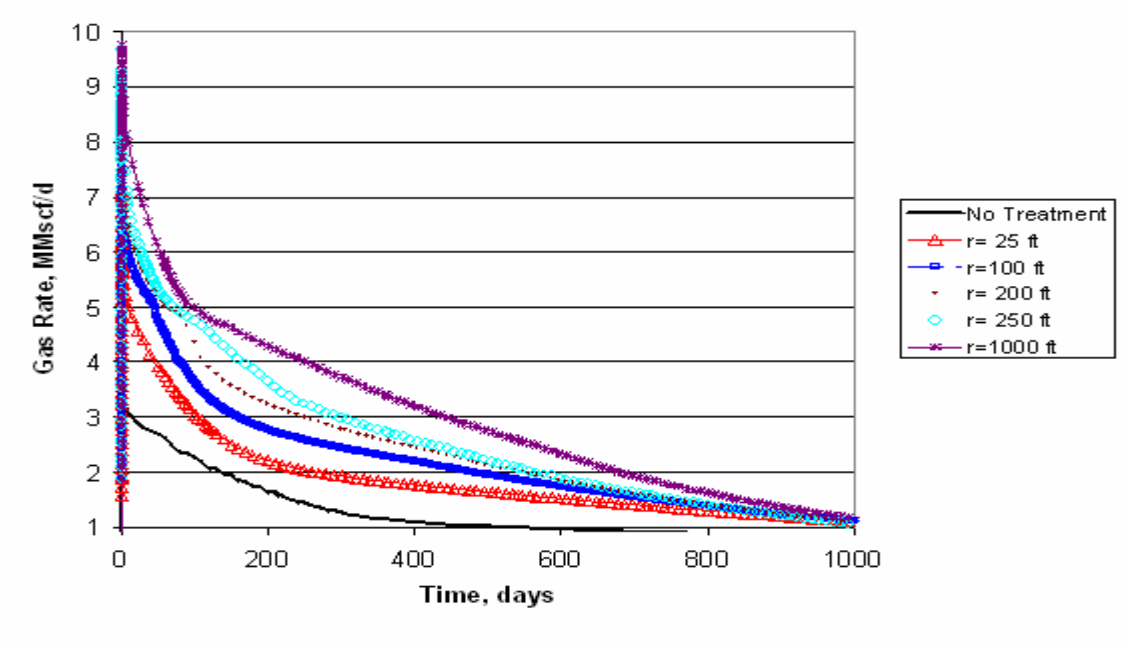

Fig. D.25 Gas Production Rate vs Time for Several Radius of Treatment, Fluid B (8 mole % C7+), Swi=0.41, h=10 feet, k=10 mD

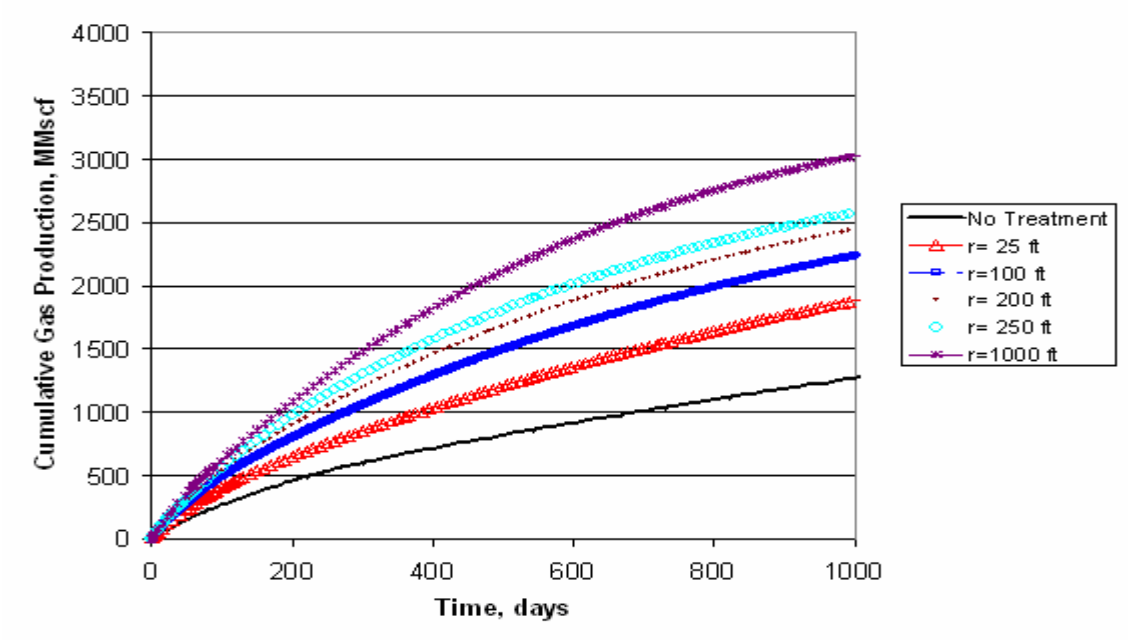

Fig. D.26 Cumulative Gas Production vs Time for Several Radius of Treatment, Fluid B (8 mole % C7+), Swi=0.41, h=10 feet, k=10 mD

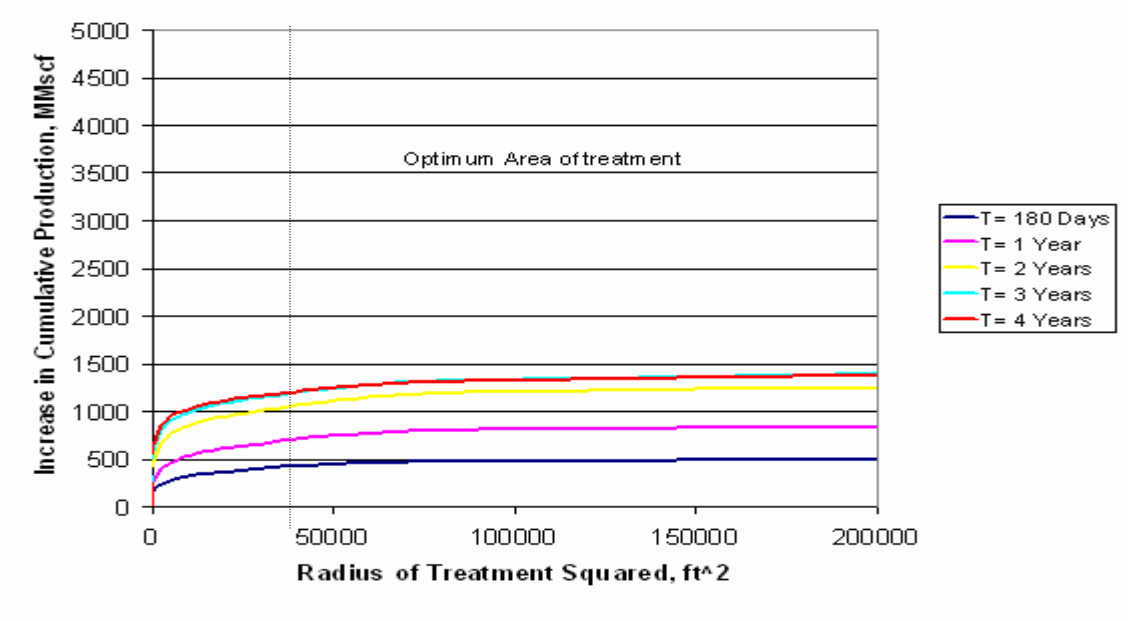

Fig. D.27 Increment in Cumulative Gas Production vs Radius of Treatment Squared , Fluid B (8 mole % C7+), Swi=0.41, h=10 feet, k=10 mD

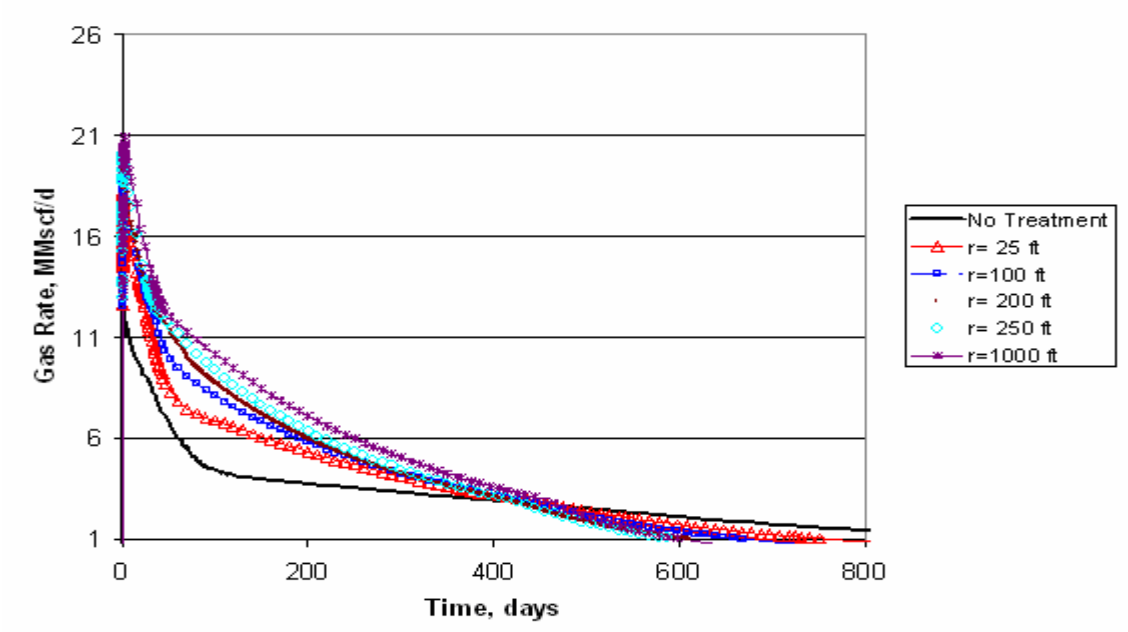

Fig. D.28 Gas Production Rate vs Time for Several Radius of Treatment, Fluid B (8 mole % C7+), Swi=0.41, h=10 feet, k=50 mD

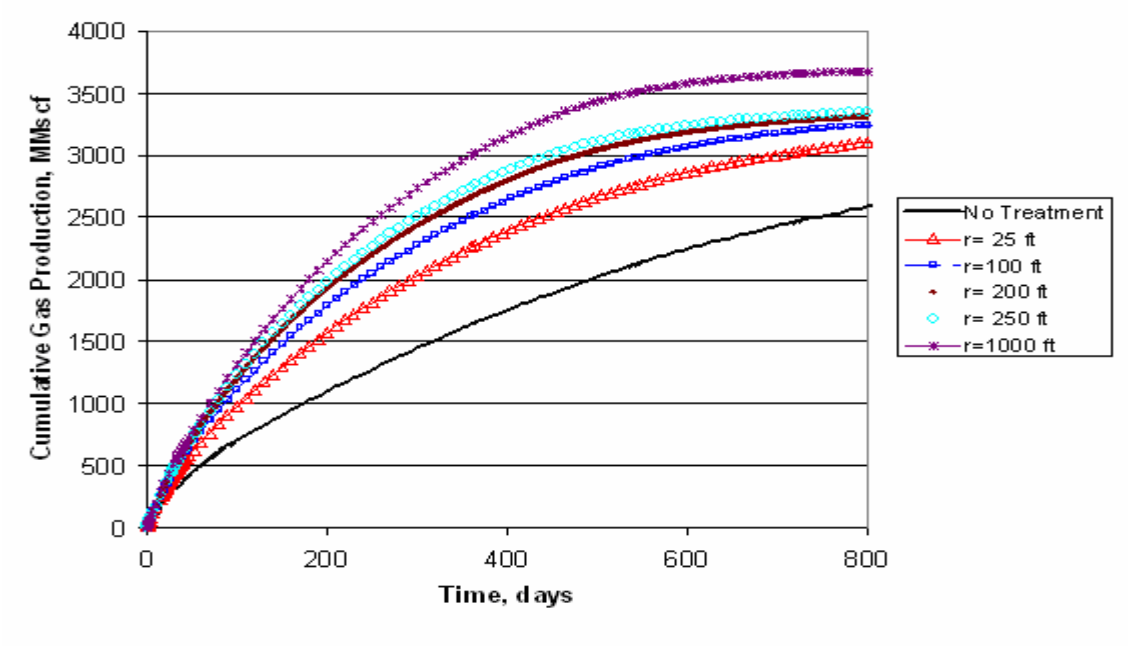

Fig. D.29 Cumulative Gas Production vs Time for Several Radius of Treatment, Fluid B (8 mole % C7+), Swi=0.41, h=10 feet, k=50 mD

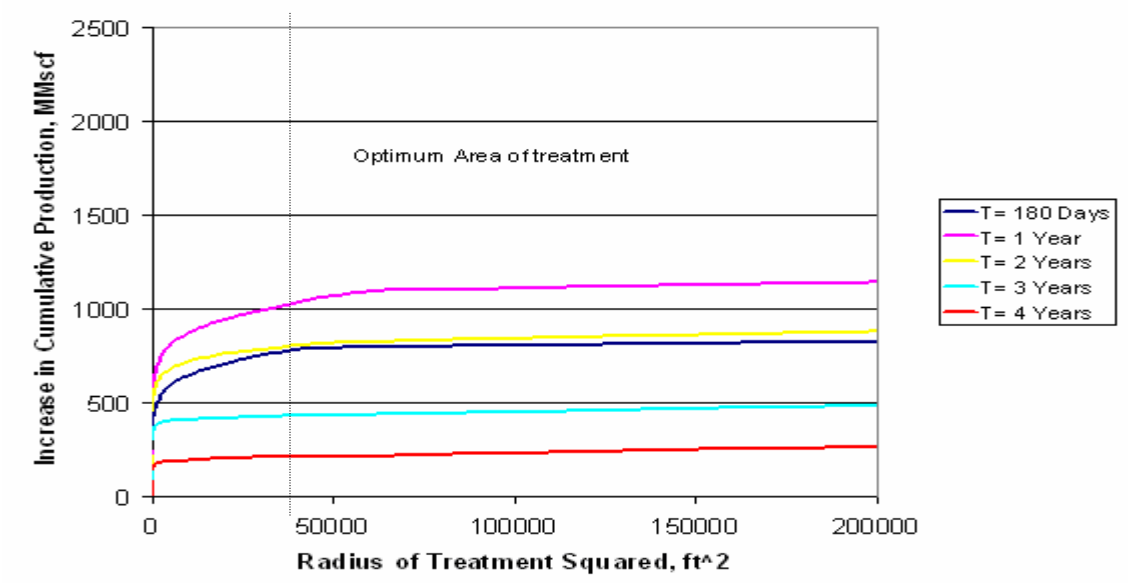

Fig. D.30 Increment in Cumulative Gas Production vs Radius of Treatment Squared , Fluid B (8 mole % C7+), Swi=0.41, h=10 feet, k=50 mD

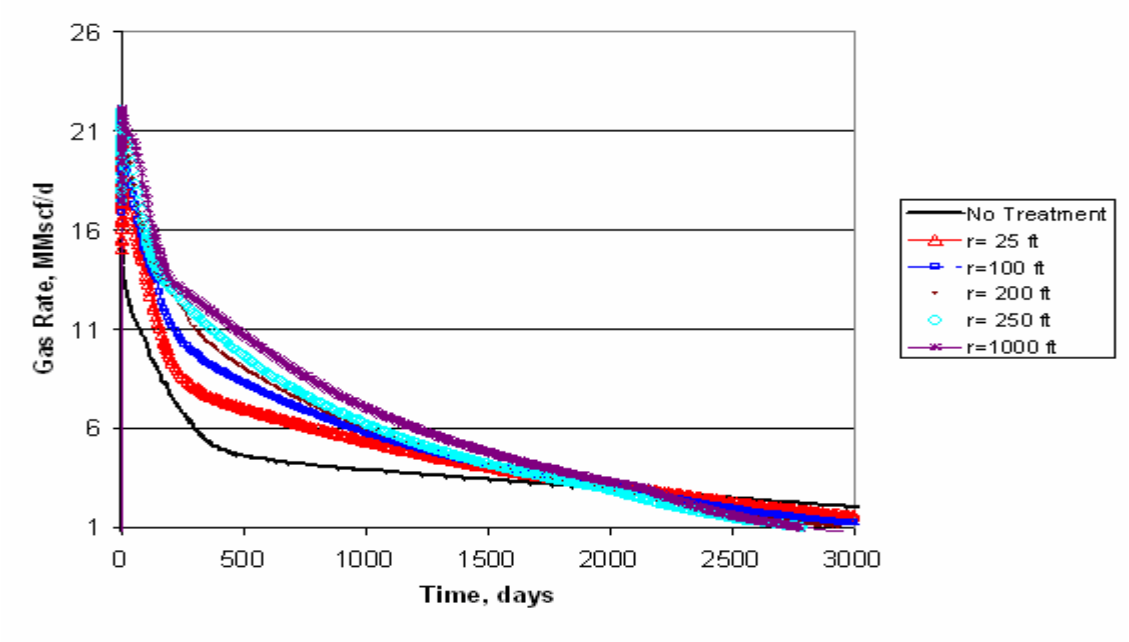

Fig. D.31 Gas Production Rate vs Time for Several Radius of Treatment, Fluid B (8 mole % C7+), Swi=0.41, h=50 feet, k=10 mD

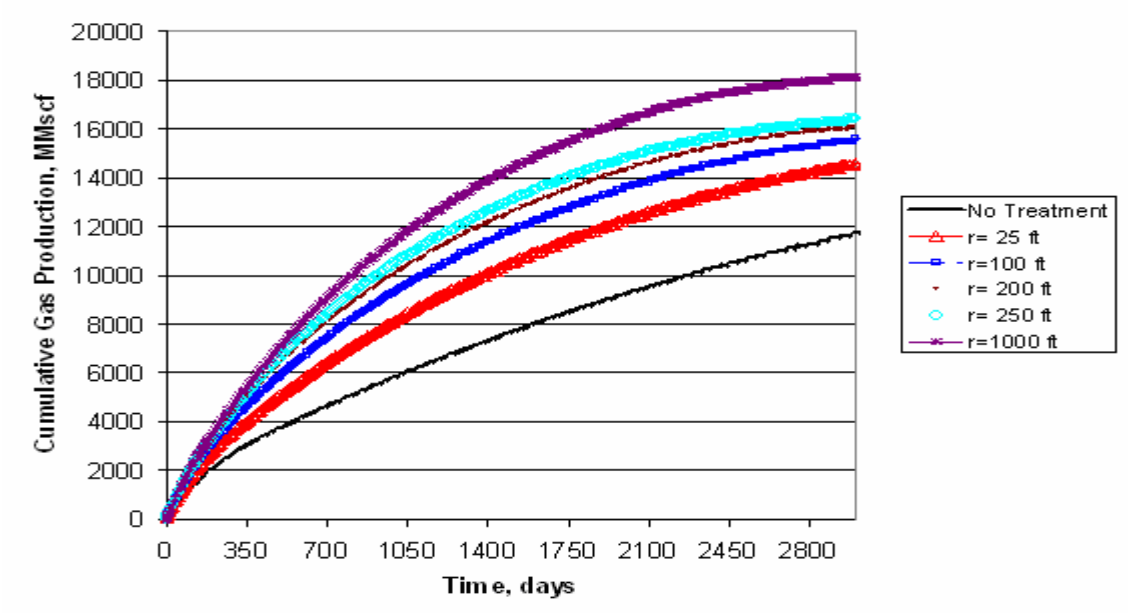

Fig. D.32 Cumulative Gas Production vs Time for Several Radius of Treatment, Fluid B (8 mole % C7+), Swi=0.41, h=50 feet, k=10 mD

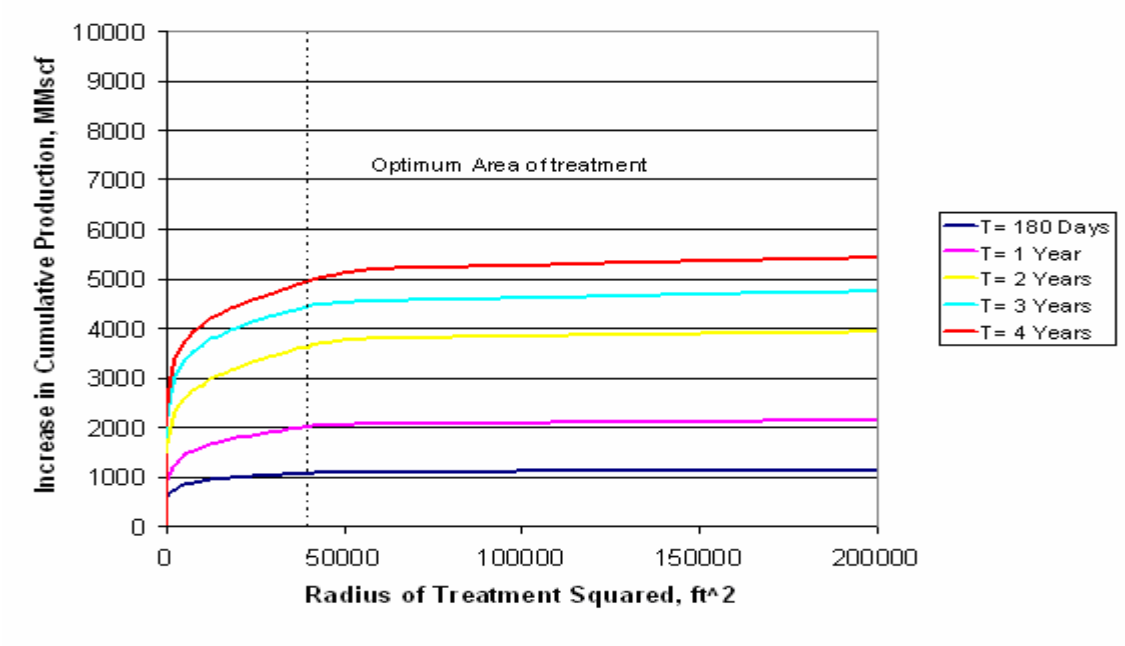

Fig. D.33 Increment in Cumulative Gas Production vs Radius of Treatment Squared , Fluid B (8 mole % C7+), Swi=0.41, h=50 feet, k=10 mD

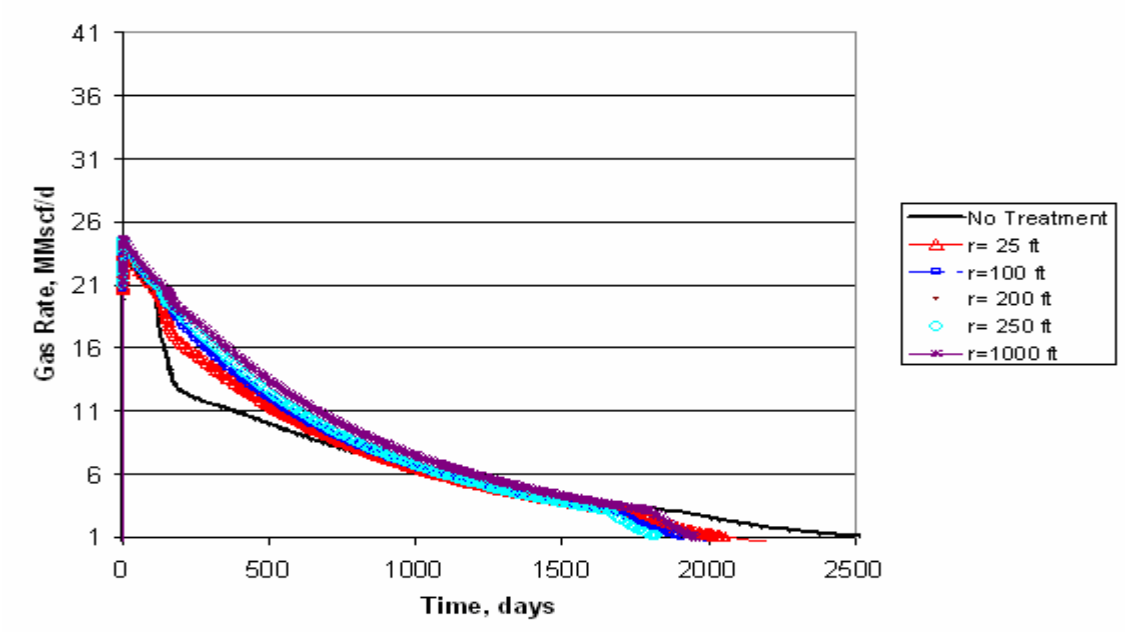

Fig. D.34 Gas Production Rate vs Time for Several Radius of Treatment, Fluid B (8 mole % C7+), Swi=0.41, h=50 feet, k=50 mD

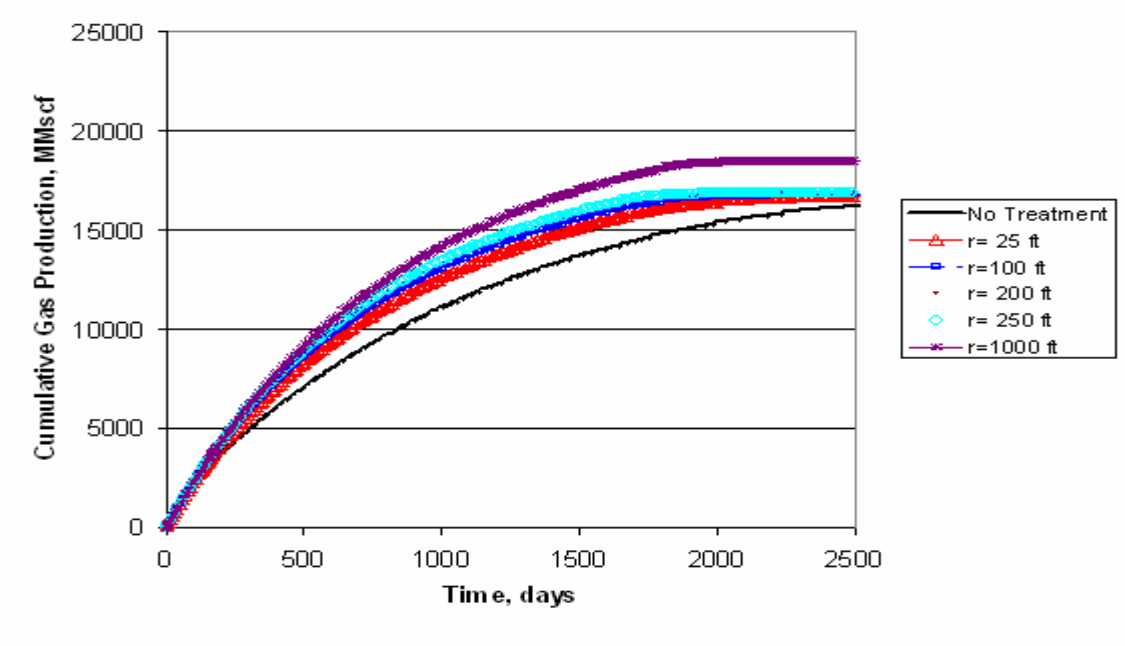

Fig. D.35 Cumulative Gas Production vs Time for Several Radius of Treatment, Fluid B (8 mole % C7+), Swi=0.41, h=50 feet, k=50 mD

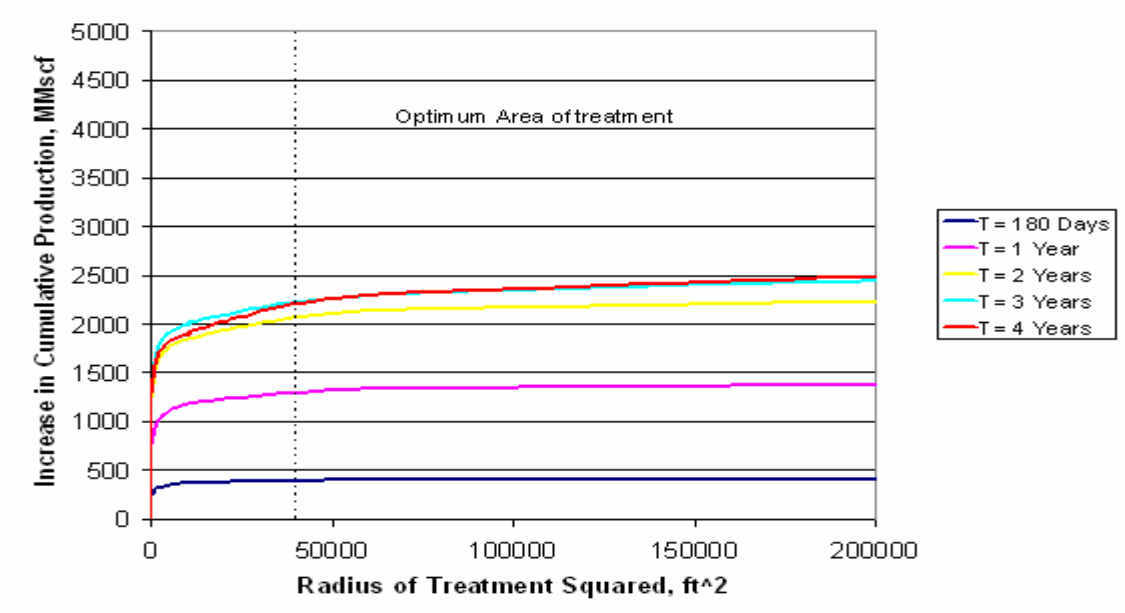

Fig. D.36 Increment in Cumulative Gas Production vs Radius of Treatment Squared , Fluid B (8 mole % C7+), Swi=0.41, h=50 feet, k=50 mD

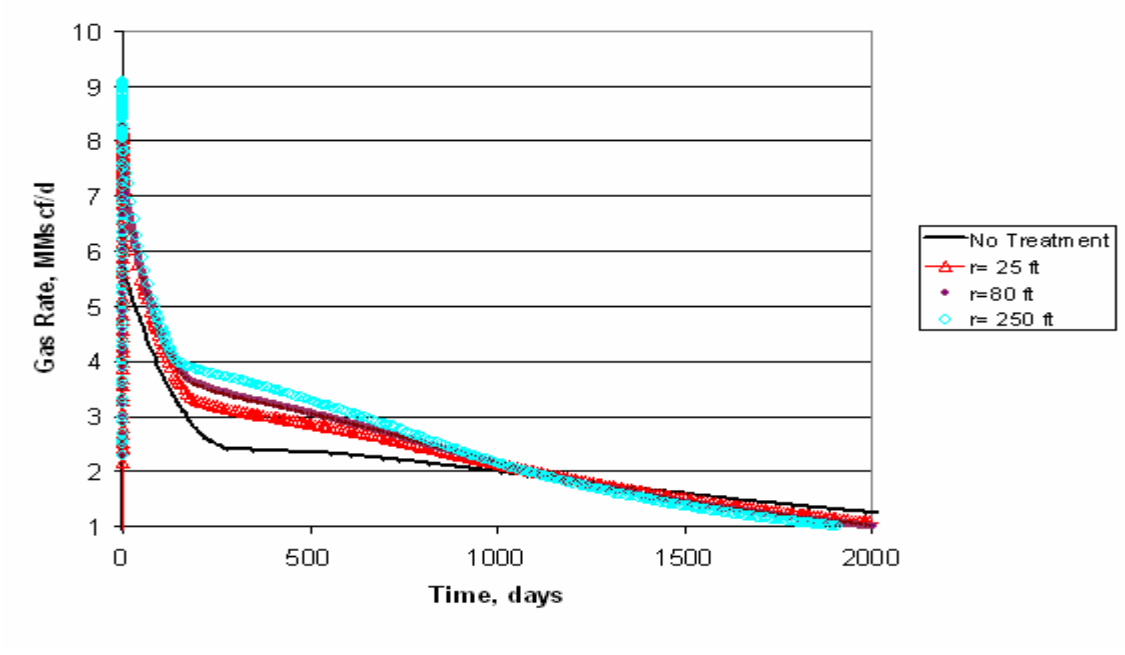

Fig. D.37 Gas Production Rate vs Time for Several Radius of Treatment, Fluid B (8 mole % C7+), Swi=0.2, h=10 feet, k=10 mD

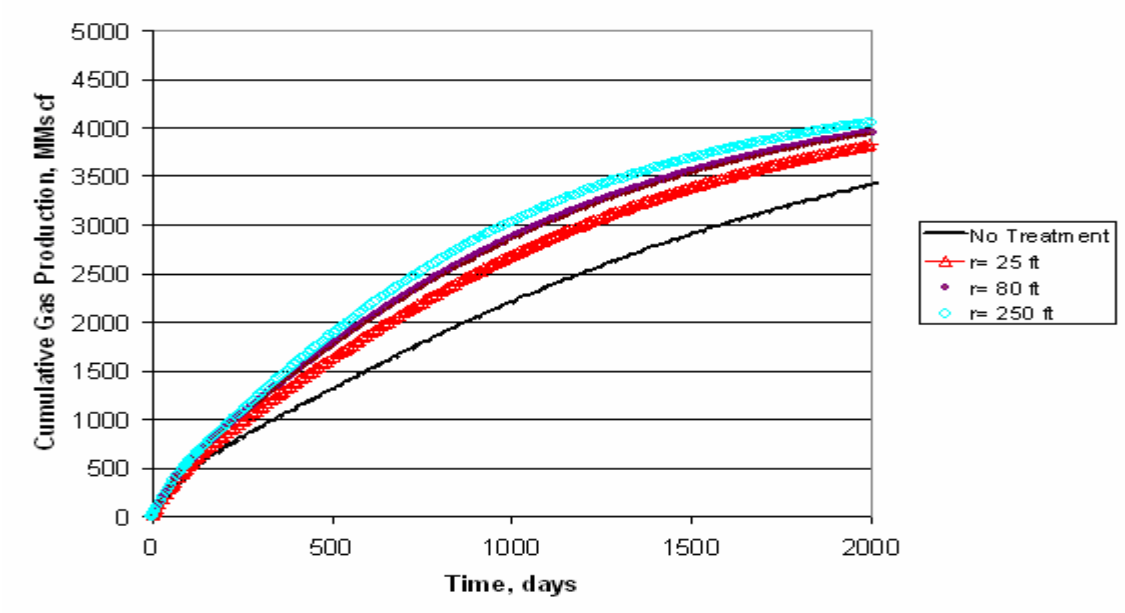

Fig. D.38 Cumulative Gas Production vs Time for Several Radius of Treatment, Fluid B (8 mole % C7+), Swi=0.2, h=10 feet, k=10 mD

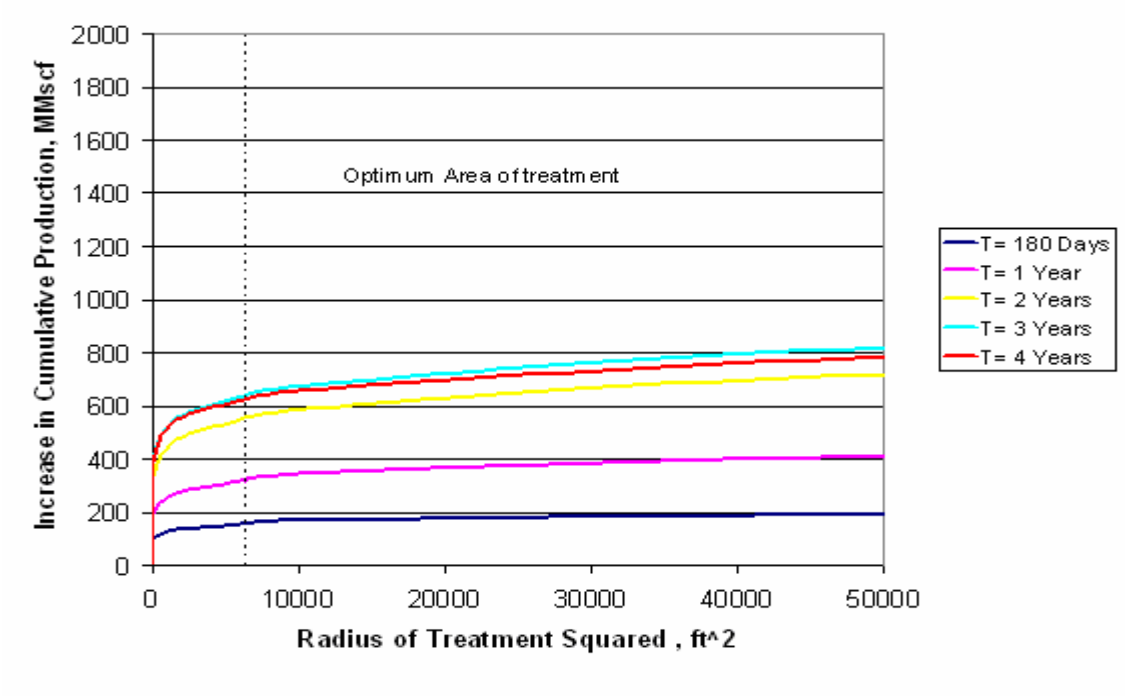

Fig. D.39 Increment in Cumulative Gas Production vs Radius of Treatment Squared , Fluid B (8 mole % C7+), Swi=0.2, h=10 feet, k=10 mD

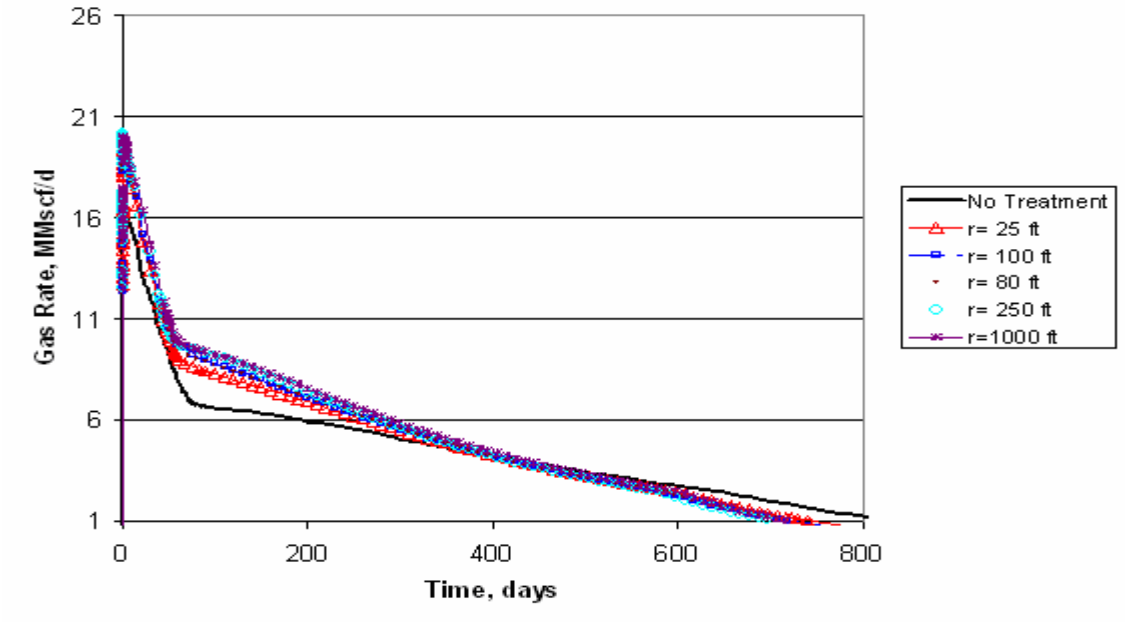

Fig. D.40 Gas Production Rate vs Time for Several Radius of Treatment, Fluid B (8 mole % C7+), Swi=0.2, h=10 feet, k=50 mD

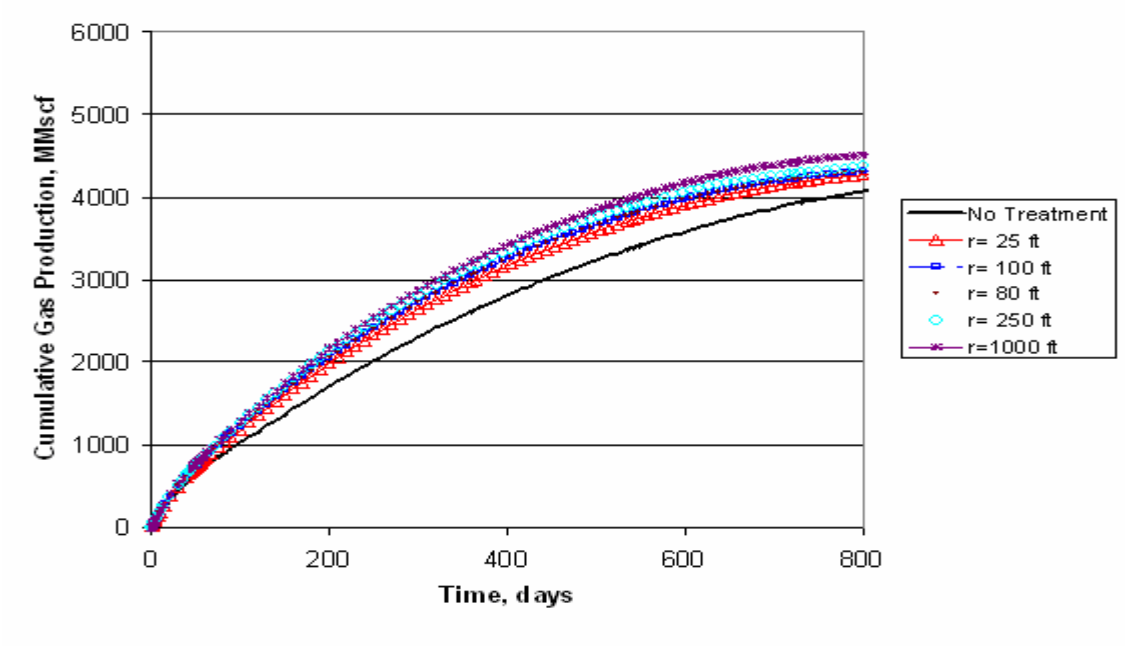

Fig. D.41 Cumulative Gas Production vs Time for Several Radius of Treatment, Fluid B (8 mole % C7+), Swi=0.2, h=10 feet, k=50 mD

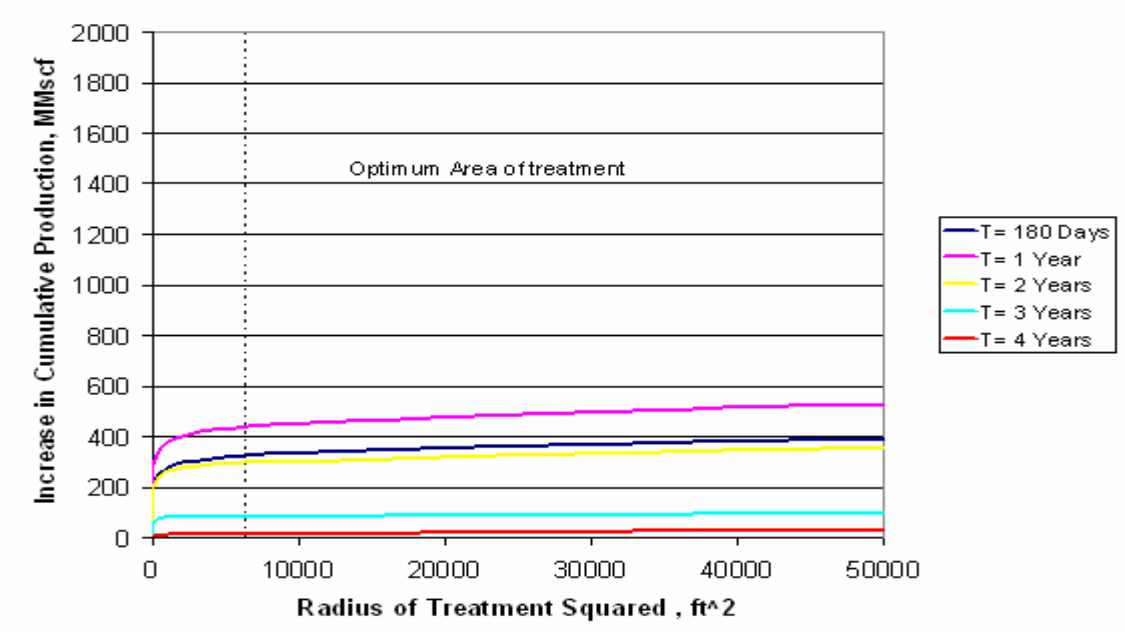

Fig. D.42 Increment in Cumulative Gas Production vs Radius of Treatment Squared , Fluid B (8 mole % C7+), Swi=0.2, h=10 feet, k=50 mD

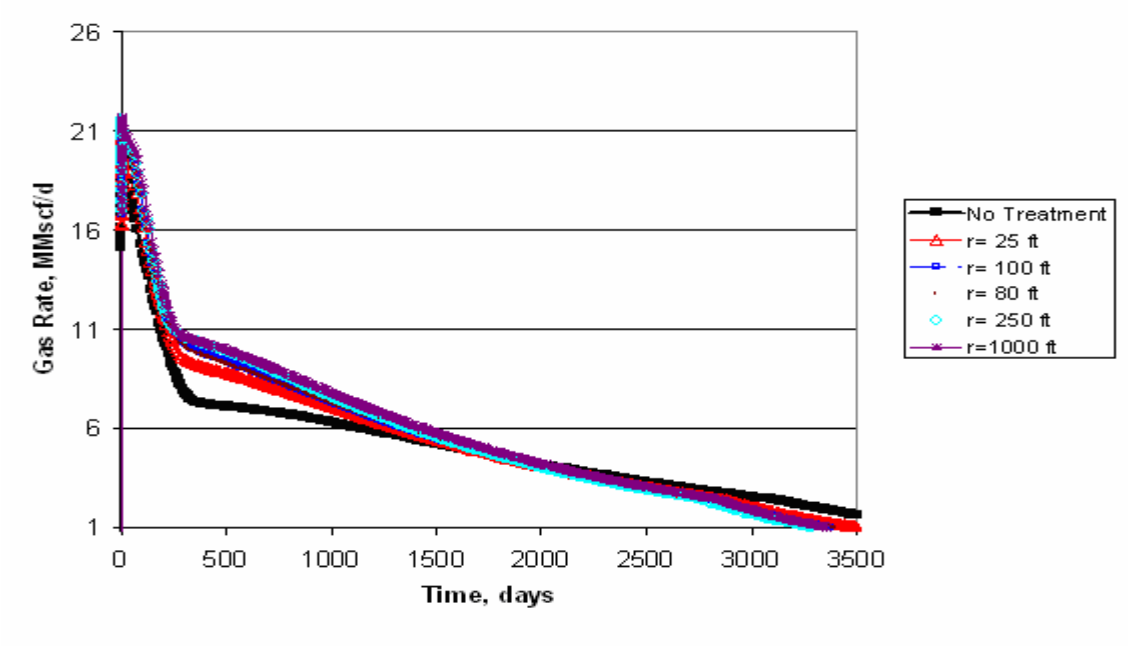

Fig. D.43 Gas Production Rate vs Time for Several Radius of Treatment, Fluid B (8 mole % C7+), Swi=0.2, h=50 feet, k=10 mD

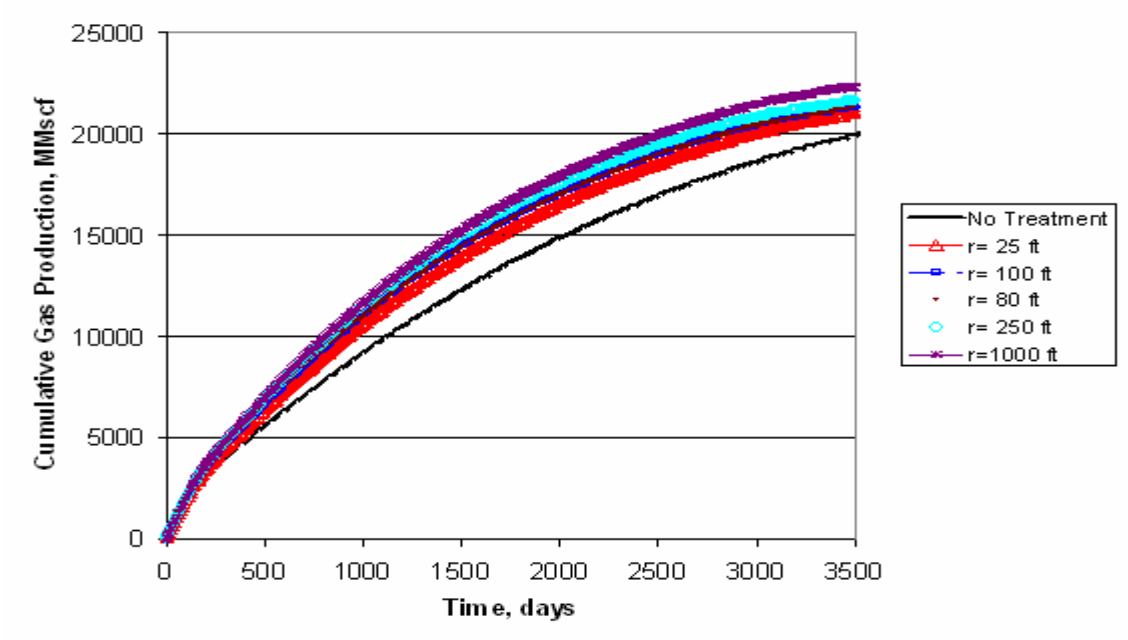

Fig. D.44 Cumulative Gas Production vs Time for Several Radius of Treatment, Fluid B (8 mole % C7+), Swi=0.2, h=50 feet, k=10 mD

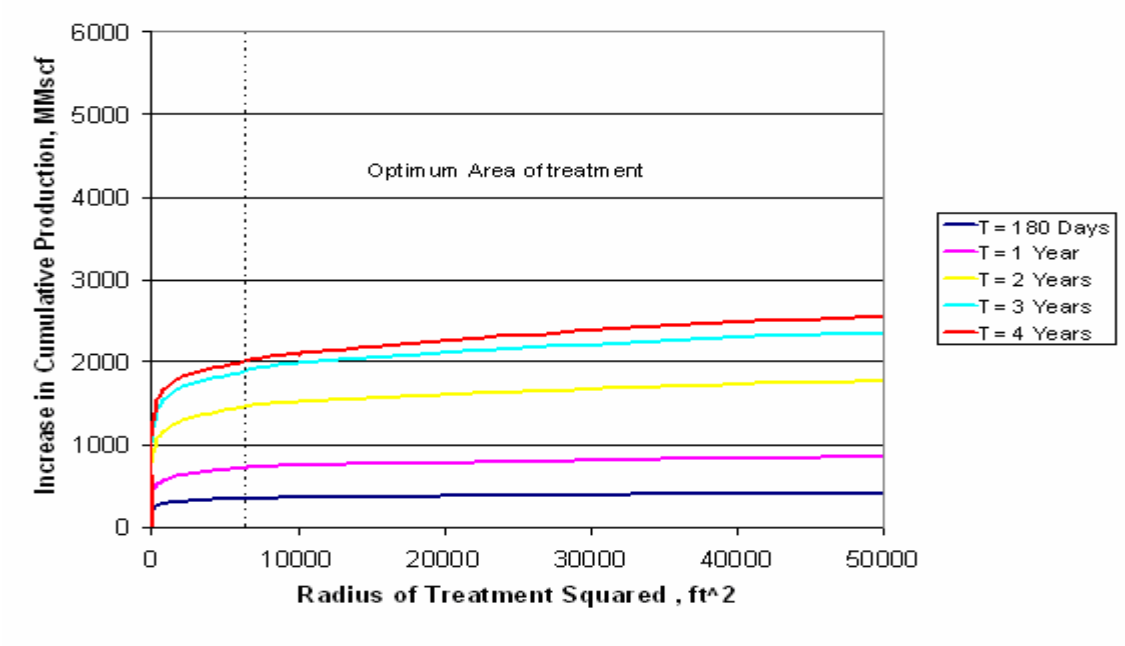

Fig. D.45 Increment in Cumulative Gas Production vs Radius of Treatment Squared , Fluid B (8 mole % C7+), Swi=0.2, h=50 feet, k=10 mD

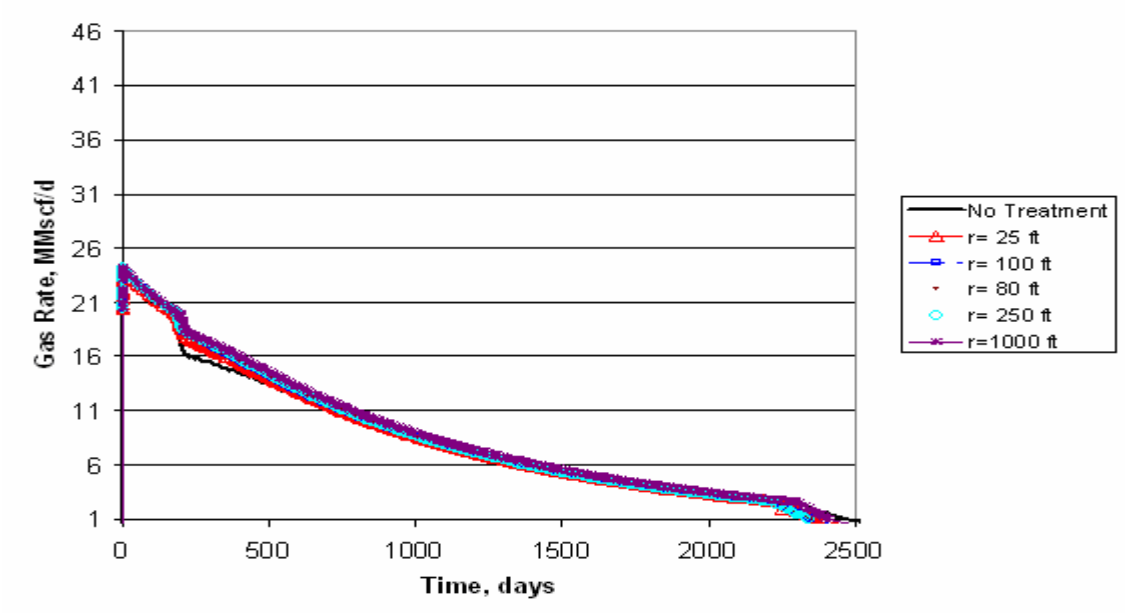

Fig. D.46 Gas Production Rate vs Time for Several Radius of Treatment, Fluid B (8 mole % C7+), Swi=0.2, h=50 feet, k=50 mD

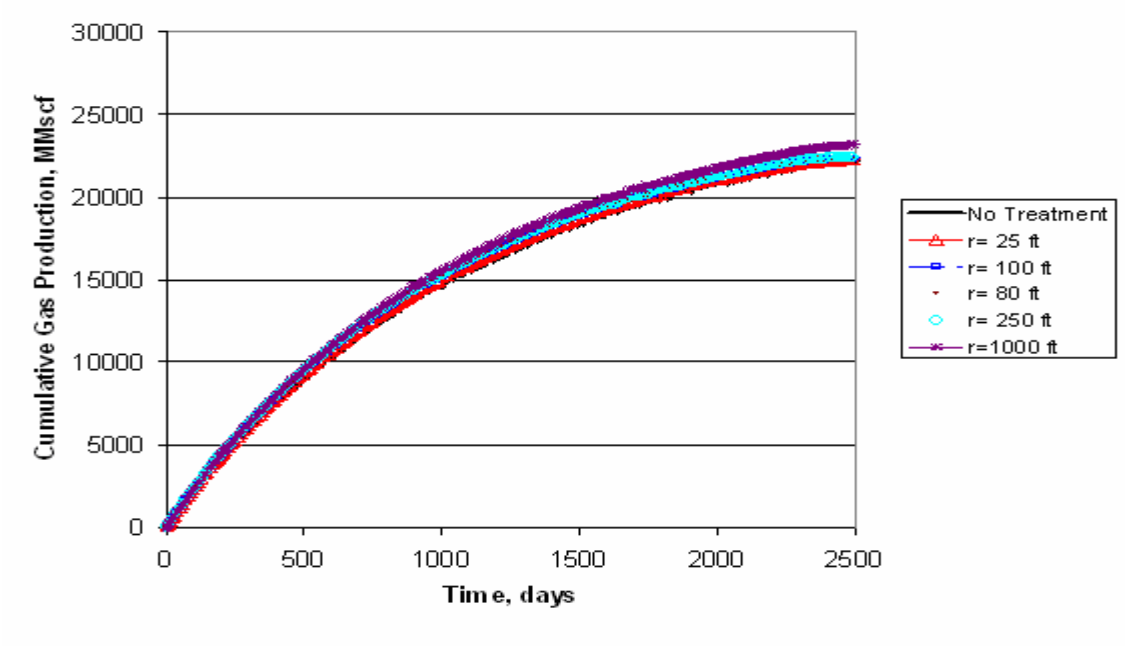

Fig. D.47 Cumulative Gas Production vs Time for Several Radius of Treatment, Fluid B (8 mole % C7+), Swi=0.2, h=50 feet, k=50 mD

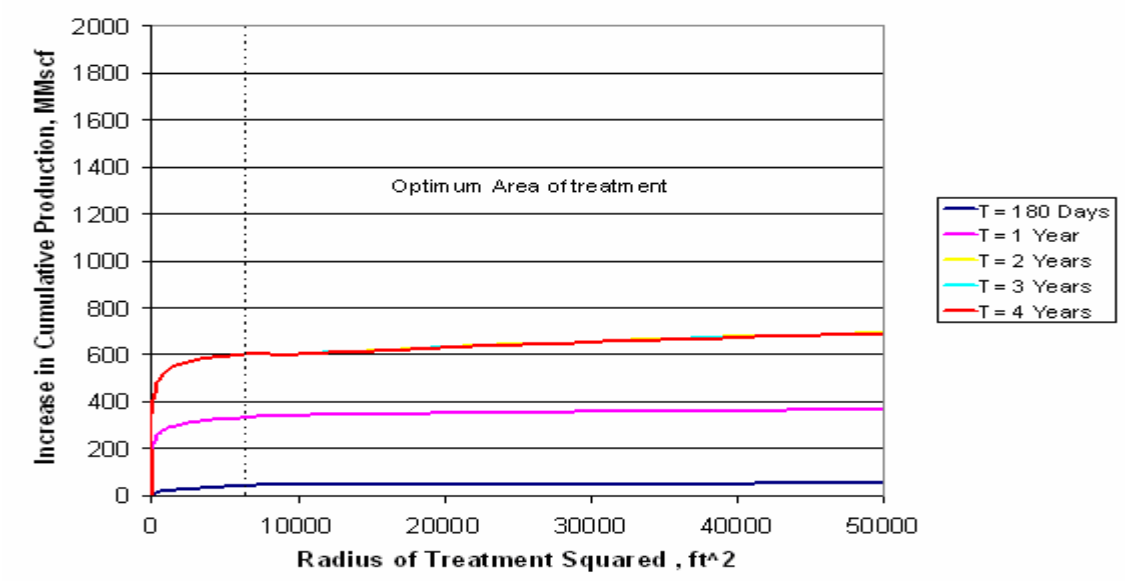

Fig. D.48 Increment in Cumulative Gas Production vs Radius of Treatment Squared , Fluid B (8 mole % C7+), Swi=0.2, h=50 feet, k=50 mD

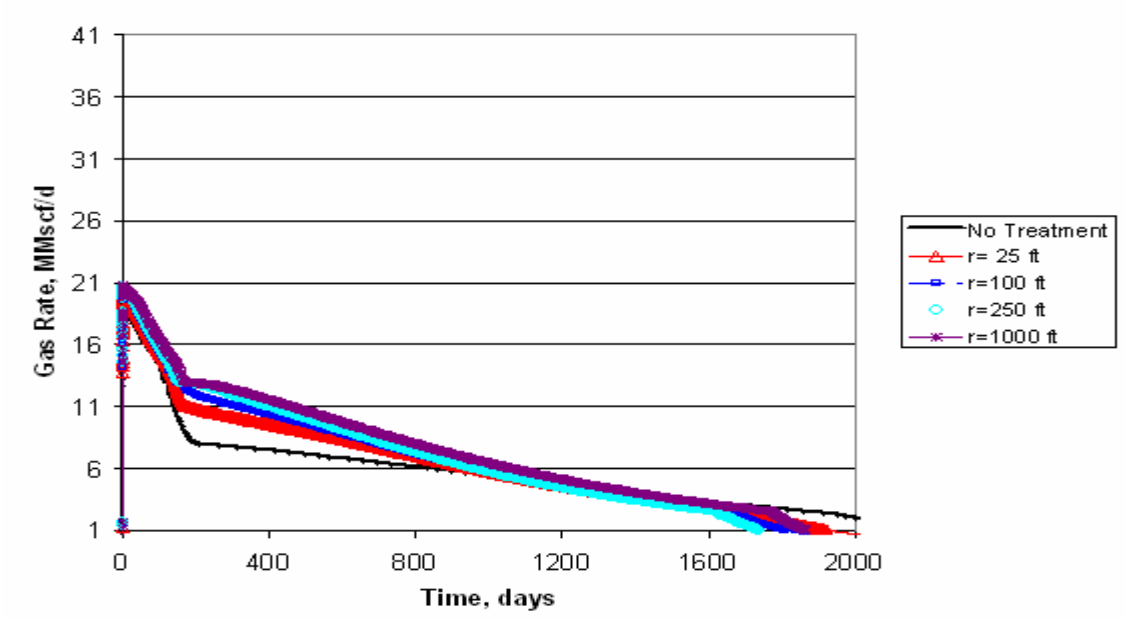

Fig. D.49 Gas Production Rate vs Time for Several Radius of Treatment, Fluid C (11 mole % C7+), Swi=0.41, h=50 feet, k=50 mD

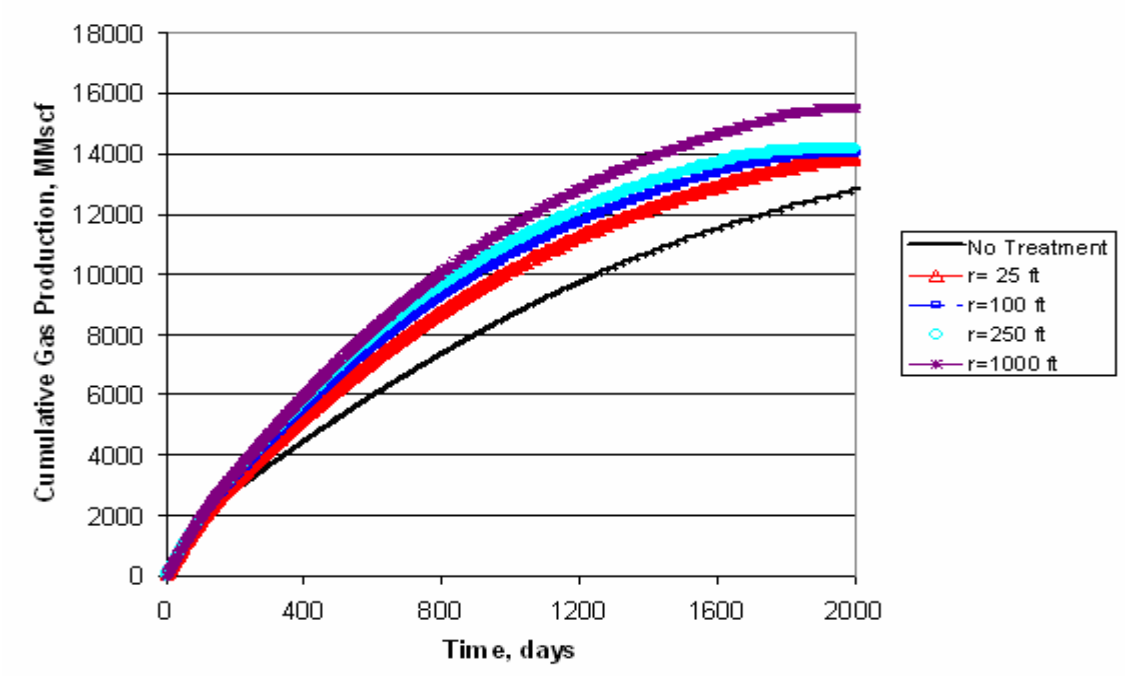

Fig. D.50 Cumulative Gas Production vs Time for Several Radius of Treatment, Fluid C (11 mole % C7+), Swi=0.41, h=50 feet, k=50 mD

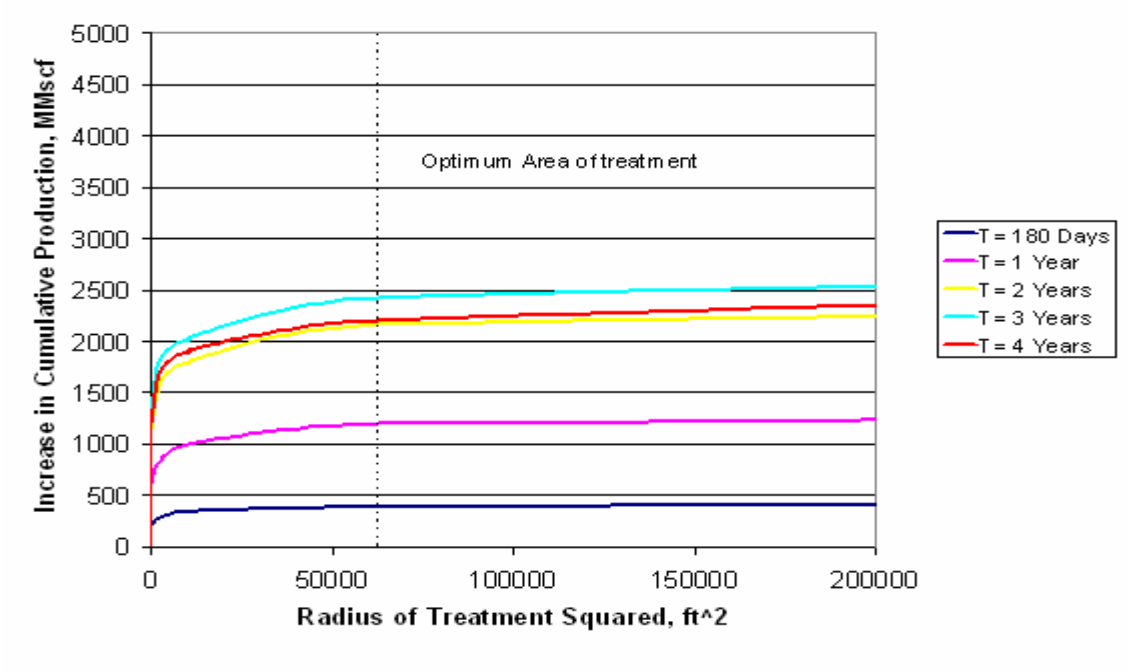

Fig. D.51 Increment in Cumulative Gas Production vs Radius of Treatment Squared , Fluid C (11 mole % C7+), Swi=0.41, h=50 feet, k=50 mD

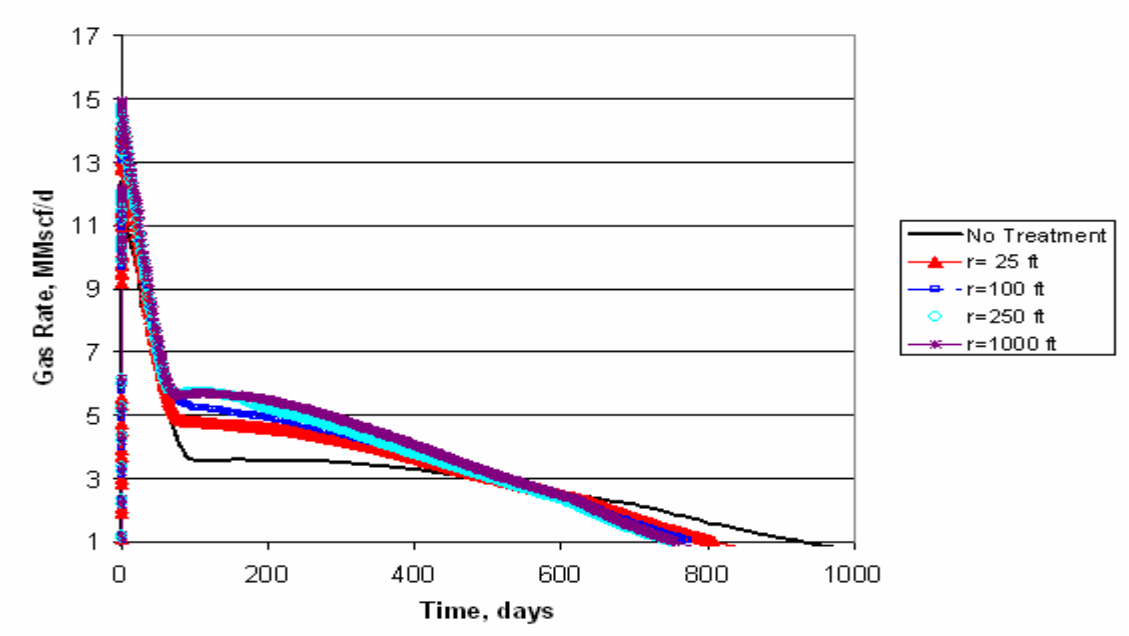

Fig. D.52 Gas Production Rate vs Time for Several Radius of Treatment, Fluid C (11 mole % C7+), Swi=0.2, h=10 feet, k=50 mD

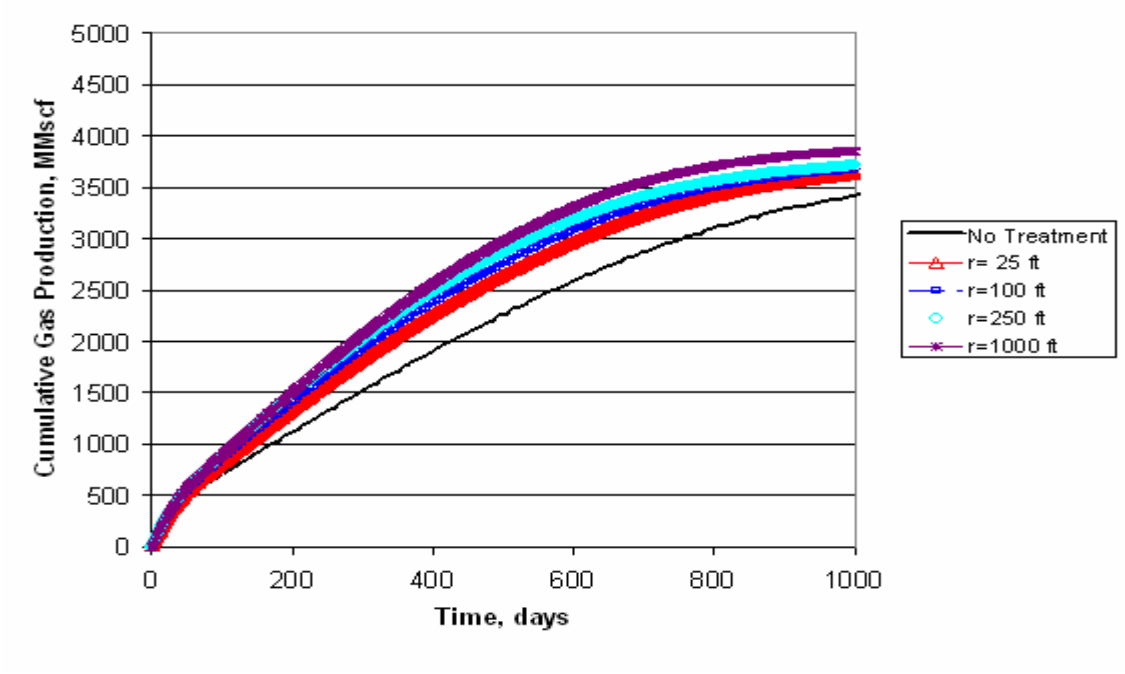

Fig. D.53 Cumulative Gas Production vs Time for Several Radius of Treatment, Fluid C (11 mole % C7+), Swi=0.2, h=10 feet, k=50 mD

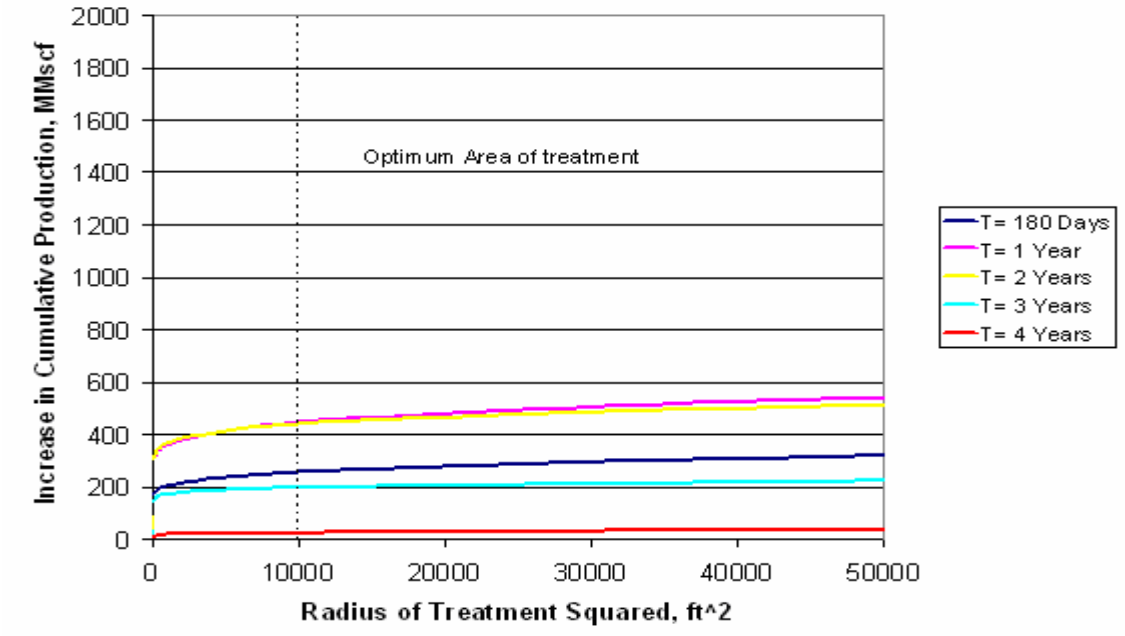

Fig. D.54 Increment in Cumulative Gas Production vs Radius of Treatment Squared , Fluid C (11 mole % C7+), Swi=0.2, h=10 feet, k=50 mD

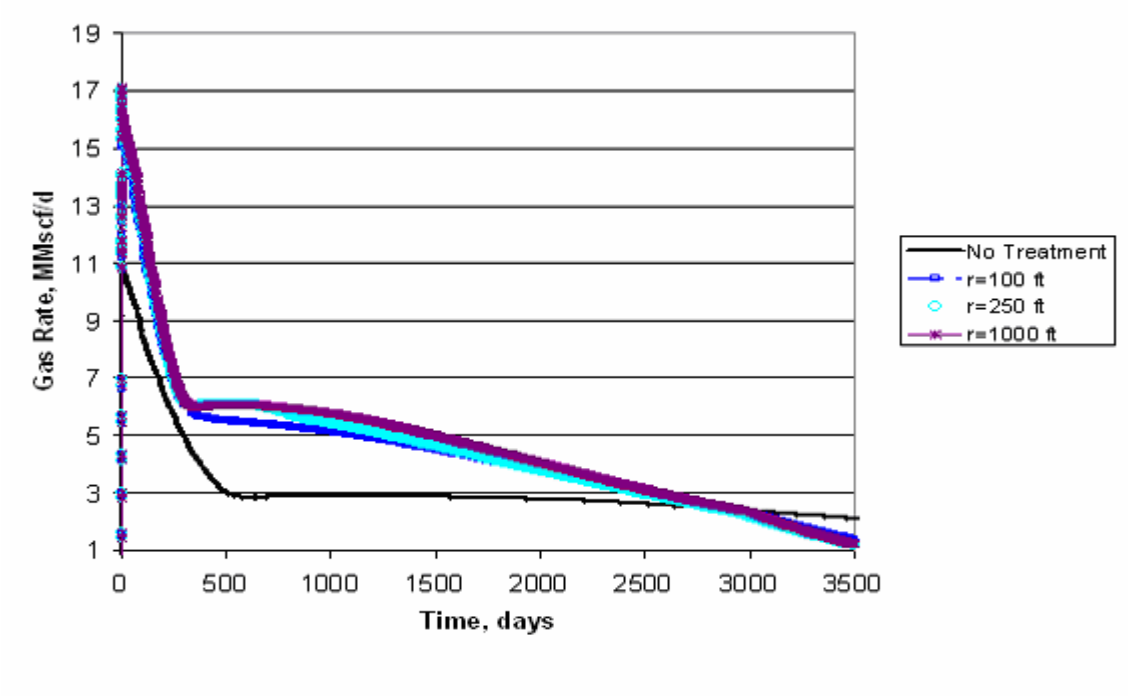

Fig. D.55 Gas Production Rate vs Time for Several Radius of Treatment, Fluid C (11 mole % C7+), Swi=0.2, h=50 feet, k=10 mD

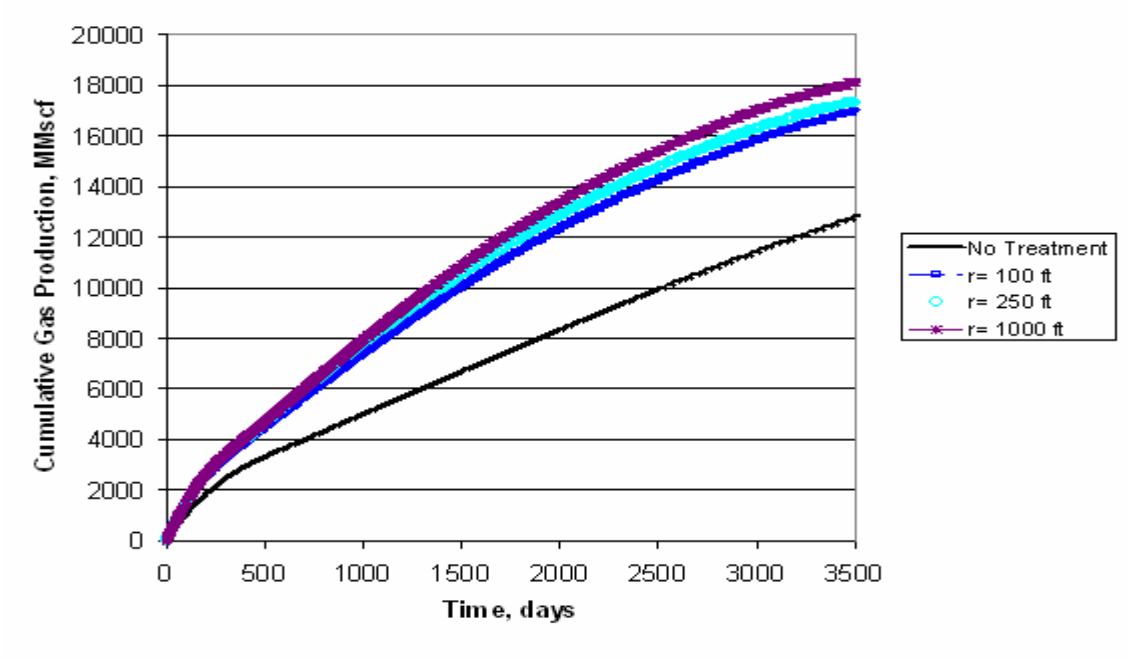

Fig. D.56 Cumulative Gas Production vs Time for Several Radius of Treatment, Fluid C (11 mole % C7+), Swi=0.2, h=50 feet, k=10 mD

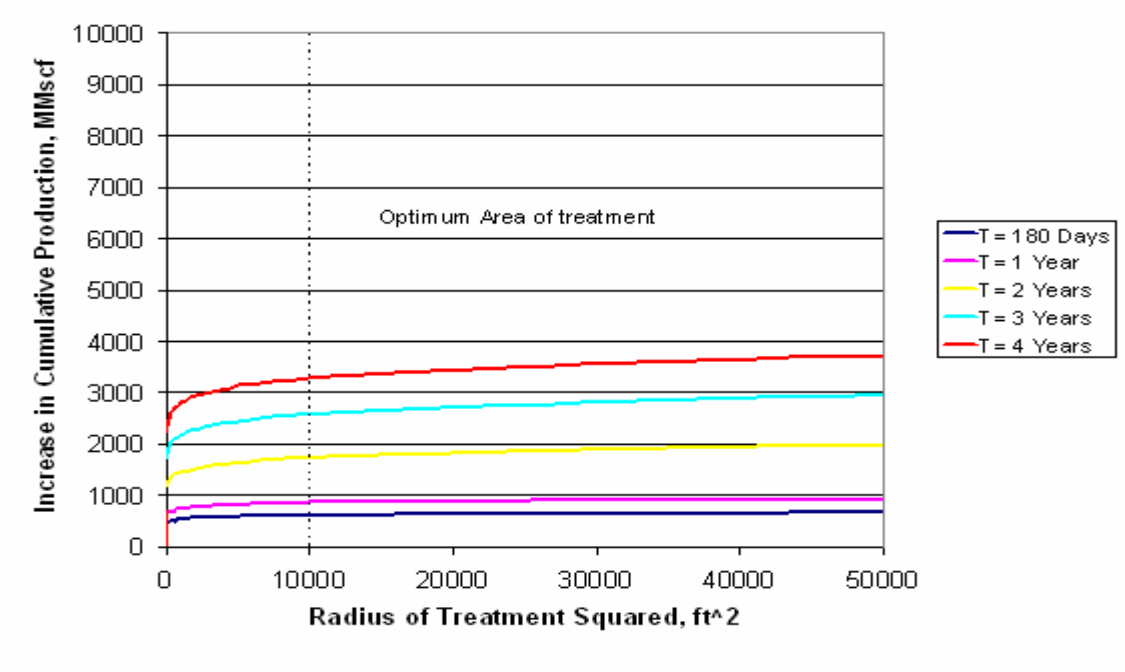

Fig. D.57 Increment in Cumulative Gas Production vs Radius of Treatment Squared , Fluid C (11 mole % C7+), Swi=0.2, h=50 feet, k=10 mD

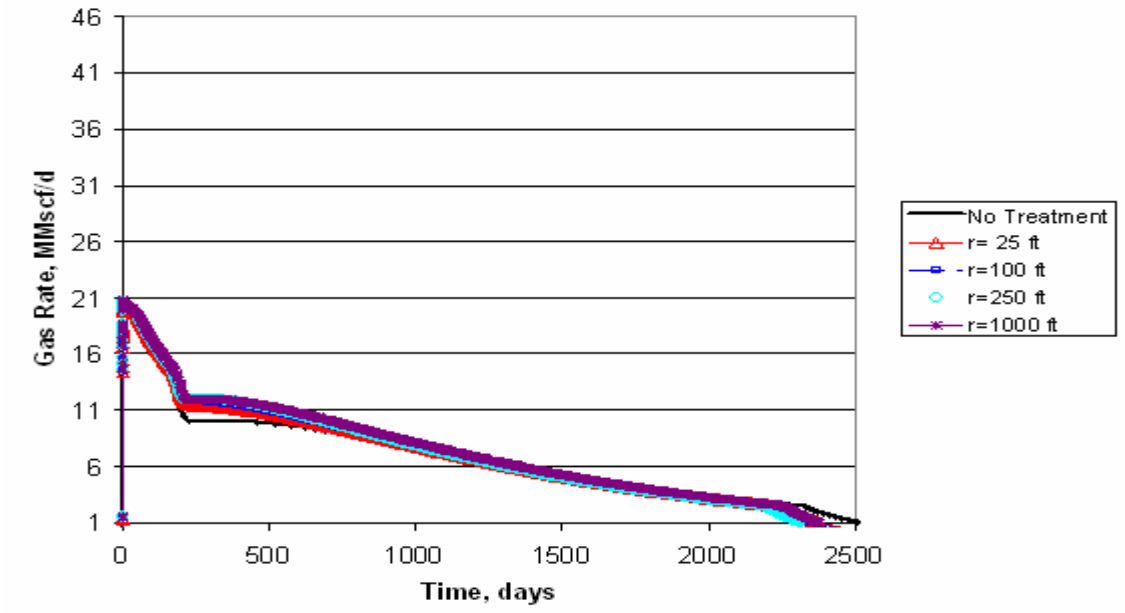

Fig. D.58 Gas Production Rate vs Time for Several Radius of Treatment, Fluid C (11 mole % C7+), Swi=0.2, h=50 feet, k=50 mD

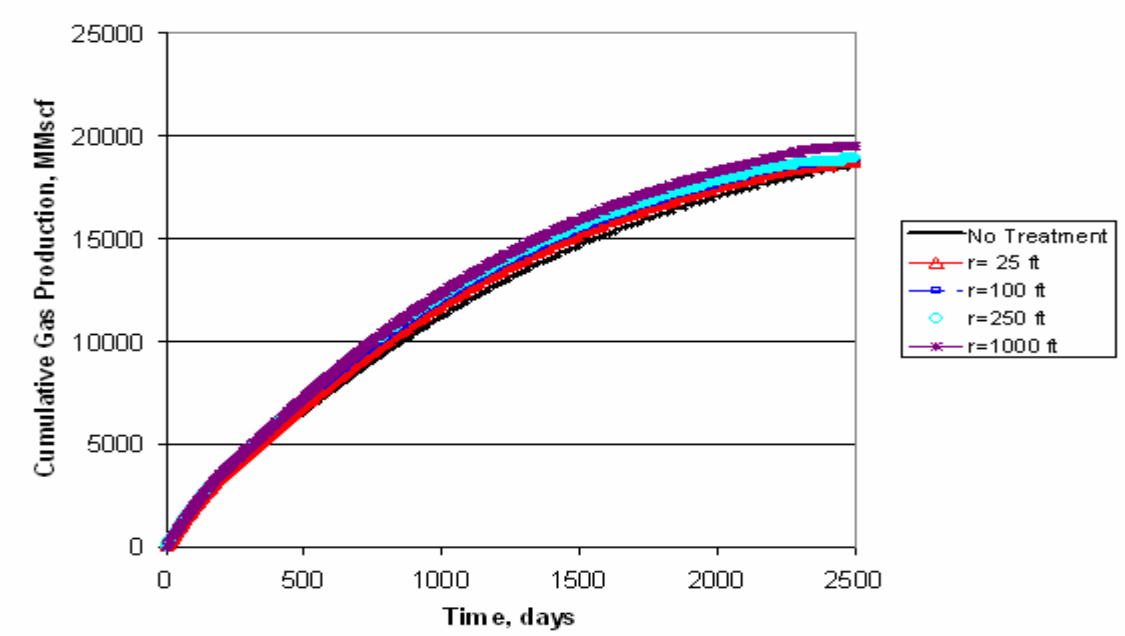

Fig. D.59 Cumulative Gas Production vs Time for Several Radius of Treatment, Fluid C (11 mole % C7+), Swi=0.2, h=50 feet, k=50 mD

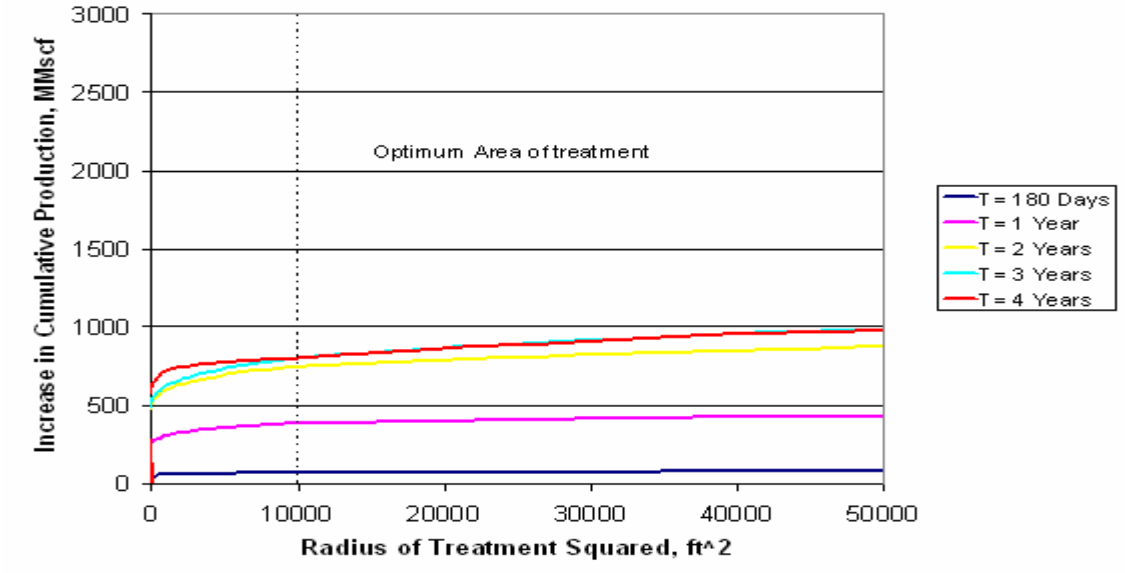

Fig. D.60 Increment in Cumulative Gas Production vs Radius of Treatment Squared , Fluid C (11 mole % C7+), Swi=0.2, h=50 feet, k=50 mD

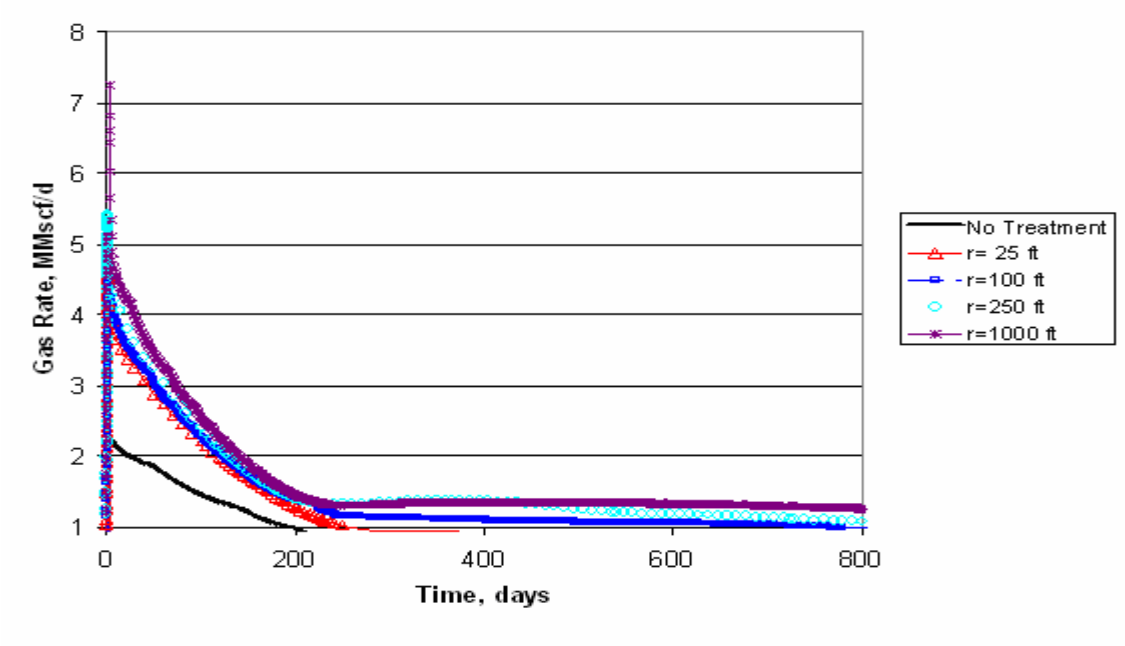

Fig. D.61 Gas Production Rate vs Time for Several Radius of Treatment, Fluid C (11 mole % C7+), Swi=0.2, h=10 feet, k=10 mD

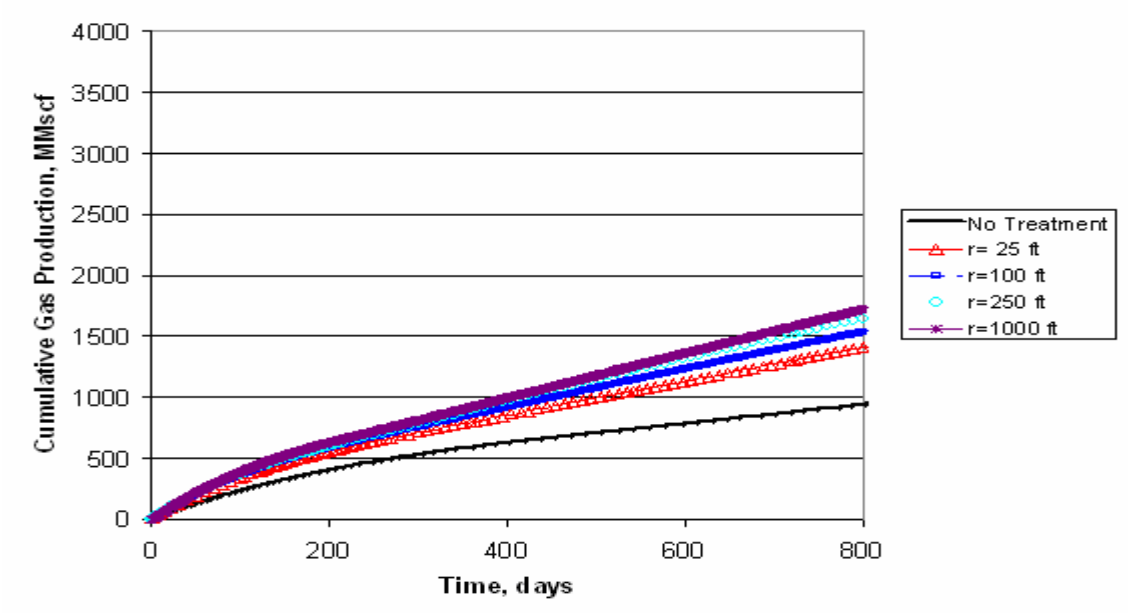

Fig. D.62 Cumulative Gas Production vs Time for Several Radius of Treatment, Fluid C (11 mole % C7+), Swi=0.2, h=10 feet, k=10 mD

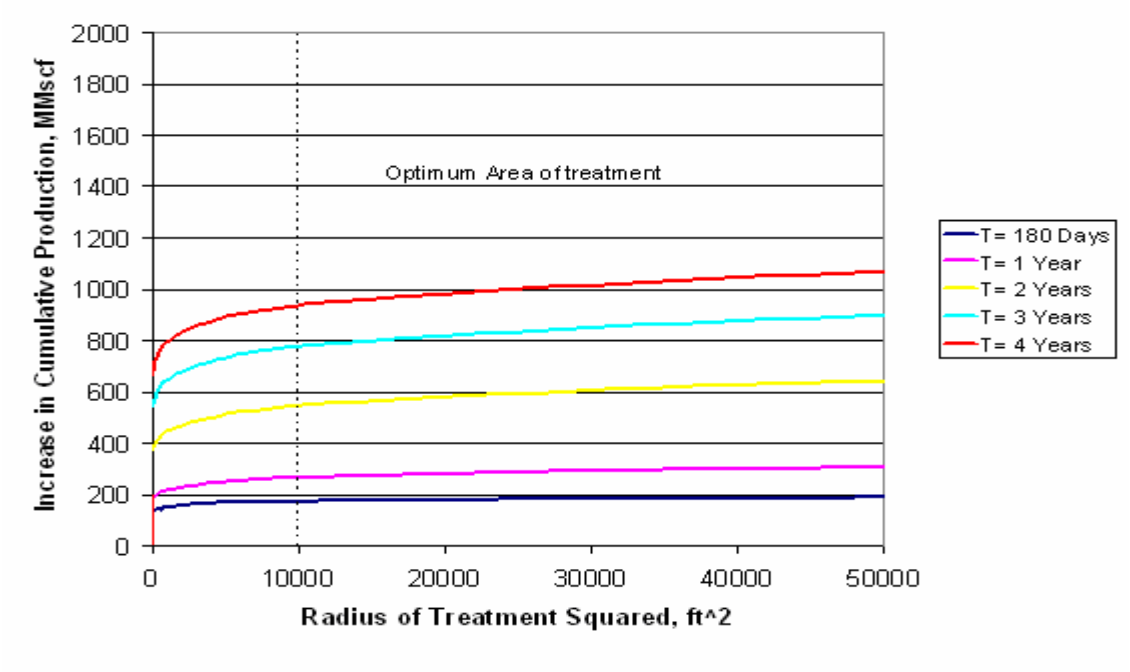

Fig. D.63 Increment in Cumulative Gas Production vs Radius of Treatment Squared , Fluid C (11 mole % C7+), Swi=0.2, h=10 feet, k=10 mD

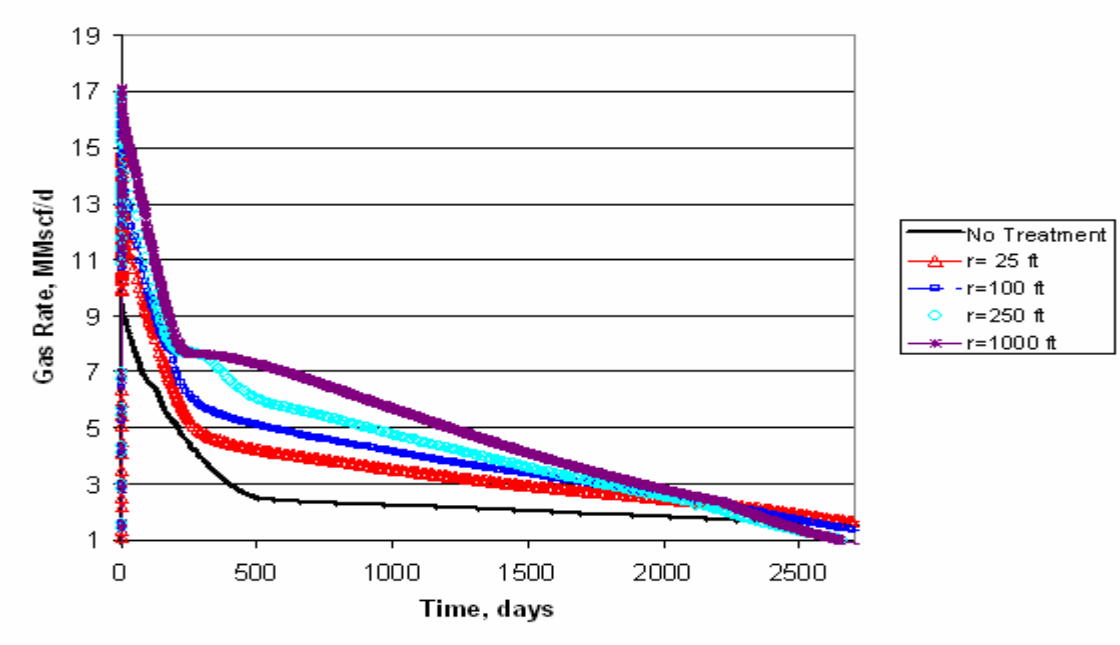

Fig. D.64 Gas Production Rate vs Time for Several Radius of Treatment, Fluid C (11 mole % C7+), Swi=0.41, h=50 feet, k=10 mD

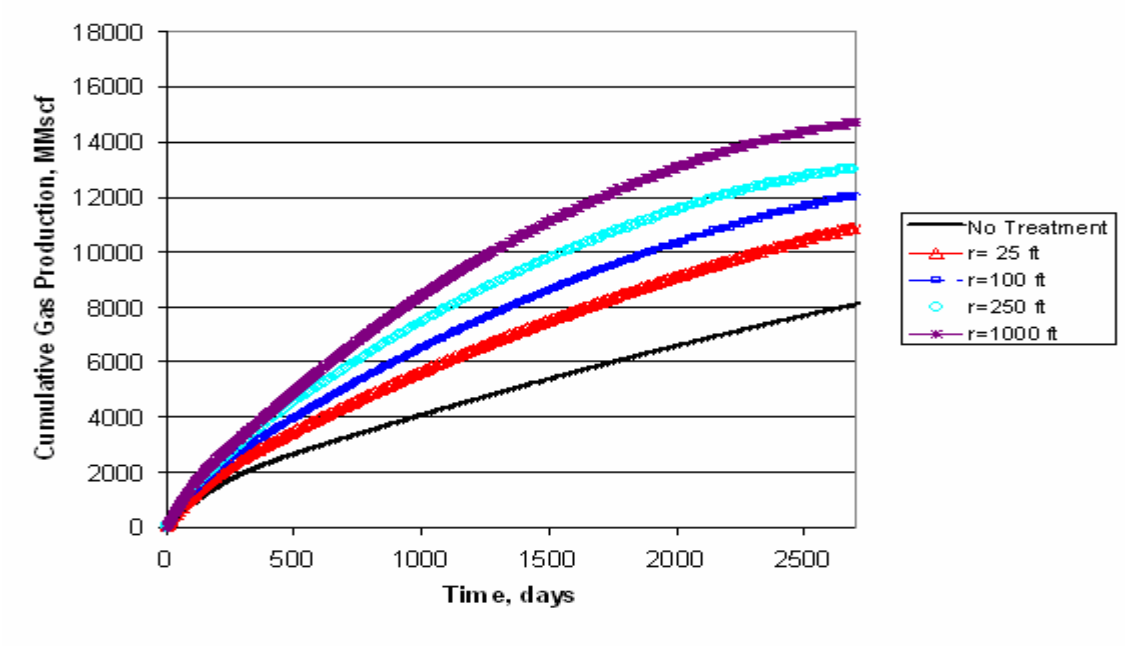

Fig. D.65 Cumulative Gas Production vs Time for Several Radius of Treatment, Fluid C (11 mole % C7+), Swi=0.41, h=50 feet, k=10 mD

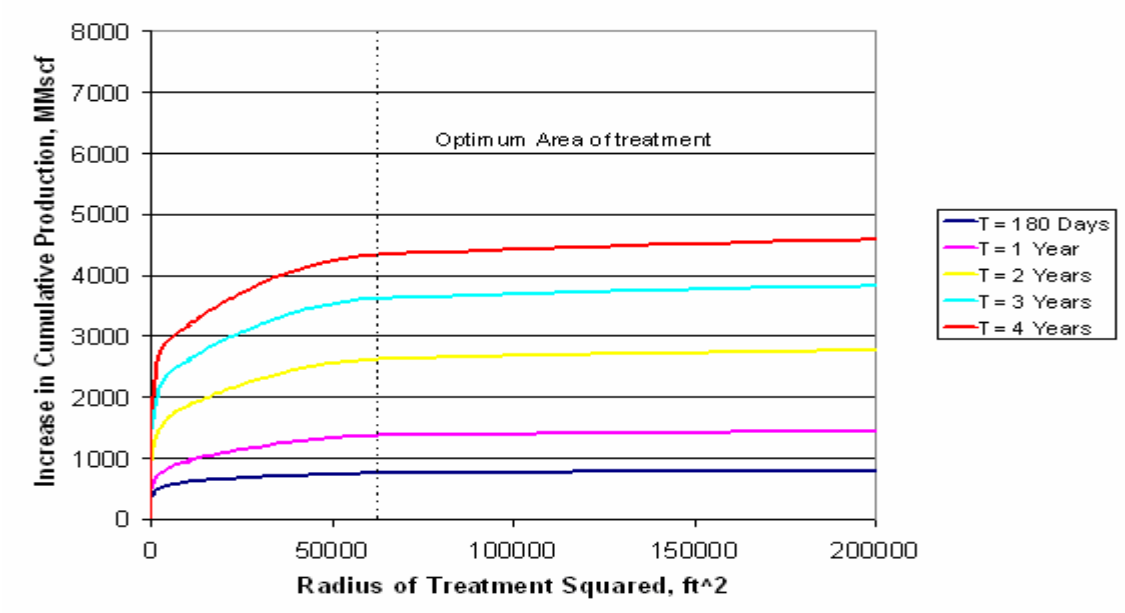

Fig. D.66 Increment in Cumulative Gas Production vs Radius of Treatment Squared , Fluid C (11 mole % C7+), Swi=0.41, h=50 feet, k=10 mD

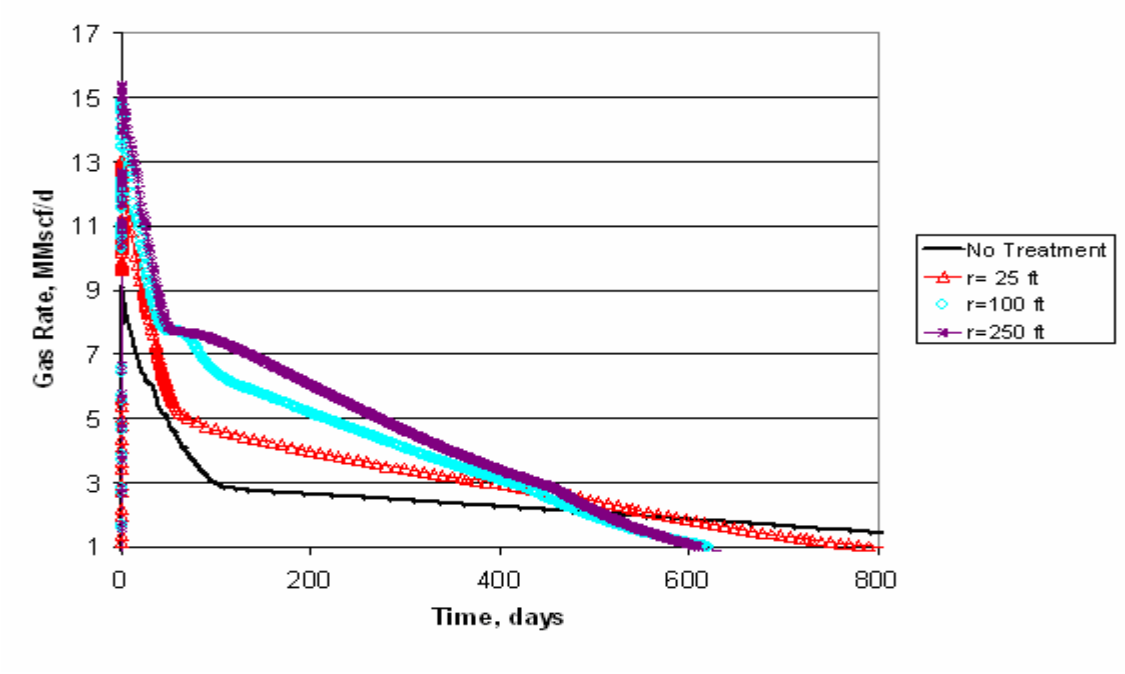

Fig. D.67 Gas Production Rate vs Time for Several Radius of Treatment, Fluid C (11 mole % C7+), Swi=0.41, h=10 feet, k=50 mD

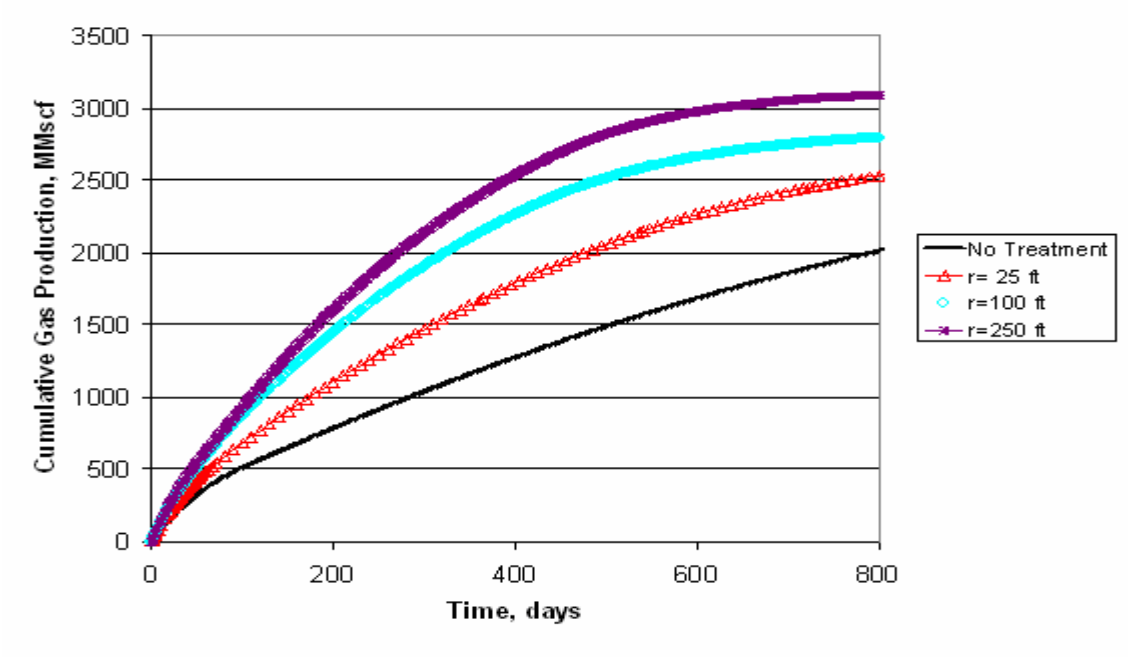

Fig. D.68 Cumulative Gas Production vs Time for Several Radius of Treatment, Fluid C (11 mole % C7+), Swi=0.41, h=10 feet, k=50 mD

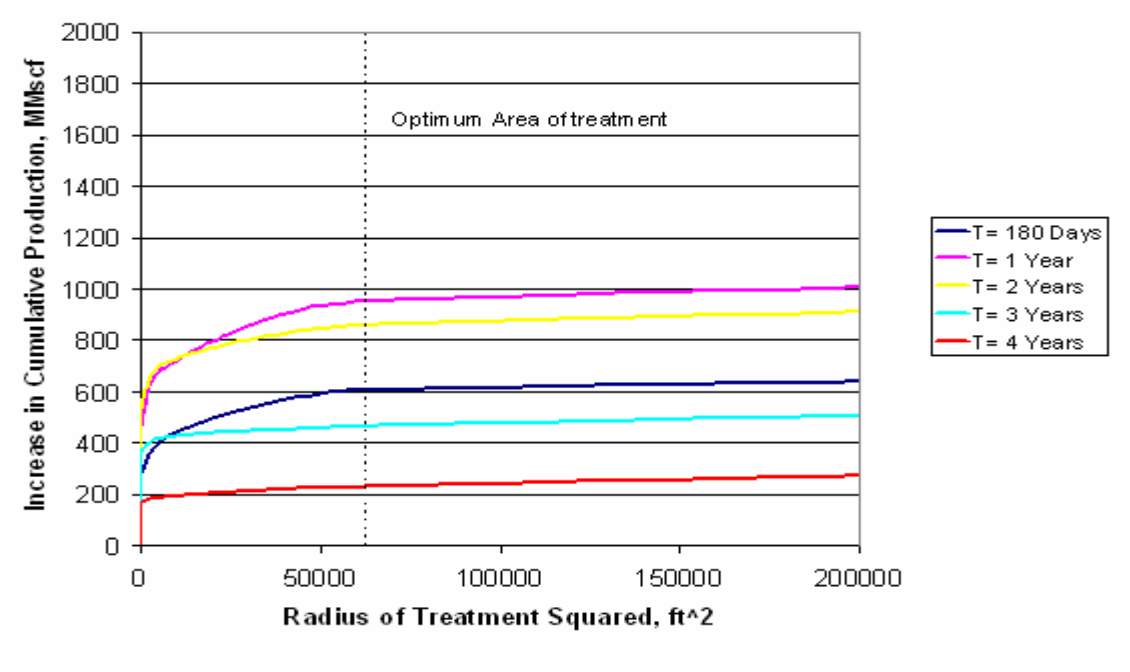

Fig. D.69 Increment in Cumulative Gas Production vs Radius of Treatment Squared , Fluid C (11 mole % C7+), Swi=0.41, h=10 feet, k=50 mD

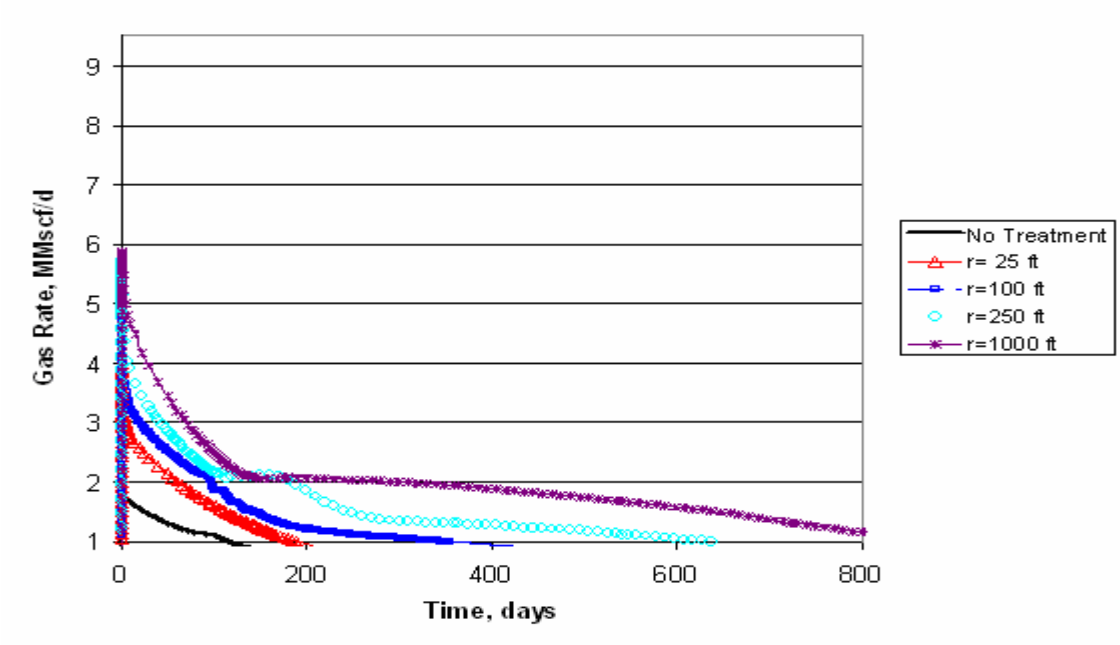

Fig. D.70 Gas Production Rate vs Time for Several Radius of Treatment, Fluid C (11 mole % C7+), Swi=0.41, h=10 feet, k=10 mD

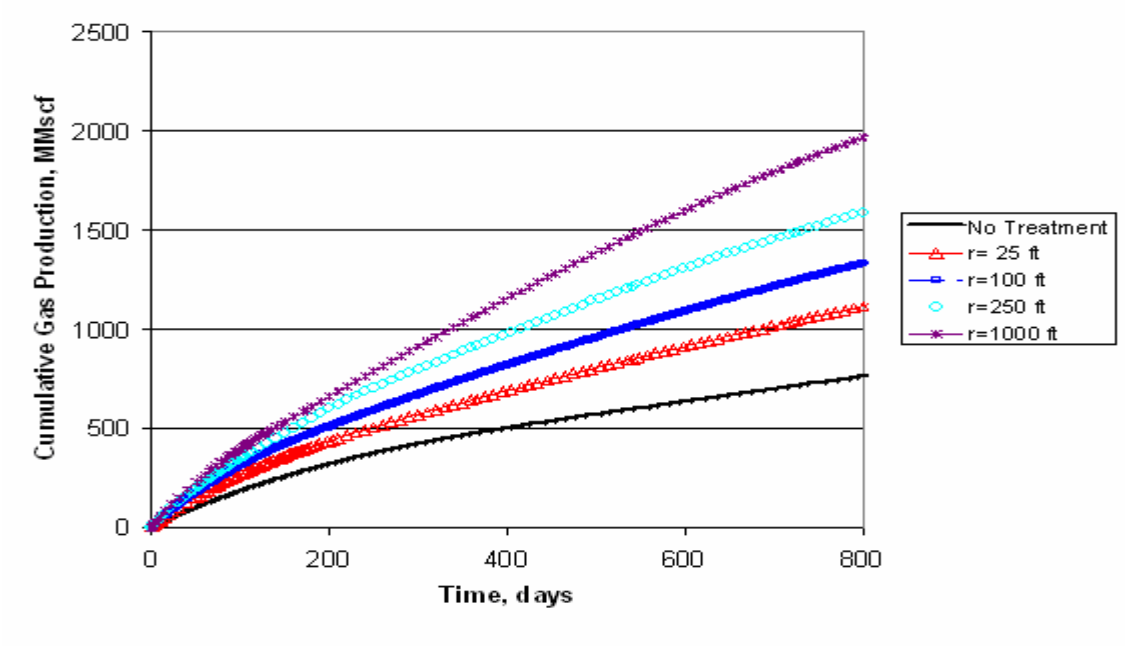

Fig. D.71 Cumulative Gas Production vs Time for Several Radius of Treatment, Fluid C (11 mole % C7+), Swi=0.41, h=10 feet, k=10 mD

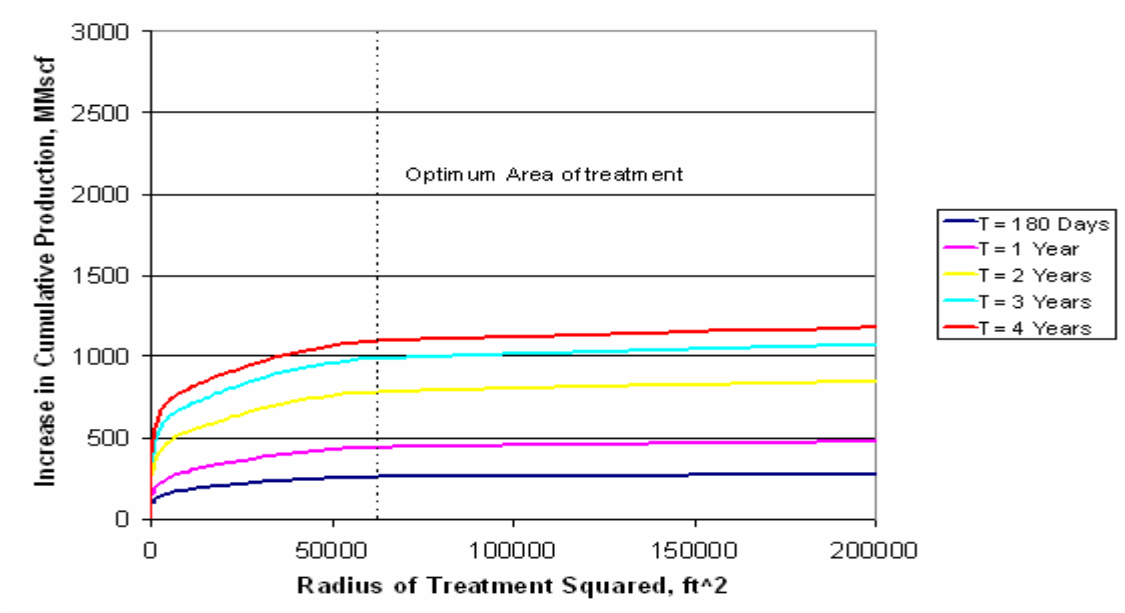

Fig. D.72 Increment in Cumulative Gas Production vs Radius of Treatment Squared , Fluid C (11 mole % C7+), Swi=0.41, h=10 feet, k=10 mD

APPENDIX E
EFFECT OF TUBING DIAMETER

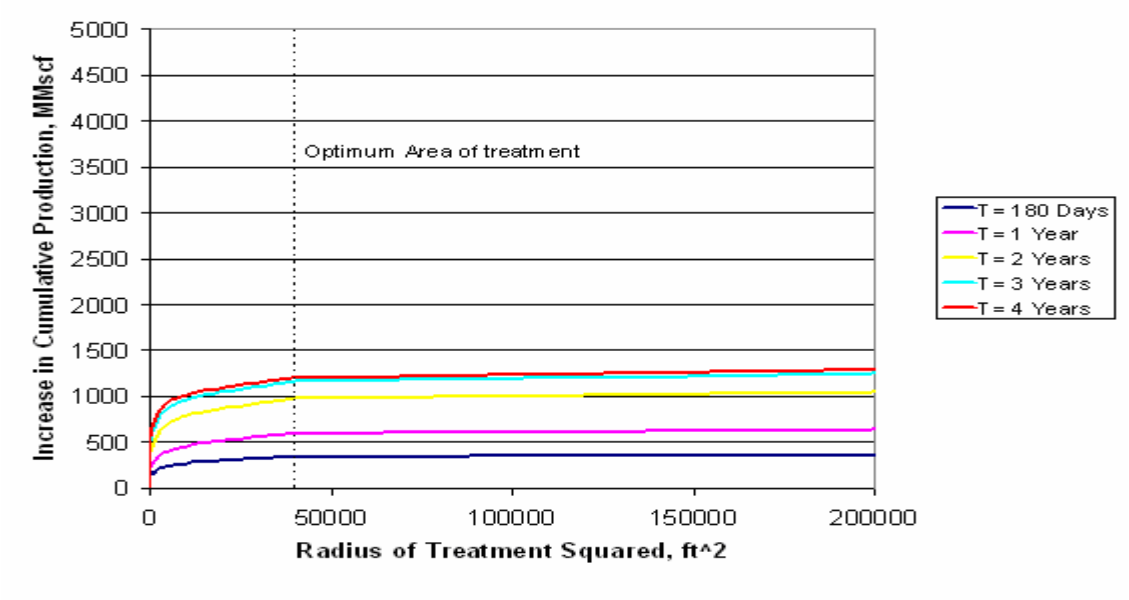

Fig. E.1 Increase in Cumulative Gas Production Vs Time for Fluid B (4 mole % C7+), Swi=0.41, h=10 feet, k=10 mD, Tub Diam= 3.5 inches

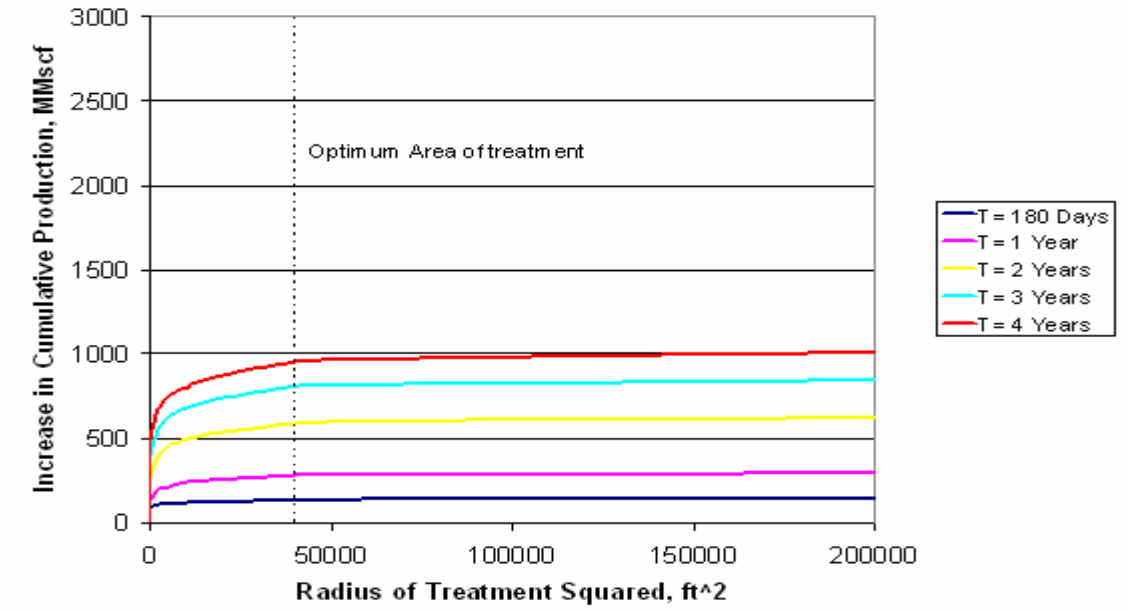

Fig. E.2 Increase in Cumulative Gas Production Vs Time for Fluid B (4 mole % C7+), Swi=0.41, h=10 feet, k=10 mD, Tub Diam= 2.875 inches

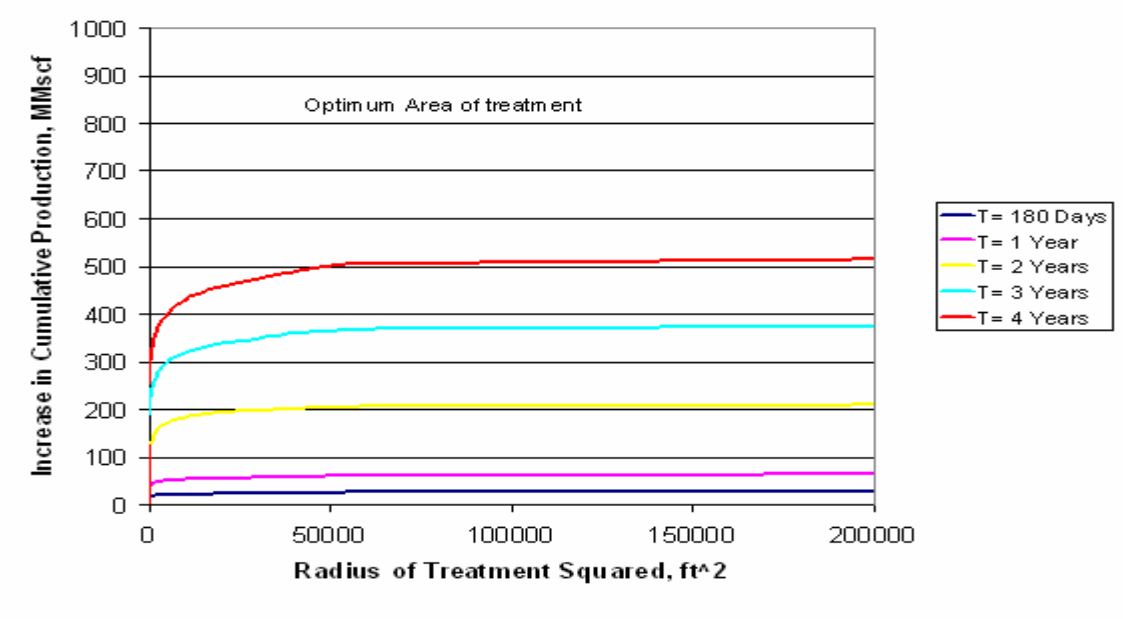

Fig. E.3 Increase in Cumulative Gas Production Vs Time for Fluid B (4 mole % C7+), Swi=0.41, h=10 feet, k=10 mD, Tub Diam= 2.375 inches

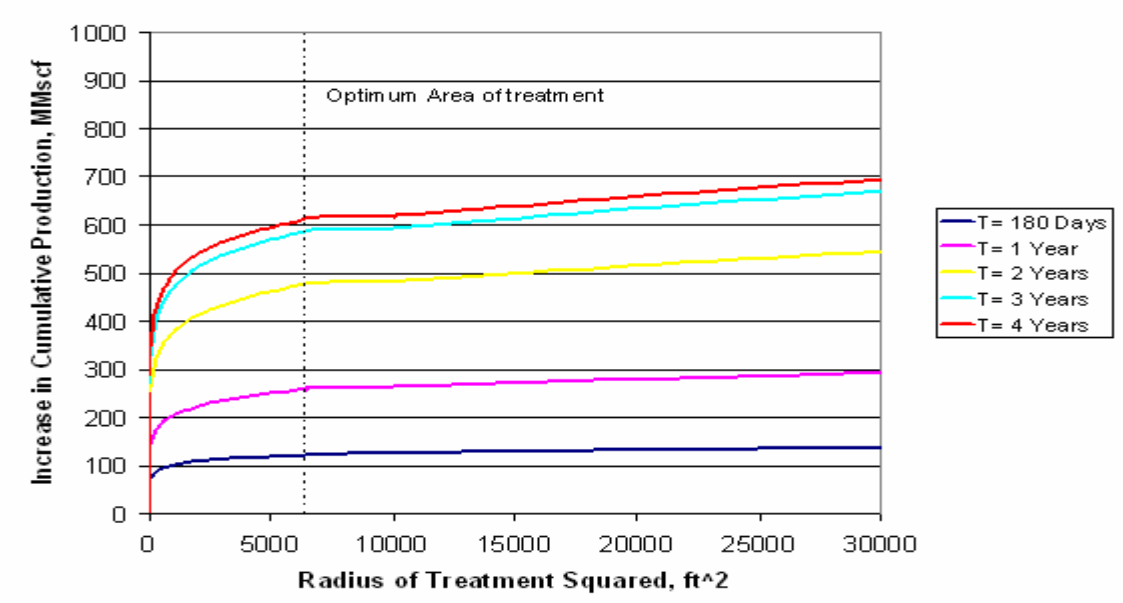

Fig. E.4 Increase in Cumulative Gas Production Vs Time for Fluid B (4 mole % C7+), Swi=0.2, h=10 feet, k=10 mD, Tub Diam= 3.5 inches

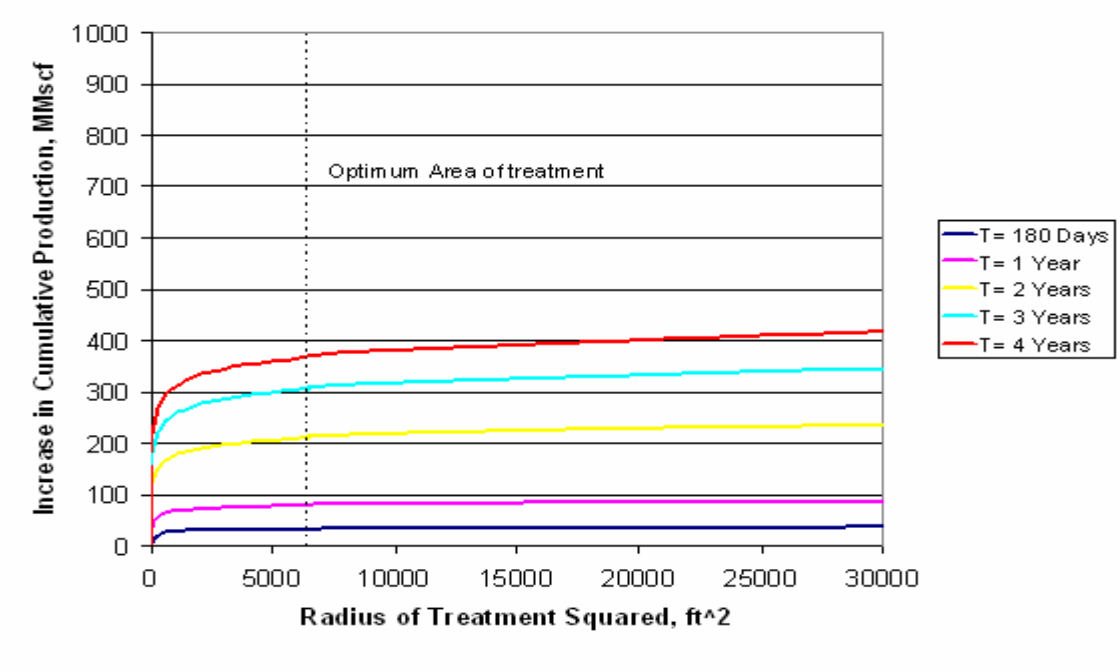

Fig. E.5 Increase in Cumulative Gas Production Vs Time for Fluid B (4 mole % C7+), Swi=0.2, h=10 feet, k=10 mD, Tub Diam= 2.875 inches

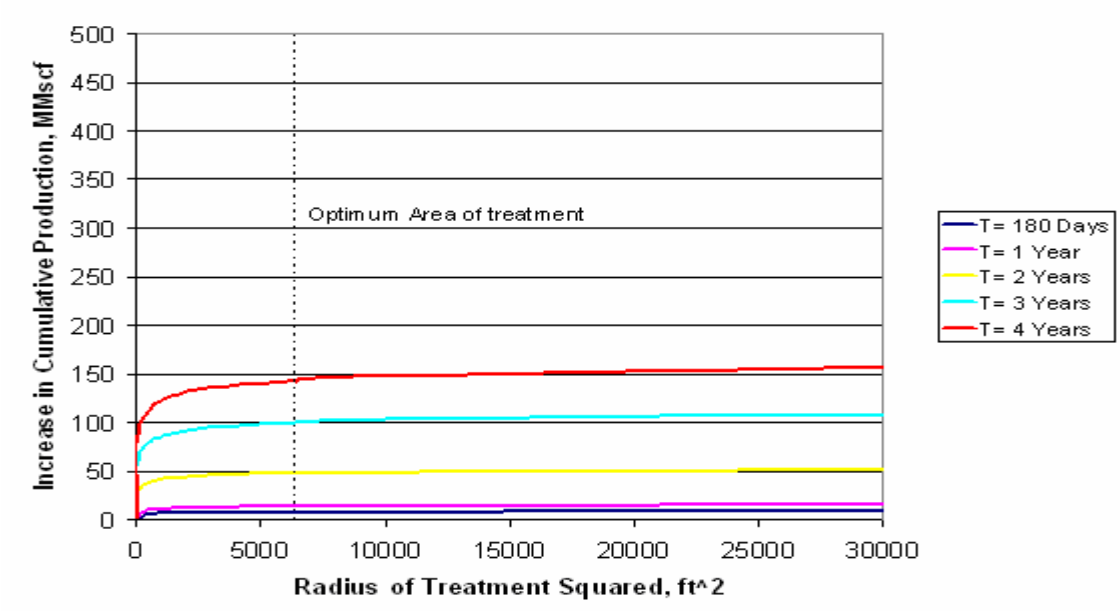

Fig. E.6 Increase in Cumulative Gas Production Vs Time for Fluid B (4 mole % C7+), Swi=0.2, h=10 feet, k=10 mD, Tub Diam= 2.375 inches

VITA

Name:	Jose Gilberto Carballo Salas
Date of Birth:	April 24, 1978
Place of Birth:	Lecherias, Anzoategui, Venezuela
Parents:	G. Carballo N. Salas
Permanent Address:	2 Bd. Des Pyrénées, 64000 Pau France.
Education:	B.S. Chemical Engineering Universidad Simon Bolivar Venezuela, (1999) Ingénieur de L'Ecole de Petrole et des Moteurs IFP France, (2000)
Experience:	Total Oil and Gas Venezuela (Sept. 2000 – Jan 2003)